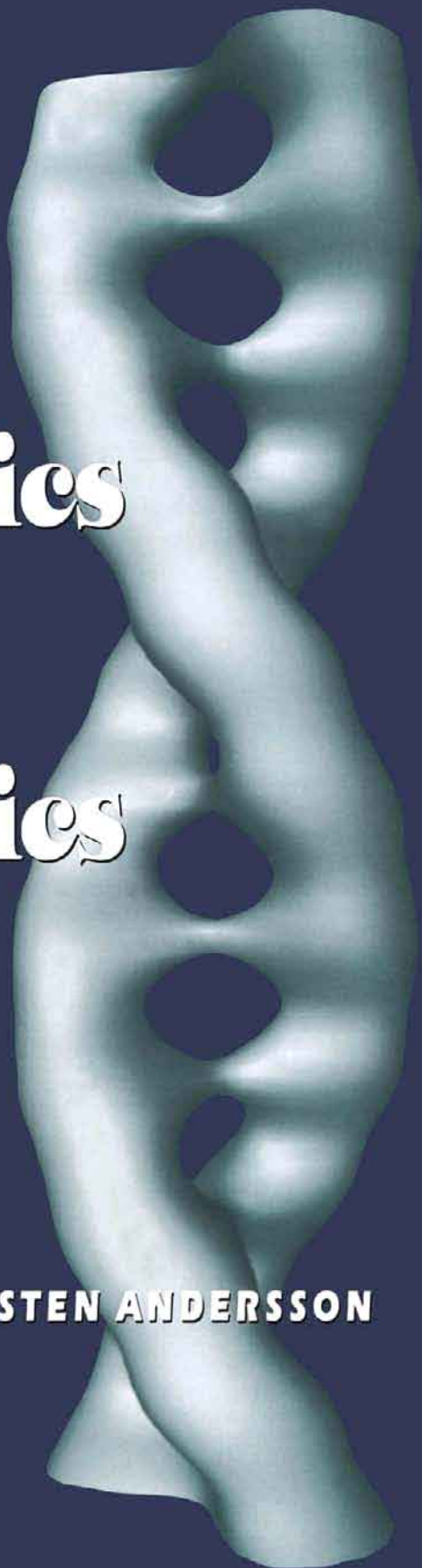


The nature of mathematics and the mathematics of nature

BY MICHAEL JACOB AND STEN ANDERSSON

Elsevier



The Nature of Mathematics and the Mathematics of Nature

This Page Intentionally Left Blank

The Nature of Mathematics and the Mathematics of Nature

by

Michael Jacob

Department of Inorganic Chemistry
Arrhenius Laboratory
University of Stockholm
S-10691 Stockholm, Sweden

and

Sten Andersson

Sandviks Forskningsinstitut
S. Långgatan 27
S-38074 Lötörp, Sweden



1998

ELSEVIER

AMSTERDAM . LAUSANNE . NEWYORK . OXFORD . SHANNON . SINGAPORE . TOKYO

ELSEVIER SCIENCE B.V.
Sara Burgerhartstraat 25
P.O. Box 211, 1000 AE Amsterdam, The Netherlands

ISBN: 0-444-82994-6

Library of Congress Cataloging-in-Publication Data

Jacob, Michael.

The nature of mathematics and the mathematics of nature / Michael
Jacob, Sten Andersson.

p. cm.

Includes bibliographical references and index.

ISBN 0-444-82994-6 (alk. paper)

1. Mathematics. I. Andersson, Sten. II. Title.

QA39.2.J313 1998

510--dc21

98-36663

CIP

© 1998 Elsevier Science B.V. All Rights Reserved.

No part of this publication may be reproduced, stored in a retrieval system or transmitted in any form or by any means, electronic, mechanical, photocopying, recording or otherwise, without the prior written permission of the publishers, Elsevier Science B.V., Copyright & Permissions Department, P.O. Box 521, 1000 AM Amsterdam, The Netherlands.

Special regulations for readers in the U.S.A.- This publication has been registered with the Copyright Clearance Center Inc. (CCC), 222 Rosewood Drive, Danvers, MA 01923. Information can be obtained from the CCC about conditions under which photocopies of parts of this publication may be made in the U.S.A. All other copyright questions, including photocopying outside of the U.S.A., should be referred to the publisher.

© The paper used in this publication meets the requirements of ANSI/NISO Z39.48-1992 (Permanence of Paper).

Printed in The Netherlands.

Contents

Chapter 1

| | |
|---|---|
| 1 Introduction | 1 |
| References 1 | 4 |
| Publications on 'The Exponential Scale' | 5 |

Chapter 2

| | |
|---|----|
| 2 The Roots of Mathematics - the Roots of Structure | 7 |
| 2.1 Multiplication of Polynomials | 7 |
| 2.2 Addition of Polynomials | 16 |
| 2.3 Saddles | 26 |
| Exercises 2 | 31 |
| References 2 | 38 |

Chapter 3

| | |
|--|----|
| 3 The Natural Function and the Exponential Scale | 39 |
| 3.1 Polygons and Planar Geometry | 39 |
| 3.2 Polyhedra and Geometry | 47 |
| 3.3 Curvature | 52 |
| 3.4 The Fundamental Polyhedra - and Others | 55 |
| 3.5 Optimal Organisation and Higher Exponentials | 62 |
| Exercises 3 | 67 |
| References 3 | 71 |

Chapter 4

| | |
|---|----|
| 4 Periodicity and the Complex Exponential | 73 |
| 4.1 The Translation Vector | 73 |
| 4.2 The Complex Exponential and Some Variants | 80 |
| 4.3 Some Other Exponentials | 88 |
| Exercises 4 | 94 |
| References 4 | 98 |

Chapter 5

| | |
|--|-----|
| 5 The Screw and the Finite Periodicity with the Circular Punctions | 99 |
| 5.1 Chirality, the Screw and the Multi Spiral | 99 |
| 5.2 The Bending of a Helix | 109 |
| 5.3 Finite Periodicity - Molecules and the Larsson Cubosomes | 112 |
| Exercises 5 | 119 |
| References 5 | 122 |

Chapter 6

| | |
|--|-----|
| 6 Multiplication, Nets and Planar Groups | 123 |
| 6.1 Lines and Saddles | 123 |
| 6.2 Nets with Two Planes, and Variations | 125 |
| 6.3 Nets with Three Planes, and Variations | 127 |
| 6.4 Nets with Four Planes, and Variations | 130 |
| 6.5 Structures in 3D from the Nets | 132 |
| 6.6 Quasi | 136 |
| 6.6.1 Four Planes and Quasi | 136 |
| 6.6.2 Five Planes and Quasi | 137 |
| Exercises 6 | 139 |
| References 6 | 146 |

Chapter 7

| | |
|---|-----|
| 7 The Gauss Distribution Function | 147 |
| 7.1 The GD Function and Periodicity | 147 |
| 7.1.1 Handmade Periodicity | 155 |
| 7.2 The GD Function and Periodicity in 3D | 156 |
| 7.3 The BCC and Diamond Symmetries | 161 |
| 7.4 The Link to Cosine | 176 |
| Exercises 7 | 186 |
| References 7 | 190 |

Chapter 8

| | |
|---|-----|
| 8 Handmade Structures and Periodicity | 191 |
| 8.1 Prelude | 191 |
| 8.2 Simplest of Periodic Structures | 201 |
| 8.3 Contact of Spheres in Space - Structures and Surfaces | 205 |
| 8.4 How Tetrahedra and Octahedra meet in Space | 226 |
| Exercises 8 | 229 |
| References 8 | 236 |

Chapter 9

| | |
|---|-----|
| 9 The Rods in Space | 237 |
| 9.1 Primitive Packing of Rods | 237 |
| 9.2 Body Centred Packing of Rods | 242 |
| 9.3 Tetragonal and Hexagonal Packing of Rods | 246 |
| 9.4 Larsson Cubosomes of Rods | 253 |
| 9.5 Packing of Rods, and their Related Surfaces | 258 |
| Exercises 9 | 262 |
| References 9 | 265 |

| | |
|---|-----|
| Chapter 10 | |
| 10 The Rings, Addition and Subtraction | 267 |
| 10.1 Some Simple Examples of Subtraction and Addition in 3D | 267 |
| 10.2 The Rings | 273 |
| 10.3 More Ways to make Rings | 278 |
| 10.4 More Subtraction - Hyperbolic Polyhedra | 283 |
| Exercises 10 | 289 |
| References 10 | 292 |
| Chapter 11 | |
| 11 Periodic Dilatation - Concentric Symmetry | 293 |
| 11.1 Dilatation and Translation in 2D | 293 |
| 11.2 Dilatation and Translation in 3D | 300 |
| 11.3 Pure Dilatation | 312 |
| Exercises 11 | 320 |
| References 11 | 324 |
| Appendix 1 | |
| Mathematica | 325 |
| Appendix 2 | |
| Curvature and Differential Geometry | 327 |
| Appendix 3 | |
| Formal Way to Derive the Shapes of Polyhedra | 330 |
| Appendix 4 | |
| More Curvature | 333 |
| Appendix 5 | |
| Raison d'être | 335 |
| Subject Index | 339 |

This Page Intentionally Left Blank

1 Introduction

'every chapter is an introduction' (from D'Arcy Thompson)

We are chemists, and as chemists we find it necessary to build models for the understanding and description of structures in science. This book concerns the tool we found in order to build and describe structures with the use of mathematics.

Chemistry, as well as the rest of natural science, is awfully complicated - because it is Nature. Mathematics is man-made and therefore not as complicated. We found good use of it from group theory for crystal structure determination and description [1], and we used the intrinsic curvature to explain reactions and structures in inorganic solid state chemistry. We dealt with minimal surfaces, isometric transformations and applications in natural science [2]. Together with mathematicians and biologists THE LANGUAGE OF SHAPE [3] was born.

We found the daily use of the mathematics involved somewhat heavy, for instance the differential geometry, Riemann surfaces or Bonnet transformations. As chemists we are, we tried new routes - other branches - of mathematics.

We introduced the Exponential Scale a few years ago, and the articles published are collected below. The field is unusually rich, and instead of writing more articles we decided to write this book, and search as deep as possible into the mathematics.

We found that the 3D representations of the hyperbolic functions are the concave adding of planes, and the convex subtraction of planes. These give polyhedra in the first case, and saddles in the second.

We also found that the multiplication of planes give the general saddle equations and the multispirals. And that the simplest complex exponential in 3D (also composed of planes) is a fundamental nodal surface, within 0.5 % the same as the famous Schwartz minimal surface as found by Schwartz himself. This surface is in a way identical to a classical chemical structure. We found that the functions we do can be dissecting into planes or lines, which may be the roots that build the fundamental theorem of algebra, and our finite periodicity.

Here the natural exponential, e^x , in 3D is a cube corner, and the Platonic polyhedra are the $\cosh(x)$ function. The complex exponentials with the general permutations in space are the same as the fundamental cubic symmetries as represented by primitive packing of bodies, face centred cubic packing, body centred packing and diamond packing.

We derive the equation of symmetry, which really contains the exponential scale with its functions for solids, the complex exponentials with all the nodal surfaces, and the GD (gauss distribution) mathematics.

We study the three dimensional structures of mathematical functions, such as the polynoms of the fundamental theorem of the algebra, the natural exponential, the circular functions, and the GD functions. And combinations of these. Doing this we can study the reaction of a sphere with itself or with a plane, or a complex exponential. And the same for a polyhedron, and also make the hyperbolic polyhedra. We do the same with rods or cylinders, or with other objects.

And very important, we study finite, or infinite, periodicity of spheres, cylinders, or anything.

We study the addition, the subtraction and the multiplication of functions.

This is what we call the Nature of Mathematics.

During the work with this book we were surprised to realise that some earlier work in chemistry came to daylight again - but now in form of mathematics. Starting almost 30 years ago, inorganic crystal structures in the solid state were systematically organised in an axiomatic and hierarchic way. The crystallographic operations translation, rotation and reflection were applied to fundamental building blocks in order to describe complicated structures. The work was finally summarised in a monograph [5], and later the rod packings were derived [6,7]. All this was 'handmade'.

Piece by piece we found our descriptions of structures and the structure building operations in form of mathematical functions. The description of a structure is the nature of mathematics itself. We are now tempted to say that crystal structures and 3D mathematics are synonyms.

We also found functions for the rod packings, and for defects in solids. And the mathematics for giant molecules like the cubosomes, the DNA double helix [8], and certain building blocks in protein structures. With the mathematics for dilatation we make twins, trillings, furlings and sixlings. With the GD mathematics we make them periodic.

Some beautiful work in chemistry has been carried out using the ELF (electron localisation function) method from quantum physics the recent years. The ELF descriptions of the boron hydrides are of particular interest [4] here as they also are described by fundamental functions in several different kinds of mathematics. They show up as simple roots to the fundamental theorem of algebra. They also show up in the 'cubosome' mathematics, in the GD mathematics and also as products of GD functions and complex exponentials.

We conclude:

We see topologies, more or less by accident, that are relevant to natural sciences.

We see motion, attraction, or repulsion without the notions of time, speed or acceleration.

We see molecules or crystal structure, without the notion of energy.

We make molecules or structures from the fundamental theorem of algebra.

We make molecules or structures from the Gauss distribution function.

This is what we call the Mathematics of Nature.

So we had the name to this book.

We found we had - unintentionally - written a continuation of THE LANGUAGE OF SHAPE.

Michael Jacob
Sten Andersson

*Stockholm, Sweden
Sandvik, Öland
March 1998*

References 1

1. Q.-B. Yang, and S. Andersson, Application of coincidence site lattices for crystal structure description, Part I: $\Sigma=3$, *Acta Cryst.* **B43** (1987) 1-14.
2. S. Andersson, S.T. Hyde, K. Larsson, S. Lidin, Minimal surfaces and structures: From inorganic and metal crystals to cell membranes and biopolymers, *Chemical Reviews*, **88** (1988) 221-242.
3. S.T. Hyde, S. Andersson, K. Larsson, Z. Blum, T. Landh, S. Lidin, and B. Ninham, *THE LANGUAGE OF SHAPE*, the role of curvature in condense matter: physics, chemistry and biology, Elsevier, Amsterdam, 1997.
4. A. Burkhardt, U. Wedig, H.G. von Schnering and A. Savin, Die Elektronen-Lokalisierungs-Funktion in *closo*-Bor-Clustern, *Z. anorg. allg. Chem.* **619**, 437 (1993).
5. B.G. Hyde and S. Andersson, *INORGANIC CRYSTAL STRUCTURES*, Wiley, New York, 1988.
6. S. Lidin, M. Jacob and S. Andersson, A mathematical analysis of rod packings, *J. Solid State Chem.* **114**, 36 (1995).
7. M. O'Keeffe and S. Andersson, Rod packings and crystal chemistry, *Acta Cryst. A* **33**, 914 (1977).
8. M. Jacob, Saddle, Tower and Helicoidal surfaces, *J.Phys. II France* **7** (1997) 1035-1044.

Publications on ‘The Exponential Scale’

- I S. Andersson, M. Jacob, S. Lidin, On the shapes of crystals, *Z. Kristallogr.* **210**, 3-4 (1995).
- II S. Andersson, M. Jacob, K. Larsson, S. Lidin, Structure of the Cubosome - a closed Lipid Bilayer Aggregate, *Z. Kristallogr.* **210** (1995) 315-318.
- III S. Andersson, M. Jacob, S. Lidin, The exponential Scale and Crystal Structures, *Z. Kristallogr.* **210** (1995) 826-831.
- IV K. Larsson, M. Jacob, S. Andersson, Lipid bilayer standing waves in cell membranes, *Z. Kristallogr.* **211** (1996) 875-878
- V M. Jacob, K. Larsson, S. Andersson, Lipid bilayer standing wave conformations in aqueous cubic phases, *Z. Kristallogr.* **212** (1997) 5-8.
- VI S. Andersson, M. Jacob, On the structure of mathematics and crystals, *Z. Kristallogr.* **212** (1997) 334-346.
- VII M. Jacob, Saddle, Tower and Helicoidal surfaces, *J.Phys. II France* **7** (1997) 1035-1044.
- VIII M. Jacob, S. Andersson, Finite Periodicity and Crystal Structures, *Z. Kristallogr.* **212** (1997) 486-492.
- IX S. Andersson, M. Jacob, *The exponential Scale*, Supplement No. 13 of *Zeitschrift für Kristallographie*, R. Oldenbourg Verlag, München, 1997.
- X M. Jacob, S. Andersson, Finite periodicity, chemical systems and Ninham forces, *Colloids and Surfaces* **129-130** (1997) 227-237.
- XI M. Jacob, S. Andersson, The Exponential Scale: The Mathematics of Structures, Toyota 11th Conference. In print.

This Page Intentionally Left Blank

2 The Roots of Mathematics - the Roots of Structure

Kant had said that it was Nature herself, and not the mathematician, who brings mathematics into natural philosophy (D'Arcy Thompson [1]).

Here we describe the fundamental theorem of algebra in two and three dimensions, and show that functions often can be dissected into straight lines or planes. Polynomial products with suitable roots contain the commencement of periodicity and we give the link to the sinus function. Permutations of variables, and polynomial additions in three dimensions give the fundamental polyhedra, structure of simple molecules in natural science, and the core of the fundamental sphere packings.

We give the link to The Exponential Scale.

We study saddles, and also some important minimal surfaces.

In Appendix 1 we introduce you to Mathematica, differential geometry, shapes of polyhedra and curvature.

2.1 Multiplication of Polynomials

The idea with this book is to study the variation of the variables x , y and z , which includes geometry. We will mainly work in 3D space, and only in 2D or 1D to clarify.

Mathematics have *numbers*, negative and positive, with the important zero in between.

For *functions* there are variables, and we explain these following Hardy [2]: When a volume V of a gas is compressed with a pressure p , the product of p and V is constant (Boyle's law - this is natural science so there are deviations, but we assume it is ideal).

$$pV = C$$

2.1.1

With C being the constant, this means that if p is large, V is small and vice versa, just like using a manual pump for the filling of air in an empty tube to your bike. We have here described variables, but normally we call them x in one dimension, x and y in two dimensions, and x , y and z in three dimensions.

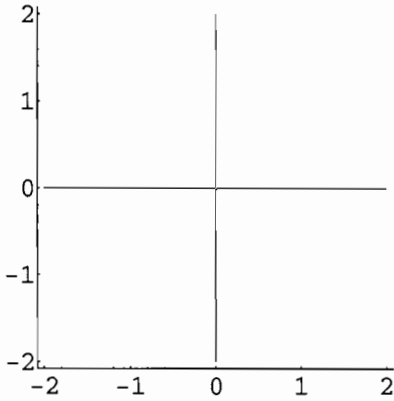


Fig. 2.1.1. Equation after 2.1.2 with $C=0$.

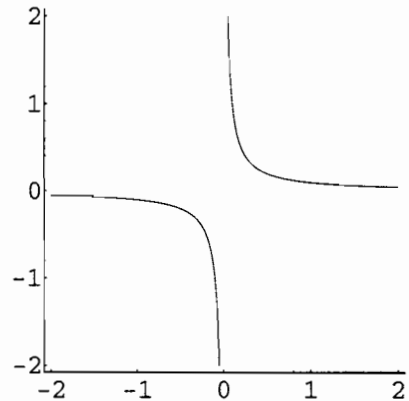


Fig. 2.1.2. $C=0.1$

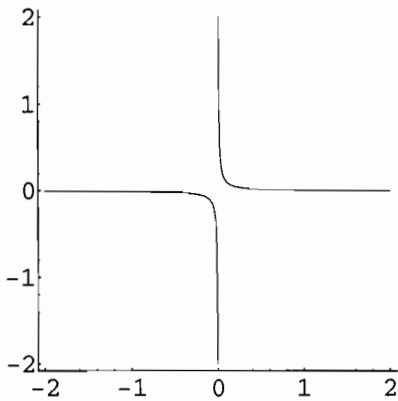


Fig. 2.1.3. $C=0.01$

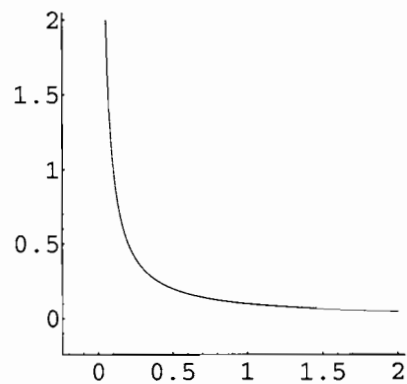


Fig. 2.1.4. $C=0.1$

We plot this our first function after equation 2.1.2 (capital C means isosurface constant throughout this study).

$$xy = C$$

2.1.2

With $C=0, 0.1, 0.01$ and 0.1 we get figures 2.1.1, 2.1.2, 2.1.3 and 2.1.4. When $C=0$, two lines intersect as in 2.1.1, and as soon as $C \neq 0$ as in 2.1.2 and 2.1.3 the lines divide. Figure 2.1.4 is the part of the function that corresponds to Boyle's law above, with only positive values for the variables.

From this we learn that this function is described by two lines that cross each other without intersection for C different from 0.

We bring in the roots

$$(x)(x-1)$$

and

$$x^3 - 2x^2 + x = (x)(x-1)(x+1)$$

and study these in two dimensions, x and y:

$$(x)(x-1)(y)(y-1) = C \tag{2.1.3}$$

and

$$(x)(x-1)(x+1)(y)(y-1)(y+1) = C \tag{2.1.4}$$

In figures 2.1.5 and 2.1.7 C=0, and in 2.1.6 and 2.1.8 C=0.01.

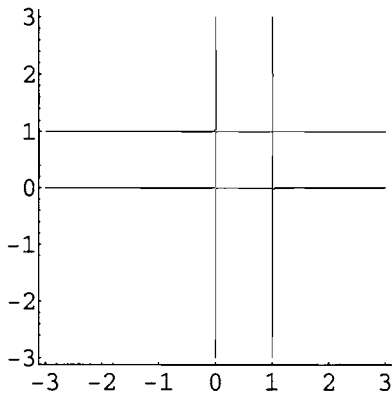


Fig. 2.1.5. Equation after 2.1.3 with C=0.

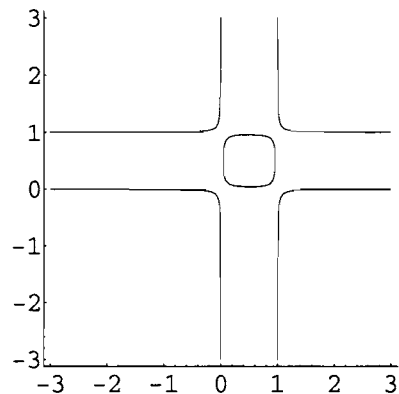


Fig. 2.1.6. C=0.01

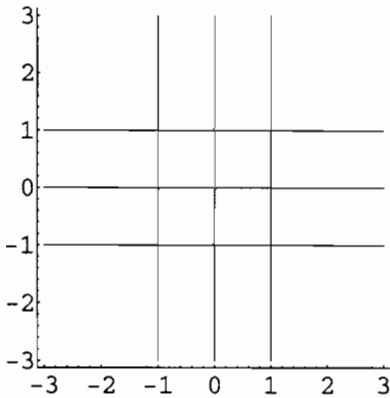


Fig. 2.1.7. Equation after 2.1.4 with $C=0$.

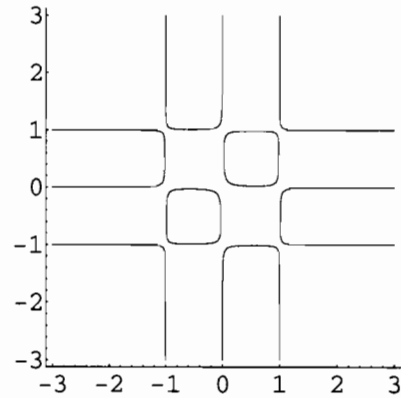


Fig. 2.1.8. $C=0.01$

We have seen one of the most important properties of science: the commencement of periodicity itself and how it comes from the roots of an algebraic equation. The idea is to show how such an equation looks like in two and three dimensions - we have chosen roots that give equidistant translation in order to keep complexity down. In figure 2.1.7 the output is more than the input, here there are 9 points identical via translation originating from the three points in x and three in y . $C=0.01$ in equation 2.1.4 produces a structure of a continuous function of separated particles in figure 2.1.8.

We continue with the equation of the seventh degree:

$$x^7 - 14x^5 + 49x^3 - 36x = C$$

or

$$x(x-1)(x+1)(x-2)(x+2)(x-3)(x+3) = C \quad 2.1.5$$

The periodicity in 2D is shown in figure 2.1.9 after equation 2.1.6.

$$\begin{aligned} &x(x-1)(x+1)(x-2)(x+2)(x-3)(x+3) \\ &\cdot y(y-1)(y+1)(y-2)(y+2)(y-3)(y+3) = C = 0 \end{aligned} \quad 2.1.6$$

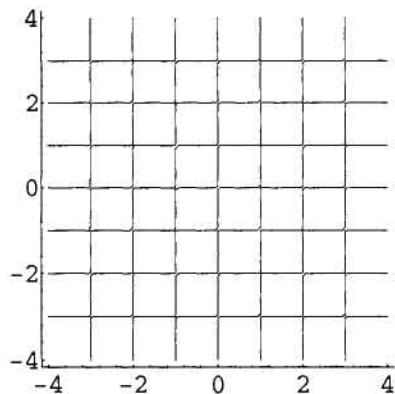


Fig. 2.1.9. Periodicity after equation 2.1.6.

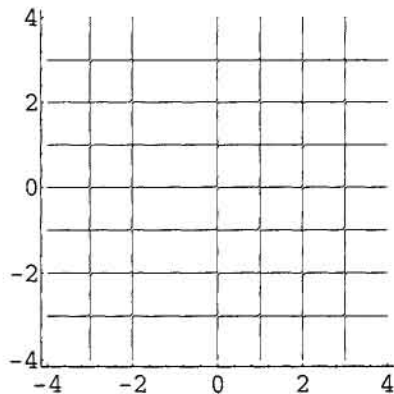


Fig. 2.1.10. Defect structure after equation 2.1.7.

We can make a defect structure as well, by omitting one line in equation 2.1.7 as shown in figure 2.1.10.

$$\begin{aligned}
 &x(x-1)(x-2)(x+2)(x-3)(x+3) \\
 &\cdot y(y-1)(y+1)(y-2)(y+2)(y-3)(y+3) = C = 0
 \end{aligned}
 \tag{2.1.7}$$

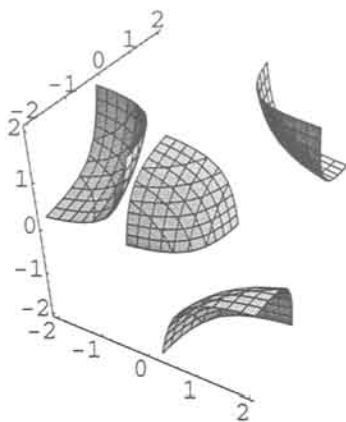


Fig. 2.1.11. Equation after 2.1.8 with C=1.

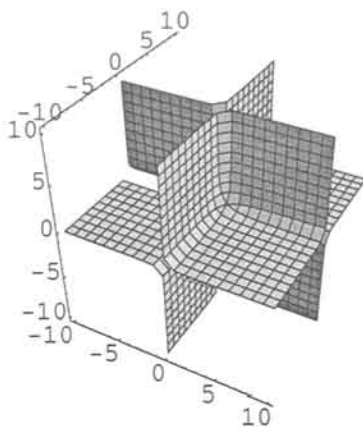


Fig. 2.1.12. Equation after 2.1.8 with C=-1.

We extend to 3D with the function in 2.1.8 as shown in figure 2.1.11 with C=1. In 2.1.12 C=-1 to show the reverse tetrahedral symmetry with larger

boundaries and changed sign of the constant. This also to show the planes which build up the surface.

$$xyz = C \quad 2.1.8$$

This space contains symmetry, the structure is tetrahedral with four identical surfaces from three variables. Increased boundaries show four "cube corners" that make the first fragment of periodicity. The total structure at $C \neq 0$ is built of perpendicular and non-intersecting planes.

More roots show extended periodicity using the polynomial 2.1.9.

$$\begin{aligned} & (x)(y)(z)(x-1)(x+1)(x-2)(x+2) \\ & \cdot (y-1)(y+1)(y-2)(y+2) \\ & \cdot (z-1)(z+1)(z-2)(z+2) = 0.1 \end{aligned}$$

or the identical

$$\begin{aligned} & (x)(y)(z)(x^2-1)(y^2-1)(z^2-1) \\ & \cdot (x^2-4)(y^2-4)(z^2-4) = 0.1 \end{aligned} \quad 2.1.9$$

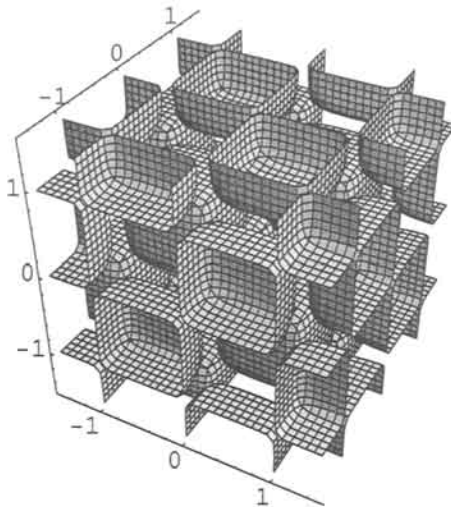


Fig. 2.1.13. Equation after 2.1.9 with $C=0.1$.

In figure 2.1.13 the central part of the function is shown which is the structure of face centred cubic arrangements of bodies. With larger boundaries and the same function 2.1.9, we see the formidable periodicity in figure 2.1.14.

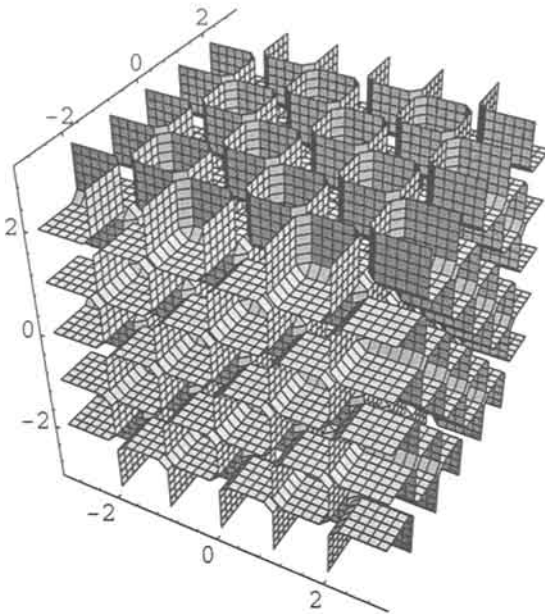


Fig. 2.1.14. Equation after 2.1.9 with larger boundaries shows periodicity of the fundamental theorem of algebra.

The result above is very similar to the fundamental solution of the wave equation:

$$\sin x \sin y \sin z = 0 \quad 2.1.10$$

How comes? We have seen that periodicity itself is simple, exact and easily obtained with well chosen equations. But this periodicity is *finite*, as most phenomena in nature are. Going infinite means infinite products and we arrive at one of the definitions of sine as shown in 2.1.11.

$$\sin x = x \left(1 - \frac{x^2}{\pi^2}\right) \left(1 - \frac{x^2}{2^2 \pi^2}\right) \left(1 - \frac{x^2}{3^2 \pi^2}\right) \dots \quad 2.1.11$$

or

$$\sin x = x \prod_{r=1}^{\infty} \left(1 - \frac{x^2}{r^2 \pi^2} \right)$$

A first rearrangement gives equation 2.1.12,

$$\sin x = (\pi^n n!)^{-2} x(x^2 - \pi^2)(x^2 - 2^2 \pi^2)(x^2 - 3^2 \pi^2)(x^2 - 4^2 \pi^2) \dots (x^2 - n^2 \pi^2) \dots 2.1.12$$

and finally polynomials as 2.1.13.

$$\sin \pi x = \frac{\pi}{(n!)^2} x(x^2 - 1)(x^2 - 4)(x^2 - 9) \dots (x^2 - n^2) \tag{2.1.13}$$

This clearly shows the relationship between sinus and the algebra, the roots of the polynomial are the nodes of the circular function.

For $n=12$ we have plotted this function together with $\sin \pi x$ in figure 2.1.15.

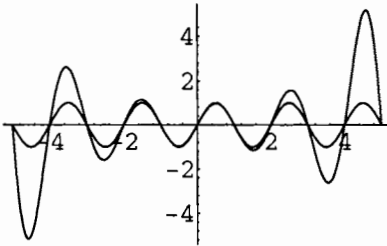


Fig. 2.1.15. Equation 2.1.13 with twelve roots compared with $\sin \pi x$.

The description of a structure with an algebraic equation has advantages - one is that changes can be introduced as a part of the function. We did so above in 2D and do so using equation 2.1.9 in 3D and take away one plane as in 2.1.14, which is shown in figure 2.1.16.

$$(y)(z)(x-1)(x+1)(x-2)(x+2) \cdot (y-1)(y+1)(y-2)(y+2)(z-1)(z+1)(z-2)(z+2) = 0.1 \tag{2.1.14}$$

Instead of taking away the plane we can move it after equation 2.1.15 which is shown in 2.1.17.

$$(x-0.3)(y)(z)(x-1)(x+1)(x-2)(x+2) \cdot (y-1)(y+1)(y-2)(y+2)(z-1)(z+1)(z-2)(z+2) = 0.1 \quad 2.1.15$$

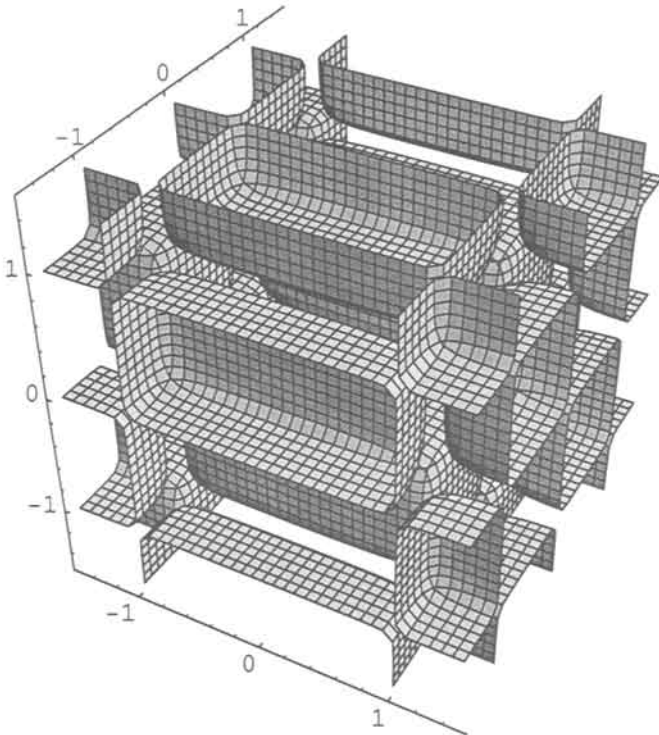


Fig. 2.1.16. One plane is missing after equation 2.1.14.

We may choose any roots and as there are two or three variables whose combinations give more roots, the output becomes larger than the input. Another way to say this is that lines in 2D - or planes in 3D - meet. Any roots produces lines or planes, which may be irregularly spaced, but as the planes or lines are parallel, there is a structure. It may or may not have a sharp Fourier transform indicating long range order. Algebra offers beautiful models via its roots for natural solids and supports the structure building principles and the models for planar defects as developed for crystals [3].

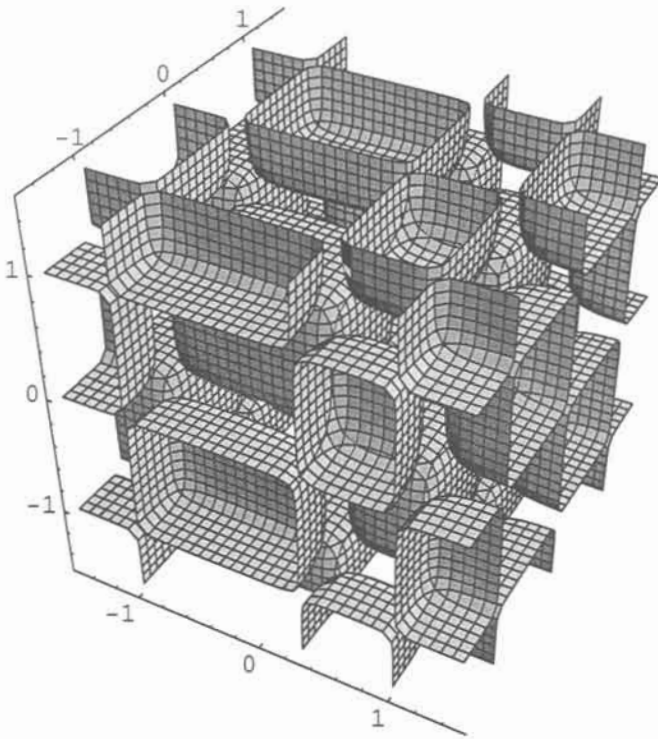


Fig. 2.1.17. The plane is back but moved.

2.2 Addition of Polynomials

The fundamental theorem of algebra says that every algebraic equation has a root, which means that a polynomial like

$$f(z) = a_n x^n + a_{n-1} x^{n-1} + \dots + a_1 x + a_0 \quad 2.2.1$$

always can be written as a product of the roots:

$$f(z) = k(x - x_1)(x - x_2) \dots (x - x_n) \quad 2.2.2$$

We just studied this theorem in 3D by multiplying the x , y and z terms. Addition is the next step, and the first formula is the simplest;

$$x^n + y^n + z^n = C$$

2.2.3

With $n=2$ there is the sphere, and $n=4$ brings out the character of the planes with a constant of 100 in figure 2.2.1.

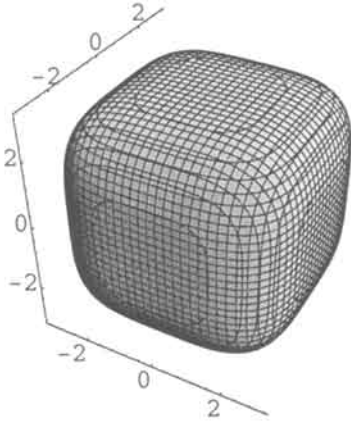


Fig. 2.2.1. Equation 2.2.3 with $n=4$.

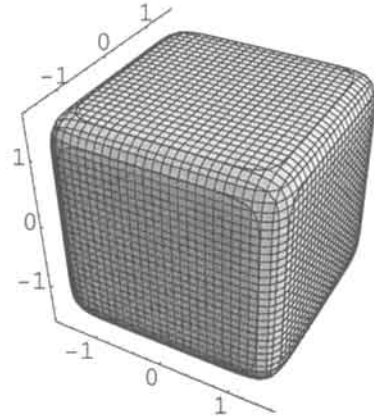


Fig. 2.2.2. Equation 2.2.3 with $n=10$.

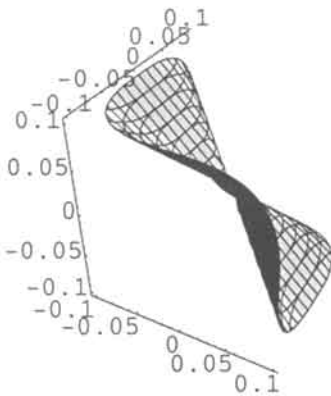


Fig. 2.2.3. Equation 2.2.3 with $n=3$ and $C=0$.

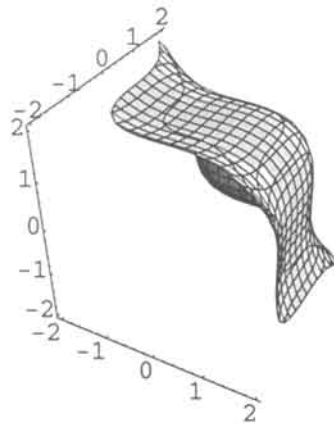


Fig. 2.2.4. Equation 2.2.3 with $n=3$ and $C=5$.

For $n=10$ and the same constant there is figure 2.2.2, and we see that the curvature of the corners increases with n . Similarly the permutations of variables in space give the octahedron, the tetrahedron and the rhombic dodecahedron. But more about that in the next chapter.

Odd n in equation 2.2.3 brings in negative numbers, and the result is hyperbolic geometry where planes meet in a centre point. Adding a constant brings in a cube corner and with this elliptic geometry. Figures 2.2.3 and 2.2.5 are for $n=3$ and $n=5$, both with $C=0$. Figures 2.2.4 and 2.2.6 are for $n=3$ and 5, and $C=5$. Higher exponentials increase sharpness and plane character, and curvature.

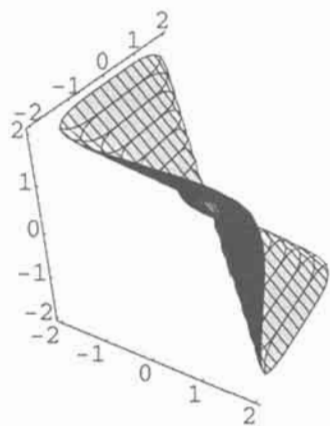


Fig. 2.2.5. Equation 2.2.3 and $n=5$ and $C=0$.

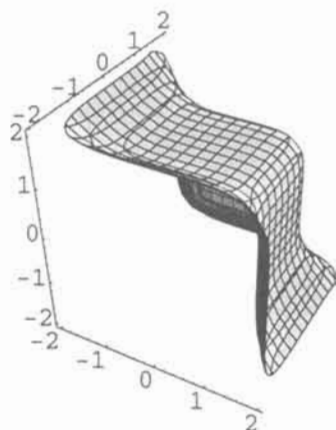


Fig. 2.2.6. Equation 2.2.3 and $n=5$ and $C=5$.

The observations above are contained in the power expansions of the natural function

$$e^x = \cosh x + \sinh x \quad 2.2.4$$

where

$$\cosh x = \frac{1}{2}(e^x + e^{-x})$$

and

$$\sinh x = \frac{1}{2}(e^x - e^{-x})$$

This is beautiful in three dimensions - *cosh* is elliptic and gives the polyhedra and morphology of crystals, whereas *sinh* is hyperbolic and gives the monkey saddles, which is the commencement of periodicity. The expansions below show that the geometry above is contained in the general functions:

$$\begin{aligned} \cosh x + \cosh y + \cosh z &= \\ &= 3 + \frac{1}{2!}(x^2 + y^2 + z^2) + \frac{1}{4!}(x^4 + y^4 + z^4) \dots = \\ &= e^x + e^y + e^z + e^{-x} + e^{-y} + e^{-z} \end{aligned} \tag{2.2.5}$$

Clearly it will become more cubic with more terms.

The other expansion is

$$\begin{aligned} \sinh x + \sinh y + \sinh z &= \\ &= x + y + z + \frac{1}{3!}(x^3 + y^3 + z^3) + \frac{1}{5!}(x^5 + y^5 + z^5) \dots = \\ &= e^x + e^y + e^z - e^{-x} - e^{-y} - e^{-z} \end{aligned} \tag{2.2.6}$$

The exponential functions are the general case and we have said they belong to the Exponential Scale [4]. This will be further developed in the next chapter.

We recall equation 2.2.3 again and point out that for n even we had elliptic geometry, and for n odd we had hyperbolic geometry.

Bringing in roots as in equation 2.2.7 means (finite) periodicity. And how a cube gradually turns into a cubic periodic structure.

$$x(x-1)(x+1) + y(y-1)(y+1) + z(z-1)(z+1) = 0 \tag{2.2.7}$$

The result is shown in fig. 2.2.7, and with larger boundaries and a different direction in 2.2.8. We use this topology to give the mechanism for how matter goes through a wall without making a hole in it (much has been written about the cubic equation but we doubt there is anything like this);

$$x^3 - 2x^2 + x + y^3 - 2y^2 + y + z^3 - 2z^2 + z = C \tag{2.2.8}$$

With a C of -0.5 we have figure 2.2.9, with a const of 0 figure 2.2.7 and 8, and for a constant of 0.5 figure 2.2.10.

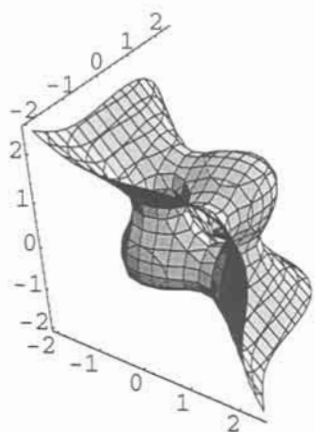


Fig. 2.2.7. The cubic equation from 2.2.7 with $C=0$.

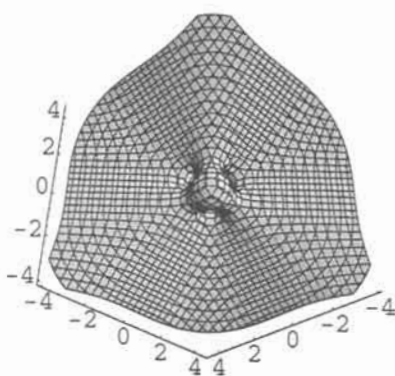


Fig. 2.2.8. As Fig. 2.2.7 but with larger boundaries and different direction.

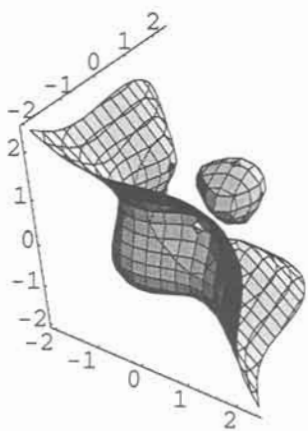


Fig. 2.2.9. The cubic equation with $C=-0.5$.

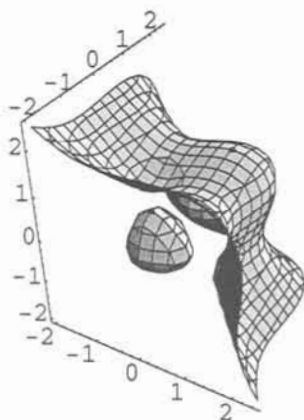


Fig. 2.2.10. $C=0.5$

Figure 2.2.7 is the origin of the P surface (see appendix 2) and is as this periodic, and steadily growing out of a surrounding surface by expanding each equation with more roots as in the following few figures. We start doing this in equation 2.2.9 with one more term and its figure 2.2.11, which is close to the electron structure of our first molecule, B_6H_6 [5]. This dual

form of the molecule is now a finite periodic structure as shown in figure 2.2.12 for a constant of 36, and which also is a primitive cubic structure.

$$\begin{aligned} x(x-1)(x+1)(x-2)+y(y-1)(y+1)(y-2) \\ +z(z-1)(z+1)(z-2)=-1 \end{aligned} \quad 2.2.9$$

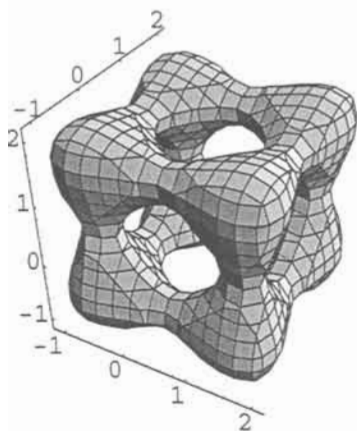


Fig. 2.2.11. Equation from 2.2.9 gives electron structure of B_6H_6 , as a larger part of the P surface.

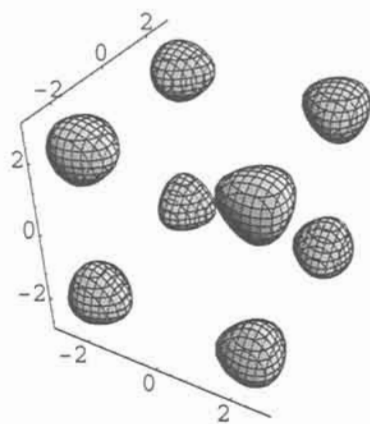


Fig. 2.2.12. Constant of 36 gives a finite primitive arrangement of bodies.

Still another term, as in equation 2.2.10, gives figure 2.2.13 with a larger part of the P surface in the centre of the monkey saddle.

$$\begin{aligned} x(x-1)(x+1)(x-2)(x+2)+y(y-1)(y+1)(y-2)(y+2) \\ +z(z-1)(z+1)(z-2)(z+2)=0 \end{aligned} \quad 2.2.10$$

Finally in equations 2.2.11 and 2.2.12 there are more terms and the corresponding figures are 2.2.14 and 2.2.15 with still larger parts of the P surface. Figure 2.2.14 has been made more P-like by adding a constant.

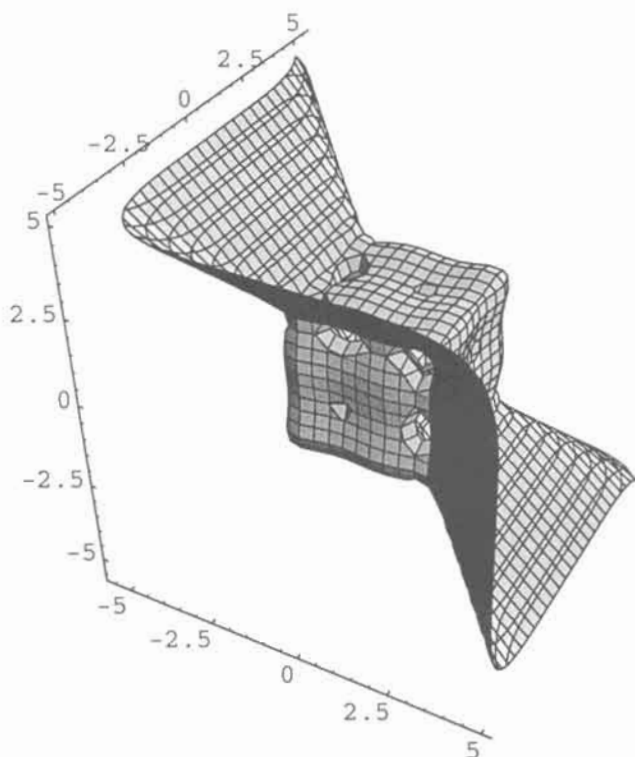


Fig. 2.2.13. More roots give a larger part of the P surface.

$$\begin{aligned}
 &x(x-1)(x+1)(x-2)(x+2)(x-3)(x+3) \\
 &\cdot (x-4)(x+4)(x-5)(x+5)(x-6) \\
 &+y(y-1)(y+1)(y-2)(y+2)(y-3)(y+3) \\
 &\cdot (y-4)(y+4)(y-5)(y+5)(y-6) \\
 &+z(z-1)(z+1)(z-2)(z+2)(z-3)(z+3) \\
 &\cdot (z-4)(z+4)(z-5)(z+5)(z-6) = 20000
 \end{aligned}
 \tag{2.2.11}$$

$$\begin{aligned}
 &x(x-1)(x+1)(x-2)(x+2)(x-3)(x+3) \\
 &\cdot (x-4)(x+4)(x-5)(x+5)(x-6)(x+6) \\
 &+y(y-1)(y+1)(y-2)(y+2)(y-3)(y+3) \\
 &\cdot (y-4)(y+4)(y-5)(y+5)(y-6)(y+6) \\
 &+z(z-1)(z+1)(z-2)(z+2)(z-3)(z+3) \\
 &\cdot (z-4)(z+4)(z-5)(z+5)(z-6)(z+6) = 0
 \end{aligned}
 \tag{2.2.12}$$

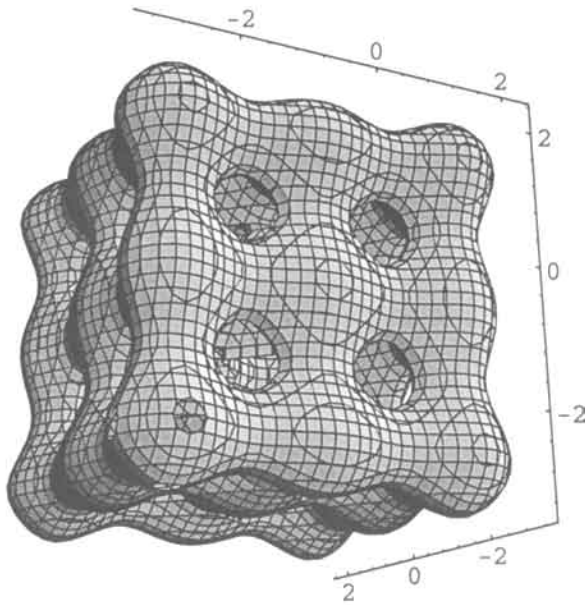


Fig. 2.2.14. Roots after equation 2.2.11.

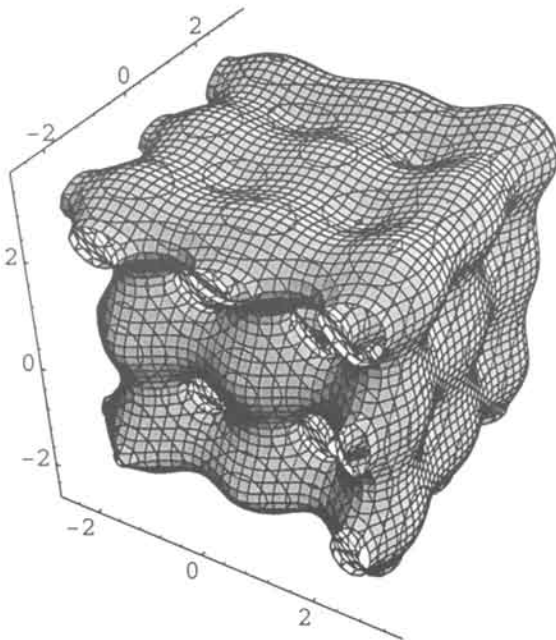


Fig. 2.2.15. Roots after equation 2.2.12.

We continue with the simplest permutations of the variables x , y and z , which are $(x+y)$, $(x+z)$, $(y+z)$, $(x-y)$, $(x-z)$, $(y-z)$ and $(x+y+z)$, $(x-y-z)$, $(-x-y+z)$, $(-x+y-z)$. We have already made the cube from equation 2.2.3, and as said it is easy in the same way to show the rest of the symmetry of space with the other fundamental polyhedra - the octahedron, the tetrahedron and the rhombic dodecahedron. As the general case is the use of the exponential scale instead of algebra or classic geometry, this will be developed in the next chapter.

Bringing in the roots after translation in these permutations of the 3D variables give the first fragments of periodicity. We have already done the beginning of the primitive cubic packing and the related molecule B_6H_6 [5] above and continue with the octahedron of a presumptive B_8H_8 with the equation

$$\begin{aligned} & [(x+y+z)^2 - 1][(x+y+z)^2 - 9] \\ & + [(x-y-z)^2 - 1][(x-y-z)^2 - 9] \\ & + [(-x-y+z)^2 - 1][(-x-y+z)^2 - 9] \\ & + [(-x+y-z)^2 - 1][(-x+y-z)^2 - 9] = -10 \end{aligned} \quad 2.2.13$$

The structure is shown in figure 2.2.16, which is the beginning of the cubic close packing. Next is the tetrahedron, or B_4H_4 , the equation of which is 2.2.14, and the molecule in figure 2.2.17 gives the beginning of the diamond structure.

$$\begin{aligned} & (x+y+z)(x+y+z-1)(x+y+z+1)(x+y+z-2) \\ & + (x-y-z)(x-y-z-1)(x-y-z+1)(x-y-z-2) \\ & + (-x-y+z)(-x-y+z-1)(-x-y+z+1)(-x-y+z-2) \\ & + (y-z-x)(y-z-x-1)(y-z-x+1)(y-z-x-2) = -0.6 \end{aligned} \quad 2.2.14$$

Equation 2.2.15 has the symmetry of the rhombic dodecahedron, with its compressed octahedron as shown in figure 2.2.18, and which is the beginning of body centred packing of bodies.

$$\begin{aligned} & [(x+y)^2 - 1][(x+y)^2 - 9] + [(x-y)^2 - 1][(x-y)^2 - 9] \\ & + [(x+z)^2 - 1][(x+z)^2 - 9] + [(x-z)^2 - 1][(x-z)^2 - 9] \\ & + [(y+z)^2 - 1][(y+z)^2 - 9] + [(y-z)^2 - 1][(y-z)^2 - 9] = -23 \end{aligned} \quad 2.2.15$$

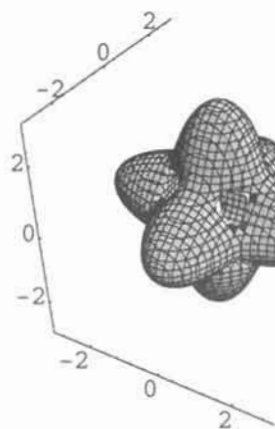


Fig. 2.2.16. From equation 2.2.13 the structure is the electron density of B_8H_8 , dual of the molecule and beginning of the cubic close packing of bodies.

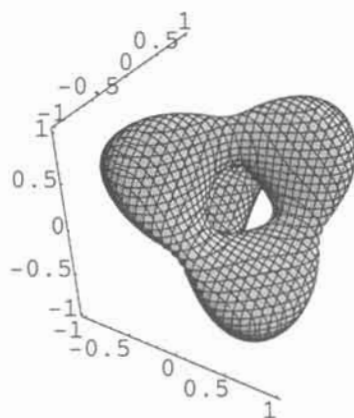


Fig. 2.2.17. From equation 2.2.14 the structure is B_4H_4 , the beginning of the diamond structure.

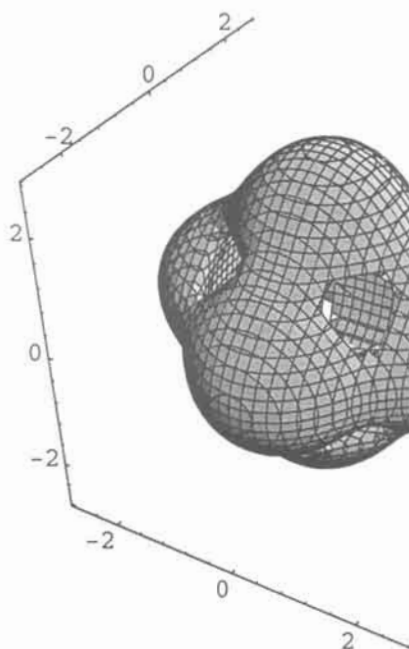


Fig. 2.2.18. From equation 2.2.15 the structure is the beginning of the body centred packing of bodies.

As was the case with the primitive cubic structure and the P surface above in figures 2.2.11 and 2.2.12, these polyhedra also constitute small parts of translation structures. The nodal surfaces [6] - topologically related to the periodic minimal surfaces [7] - are here the FRD-surface for the octahedron, the D-surface for the tetrahedron and the IWP-surface for the rhombic dodecahedron.

The simplicity is astonishing. The roots of these functions are the symmetry of space and also the roots of structure and mathematics. How is it that they are also very close to the ELF structures of molecules? Symmetry brings the fundamentals of chemistry and mathematics together.

There are of course many ways to mix addition and multiplication in space and we shall just do one more, a simple, but important one in the section to follow.

2.3 Saddles

The classical saddle equation is

$$x^2 - y^2 - z = (x+y)(x-y) - z = 0 \quad 2.3.1$$

and in figure 2.3.1 there are planes, $(x+y)$ and $(x-y)$, multiplied with each other in equation 2.3.1, and subtracted by z . Only a rotation of $\pi/4$ differs this equation from $xy-z=0$ (see below).

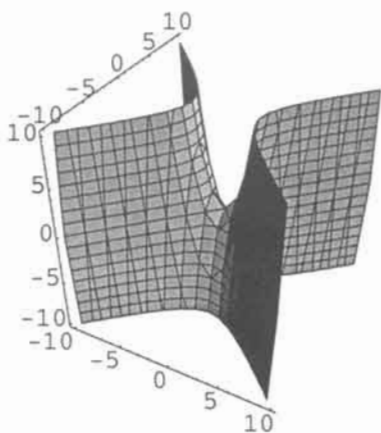


Fig. 2.3.1. Multiplication of two planes as in equation 2.3.1 gives the classical saddle.

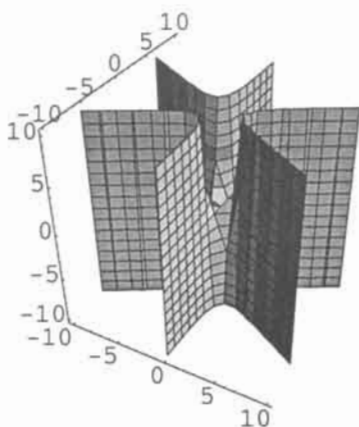


Fig. 2.3.2. Multiplication of three planes as in equation 2.3.2 gives the classical monkey saddle.

The planes are perpendicular and with a set of three meeting and non-intersecting planes separated by $\pi/3$ there is the classic monkey saddle as in equation 2.3.2 and figure 2.3.2.

$$x(x^2 - 3y^2) - z = 0 \tag{2.3.2}$$

The saddle function becomes periodic along z by using a circular function, as $\cos(z)$;

$$(x + y)(x - y) - \cos \pi z = 0 \tag{2.3.3}$$

Its surface in figure 2.3.3 is very similar to a classical minimal surface, the so-called Scherk's surface (exercise 2.4).

The corresponding tower surface for the monkey saddle is

$$x(x^2 - 3y^2) - \cos \pi z = 0 \tag{2.3.4}$$

which is shown in 2.3.4.

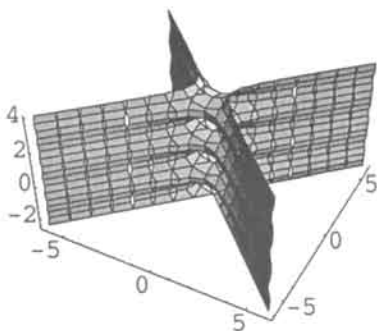


Fig. 2.3.3. The saddle is repeated along z after equation 2.3.3 and form a tower surface.

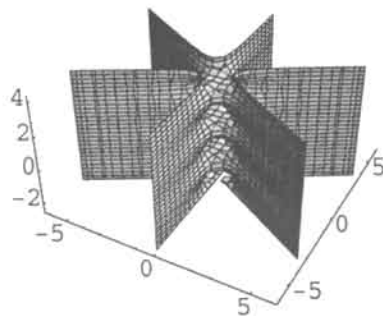


Fig. 2.3.4. This tower surface is derived from the monkey saddle as in equation 2.3.4.

The concept of deriving saddles by non-intersecting planes can be generalised [8] to

$$\prod_{i=0}^{i < n} [x \cos(\frac{i\pi}{n}) + y \sin(\frac{i\pi}{n})] - z = 0 \tag{2.3.5}$$

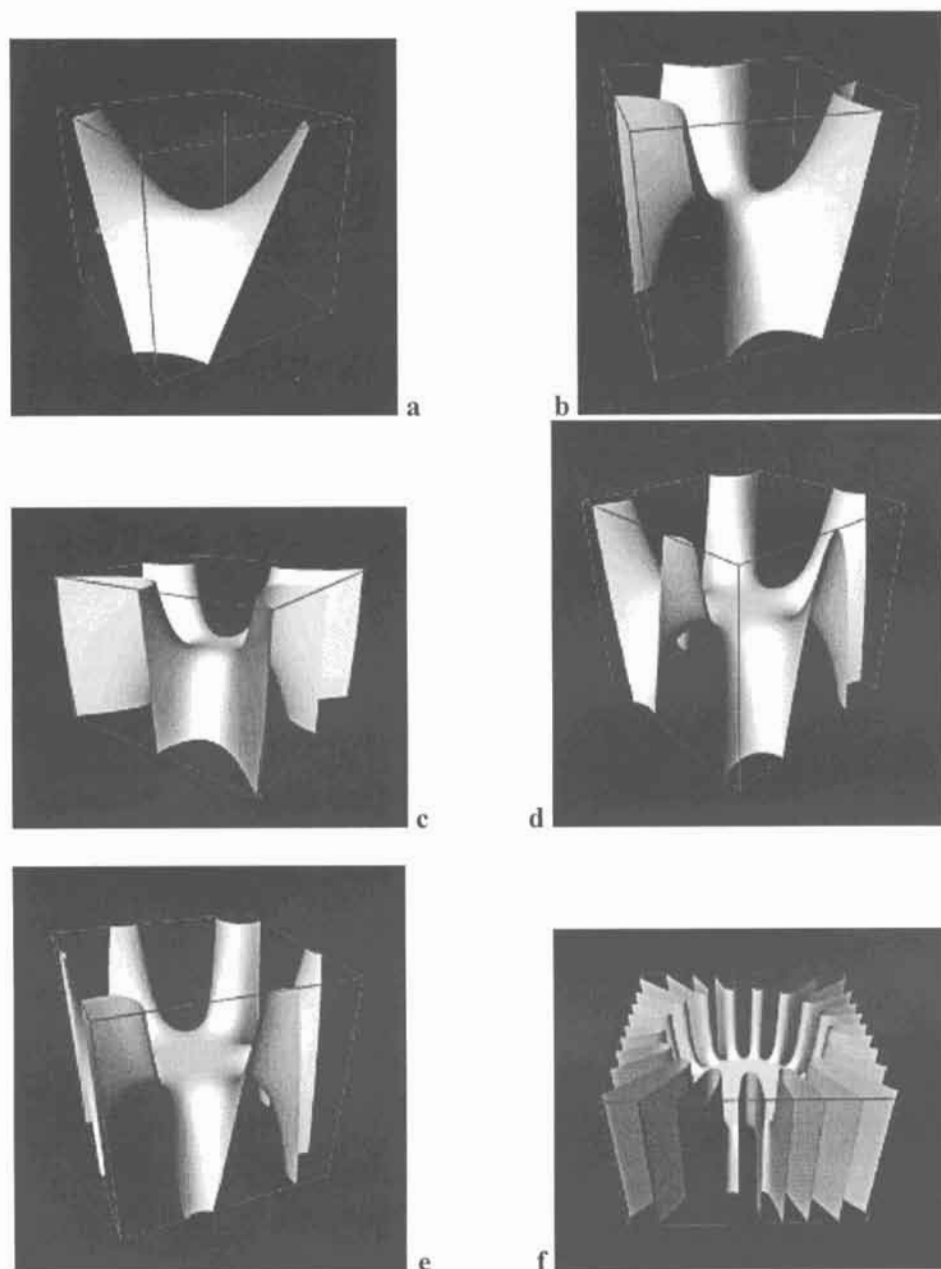


Fig. 2.3.5. Illustration of the general saddle equation 2.3.5. (a) Two-fold saddle created with $n=2$, in the region $-2 < x, y, z < 2$. (b) Three-fold saddle with $n=3$ in the region $-3 < x, y, z < 3$. (c) Four-fold saddle with $n=4$, $-3 < x, y < 3$, $-2 < z < 2$. (d) Five-fold saddle with $n=5$, $-2 < x, y, z < 2$. (e) Six-fold saddle with $n=6$, $-2 < x, y, z < 2$. (f) 17-fold saddle, $n=17$, $-3 < x, y < 3$, $-2 < z < 2$.

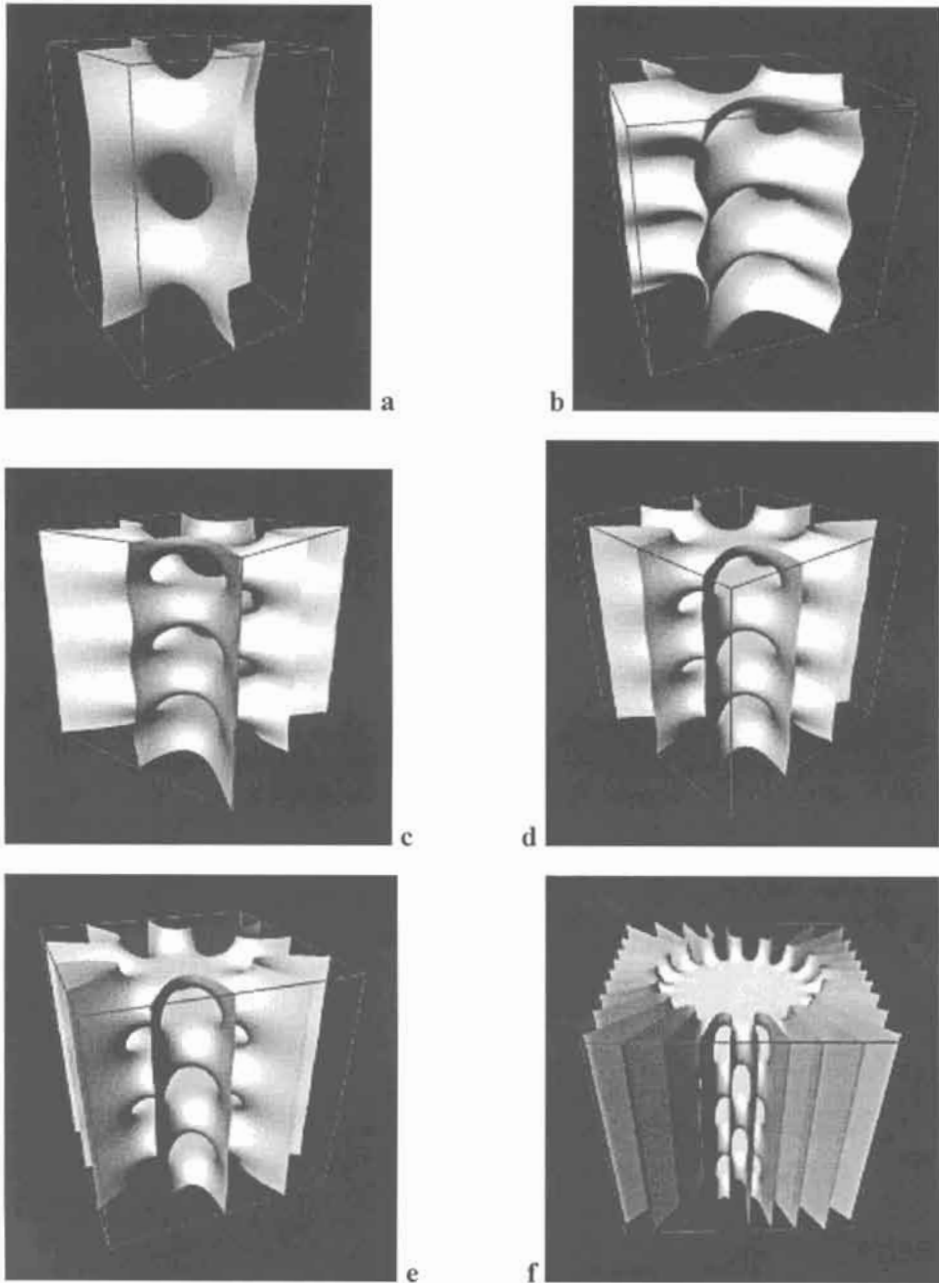


Fig. 2.3.6 Equation 2.3.6 for saddle tower surfaces at corresponding n -values to Fig. 2.3.5. (a) Saddle tower surface with $n=2$ and $p=1.0$. Illustrated in the region $-4 < x, y < 4$, $-6 < z < 6$. (b) Three-fold saddle tower ($n=3$, $p=\pi$), $-3 < x, y, z < 3$. (c) Four-fold saddle tower ($n=4$, $p=\pi$), $-3 < x, y, z < 3$. (d) Five-fold saddle tower ($n=5$, $p=\pi$), $-3 < x, y, z < 3$ (e) Six-fold saddle tower ($n=6$, $p=\pi$), $-3 < x, y, z < 3$. (f) 17-fold tower, $n=17$.

and in figures **2.3.5 a-f** there are saddles for $n=2, 3, 4, 5, 6$ and 17, the last one to indicate the generality.

And as above these saddles can be repeated after z using a circular function, and beautiful surfaces are obtained, topologically the same as the minimal surfaces called tower surfaces. The general equation for these surfaces is

$$\prod_{i=0}^{i<n} [x \cos(\frac{i\pi}{n}) + y \sin(\frac{i\pi}{n})] - \cos(pz) = 0 \quad 2.3.6$$

where p is the distance between saddles. The surfaces corresponding to the saddles above are shown in figures **2.3.6 a-f**.

Exercises 2

Exercise 2.1. $\cosh x + \cosh y + \cosh z - 10 = 0$ is a rounded cube. Make it more cube-like by subtracting a sphere according to the expansion.

Exercise 2.2. Square equation 2.28 and study the surface.

Exercise 2.3. Find a Fibonacci structure in two dimensions using polynoms.

Exercise 2.4. Plot the real Scherk minimal tower surface $\sin z = \sinh x \sinh y$.

Exercise 2.5. Plot the Scherk' first surface $e^z \cos x = \cos y$, which also is a minimal surface.

Exercise 2.6. Plot the surface $e^z \cos \pi x = y$. Extended boundaries ($\pm 3, \pm 3, \pm 5$ of x, y, z) reveal an incredible transformation of an infinite number of planes into a single one. This equation is also a solution to the heat equation and was found to describe the seasonal variation of temperature below ground as a fraction of surface temperature [9]. This function has also been found to describe the potentials of a field between parallel electrodes terminated by a plane electrode [10].

Exercise 2.7. Describe the first tower surface and the helicoid with polynoms to show that finite periodicity is useful. The equations are $xy + \cos z = 0$ and $x \sin z + y \cos z = 0$.

Answer 2.1

a. `ContourPlot3D[Cosh[x]+Cosh[y]+Cosh[z]-.5 (x^2+y^2+z^2)-10, {x,-4,4},{y,-4,4},{z,-4,4},MaxRecursion->2,PlotPoints->{{5,3},{5,3},{5,3}},Boxed->False,Axes->True,AxesLabel->{x,y,z}]`

b. `ContourPlot3D[Cosh[x]+Cosh[y]+Cosh[z]-10, {x,-4,4}, {y,-4,4}, {z,-4,4},MaxRecursion->2,PlotPoints->{{5,3},{5,3},{5,3}},Boxed->False,Axes->True,AxesLabel->{x,y,z}]`

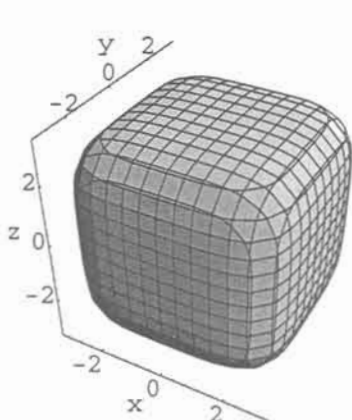


Fig. 2.1. a.

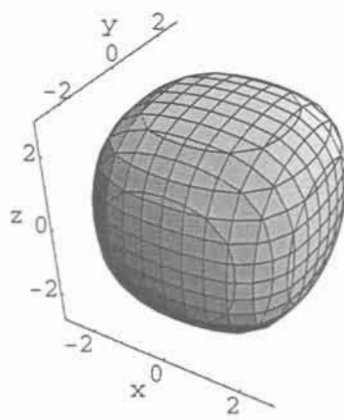


Fig. 2.1. b.

Answer 2.2

`ContourPlot3D[(x y z)^2-1,{x,2,-2},{y,2,-2},{z,2,-2},MaxRecursion->2,PlotPoints->{{5,3},{5,3},{5,3}},Boxed->False,Axes->True]`

Answer 2.3

`ImplicitPlot[(x-1) (x-2) (x-3) (x-5) (x-8) (x-13) (y-1) (y-2) (y-3) (y-5) (y-8) (y-13) ==0,{x,-1,14},{y,-1,14},PlotPoints->200]`

Answer 2.4

`ContourPlot3D[Sin[Piz]-Sinh[Piy]Sinh[Pix],{x,-3,3},{y,-3,3},{z,-2.1,2.1},MaxRecursion->2,PlotPoints->{{4,4},{4,4},{4,4}},Boxed->False,Axes->True]`

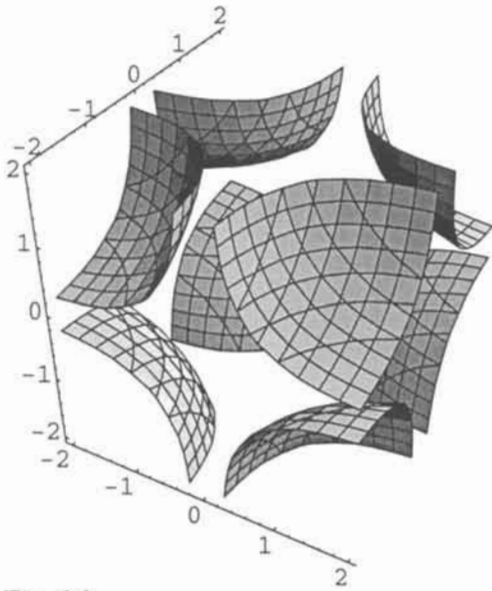


Fig. 2.2.

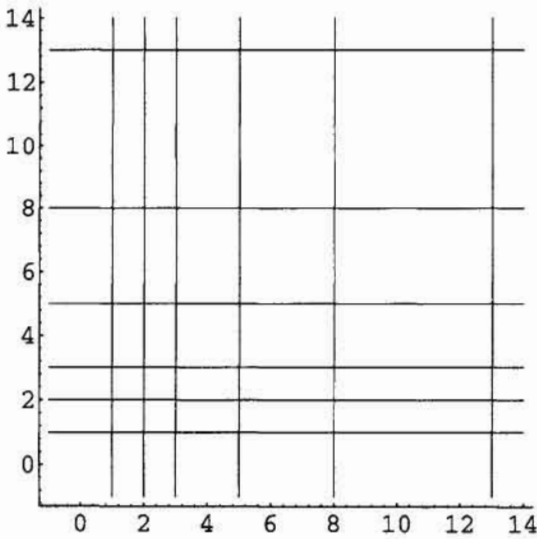


Fig. 2.3.

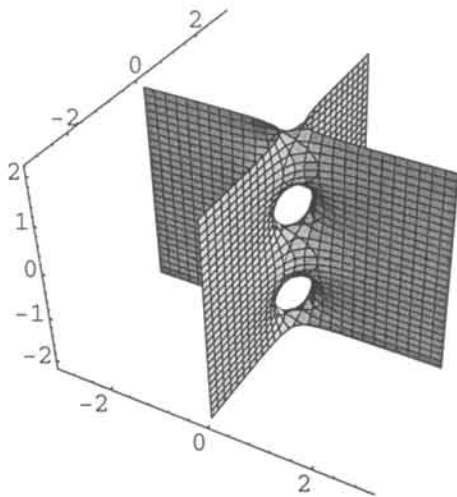


Fig. 2.4.

Answer 2.5

```
ContourPlot3D[Cos[Pi x] E^z-(Cos[Pi y]),{x,2,-2},{y,2,-2},{z,4,-4},
MaxRecursion->2,PlotPoints->{{5,3},{5,3},{4,4}},
Boxed->False,Axes->True]
```

Note the different resolution in z.

Answer 2.6

```
ContourPlot3D[Cos[Pi x] E^z -y,{x,3,-3},{y,3,-3},{z,5,-5},
MaxRecursion->2,PlotPoints->{{3,5},{3,5},{3,5}},
Boxed->False,Axes->True]
```

Answer 2.7. We use the fundamental theorem of algebra just as a translation function:

$$x y + z (z+.5) (z-.5) (z+1) (z-1) (z+1.5) (z-1.5)=0$$

and the result is in **2.7.a** and is nearly identical with the minimal surface of Scherk in **2.7.b**.

The helicoid is also a saddle function

$$x \sin z + y \cos z = 0$$

We construct an equation with the polynomials of the algebra, with proper phase shifts to give the helicoid surface:

$$xz(z+1)(z-1)(z+2)(z-2)(z+3)(z-3)+ \\ +y(z+0.5)(z-0.5)(z+1.5)(z-1.5)(z+2.5)(z-2.5)=0$$

The result is below and the similarity with the screw surface as calculated from the circular function is extraordinary, as the reader may find out for himself.

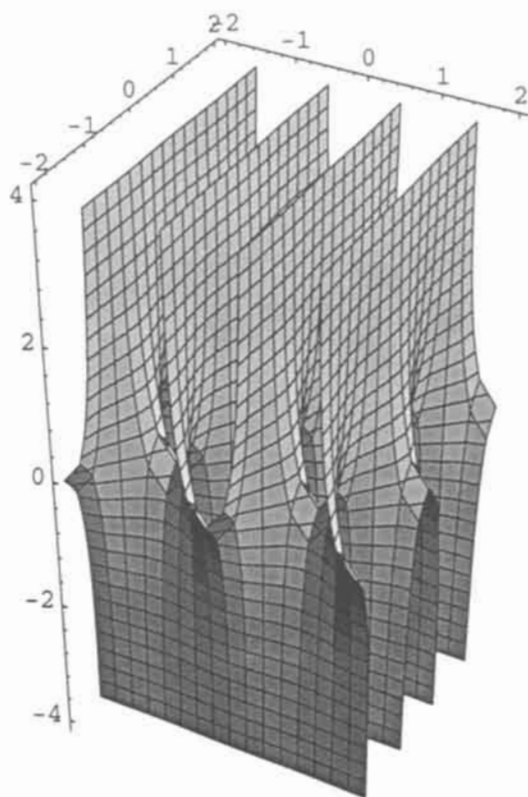
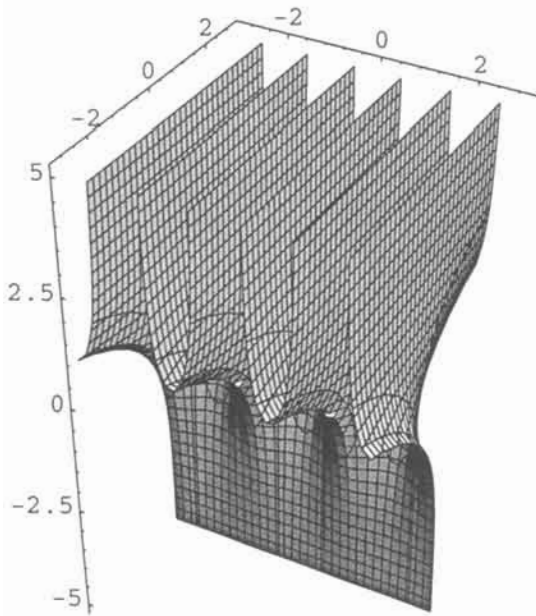
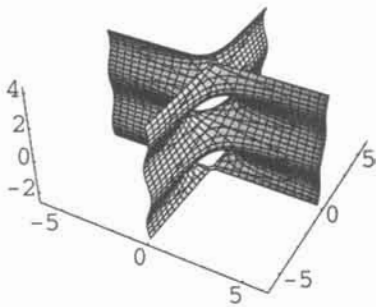
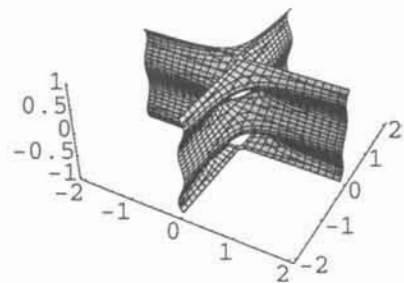


Fig. 2.5.

**Fig. 2.6.****Fig. 2.7.b.****Fig. 2.7.a.**

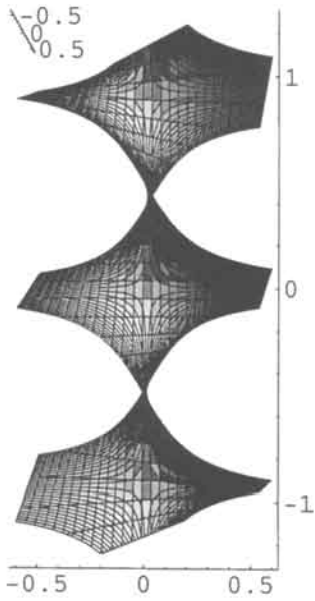


Fig. 2.7.c.

References 2

- 1 D'Arcy Wentworth Thompson, *ON GROWTH AND FORM*, Cambridge University press, 1942, page 2.
- 2 G.H. Hardy, *PURE MATHEMATICS*, Cambridge University press, 1975.
- 3 B.G. Hyde and S. Andersson, *INORGANIC CRYSTAL STRUCTURES*, Wiley, New York, 1988.
- 4 S. Andersson and M.Jacob, *THE MATHEMATICS OF STRUCTURES, THE EXPONENTIAL SCALE*, Oldenbourg, München, 1997.
- 5 A. Burkhardt, U. Wedig, H.G. von Schnering and A. Savin, *Z. anorg. allg. Chem.* **619** (1993) 437.
- 6 H.G. von Schnering and R. Nesper, *Z. Phys. B - Condensed Matter* **83** (1991) 407.
- 7 U. Dierkes, S. Hildebrandt, A. Kuster and O. Wohlrab, *MINIMAL SURFACES 1 and 2*, Springer Verlag, Berlin, 1991.
- 8 M. Jacob, *J.Phys. II France* **7** (1997) 1035-1044.
- 9 G. B. Thomas and R.L. Finney, *CALCULUS AND ANALYTIC GEOMETRY*, p. 797, Addison-Wesley, sixth ed. 1984.
- 10 P. Lorrain, D.P. Corson and F. Lorrain, *ELECTOMAGNETIC FIELDS AND WAVES*, p. 222, Freeman, NewYork, 1988.

3 The Natural Function and the Exponential Scale

'for the present the reader may be content to draw his curves as common sense dictates' (Hardy) [1].

Here we give functions to polygons and polyhedra using the Exponential Scale. We calculate curvature. We derive the equation of symmetry in space and the fundamental polyhedra; the cube, the tetrahedron, the octahedron and the rhombic dodecahedron. We derive the equations for the icosahedron and the pentagonal dodecahedron from the equations of fundamental polyhedra. We give the mathematics for hierarchy and the compound polyhedra.

3.1 Polygons and Planar Geometry

The function

$$y = e^x \tag{3.1.1}$$

is $y = e \cdot e \cdot e \dots$ multiplied x times. This is called the natural exponential, which we will have great use of in this book.

The natural number e was invented by Euler and he realised it to be so important that he named it after himself. The easiest way to define it is via its expansion:

$$e^x = 1 + \frac{x}{1!} + \frac{x^2}{2!} + \frac{x^3}{3!} + \frac{x^4}{4!} + \dots \tag{3.1.2}$$

The number e itself is calculated by making $x=1$, and results in $e=2.718\dots$

The important property that its derivative is identical with the function itself, $\frac{de^x}{dx} = e^x$, is easily realised from the expansion by derivating it.

The first function is equation 3.1.3, in fig 3.1.1. This is really two straight lines, continuously transforming into each other.

$$y + e^x = 0 \quad 3.1.3$$

We continue with a number of functions below.

$$e^x = 0 \quad 3.1.4$$

$$e^y = 0 \quad 3.1.5$$

$$e^x + e^y = 1 \quad 3.1.6$$

$$x + y = 0 \quad 3.1.7$$

$$e^{x+y} = 1 \quad 3.1.8$$

First we look at $e^x = 0$ which is a straight line in the same way as e^y is, in figs 3.1.2 and 3.1.3. Adding the two after eq. 3.1.6 gives us the remarkable corner of 3.1.4. Just adding $x+y$ gives the straight line in 3.1.5 which is the tangent to the corner as shown below. We see in 3.1.6 that e^{x+y} also is a straight line.

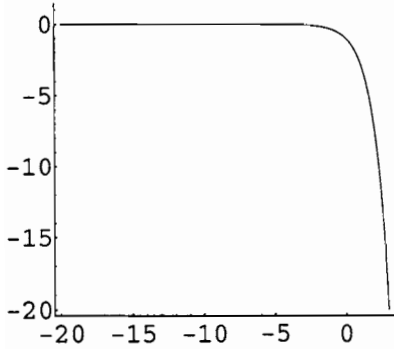


Fig. 3.1.1. After equation 3.1.3.

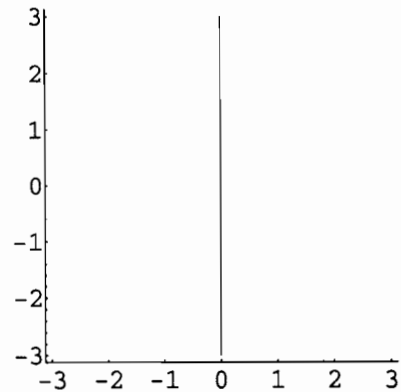


Fig. 3.1.2. After equation 3.1.4.

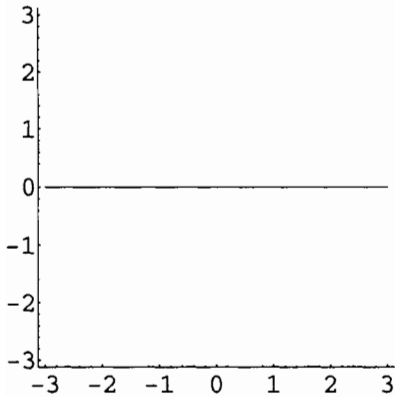


Fig. 3.1.3. After equation 3.1.5.

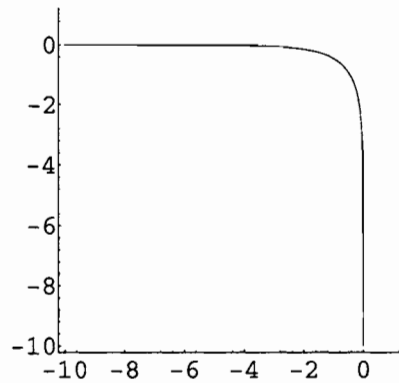


Fig. 3.1.4. After equation 3.1.6.

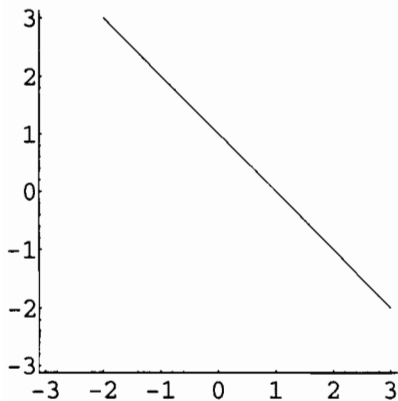


Fig. 3.1.5. After equation 3.1.7.

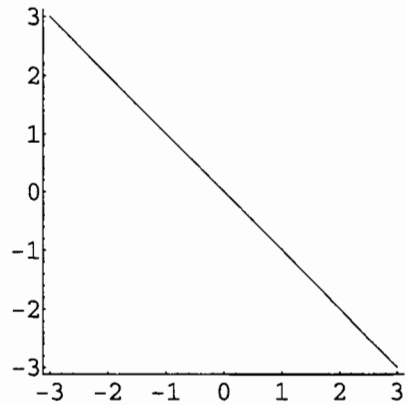


Fig. 3.1.6. After equation 3.1.8.

We add two more lines to eq. 3.1.6,

$$e^x + e^y + e^{-x} + e^{-y} = C \tag{3.1.9}$$

and for a constant of respectively 10^2 and 10^{11} we have the squares in figures 3.1.7 and 8. By calculating curvature (see Appendix 4) of the square corner we find it approaches a constant value of $\sqrt{2}/2$ with size; it is the size difference that makes the square in fig. 3.1.8 having sharper corners. Exponential addition in 3.1.10 of a tangent truncates the square in fig. 3.1.9.

By subtracting the tangent we open the square as in fig. 3.1.10 and by adding all the tangents we get the formidable octagon in fig. 3.1.11. Subtracting all the tangents give the beautiful figures in 3.1.12 and 13.

$$e^x + e^y + e^{-x} + e^{-y} + e^{0.65(x+y)} = 10^{11} \quad 3.1.10$$

$$e^x + e^y + e^{-x} + e^{-y} - e^{0.55(x+y)} = 10^4 \quad 3.1.11$$

$$e^x + e^y + e^{-x} + e^{-y} + e^{0.65(x+y)} + e^{-0.65(x+y)} + e^{0.65(x-y)} + e^{-0.65(x-y)} = 10^{11} \quad 3.1.12$$

$$e^x + e^y + e^{-x} + e^{-y} - e^{0.65(x+y)} - e^{-0.65(x+y)} - e^{0.65(x-y)} - e^{-0.65(x-y)} = 0 \quad 3.1.13$$

$$e^x + e^y + e^{-x} + e^{-y} - e^x + e^y + e^{-x} + e^{-y} - e^{0.65(x+y)} - e^{-0.65(x+y)} - e^{0.65(x-y)} - e^{-0.65(x-y)} = 10^5 \quad 3.1.14$$

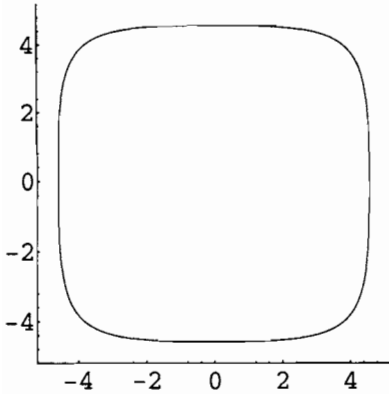


Fig. 3.1.7. After equation 3.1.9.

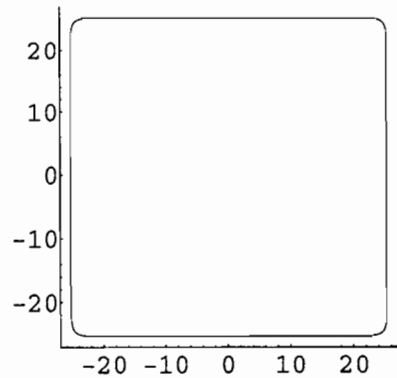


Fig. 3.1.8. After equation 3.1.9.

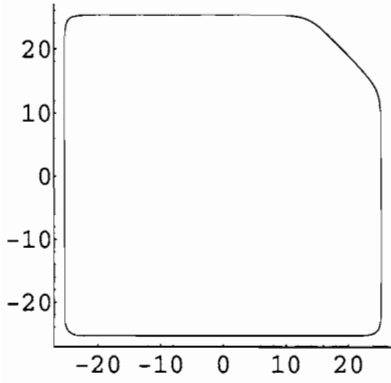


Fig. 3.1.9. After equation 3.1.10.

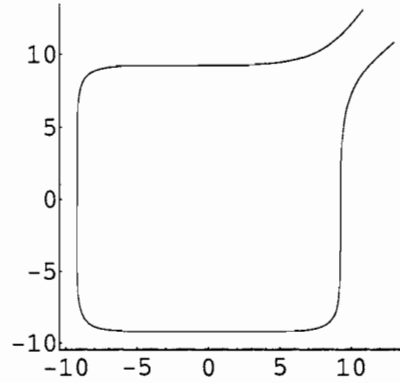


Fig. 3.1.10. After equation 3.1.11.

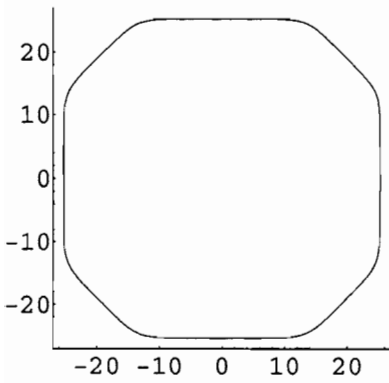


Fig. 3.1.11. After equation 3.1.12.

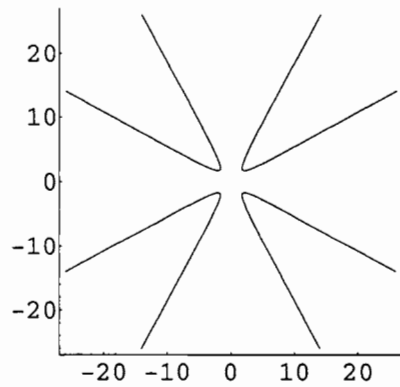


Fig. 3.1.12. After equation 3.1.13.

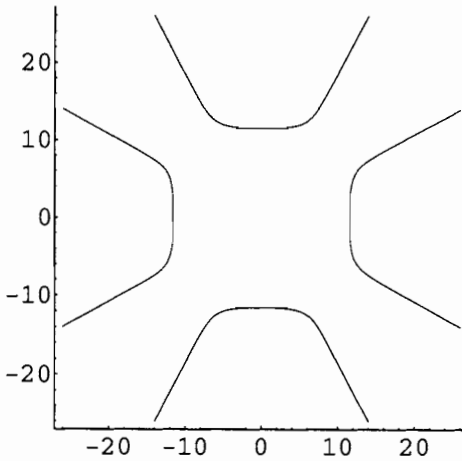


Fig. 3.1.13. After equation 3.1.14.

On the exponential scale the addition of lines gives circular geometry, while subtracting gives hyperbolic.

A great deal of classic geometry the last 2300 years consisted of adding lines or planes to construct more and more complicated polygons or polyhedra. This is easily done with the exponential scale. We derive general expressions for polygons, and use the formula 3.1.15 to find the lines to be added in 2 D for an m-gon.

$$\sum_{i=0}^{i \leq m} (x \cos(\frac{i\pi}{m}) + y \sin(\frac{i\pi}{m})) \tag{3.1.15}$$

and the general expression for any polygon becomes

$$\sum_{i=0}^{i \leq m} e^{(x \cos(i\pi/m) + y \sin(i\pi/m))^n} = C \tag{3.1.16}$$

Fig 3.1.14 is a triangle, m=3, n=1 and C=20. In fig. 3.1.15 n=3, and the advantage of higher exponential is obvious. The equation for the triangle is in eq. 3.1.17, and we continue with the equations for the square, the pentagon, the hexagon and the heptagon.

In the examples below n=4 for m even, and n=3 for m odd.

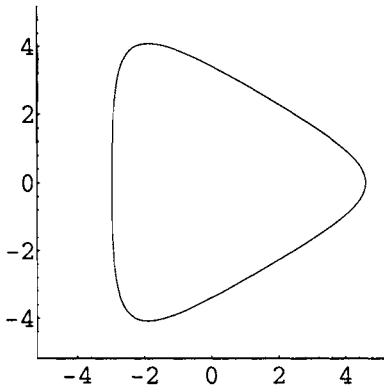


Fig. 3.1.14. After equation 3.1.16, $m=3$, $n=1$ and $C=20$.

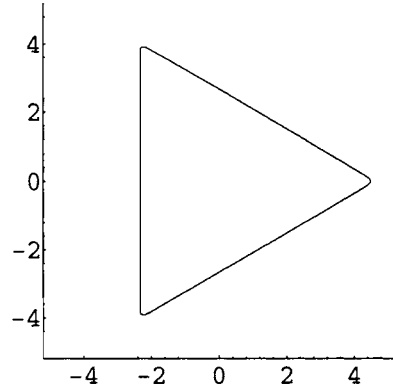


Fig. 3.1.15. After equation 3.1.17.

Triangle

$$e^{(x\cos(\pi/3)+y\sin(\pi/3))^3} + e^{(x\cos(2\pi/3)+y\sin(2\pi/3))^3} + e^{(x\cos(3\pi/3)+y\sin(3\pi/3))^3} = 2 \cdot 10^5 \quad 3.1.17$$

Square

$$e^{(x\cos(\pi/2)+y\sin(\pi/2))^4} + e^{(x\cos(2\pi/2)+y\sin(2\pi/2))^4} = 2 \cdot 10^5 \quad 3.1.18$$

Pentagon

$$e^{(x\cos(\pi/5)+y\sin(\pi/5))^3} + e^{(-x\cos(2\pi/5)-y\sin(2\pi/5))^3} + e^{(x\cos(3\pi/5)+y\sin(3\pi/5))^3} + e^{(-x\cos(4\pi/5)-y\sin(4\pi/5))^3} + e^{(x\cos(5\pi/5)+y\sin(5\pi/5))^3} = 2 \cdot 10^5 \quad 3.1.19$$

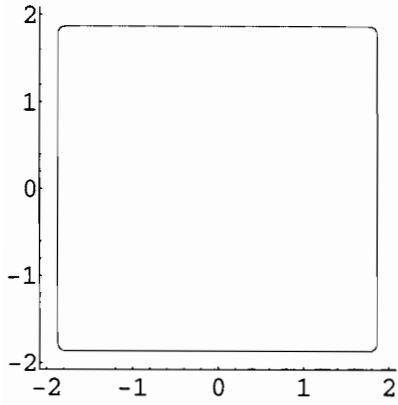


Fig. 3.1.16. After equation 3.1.18.

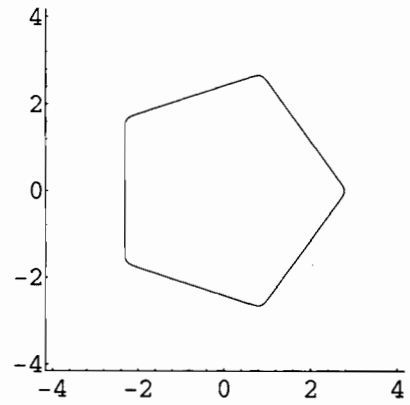


Fig. 3.1.17. After equation 3.1.19.

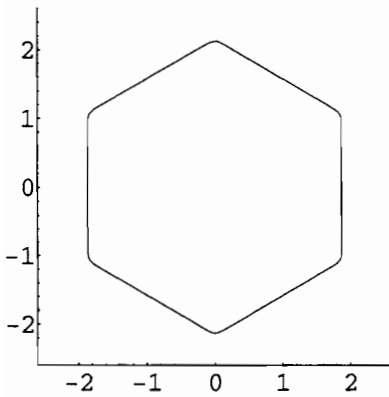


Fig. 3.1.18. After equation 3.1.20.

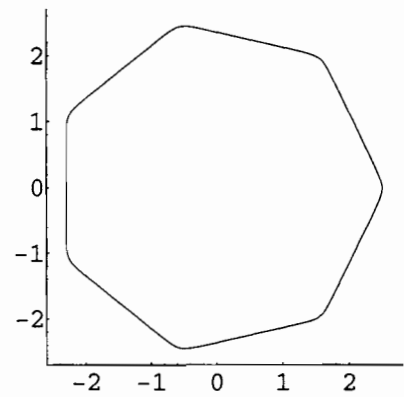


Fig. 3.1.19. After equation 3.1.21.

Hexagon

$$\begin{aligned}
 &e^{(x\cos(\pi/3)+y\sin(\pi/3))^4} + e^{(x\cos(2\pi/3)+y\sin(2\pi/3))^4} \\
 &+ e^{(x\cos(3\pi/3)+y\sin(3\pi/3))^4} = 2 \cdot 10^5
 \end{aligned}
 \tag{3.1.20}$$

Heptagon

$$\begin{aligned}
 & e^{(x\cos(\pi/7)+y\sin(\pi/7))^3} + e^{(-x\cos(2\pi/7)-y\sin(2\pi/7))^3} \\
 & + e^{(x\cos(3\pi/7)+y\sin(3\pi/7))^3} + e^{(-x\cos(4\pi/7)-y\sin(4\pi/7))^3} \\
 & + e^{(x\cos(5\pi/7)+y\sin(5\pi/7))^3} + e^{(-x\cos(6\pi/7)-y\sin(6\pi/7))^3} \\
 & + e^{(x\cos(7\pi/7)+y\sin(7\pi/7))^3} = 2 \cdot 10^5
 \end{aligned}
 \tag{3.1.21}$$

3.2 Polyhedra and Geometry

We apply the polygon results in 3D. In fig. 3.2.1 we have added two planes on the exponential level, in fig. 3.2.2 three planes, and in 3.2.3 six planes and the equations are 3.2.1, 3.2.2 and 3.2.3 respectively.

$$10^x + 10^y - 10^5 = 0 \tag{3.2.1}$$

$$10^x + 10^{-x} + 10^y - 10^5 = 0 \tag{3.2.2}$$

$$10^x + 10^{-x} + 10^y + 10^{-y} + 10^z + 10^{-z} - 10^5 = 0 \tag{3.2.3}$$

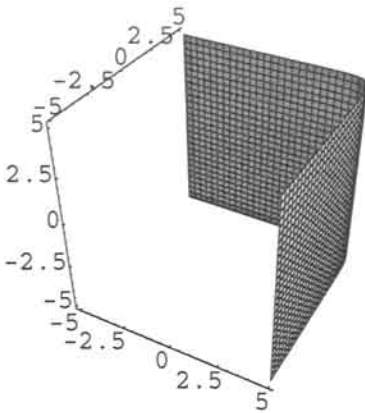


Fig. 3.2.1. Two planes meet on the exponential scale.

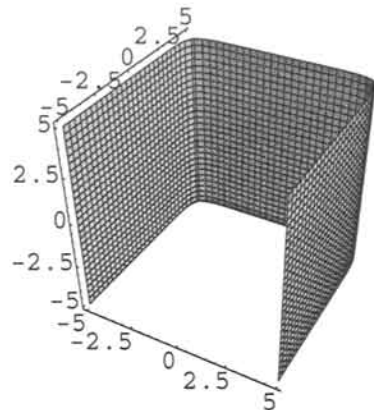


Fig. 3.2.2. Three planes meet on the exponential scale.

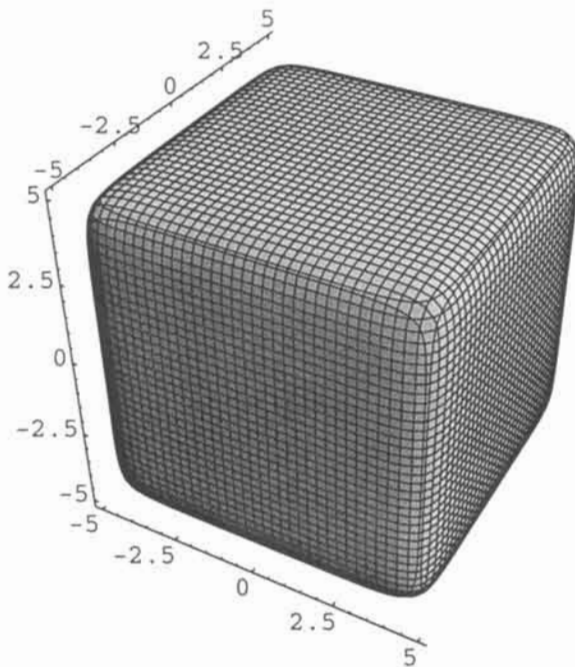


Fig. 3.2.3. A cube after equation 3.2.3.

We can of course make the rest of the Platonic solid. We can calculate all sorts of crystal shapes. You can invent your own polyhedra and calculate them. We show you how with the tetrahedron in Appendix 3.

We show the tetrahedron and the octahedron with their equations.

$$e^{(x+y+z)} + e^{(x-y-z)} + e^{(-x-y+z)} + e^{(-x+y-z)} = 400 \quad 3.2.4$$

$$\begin{aligned} &e^{(x+y+z)} + e^{(x-y-z)} + e^{(-x-y+z)} + e^{(-x+y-z)} \\ &+ e^{-(x+y+z)} + e^{-(x-y-z)} + e^{-(-x-y+z)} + e^{-(-x+y-z)} = 40000 \end{aligned} \quad 3.2.5$$

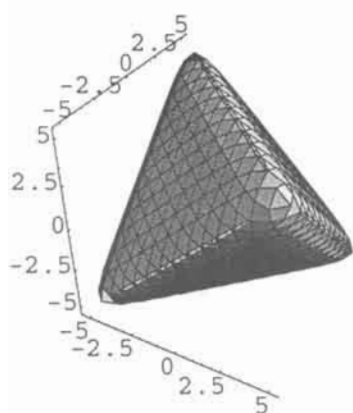


Fig. 3.2.4. A tetrahedron after equation 3.2.4.

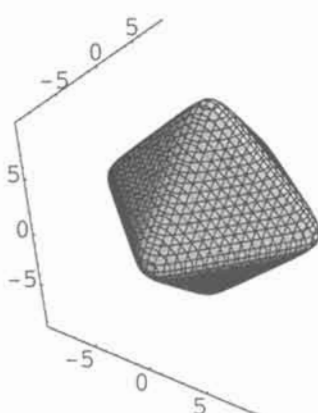


Fig. 3.2.5. An octahedron after equation 3.2.5.

Another way saying this is that $e^{(x+y+z)}$ is a plane, and we call it an exponential plane. If such planes are added together we can construct morphological shapes with continuous mathematical functions.

By adding eight octahedral planes with weighting after eq. 3.2.6 the cube is truncated as in fig. 3.2.6, and by changing sign for one of the terms $(x+y+z)$ as in eq. 3.2.7 we get the picture of 3.2.7. As in two dimensions.

$$\begin{aligned}
 &10^{(x+y+z)} + 10^{(x-y-z)} + 10^{(-x-y+z)} + 10^{(-x+y-z)} \\
 &+ 10^{-(x+y+z)} + 10^{-(x-y-z)} + 10^{-(x-y+z)} + 10^{-(x+y-z)} \quad 3.2.6 \\
 &+ 10^{2.3x} + 10^{-2.3x} + 10^{2.3y} + 10^{-2.3y} + 10^{2.3z} + 10^{-2.3z} = 10^{10}
 \end{aligned}$$

$$\begin{aligned}
 &-10^{(x+y+z)} + 10^{(x-y-z)} + 10^{(-x-y+z)} + 10^{(-x+y-z)} \\
 &+ 10^{-(x+y+z)} + 10^{-(x-y-z)} + 10^{-(x-y+z)} + 10^{-(x+y-z)} \quad 3.2.7 \\
 &+ 10^{2.3x} + 10^{-2.3x} + 10^{2.3y} + 10^{-2.3y} + 10^{2.3z} + 10^{-2.3z} = 10^{10}
 \end{aligned}$$

We do the same with the rest of the corners (eq. 3.2.8) and have the formidable fig. 3.2.8.

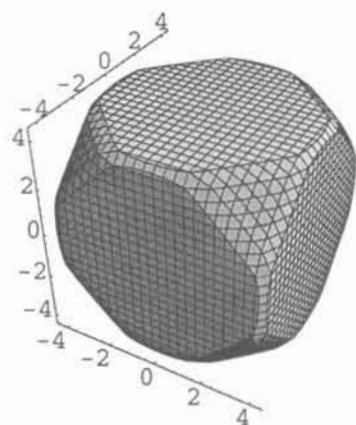


Fig. 3.2.6. A truncated cube after equation 3.2.6.

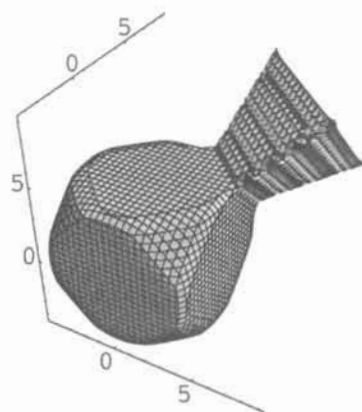


Fig. 3.2.7. Subtraction of one truncation opens the cube after equation 3.2.7.

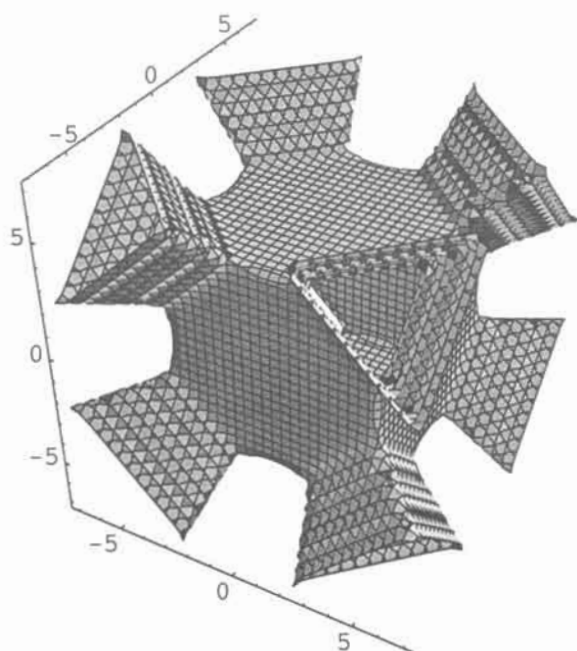


Fig. 3.2.8. Subtraction of all truncations opens all corners of the cube after equation 3.2.8.

$$\begin{aligned}
 & -10^{(x+y+z)} - 10^{(x-y-z)} - 10^{(-x-y+z)} - 10^{(-x+y-z)} \\
 & -10^{-(x+y+z)} - 10^{-(x-y-z)} - 10^{-(x-y+z)} - 10^{-(x+y-z)} \quad 3.2.8 \\
 & +10^{2.3x} + 10^{-2.3x} + 10^{2.3y} + 10^{-2.3y} + 10^{2.3z} + 10^{-2.3z} = 10^{10}
 \end{aligned}$$

Another simple way to show this effect is by changing sign for one of the terms in the equation for the cube:

$$e^x + e^y + e^z + e^{-x} + e^{-y} - e^{-z} = 100 \quad 3.2.9$$

This is shown in fig. 3.2.9, and with 3.2.10 we get two more catenoidic openings as shown in figs. 3.2.10 and 11, with constants of $C=-30$ in fig. 10 and $C=+30$ in 11. The monkey saddle in fig. 3.2.12 (with planes (110)) is clearly a transition state at zero constant and also clean hyperbolic geometry.

$$e^x + e^y + e^z - e^{-x} - e^{-y} - e^{-z} = C \quad 3.2.10$$

We have now some rules: Adding planes means positive (elliptic) curvature, while subtracting means negative (hyperbolic) curvature.

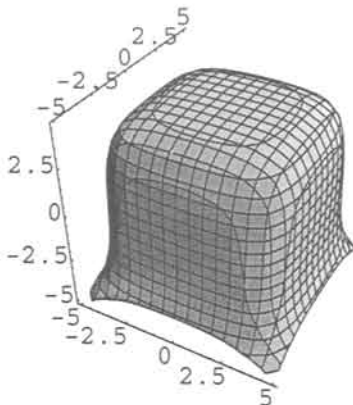


Fig. 3.2.9. Subtraction of a side of the cube after equation 3.2.9 opens the cube.

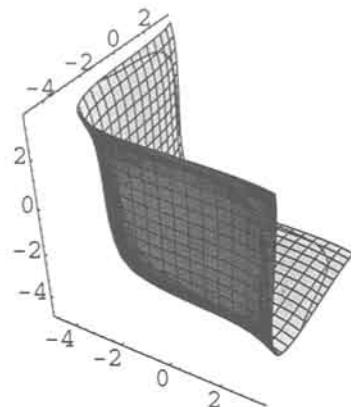


Fig. 3.2.10. Three sides subtracted with negative constant.

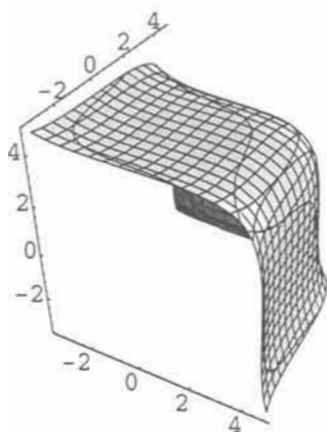


Fig. 3.2.11. Three sides subtracted with positive constant.

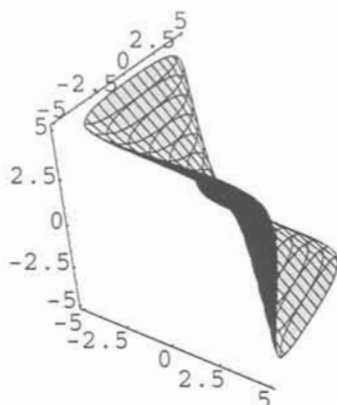


Fig. 3.2.12. Three sides subtracted with zero constant give a monkey saddle.

3.3 Curvature

A larger isosurface constant, C , results in sharper corners for the polyhedron. But how does the size of the polyhedra actually change the curvature? We study the cube. For calculating the Gaussian and mean curvature we use the Mathematica scripts in Appendix 4.

With the base e , the equation for the cube is

$$e^x + e^y + e^z + e^{-x} + e^{-y} + e^{-z} = C \quad 3.3.1$$

We simplify the expressions of the curvatures by looking at three special cases, a vertex, an edge and the middle of a face.

At a vertex the coordinates are one of the eight permutations of $x=y=z$, and the Gaussian curvature in such a point is

$$K = \frac{2 - \frac{1}{e^{4x}} - e^{4x}}{(-e^{-x} + e^x)^2 (6 - \frac{3}{e^{2x}} - 3e^{2x})} \quad 3.3.2$$

and the mean curvature

$$H = \frac{-\sqrt{3}\left(\frac{1}{e^{3x}} - \frac{1}{e^x} - e^x + e^{3x}\right)}{(-e^{-x} + e^x)\left(6 - \frac{3}{e^{2x}} - 3e^{2x}\right)} \quad 3.3.3$$

The free variable, x , is the size of the cube. From this we see that the two curvatures decrease with increased size, to reach a constant value for larger cubes. The Gaussian curvature converges to $K = \frac{1}{3}$ and the mean to $H = \frac{1}{\sqrt{3}}$, which is seen in diagrams 1a and b.

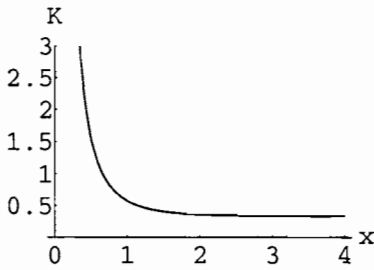


Diagram 1a. Gaussian curvature of a corner of the exponential scale cube.

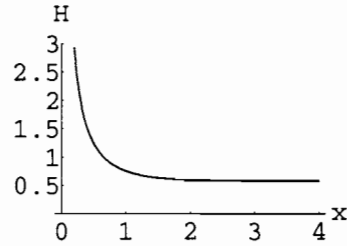


Diagram 1b. Mean curvature of a corner.

At an edge, $x=y$, while $z=0$. The curvatures at this point are

$$K = \frac{2\left(\frac{-1}{e^{3x}} + \frac{1}{e^x} + e^x - e^{3x}\right)}{(-e^{-x} + e^x)^2\left(4 - \frac{2}{e^{2x}} - 2e^{2x}\right)} \quad 3.3.4$$

$$H = \frac{-\left(-4 + \frac{1}{e^{3x}} + \frac{2}{e^{2x}} - \frac{1}{e^x} - e^x - 2e^{2x} + e^{3x}\right)}{\sqrt{2}(-e^{-x} + e^x)\left(4 - \frac{2}{e^{2x}} - 2e^{2x}\right)} \quad 3.3.5$$

These plots are shown in diagram 2a and b.

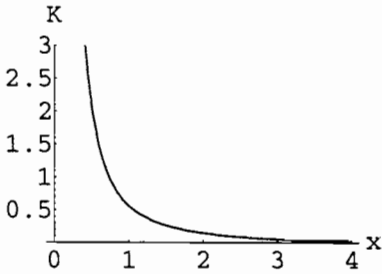


Diagram 2a. Gaussian curvature of an edge.

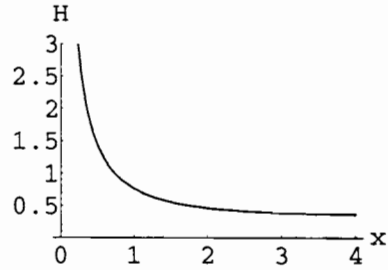


Diagram 2b. Mean curvature of an edge

As expected the Gaussian curvature converges to zero, since the edge is similar to a cylinder and thus has parabolic geometry. The mean curvature converges to $\frac{1}{2\sqrt{2}}$.

At the middle of a face the two curvatures converge to zero because the face turns more and more planar. The curvatures are

$$K = \frac{8 - \frac{4}{e^{2x}} - 4e^{2x}}{(-e^{-x} + e^x)^2(2 - e^{-2x} - e^{2x})} \tag{3.3.6}$$

$$H = \frac{4 - \frac{2}{e^{2x}} - 2e^{2x}}{(-e^{-x} + e^x)(2 - e^{-2x} - e^{2x})} \tag{3.3.7}$$

and their plots are shown in diagram 3a and b.

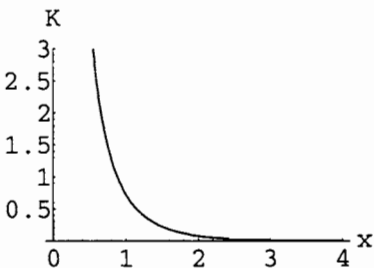


Diagram 3a. Gaussian curvature of a face in the exponential scale cube.

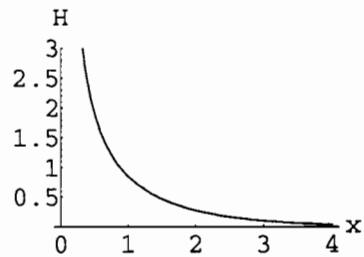


Diagram 3b. Mean curvature of a face

Thus, all polyhedra in the exponential scale converge their Gaussian and mean curvatures when they grow with the isosurface constant. At faces, both of them are zero, and at edges the Gaussian curvature is zero.

The smaller the polyhedra, the lower the constant and the more each vertex gets affected by the others which results in the polyhedra turning spherical and the curvatures increase.

3.4 The Fundamental Polyhedra - and Others

We shall now in particular study polyhedra, or bodies related to polyhedra. We take the complete permutations of the space variables x, y, z in the formula

$$\begin{aligned}
 &e^{(x+y+z)^n} + e^{(-x+y+z)^n} + e^{(x+y-z)^n} + e^{(x-y+z)^n} \\
 &+ e^{(x+y)^m} + e^{(-x+y)^m} + e^{(z+x)^m} + e^{(z-x)^m} \\
 &+ e^{(y+z)^m} + e^{(y-z)^m} + e^{(x)^p} + e^{(y)^p} + e^{(z)^p} = C
 \end{aligned}
 \tag{3.4.1}$$

This is a formula of symmetry in space and is particularly useful for describing shapes and forms of polyhedra and the transformation of one solid into another. It has often been said that topology is mathematics without equations. With this equation we can do topology with equations.

For $n,m=0$ and $p=1$ we have the natural exponential in 3D, which then also is a cube corner in fig. 3.4.1.

$$e^x + e^y + e^z = 200
 \tag{3.4.3}$$

$$e^{x^3} + e^{y^3} + e^{z^3} = 200
 \tag{3.4.4}$$

And for $p=3$ we show the effect of going up in the exponent in fig. 3.4.2.

For p even we have the cube, and we show it for $p=4$ in fig. 3.4.3.

$$e^{x^4} + e^{y^4} + e^{z^4} = 10^{10}
 \tag{3.4.5}$$

For $n,p=0, m=6$ we have the equation for the rhombic dodecahedron with a constant of 10^4 and the base of e as shown in fig. 3.4.4.

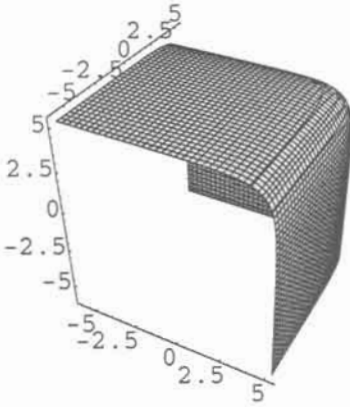


Fig. 3.4.1. Natural exponential or cube corner after equation 3.4.3.

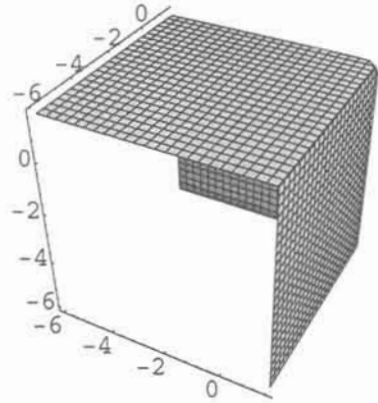


Fig. 3.4.2. Cube corner with higher exponential after equation 3.4.4.

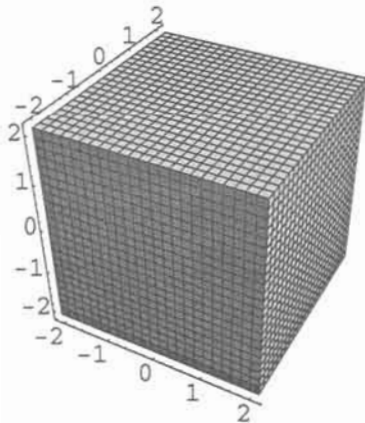


Fig. 3.4.3. Cube after equation 3.4.5.

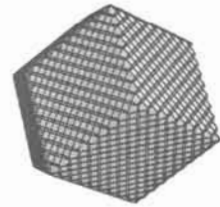


Fig. 3.4.4. Rhombic dodecahedron after equation 3.4.9.

For $m,p=0$ and n odd we have the tetrahedron which we show for a constant of 40000 and $n=3$ in fig. 3.4.5.

For $m=0, p=0$ and n even we have the octahedron, and we have chosen $C=4000$ and $n=4$ in fig. 3.4.6.

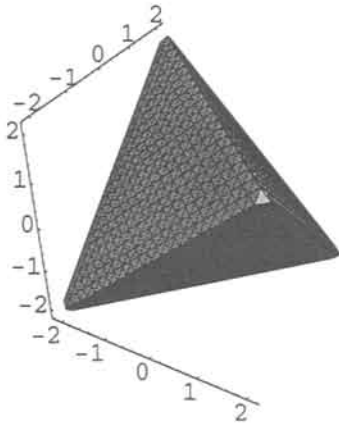


Fig. 3.4.5. Tetrahedron after equation 3.4.7.

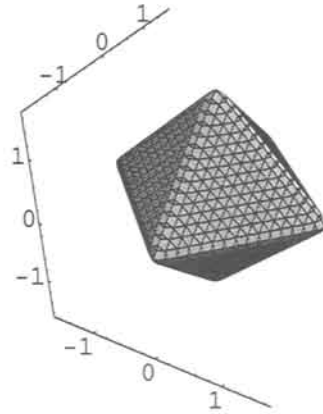


Fig. 3.4.6. Octahedron after equation 3.4.8.

From these kinds of mathematics we learn that the fundamental polyhedra are the cube, the tetrahedron, the octahedron and the rhombic dodecahedron, and we summarise:

cube

$$e^{x^4} + e^{y^4} + e^{z^4} = 10^{10} \tag{3.4.6}$$

tetrahedron

$$e^{(x+y+z)^3} + e^{(x-y-z)^3} + e^{(-x-y+z)^3} + e^{(-x+y-z)^3} = 4 \cdot 10^4 \tag{3.4.7}$$

octahedron

$$e^{(x+y+z)^4} + e^{(x-y-z)^4} + e^{(-x-y+z)^4} + e^{(-x+y-z)^4} = 4 \cdot 10^3 \tag{3.4.8}$$

rhombic dodecahedron

$$\begin{aligned} e^{(x+y)^6} + e^{(x-y)^6} + e^{(z+x)^6} \\ + e^{(z-x)^6} + e^{(y+z)^6} + e^{(y-z)^6} = 10^4 \end{aligned} \quad 3.4.9$$

We do the classic truncations of the first three just by adding equations for polyhedra:

$$\begin{aligned} e^{(x+y+z)^4} + e^{(x-y-z)^4} + e^{(-x-y+z)^4} + e^{(-x+y-z)^4} \\ + e^{x^8} + e^{y^8} + e^{z^8} = 10^7 \end{aligned} \quad 3.4.10$$

$$\begin{aligned} e^{(x+y+z)^2} + e^{(x-y-z)^2} + e^{(-x-y+z)^2} + e^{(-x+y-z)^2} \\ + e^{x^8} + e^{y^8} + e^{z^8} = 10^5 \end{aligned} \quad 3.4.11$$

$$\begin{aligned} e^{(x+y+z)^2} + e^{(x-y-z)^2} + e^{(-x-y+z)^2} + e^{(-x+y-z)^2} \\ + e^{(x+y+z)^3} + e^{(x-y-z)^3} + e^{(-x-y+z)^3} + e^{(-x+y-z)^3} = 4 \cdot 10^6 \end{aligned} \quad 3.4.12$$

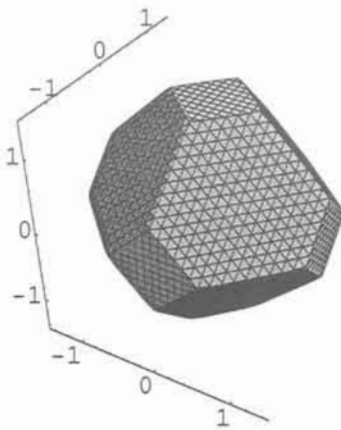


Fig. 3.4.7. Truncated octahedron after equation 3.4.10.

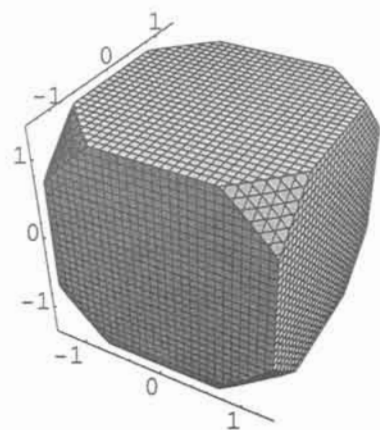


Fig. 3.4.8. Truncated cube after equation 3.4.11.

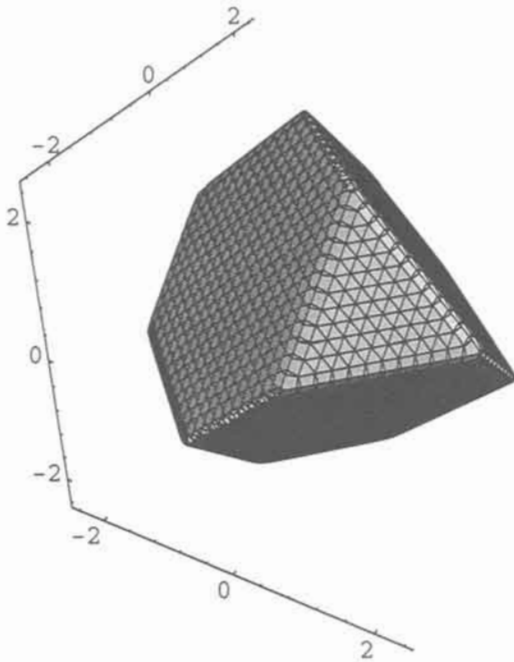


Fig. 3.4.9. Truncated tetrahedron after equation 3.4.12.

We have earlier found the equation for the icosahedron from the face vectors. The same equation is found from the addition of the octahedron and the rhombic dodecahedron as in equation 3.4.13. The constants a and b are varied from $a=1$, $b=1.2$ for fig 3.4.10, $a=1$, $b=1.5$ for fig. 3.4.11, and $a=1.5$, $b=2.5$ for 3.4.12. For $a=1.618$ (τ), $b=2.168$ (τ^2) there is the icosahedron as in fig. 3.4.13.

$$\begin{aligned}
 &10^{a(x+y+z)^4} + 10^{a(-x+y+z)^4} + 10^{a(x+y-z)^4} + 10^{a(x-y+z)^4} \\
 &+ 10^{(x+by)^4} + 10^{(-x+by)^4} + 10^{(z+bx)^4} + 10^{(z-bx)^4} \\
 &+ 10^{(y+bz)^4} + 10^{(y-bz)^4} = 10^4
 \end{aligned}
 \tag{3.4.13}$$

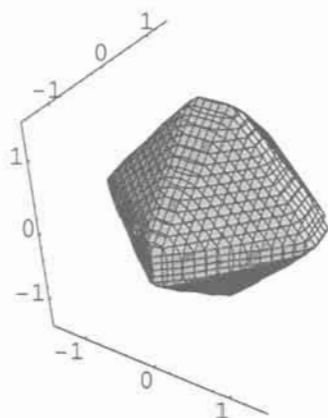


Fig. 3.4.10. The addition of the octahedron and the rhombic dodecahedron gives the icosahedron after equation 3.4.13, $a=1$, $b=1.2$.

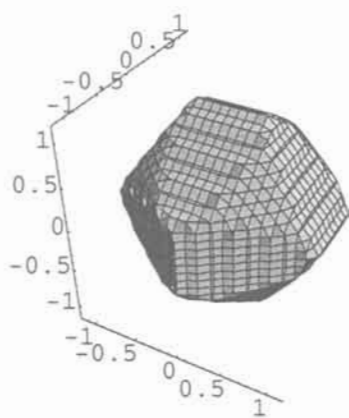


Fig. 3.4.11. $a=1$, $b=1.5$.

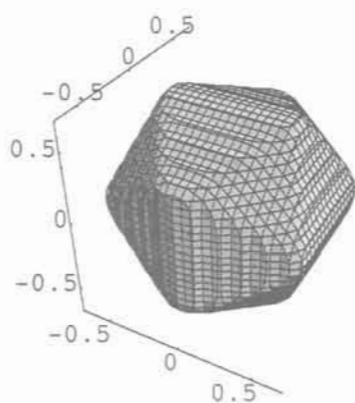


Fig. 3.4.12. $a=1.5$, $b=2.5$.

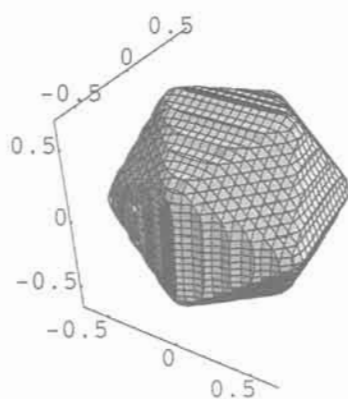


Fig. 3.4.13. $a=\tau$, $b=\tau^2$ (icosahedron)

Next is just a variation of b in the equation for the rhombic dodecahedron:

$$\begin{aligned}
 &10(x+by)^6 + 10(-x+by)^6 + 10(z+bx)^6 + 10(z-bx)^6 \\
 &+ 10(y+bz)^6 + 10(y-bz)^6 = 10^4
 \end{aligned}
 \tag{3.4.14}$$

In the remarkable series of pictures, 3.4.14 - 3.4.19, the amalgamation of the rhombic dodecahedron and the cube ($b=0$) give a number of interesting solids. The pentagonal dodecahedron is one in fig 3.4.16, the pyritohedron in fig 3.4.17 is another, and the various shapes represented by figures 3.4.18 and 19, are others. If the edges parallel to the cube axes are truncated in fig. 18 or 19, solids are obtained with great similarity to the picture of curved pyrite given by Hyde [2]. We like to thank Carlos Otero Diaz, Madrid for having given us a sample of this mineral, and stimulated this study.

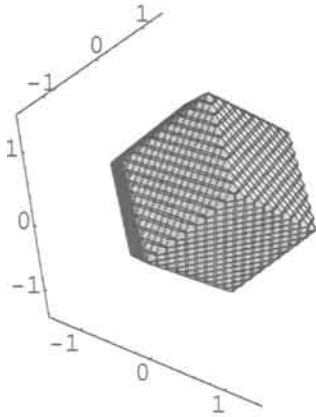


Fig. 3.4.14. $b=1$ rhombic dodecahedron.

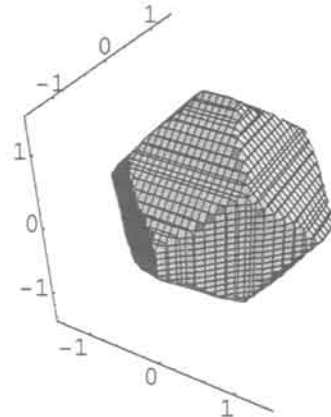


Fig. 3.4.15. $b=.85$

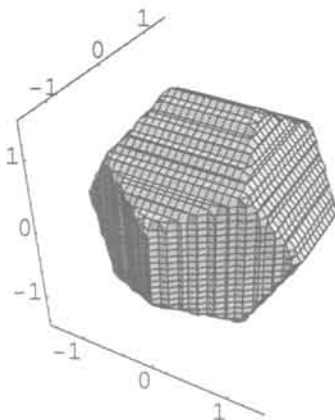


Fig. 3.4.16. $b=1/\tau$, the pentagonal dodecahedron.

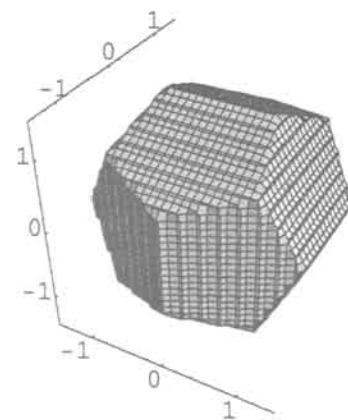
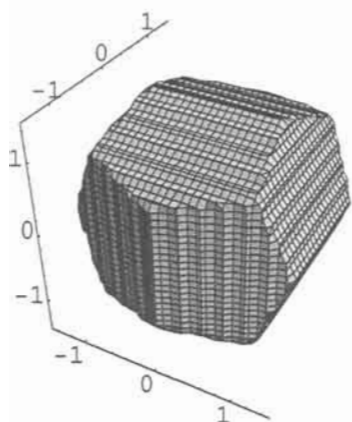
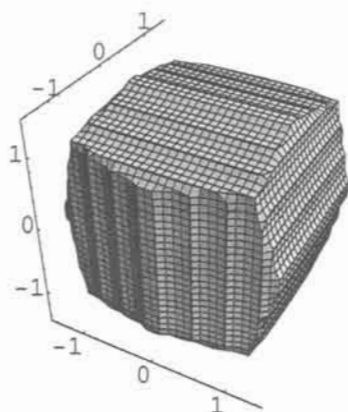


Fig. 3.4.17. $b=.5$, the pyritohedron.

Fig. 3.4.18. $b=4$.Fig. 3.4.19. $b=25$.

3.5 Optimal Organisation and Higher Exponentials

In chemistry the building block principle is common, but by no means unique for just chemistry. In astronomy it is called clustering of stars, growing to more complex structures; in biology for the building of proteins, DNA, evolution, life itself; and it exists in society as well indeed. The common dividend is the popular word hierarchy (in church), or rank (in army) or optimal organisation (science). We will show the mathematical machinery to use for the description of such structures, and also for their growth.

The exponential scale is shown below and going up in organisation means just going up in scale, and we will demonstrate that with an example where we end up using the last term in the second equation, 3.5.2, below.

$$x; e^x; e^{e^x}; e^{e^{e^x}} \quad 3.5.1$$

or

$$x^2; e^{x^2}; e^{e^{x^2}}; e^{e^{e^{x^2}}} \quad 3.5.2$$

An approach to the understanding of relations of consecutive terms in the scale is via power expansion.

We start by the addition of six parallel planes in equation 3.5.3, giving a cube in fig. 3.5.1:

$$e^{x^2} + e^{y^2} + e^{z^2} - 4 = 0 \tag{3.5.3}$$

To make it simple we add another cube but smaller, the size being determined by the constant, and the different sizes are now locked by having different exponential functions on the next higher scale as in eq. 3.5.4. It is here important to introduce a negative sign to obtain repetition and also to avoid too high numbers. This finding will be developed and used very much in structure building operations in forthcoming sections.

$$e^{-(e^{x^2} + e^{y^2} + e^{z^2} - 4)} + e^{-(e^{x^2} + e^{y^2} + e^{(z-2)^2} - 2)} - 0.2 = 0 \tag{3.5.4}$$

The shape of the original functions is kept very well in the centaur function 3.5.4, which is shown in fig. 3.5.2. The new auxiliary parameter 0.2 decides the size of the centaur function. A catenoid joins the two cubes.

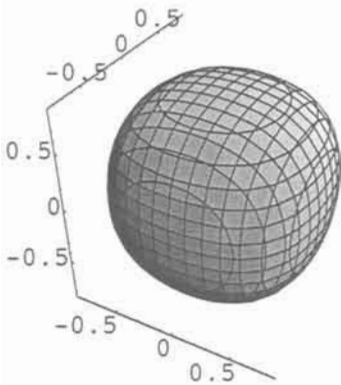


Fig. 3.5.1. Cube after equation 3.5.3.

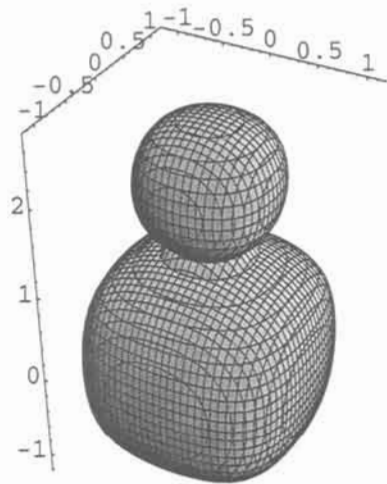


Fig. 3.5.2. Two cubes after one function equation 3.5.4.

We now have a building block, which we want to use to build a more complex structure. We shall turn the unit of two cubes up and down and

start to put the two building blocks together. We need to go up on the scale again in order to lock the original shapes and the next equation is 3.5.5.

$$\begin{aligned}
 & e^{-(e^{-x^2} + e^{y^2} + e^{z^2} - 4)} + e^{-(e^{-x^2} + e^{y^2} + e^{(z-2)^2} - 2) - 0.2} \\
 & + e^{-(e^{-(x-3)^2} + e^{y^2} + e^{z^2} - 2)} + e^{-(e^{-(x-3)^2} + e^{y^2} + e^{(z-2)^2} - 4) - 0.2} = 1.8
 \end{aligned}
 \tag{3.5.5}$$

The new auxiliary parameter, 1.8, determines of course the size of the whole thing, as seen in fig. 3.5.3.

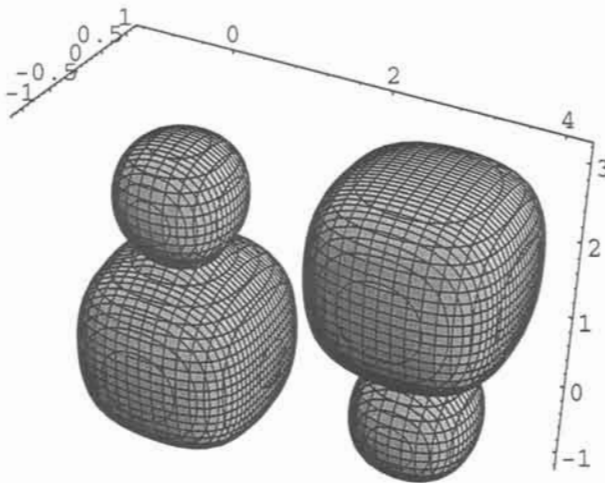


Fig. 3.5.3. Two building blocks after equation 3.5.5.

In order to make the two blocks join we change the x-parameter to equation 3.5.6.

$$\begin{aligned}
 & e^{-(e^{-x^2} + e^{y^2} + e^{z^2} - 4)} + e^{-(e^{-x^2} + e^{y^2} + e^{(z-2)^2} - 2) - 0.2} \\
 & + e^{-(e^{-(x-2)^2} + e^{y^2} + e^{z^2} - 2)} + e^{-(e^{-(x-2)^2} + e^{y^2} + e^{(z-2)^2} - 4) - 0.2} = 1.8
 \end{aligned}
 \tag{3.5.6}$$

And in fig. 3.5.4 and 3.5.5 (projection) we see the finished building block with a centre of symmetry, and we can now use the equation to repeat and

build periodic structures. We can build larger building blocks by using this block to fuse with another unit, by going still higher up on the scale.

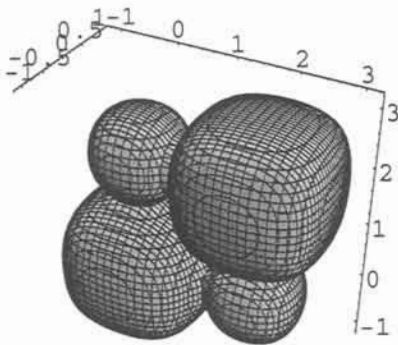


Fig. 3.5.4. The two building blocks joint to one after equation 3.5.6.

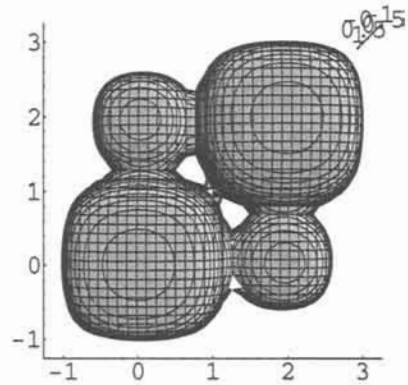


Fig. 3.5.5. The fusion of the two blocks in projection.

We shall find great use of these simple rules later on in this book. But we shall show one spectacular example here.

The octahedron can be said to consist of two sets of tetrahedral planes:

$$\begin{aligned}
 &e^{x+y+z} + e^{x-y-z} + e^{-x-y+z} + e^{-x+y-z} \\
 &+ e^{-x-y-z} + e^{-x+y+z} + e^{x+y-z} + e^{x-y+z} = C
 \end{aligned}
 \tag{3.5.7}$$

We lift them up each one separately as below on a double scale:

$$\begin{aligned}
 &e^{-(e^{(x+y+z)^3} + e^{(x-y-z)^3} + e^{(-x-y+z)^3} + e^{(-x+y-z)^3} - 200)} \\
 &+ e^{-(e^{(-x-y-z)^3} + e^{(-x+y+z)^3} + e^{(x+y-z)^3} + e^{(x-y+z)^3} - 200)} = 0.2
 \end{aligned}
 \tag{3.5.8}$$

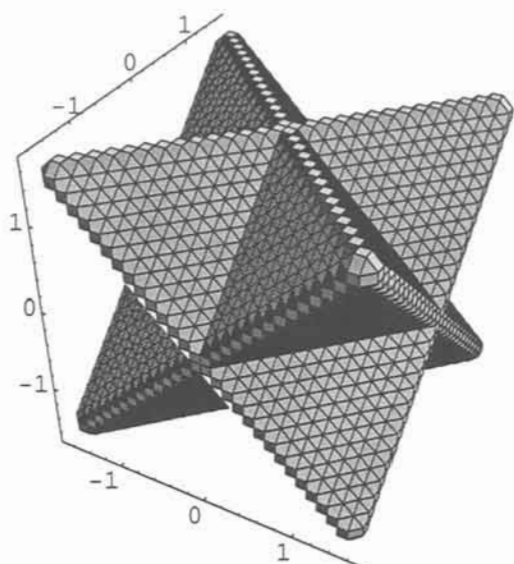


Fig. 3.5.6. Kepler's stella octangula after equation 3.5.8.

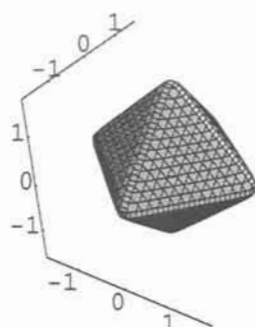


Fig. 3.5.7. The octahedron after equation 3.5.9.

With this trick of using the double scale the tetrahedra are kept, in the different orientations, and we get the formidable picture of 3.5.6. This is what is called a compound of two tetrahedra in mathematics, an interpenetration twin in mineralogy, and Kepler's stella octangula in the history of science, and a cluster called Mo_6Cl_8 in chemistry. We shall find great use of this property of the double scale later on in this book.

Just adding on the normal scale gives equation 3.5.9 and the octahedron in fig. 3.5.7.

$$\begin{aligned}
 & e^{(x+y+z)^3} + e^{(x-y-z)^3} + e^{(-x-y+z)^3} + e^{(-x+y-z)^3} \\
 & + e^{(-x-y-z)^3} + e^{(-x+y+z)^3} + e^{(x+y-z)^3} + e^{(x-y+z)^3} = 400
 \end{aligned}
 \tag{3.5.9}$$

Exercises 3

Exercise 3.1. Make higher polygons, for example the 17-gon (heptadecagon).

Exercise 3.2. Do the curvature of the 2D natural exponential ($e^x + e^y$).

Exercise 3.3. The curvature of the corner increases with increasing exponent. Show this for the function $e^{x^2} + e^{y^2} + e^{z^2}$.

Exercise 3.4. Make the polyhedron between the cube and the octahedron

Exercise. 3.5. Show how an octahedron may be transformed into a tetrahedron.

Answer 3.1

Use equation 3.1.11.

```

ImplicitPlot[
E^(y Sin[Pi/17]+x Cos[Pi/17])^9+
E^(-y Sin[Pi 2/17]-x Cos[Pi 2/17])^9+
E^(y Sin[Pi 3/17]+x Cos[Pi 3/17])^9+
E^(-y Sin[Pi 4/17]-x Cos[Pi 4/17])^9+
E^(y Sin[Pi 5/17]+x Cos[Pi 5/17])^9+
E^(-y Sin[Pi 6/17]-x Cos[Pi 6/17])^9+
E^(y Sin[Pi 7/17]+x Cos[Pi 7/17])^9+
E^(-y Sin[Pi 8/17]-x Cos[Pi 8/17])^9+
E^(y Sin[Pi 9/17]+x Cos[Pi 9/17])^9+
E^(-y Sin[Pi 10/17]-x Cos[Pi 10/17])^9+
E^(y Sin[Pi 11/17]+x Cos[Pi 11/17])^9+
E^(-y Sin[Pi 12/17]-x Cos[Pi 12/17])^9+
E^(y Sin[Pi 13/17]+x Cos[Pi 13/17])^9+
E^(-y Sin[Pi 14/17]-x Cos[Pi 14/17])^9+
E^(y Sin[Pi 15/17]+x Cos[Pi 15/17])^9+
E^(-y Sin[Pi 16/17]-x Cos[Pi 16/17])^9+
E^(y Sin[Pi 17/17]+x Cos[Pi 17/17])^9==20000000,
{x,1.4,-1.4},{y,-1.4,1.4},PlotPoints->400]

```

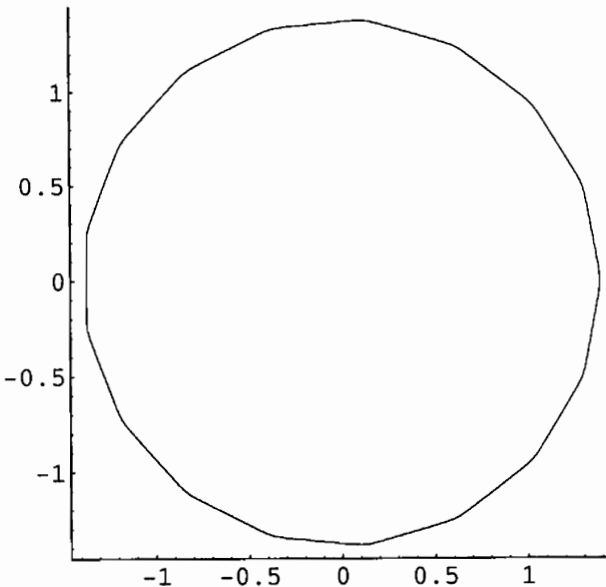


Fig. 3.1

Answer 3.2

Calculate mean curvature and plot after below

```
w[x,y,z]=E^x+E^y;
meancurv[w,x,y,z]
Plot[2(E^(2x+x)+E^(x+2x))/(2(E^(2x)+E^(2x))^(1.5)),
{x,0,1},PlotPoints->200,Axes->True]
```

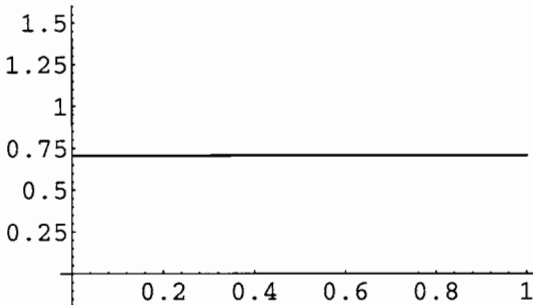


Fig. 3.2

Answer 3.3

Calculate mean curvature for the 2D case and study the exponents in the denominator and the dividend

Answer 3.4

The equation to use is

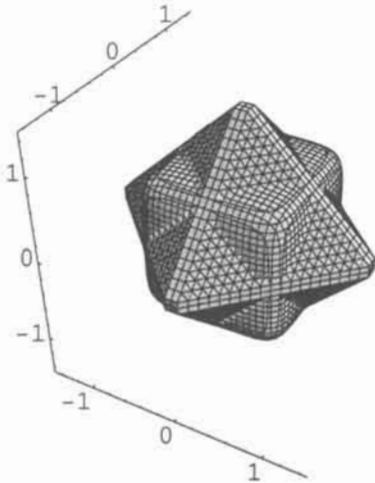
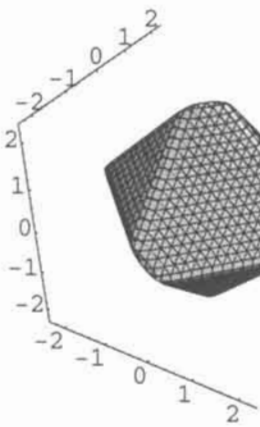
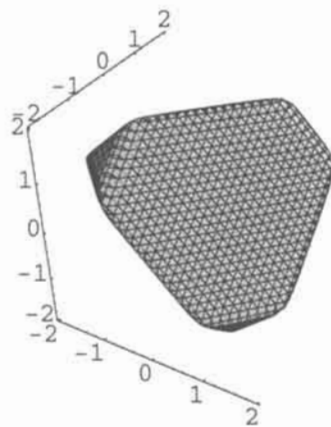
$$e^{-(e^{x^6} + e^{y^6} + e^{z^6} - 1.75)} + e^{-(e^{(x+y+z)^4} + e^{(-x+y+z)^4} + e^{(x+y-z)^4} + e^{(x-y+z)^4} - 200)} = 0.2$$

Answer 3.5

Use equation

$$e^{a(x+y+z)^2} + e^{a(x-y-z)^2} + e^{a(-x-y+z)^2} + e^{a(-x+y-z)^2} + e^{b(-x-y-z)^3} + e^{b(-x+y+z)^3} + e^{b(x+y-z)^3} + e^{b(x-y+z)^3} = 4000$$

The octahedron is for the square and the tetrahedron for cubic exponent. We show: a=1, b=.85 in 3.5 a and a=.75, b=1 in 3.5 b.

**Fig. 3.4****Fig. 3.5 a****Fig. 3.5 b**

References 3

- 1 G.H. Hardy, *PURE MATHEMATICS*, Cambridge University press 1975 page 47.
- 2 S.T. Hyde, *INFINITE PERIODIC MINIMAL SURFACES*, Thesis, Monash University, Melbourne 1986.

This Page Intentionally Left Blank

4 Periodicity and the Complex Exponential

Je dis que... (LaVallée Poussin in his description of 'fonctions circulaires' [1])

or

'although measurement is the sieve which separates grain from chaff..., measurement without imagination is only an empty sieve' (Synge [2]).

Here we describe the complex exponential in three dimensions. We show the topology of the minimal surfaces called P, D, G, IWP, FRD and O, C-TO as derived from various exponential equations. Permutation of space variables in periodic functions give pictures of crystal structures.

4.1 The Translation Vector

In mathematics things repeat with isometry or dilatation. Infinite periodicity with a translation vector describes the isometric repetition in nature. Light waves are periodically repeated, like waves on water can be. Crystals are periodically organised, which means most solids are periodic since these represent the majority of solids. Glass does not transional periodicity, as it is a solidified liquid. Enzymes can crystallise, and billions of giant enzyme molecules then know exactly where to sit in a crystal. We say "know" because the molecule has a memory function given by its structure and hence knows how to repeat in a crystal. Just like the sodium and chloride ions do in a crystal in your table salt. So why do we have the translation vector - the memory - that describes repetition? Such questions are not really allowed - they are too difficult to answer. But we can always say that the structure is the optimal state. Or go over to negations and say - without the translation vector we had no ice to float on water, we had no crystals, we had no DNA, we had no calciumphosphate to build Apatite that builds our skeleton, we had no life and would not exist to raise these questions. If of any help.

In the description of translation, the one dimensional version it is relatively simple - walking is an example, propagation of waves another.

In two dimensions the translation vectors give periodicity in two directions, and lines interact in the plane to give 2D repetition. Which is

unique. The Alhambra ornaments are one example, ordinary wall paper is another.

Our main goal in this section is to study repetition in 3D. Our approach is to take the permutation of the space variables in functions derived from the general complex exponential, e^{ix} . It quickly becomes very complicated, but to our surprise we can recognise crystal structures, even among the very difficult patterns, chemists as we are.

We were taught, and we believed, that crystal structures are physical objects and should be explained as such. We now know better and will show that the description of the arrangement of atoms in crystals may be considered as a part of the mathematics in space.

Crystals are built of atoms occupying various positions, and for a crystallographical description all the coordinate systems are necessary. The simplest case is the cubic, then comes the hexagonal, the tetragonal, the orthorhombic, the monoclinic and finally the triclinic. In the cubic case all unit vectors have equal magnitudes, and are perpendicular to each other. For the triclinic case the translation vectors all have different magnitudes, and the angles between them are all separated from 90° . Symmetry operations like mirror, rotation and their combinations, the screw and glide, give the 230 groups in space (or 17 in the plane). Group theory gives the positions for the general variables, and finding the atomic positions in a crystal - also with protein molecules - is nowadays close to a straightforward technology.

There are plenty of text books in the field, and here those that describe structures are of interest [3].

During this journey in mathematics we will find the most common of the simpler structures, and we describe them in the order we find them. That will be the way you learn crystal structures.

In chapters to come we show several kinds of repetition - the circular, the handmade and the Gauss distribution functions. We need them all for the study of this subject - periodicity in space.

Translation in natural science and mathematics is described with the circular functions, and often using the convenient relation between the complex number and the natural function, or the complex exponential. This is developed below.

For a description - or definition - of what $\sin(x)$ really is (which is in no way straightforward) we refer to textbooks of mathematics by Hardy,

LaVallée Poussin, Whittaker & Watson [4,1,5] and to chapter 2 in this book.

The symmetry operations reflection and rotation are best studied in the structures formed by translation. The very important combination rotation + translation (=the screw) will be dealt with in the next chapter.

Small changes in the expansion of the natural exponential

$$e^x = 1 + \frac{x}{1!} + \frac{x^2}{2!} + \frac{x^3}{3!} + \frac{x^4}{4!} + \frac{x^5}{5!} \dots$$

give the expansions for the circular functions

$$\cos x = 1 - \frac{x^2}{2!} + \frac{x^4}{4!} - \dots$$

and

$$\sin x = x - \frac{x^3}{3!} + \frac{x^5}{5!} - \dots$$

which are periodic and describe infinite translation.

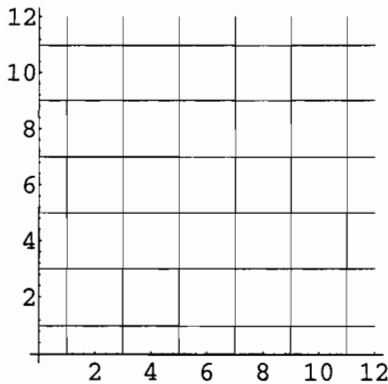


Fig. 4.1.1. The two functions $\cos x=0$ and $\cos y=0$ plotted on top of each other.

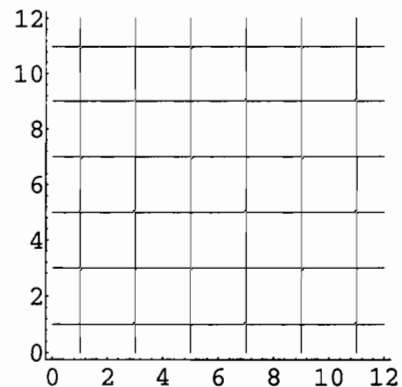


Fig. 4.1.2. The function $\cos x \cos y=0$

The function $\cos(x)=C$ is an infinite number of parallel lines in 2D, $\cos(y)$ likewise, and these two set of lines intersect in space at right angles in a Cartesian system. The two individual functions are plotted in fig 4.1.1. The combined function, the product, is plotted in 4.1.2. In fig 4.1.3 the isosurface constant is 0.02 which is increased to give 'atoms' in fig 4.1.4.

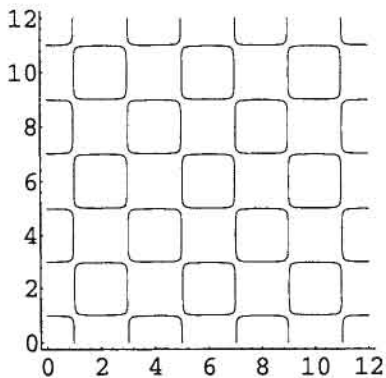


Fig. 4.1.3. The function $\cos x \cos y = 0.02$.

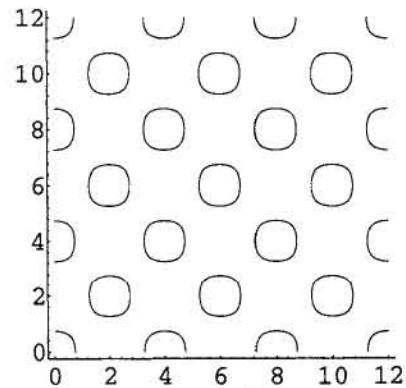


Fig. 4.1.4. The function $\cos x \cos y = 0.4$.

Going 3D with the function

$$\cos \pi x \cos \pi y \cos \pi z = C$$

4.1.1

gives of course the similar pattern as shown in fig 4.1.5 and 4.1.6, with const of 0 respectively 0.1. The bodies in space are in cubic close packing, called fcc (face centred cubic).

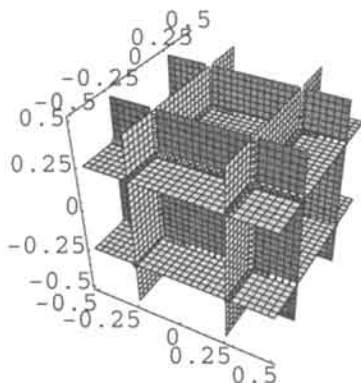


Fig. 4.1.5. Equation 4.1.1 with $C=0$.

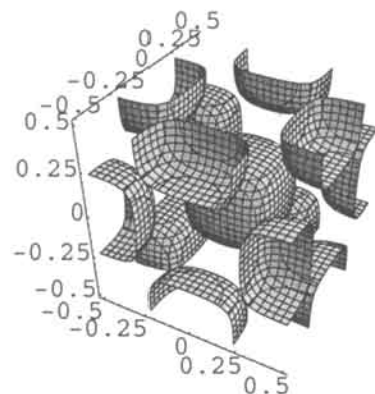


Fig. 4.1.6. Equation 4.1.1 with $C=0.1$.

We go to addition with the function

$$\cos \pi x + \cos \pi y = C \tag{4.1.2}$$

Here we again have intersecting lines, this time of the $x+y$ type in fig 4.1.7 which with an increased C become 'atoms' in fig 4.1.8.

For 3D we start with

$$\cos \pi x + \cos \pi y + \cos \pi z = C \tag{4.1.3}$$

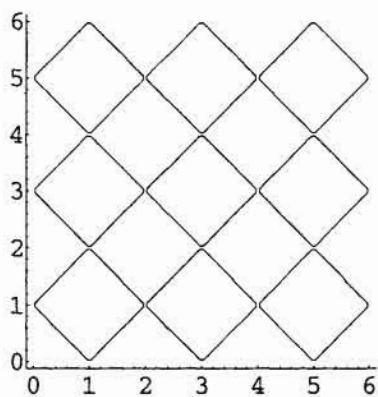


Fig. 4.1.7. Equation 4.1.2 with $C=0$.

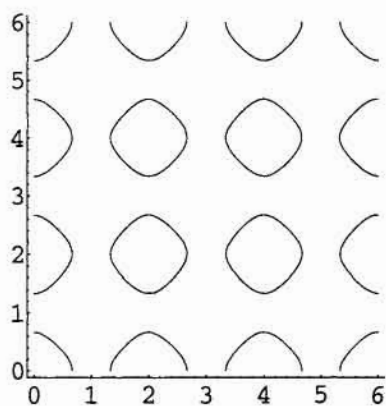


Fig. 4.1.8. Equation 4.1.1 with $C=0.5$.

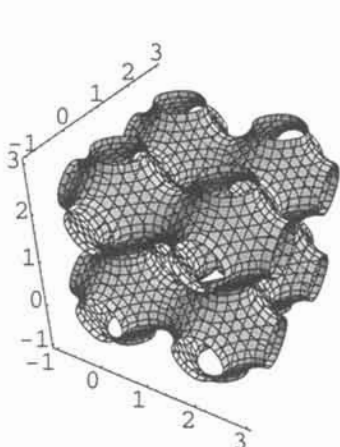


Fig. 4.1.9. Equation 4.1.3 with $C=0$.

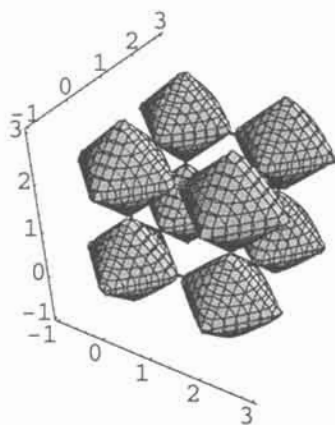


Fig. 4.1.10. Equation 4.1.3 with $C=1$.

This gives the well-known P-surface with $C=0$ in fig 4.1.9, the ReO_3 structure with $C=1$ in fig 4.1.10, and primitive cubic (pc) packing of bodies with $C=2$ in fig 4.1.11. We can now see that the so famous P-surface is easily derived from perpendicular planes in the three directions. This is certainly pronounced for the ReO_3 structure which is directly built of $x+y+z$ planes.

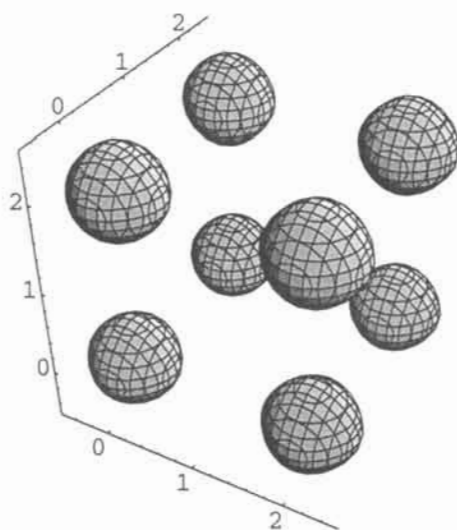


Fig. 4.1.11. Equation 4.1.3 with $C=2$.

These figures represent the two simplest structures ever - the primitive cubic packing of atoms and the so called ReO_3 structure. The ReO_3 structure has metal atoms in the centre of the octahedra, which have oxygen atoms at the vertices. In the primitive cubic (pc) packing of atoms each atom has six neighbours. In each corner of the unit cell, or cube, there is one atom. This is a bad packing for spheres, but excellent if the bodies are cubes and made to approach each other. So, how well atoms are packed in solids depends on their shape.

A simple combination as in eq. 4.1.4 gives cubes touching each other in fig 4.1.12.

$$\cos \pi x \cos \pi y + \cos \pi x \cos \pi z + \cos \pi y \cos \pi z = 0$$

4.1.4

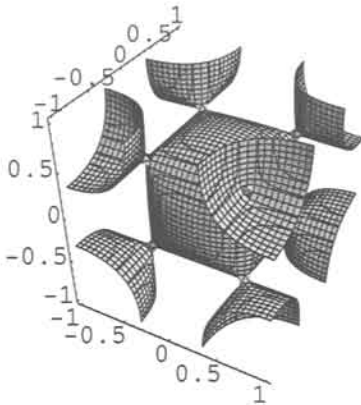


Fig. 4.1.12. Equation 4.1.4 with $C=0$.

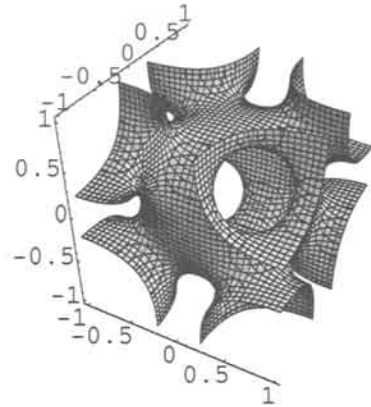


Fig. 4.1.13. Equation 4.1.4 with $C=0.5$.

Instead of zero we have to choose a constant of 0.5 to get the surface in fig. 4.1.13, which now has different volumes on the different sides of the contours. The corresponding minimal surface is IWP. These three surfaces above are the simplest periodic surfaces and they are also mathematically identical to the three fundamental constant energy (Fermi) surfaces for metals in reciprocal space. The first surface, of intersecting planes, is for a body centred cubic (bcc) metal, the second, the so called P surface is for a simple cubic metal and the IWP is for a fcc or close packed cubic metal.

Some slight changes of the trigonometric equations give more surfaces;

Eq 4.1.5 is the D surface and eq. 4.1.6 is the G surface, and both are shown and discussed separately below.

$$\cos \pi x \cos \pi y \cos \pi z + \sin \pi x \sin \pi y \sin \pi z = 0 \quad 4.1.5$$

$$\cos \pi x \sin \pi y + \sin \pi x \cos \pi z + \cos \pi y \sin \pi z = 0 \quad 4.1.6$$

The systematic mathematics for these surfaces above, and many more, were derived by von Schnering and Nesper in their description of their zero potential surfaces [6,7]. They call these surfaces nodal surfaces and they have also described their close relations to the minimal surfaces [8].

4.2 The Complex Exponential and Some Variants

We shall here use a somewhat different derivation of these nodal surfaces that makes these mathematics directly related to everything else we do.

The traditional way to handle periodicity in chemistry and physics is to use the so called complex exponential. So we explain what that is.

We start to use complex numbers. The number i is an imaginary number, it does not exist for us. Similar to minus one apple. The number i is $\sqrt{-1}$.

From the expansions of the circular functions, shown in equations 4.2.1a and 4.2.1b,

$$\sin x = x - \frac{x^3}{3!} + \frac{x^5}{5!} - \dots \quad 4.2.1a$$

$$\cos x = 1 - \frac{x^2}{2!} + \frac{x^4}{4!} - \dots \quad 4.2.1b$$

$$e^x = 1 + \frac{x}{1!} + \frac{x^2}{2!} + \frac{x^3}{3!} + \frac{x^4}{4!} + \frac{x^5}{5!} \dots \quad 4.2.2$$

it is clear that e^{ix} can be written

$$e^{ix} = \cos x + i \sin x \quad 4.2.3$$

and it is easy to show that

$$\sin x = \frac{1}{2}i(e^{ix} - e^{-ix}) \quad 4.2.4a$$

$$\cos x = \frac{1}{2}(e^{ix} + e^{-ix}) \quad 4.2.4b$$

These are the miracles in mathematics: The derivative of cos is sine and vice versa, the derivative of e^x is e^x , which is the natural function. The complex exponential is e^{ix} , and its remarkable and strange relations with the circular functions are given in eq 4.2.4a and b. And all adding up to give the periodic power expansions. We conclude giving the most beautiful formula of all, discovered by de Moivre:

$$e^{\pi i} = -1 \quad 4.2.5$$

Using e^{ix} means that the real part is $\cos x$ and the imaginary part is $\sin x$.
Or,

$$\operatorname{Re}[e^{ix}] = \cos x$$

and

$$\operatorname{Im}[e^{ix}] = \sin x$$

But the general thing to use is the complex exponential:

$$e^{\pi ix} + e^{\pi iy} + e^{\pi iz} \quad 4.2.6$$

We write

$$e^{ix} = \cos x + i \sin x$$

and the real part of the complex exponential is

$$\operatorname{Re}[e^{\pi ix} + e^{\pi iy} + e^{\pi iz}] = \cos \pi x + \cos \pi y + \cos \pi z \quad 4.2.7$$

We simplify with the famous formula

$$e^{\pi i} = -1$$

and we get

$$i^{2x} + i^{2y} + i^{2z} \quad 4.2.8$$

which is identical with 4.1.12.

This is a bit snobbish - we could as well just use $\cos x + \cos y + \cos z$. Or just use -1 as in the equation

$$(-1)^x + (-1)^y + (-1)^z = 0 \quad 4.2.9$$

since

$$(-1)^x = \cos \pi x + i \sin \pi x$$

We could use -1 as base in these equations, there is no need to use e or i , in this book. Or sin or cos. It is all built into an expression like $(-1)^x$. But we will still use e and i , as it is also useful in other kinds of mathematics.

The P nodal surface is within 0.5% identical with the P minimal surface.

Using complex numbers is simple and straightforward in Mathematica. Useful routines are shown in Exercises.

The general complex exponential is obtained from the equation of symmetry in eq. 3.4.1 by multiplying with i in the exponent:

$$\begin{aligned} & e^{[i(x+y+z)]^n} + e^{[i(-x+y+z)]^n} + e^{[i(x+y-z)]^n} + e^{[i(x-y+z)]^n} \\ & + e^{[i(x+y)]^m} + e^{[i(-x+y)]^m} + e^{[i(z+x)]^m} + e^{[i(z-x)]^m} \\ & + e^{[i(y+z)]^m} + e^{[i(y-z)]^m} + e^{[i(x)]^p} + e^{[i(y)]^p} + e^{[i(z)]^p} = 0 \end{aligned} \quad 4.2.10$$

$n, m=0, p=1$ give the P-surface, $n, p=0, m=1$ give the gyroid (Im-part) and IWP (Re-part), $m, p=0, n=1$ give the D-surface (Im+Re), $m=0, n$ and $p=1$ give the Neovius surface (Re part) *etc.* The variation of constant and various combinations give all kind of crystal structures as we have discussed elsewhere [9], and to some extent will do below.

$n, m, p=0$ or 2 give expressions of the type e^{-x^2} , or the Gaussian distribution which will be discussed in detail in chapter 7.

A variant to study is functions of type

$$e^{\text{Re}[e^{ix}]} = e^{\cos x} \quad 4.2.11$$

This we have done to some detail elsewhere [9].

Another variant of study is the square of the whole function which gives two roots, one surface on each side of the original one:

$$(\cos x + \cos y + \cos z)^2 = 0.4 \quad 4.2.12$$

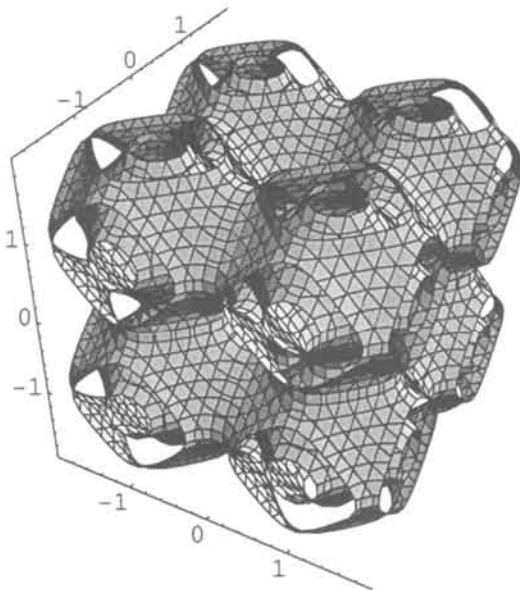


Fig. 4.2.1. Two interpenetrating P surfaces from equation 4.2.12.

This is at this constant two interpenetrating ReO_3 's and the chemical structure is that of Nb_6F_{15} as shown in fig. 4.2.1.

We continue with the complex exponential and for $n = 1$, and $C=0$, and get the so called D surface in fig 4.2.2. Changing C to 3, and increasing the boundaries, we get bodies or atoms - the diamond structure - projected along a cube axis in fig. 4.2.3. With a C of 2.5 the atoms become connected via catenoids as in fig. 4.2.4 and its projection is in fig. 4.2.5. It is easy to realise the diamond structure in which each atom is bonded to four others and the structure is also that of cristobalite, or cubic ice.

$$\begin{aligned} & \text{Re}[e^{i(x+y+z)} + e^{i(x-y-z)} + e^{i(-x-y+z)} + e^{i(-x+y-z)}] \\ & + \text{Im}[e^{i(x+y+z)} + e^{i(x-y-z)} + e^{i(-x-y+z)} + e^{i(-x+y-z)}] = C \end{aligned} \quad 4.2.13$$

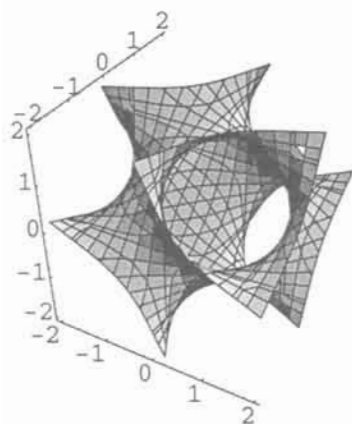


Fig. 4.2.2. D-surface after equation 4.2.13. $C=0$.

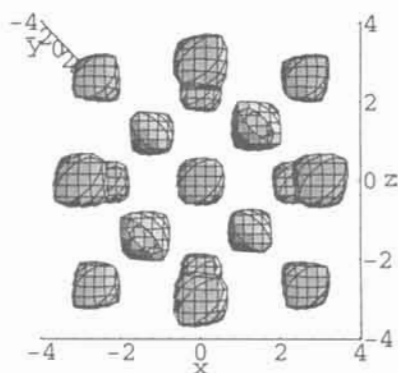


Fig. 4.2.3. Diamond structure after equation 4.2.13. $D=3$.

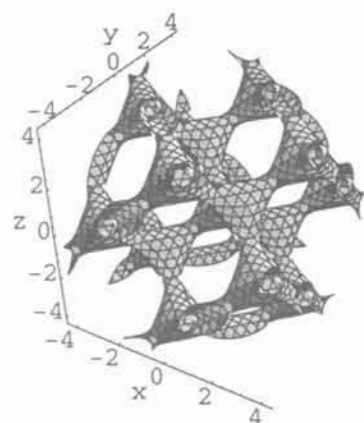


Fig. 4.2.4. Cubic ice with $C=2.5$ after equation 4.2.13.

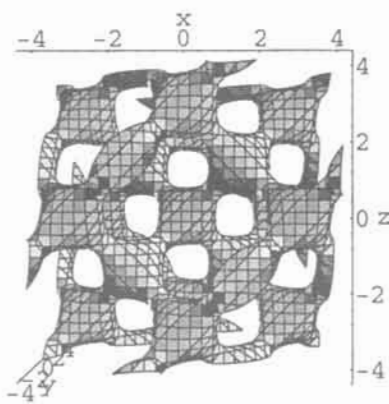


Fig. 4.2.5. Fig. 4.2.4 in projection.

We now square the function 4.2.13 as in eq. 4.2.14 below and for a constant of $C=1$ and of 6.25 there are figures 4.2.6 and 4.2.7. The latter shows the structure of the extreme high pressure form of ice which we for obvious reasons call double ice. Or double diamond, as this could be the structure of a high pressure form, a metallic bcc structure, of diamond.

$$\begin{aligned}
 & (\text{Re}[e^{i(x+y+z)} + e^{i(x-y-z)} + e^{i(-x-y+z)} + e^{i(-x+y-z)}]) \\
 & + \text{Im}[e^{i(x+y+z)} + e^{i(x-y-z)} + e^{i(-x-y+z)} + e^{i(-x+y-z)}])^2 = C
 \end{aligned}
 \tag{4.2.14}$$

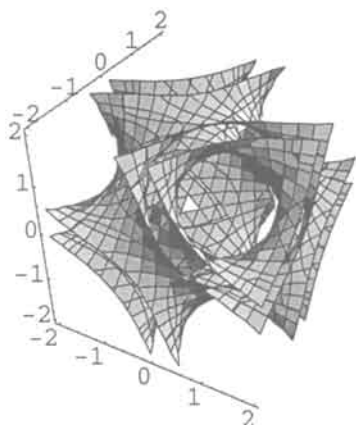


Fig. 4.2.6. Two interpenetrating D's after equation 4.2.14.

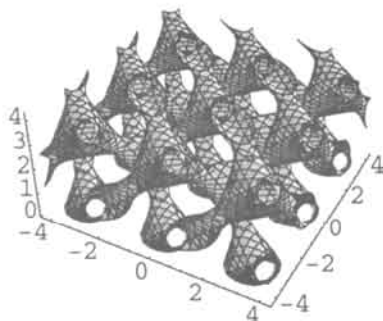


Fig. 4.2.7. Double ice (high pressure form) after equation 4.2.14.

In the pc structure as derived from the P surface, each atom had six neighbours. In the diamond structure each carbon atom has four other atoms as neighbours. We continue with the next - three neighbours. From the symmetry equation we derive the equation below:

$$e^{i(x+y)} + e^{i(x-y)} + e^{i(x+z)} + e^{i(-x+z)} + e^{i(y+z)} + e^{i(y-z)} = C \quad 4.2.15$$

For a zero constant and the Im part we get the gyroid type surface as in figures 4.2.8 and 4.2.9. In order to bring out the neighbours clearly we use the square as in the equation 4.2.16 and obtain fig. 4.2.10.

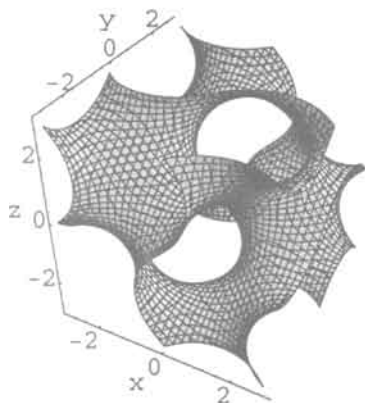


Fig. 4.2.8. Im part of equation 4.2.15 gives gyroid surface.

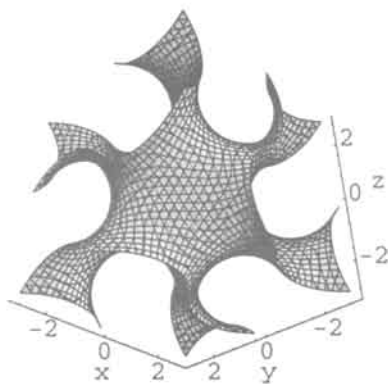


Fig. 4.2.9. Figure 4.2.8 in projection.

$$(e^{i(x+y)} + e^{i(x-y)} + e^{i(x+z)} + e^{i(-x+z)} + e^{i(y+z)} + e^{i(y-z)})^2 = 6.25 \quad 4.2.16$$

This double net is two three-connecting nets, e.g. if in one of the nets an atom is placed at the junctions, each such atom has three neighbours. This net, when it exists for itself on one side of the gyroid surface, corresponds to the Si part structure of the SrSi_2 structure, with the Sr atoms on the other side. In the case of the double net the whole structure is then of the γ -Si type (a high pressure form of Si). There is a contact between the Si atoms across the flat points of the gyroid surface completing the four coordination of silicon. The findings of these structures and nets come from Wells [10] and Nesper and von Schnering [6].

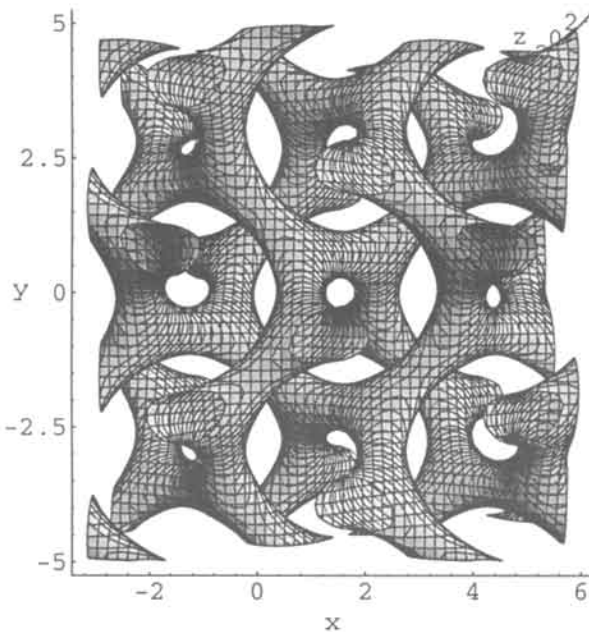


Fig. 4.2.10. Double gyroid after equation 4.2.16. $C=6.25$.

At a constant of $C=1$ in eq. 4.2.15, Re part, we have the important bcc, or body centred cubic packing of bodies in fig. 4.2.11. This is the structure for many metals and alloys (stainless steel). Each atom has here eight metal bonds to another identical atom at a distance of $\sqrt{3}/2$ of the cubic unit cell

edge. There are also another six identical metal bonds as indicated in the figure in form of fragments of atoms, with a distance of one unit cell apart. That is why this is described as 6+8 coordination for metals.

This is also the structure of CsCl with Cs and Cl atoms ordered in every second position. And every atom has eight electrostatic bonds to the other kind of atom.

We square also this equation and for a constant of 3 we have the remarkable fig. 4.2.12.

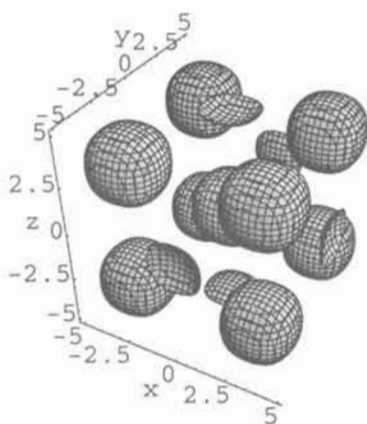


Fig. 4.2.11. Bcc pacing of bodies after equation 4.2.15, $C=1$.

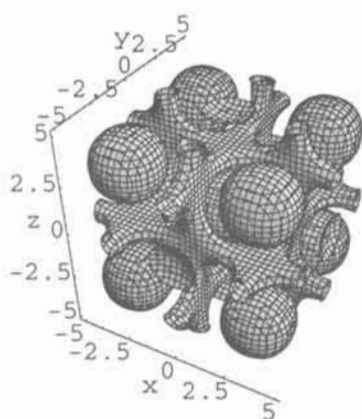


Fig. 4.2.12. The square of equation 4.2.15, $C=3$.

The beautiful four-connected net is that for the structure of NbO with Nb and O taking alternate positions of four coordination [10]. This is a very open description of the metallic structure of this oxide and we assume space is filled with electron densities localised to the spheres. This could also serve as the anti structure to the bcc metal structure, with the four connected surface as the electron density.

The IWP surface has different volumes on each side of the surface - this is the reason why this square is different from those above.

4.3 Some Other Exponentials

Another variant to study is the exponential functions below:

$$(\cos \pi x)^2 + (\cos \pi y)^2 + (\cos \pi z)^2 = 2 \quad 4.3.1$$

$$(\cos \pi x)^4 + (\cos \pi y)^4 + (\cos \pi z)^4 = 2 \quad 4.3.2$$

$$(\cos \pi x)^6 + (\cos \pi y)^6 + (\cos \pi z)^6 = 2 \quad 4.3.3$$

and we plot them in figures 4.3.1, 2 and 3. We see that the octahedra go apart, and are only joined by thin tube-like catenoids as an effect of going up in exponential.

By making x, y approach 0, the value of $(\cos z)^n$ stay close to zero over longer intervals of z , with increasing n .

Similarly we do the function

$$\begin{aligned} &(\cos \pi(x+y))^8 + (\cos \pi(x-y))^8 + (\cos \pi(x+z))^8 \\ &+ (\cos \pi(z-x))^8 + (\cos \pi(y+z))^8 + (\cos \pi(y-z))^8 = 2 \end{aligned} \quad 4.3.4$$

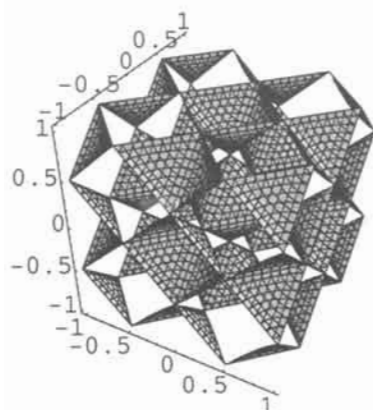


Fig. 4.3.1. The equation is 4.3.1 with $C=2$.

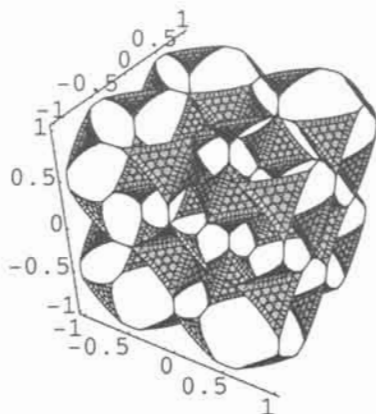


Fig. 4.3.2. The equation is 4.3.2 with $C=2$.

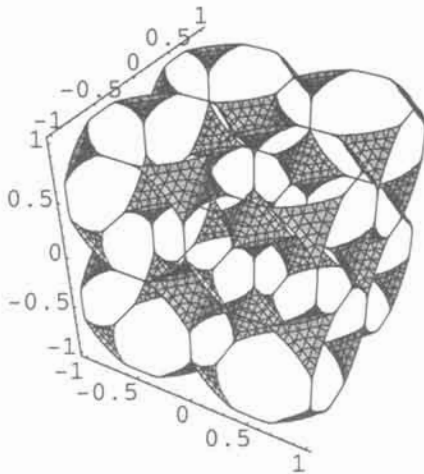


Fig. 4.3.3. The equation is 4.3.3 with $C=2$.

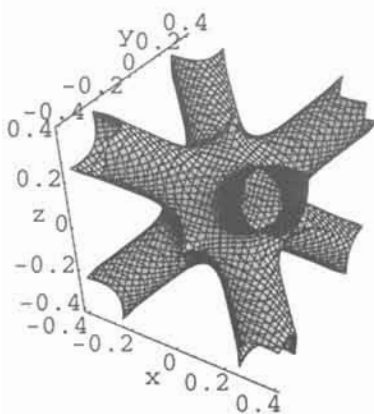


Fig. 4.3.4. Part of the O,C-TO surface from 4.3.4 with $C=2.99$.

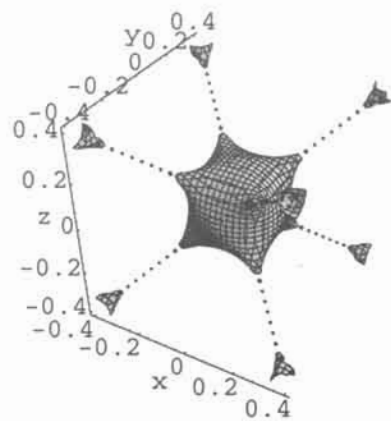


Fig. 4.3.5. $C=2$.

This is a part of the O,C-TO surface which compared with the IWP has six extra catenoids in octahedral symmetry, and which for a constant of 2 are extremely thin as seen in fig. 4.3.4. At higher constants we are coming back to the IWP as in fig. 4.3.5 calculated for a constant of 2.99.

In fig. 4.3.6 we have used equation

$$\begin{aligned} &(\cos \pi(x+y))^4 + (\cos \pi(x-y))^4 + (\cos \pi(x+z))^4 \\ &+ (\cos \pi(z-x))^4 + (\cos \pi(y+z))^4 + (\cos \pi(y-z))^4 = 1.5 \end{aligned} \quad 4.3.5$$

to describe the O,C-TO surface. Chemically this corresponds to the sodalite structure [9].

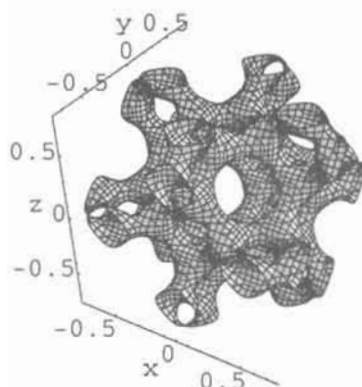


Fig. 4.3.6. Equation 4.3.5 gives O,C-TO surface or sodalite structure.

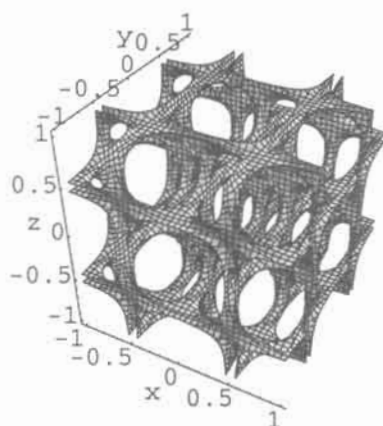


Fig. 4.3.7. Square four connected net from equation 4.3.6.

Just using squares and a constant of 2.1 according to equation 4.3.6 give an interesting distortion of the IWP. This is the square four connected net again in fig 4.3.7, now without the spheres from fig 4.2.12.

$$\begin{aligned} &(\cos \pi(x+y))^2 + (\cos \pi(x-y))^2 + (\cos \pi(x+z))^2 \\ &+ (\cos \pi(z-x))^2 + (\cos \pi(y+z))^2 + (\cos \pi(y-z))^2 = 2.1 \end{aligned} \quad 4.3.6$$

The complete permutation has an interesting development for the equation:

$$\begin{aligned}
 &(\cos \pi(x+y+z))^4 + (\cos \pi(x-y-z))^4 \\
 &+ (\cos \pi(-x-y+z))^4 + (\cos \pi(-x+y-z))^4 = C
 \end{aligned}
 \tag{4.3.7}$$

With a constant of 1 we have a beautiful Kepler star of fourteen atoms in cubic close packing. We make the atoms approach each other by changing constant, and at a value of 1.05 extra particles are created as shown in fig. 4.3.9.

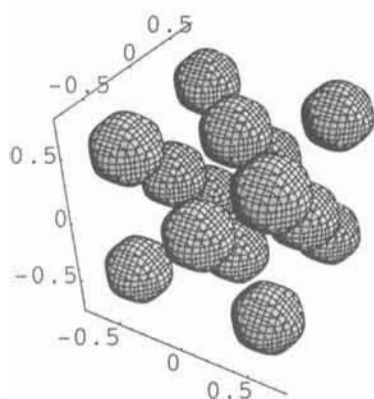


Fig. 4.3.8. Kepler star of bodies from equation 4.3.7 with $C=1$.

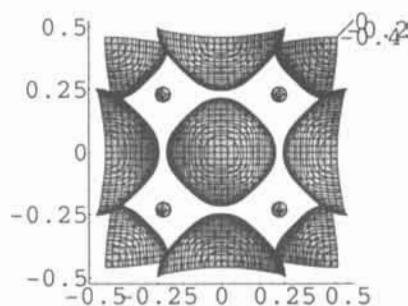


Fig. 4.3.9. Small particles appear at $C=1.05$.

When the constant increases, the small round particles grow into tetrahedral shape and finally join the larger round bodies, each at eight places via catenoids. The larger bodies become cube-like. Chemically this can be said to be the structure of TiH_2 with the larger bodies as titanium atoms in ccp, while the small atoms are the hydrogens. The structure is of the type of CaF_2 .

Each small atom is surrounded by four larger in a tetrahedral manner, which with the catenoids developed is a piece of the D-surface. The larger bodies are surrounded by eight small ones, giving a shape as a piece of the IWP surface. Two typical polyhedral parts of this FRD surface are given in figures 4.3.12 and 4.3.13, both calculated for a C of 1.5.

And in fig. 4.3.14 we give the complete FRD surface as calculated for a constant of 1.6.

For a constant of 1.97 we get a beautiful variant of FRD as seen in fig. 4.3.15.

Finally we show again the remarkable behaviour of the function for a constant of 2 in eq. 4.3.8 and fig. 4.3.16.

$$\begin{aligned} &(\cos \pi(x+y+z))^8 + (\cos \pi(x-y-z))^8 \\ &+ (\cos \pi(-x-y+z))^8 + (\cos \pi(-x+y-z))^8 = 2 \end{aligned} \quad 4.3.8$$

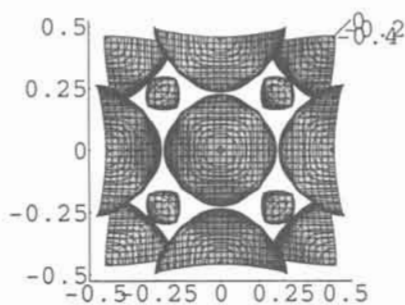


Fig. 4.3.10. At $C=1.2$ a description of the TiH_2 structure.

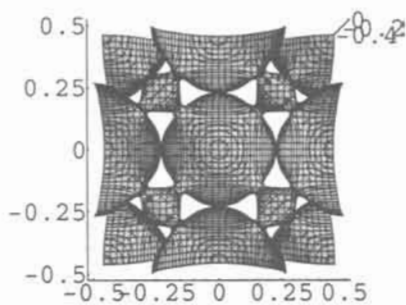


Fig. 4.3.11. At $C=1.25$ the FRD surface starts to develop.

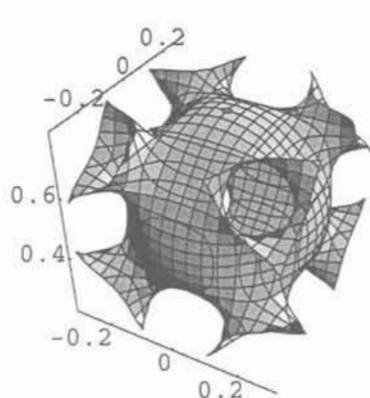


Fig. 4.3.12. At $C=1.5$ the IWP part of the FRD surface.

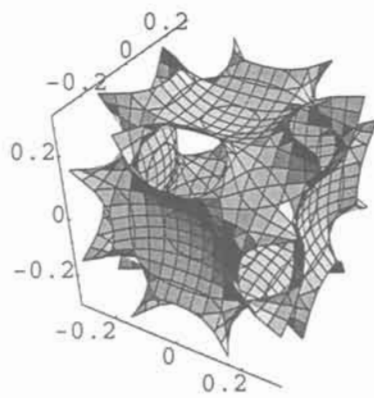


Fig. 4.3.13. At $C=1.5$ a typical part of the FRD surface, still from equation 4.3.7.

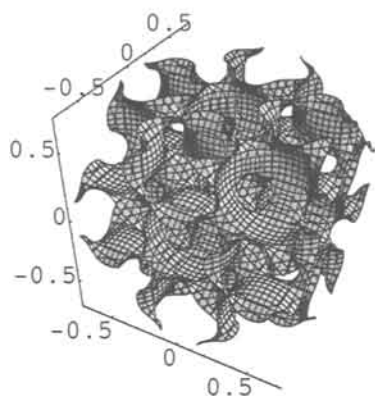


Fig. 4.3.14. At $C=1.6$ the complete part of the FRD surface.

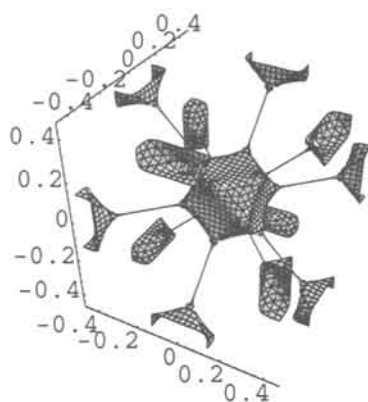


Fig. 4.3.16. At $C=2$ an interesting variation of the FRD surface as in figures 4.3.1-3.

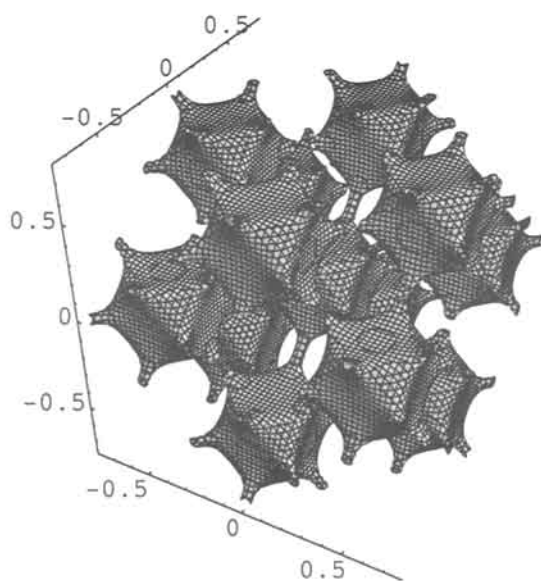


Fig. 4.3.15. At $C=1.97$ a beautiful variation of the FRD surface.

Exercises 4

Exercise 4.1 Expand e^{ix} and e^{i^2x}

Exercise 4.2 Do the equation $(-1)^{2x} + (-1)^{2y} + (-1)^{2z} = 0$, and the equation $(-\pi)^{2x} + (-\pi)^{2y} + (-\pi)^{2z} = 0$. Explain the difference.

Exercise 4.3 Plot $\text{Re}[(-1)^{2x} + (-1)^{2y} + (-1)^{2z} = 0]$ and describe the result.

Exercise 4.4 Do the calculation below (written for Mathematica) and find out what surface it is, and describe the part obtained.

```
ContourPlot3D[(((Cos[Pi(x+y-z)])^4+(Cos[Pi(x-y+z)])^4+
(Cos[Pi(-x+y+z)])^4+(Cos[Pi(-x-y-z)])^4)-1.5,{x,.5,0},{y,.5,0},{z,.5,0},
MaxRecursion->2,PlotPoints->{{5,3},{5,3},{5,3}},Boxed->False,
Axes->True]
```

Exercise 4.5 Plot the expansion of cosine using 12 terms. Compare with cosine.

Exercise 4.6 Show that the equation 4.2.13 is identical with 4.1.5.

Answer 4.1

$$\text{ComplexExpand}[E^{i x}] = \cos x + i \sin x$$

$$\text{ComplexExpand}[E^{i^2 x}] = \cos x \sin \pi x e^{\cos \pi x} + i \sin x \sin \pi x e^{\cos \pi x}$$

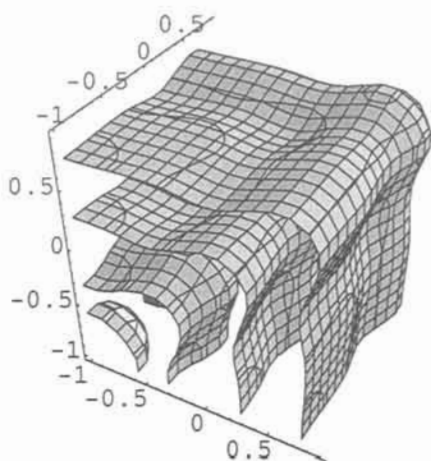
Answer 4.2

$$\text{ComplexExpand}[-1^{2x}] = (-1^{2x}) = \cos 2\pi x + i \sin 2\pi x$$

$$\text{ComplexExpand}(-\pi^{2x}) = \pi^{2x} \cos 2\pi x + i \pi^{2x} \sin 2\pi x$$

Answer 4.3

```
ContourPlot3D[Re[(-Pi)^(2x)+(-Pi)^(2y)+(-Pi)^(2z)],
{x,1,-1},{y,1,-1},{z,1,-1},MaxRecursion->2,PlotPoints
->{{5,3},{5,3},{5,3}},Boxed->False,Axes->True]
```

**Fig. 4.3**

This is a concentric structure of type described in [6]. The changing of the base from π to something closer to one, say 1.5, reveals a mechanism for a transformation to the P-surface. This means we have the topology for making a small molecule grow to a bigger, and finally ending up with an infinite lattice. Try and show how a B_6H_6 molecule grows into the P surface.

Answer 4.4

The tetrahedral part of FRD

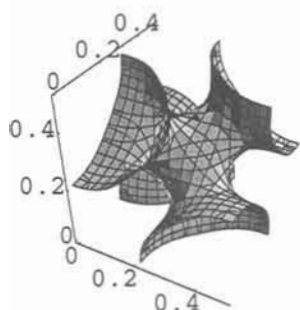


Fig. 4.4

Answer 4.5

```
Plot[{1-1/2x^2+1/(4!)x^4-1/(6!)x^6+1/(8!)x^8-
1/(10!)x^10+1/(12!)x^12-1/(14!)x^14+1/(16!)x^16-
1/(18!)x^18+1/(20!)x^20
-1/(22!)x^22+1/(24!)x^24,Cos[x]},{x,0,13},PlotPoints->200]
```

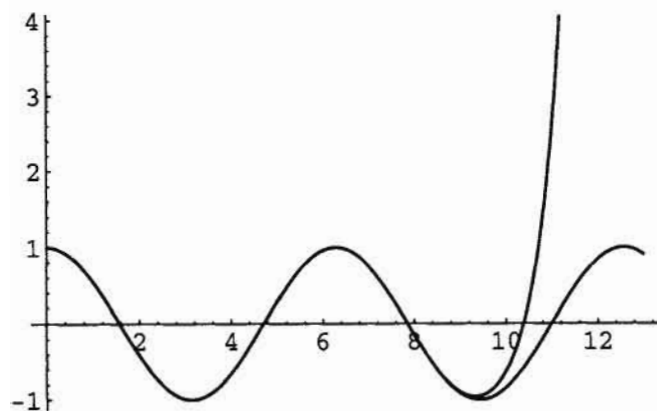


Fig. 4.5

Answer 4.6

Use Mathematica.

```
ComplexExpand[Re[E^(I(x+y+z))+E^(I(x-y-z))+E^(I(-x-y+z))+
E^(I(y-z-x))]+Im[E^(I(x+y+z))+E^(I(x-y-z))+E^(I(-x-y+z))+E^(I(y-z-x))]]
=
Cos[x-y-z]+Cos[x+y-z]+Cos[x-y+z]+Cos[x+y+z]+Sin[x-y-z]-Sin[x+y-z]-
Sin[x-y+z]+Sin[x+y+z]
Expand[%,Trig->True]
=
4 Cos[x]Cos[y]Cos[z] - 4 Sin[x]Sin[y]Sin[z]
```

References 4

- 1 Ch.-J. de la Vallée Poussin, *COURS d'Analyse Infinitésimale*, PARIS GAUTHIER-VILLARS, 1947 ,page 468.
- 2 J.L. Synge, *SCIENCE: SENSE AND NONSENSE*, Books for Libraries Press, New York, 1972, page 76
- 3 B.G. Hyde and S. Andersson, *INORGANIC CRYSTAL STRUCTURES*, Wiley, New York, 1988.
- 4 G.H. Hardy, *PURE MATHEMATICS*, CAMBRIDGE UNIVERSITY PRESS 1975.
- 5 E.T. Whittaker & G.N. Watson, *A Course of MODERN ANALYSES*, CAMBRIDGE UNIVERSITY PRESS 1988.
- 6 H.G. von Schnering and R. Nesper, *Angew. Chem. Int. Ed. Engl.* **26**, 1059 (1987).
- 7 H.G. von Schnering and R. Nesper, *Z. Phys. B - Condensed Matter* **83**, 407 (1991).
- 8 U. Dierkes, S. Hildebrandt, A. Kuster and O. Wohlrab, *Minimal Surfaces 1 and 2*, Springer Verlag, Berlin, 1991.
- 9 S. Andersson and M. Jacob, *THE MATHEMATICS OF STRUCTURES - THE EXPONENTIAL SCALE*, Oldenbourg, München, 1997.
- 10 A.F. Wells, *THREE-DIMENSINAL NETS AND POLYHEDRA*, Wiley, New York, 1977.

5 The Screw and the Finite Periodicity with the Circular Functions

The general rigid motion of space is called a screw, rotations and translations being regarded as limiting cases. (Hilbert [1]).

Here we discuss the space curves and the time parametrisation, and propose that our variation of isosurface constant is just another parametrisation. We introduce finite periodicity from circular functions. We describe the screw and the general multi-spiral. And the mathematics for giant molecules like the cubosomes, the DNA and certain building blocks in protein structures.

5.1 Chirality, the Screw and the Multi Spiral

A fundamental property of life is chirality - a good example is our two hands, one is left and the other is right. They are transformed into each other by an operation what in politics and medicine is called bilateral - we call it a mirror.

A molecule can be left or right handed. Their physical properties are identical but a molecule used as a drug must have correct chirality to be active. With wrong chirality it might have no effect at all, or it might be deadly poison. Like for example Neurosedyne, one of the enantiomorphs works as an excellent sedative, while the other damages the fetus during pregnancy. Chirality is a matter of shape and function - recognition - a left handed screw does not fit to a right handed bolt. Most enzymes are chiral and so is of course DNA.

Chirality cannot be described with energy, or minimisation. So it is not quantized. Chirality is a property of symmetry in three dimensions. The change of chirality for the screw in mathematics is easily done just by changing sign. To continuously go from one of the shapes to the other is not trivial. Special cases exist, like turning a glove in and out.

Translation and rotation are special cases of motions in space, and the combination of the two give the most fundamental motion - the screw, which is chiral.

The important one is the cylindrical helix, the shape of a stair case, and has the parametric equations

$$r = a, z = c\theta \quad 5.1.1$$

which is cylindrical coordinates, or

$$x^2 + y^2 = a^2; \frac{y}{x} = \tan \frac{z}{c} \quad 5.1.2$$

which means that the circular helix is the curve of intersection between two surfaces, the helicoid and the circular cylinder.

But we prefer to work implicit so we formulate the following equation, which is quite analogous with the parametric one above. A cylinder is added to a helicoid, and we get a surface instead of a space curve, a cylindrical helicoid - a spiral - in fig 5.1.1.

$$x \cos \pi z - y \sin \pi z + x^2 + y^2 = 0 \quad 5.1.3$$

The projection of a circular helix on a plane $x=0$ is the sine curve $y = \sin \pi z$

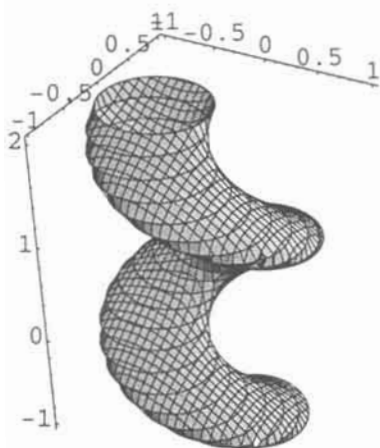


Fig. 5.1.1. A spiral surface after equation 5.1.3.

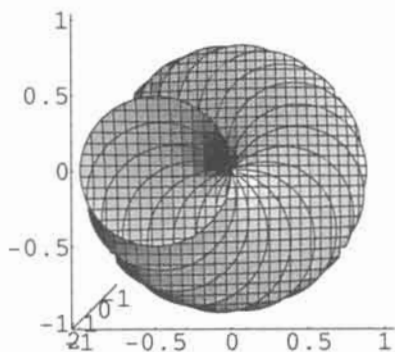


Fig. 5.1.2. A projection of fig. 5.1.1.

In order to approach a curve we have varied the constant in eq. 5.1.4. For $C=0.2$ there is fig. 5.1.3 and in 5.1.4 $C=0.2494$, and the cylindrical spiral is approaching the space curve - the cylinder gets infinitely thin.

$$x \cos \pi z - y \sin \pi z + x^2 + y^2 + C = 0 \quad 5.1.4$$

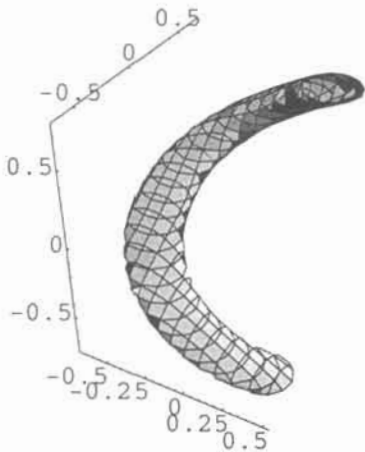


Fig. 5.1.3. $C=0.2$ from equation 5.1.4.

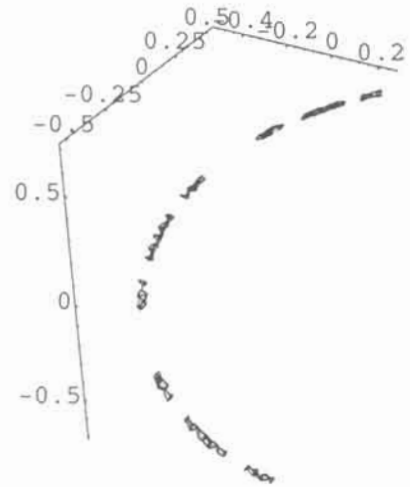


Fig. 5.1.4. $C=0.2494$ from equation 5.1.4.

We now go back to the simple function xz and make two cyclic functions, shown in fig. 5.1.5-6 and equations below:

$$y \cos \pi z = 0.05$$

$$x \sin \pi z = -0.05$$

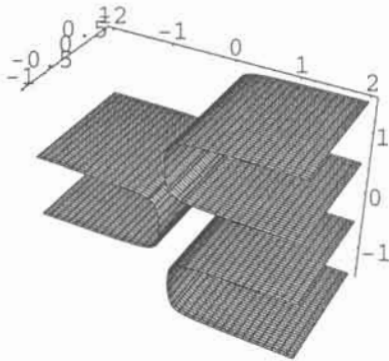


Fig. 5.1.5. Equation $y \cos \pi z = 0.05$.

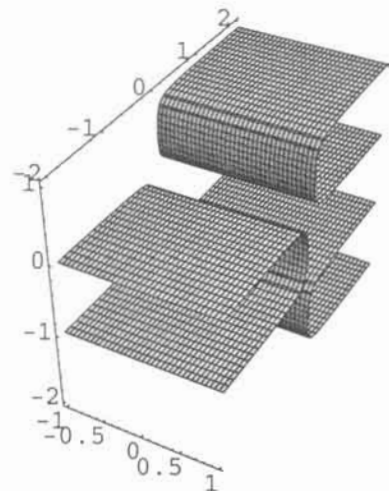


Fig. 5.1.6. Equation $x \sin \pi z = -0.05$

By adding these two we get the equation for the helicoid (5.1.5), the very famous minimal surface which also is ruled (fig 5.1.7). We clearly see that the structure of the helicoid is composed of the two simpler surfaces glued together, or x and y planes plus the dominating periodic z planes.

$$y \cos \pi z - x \sin \pi z = 0$$

5.1.5

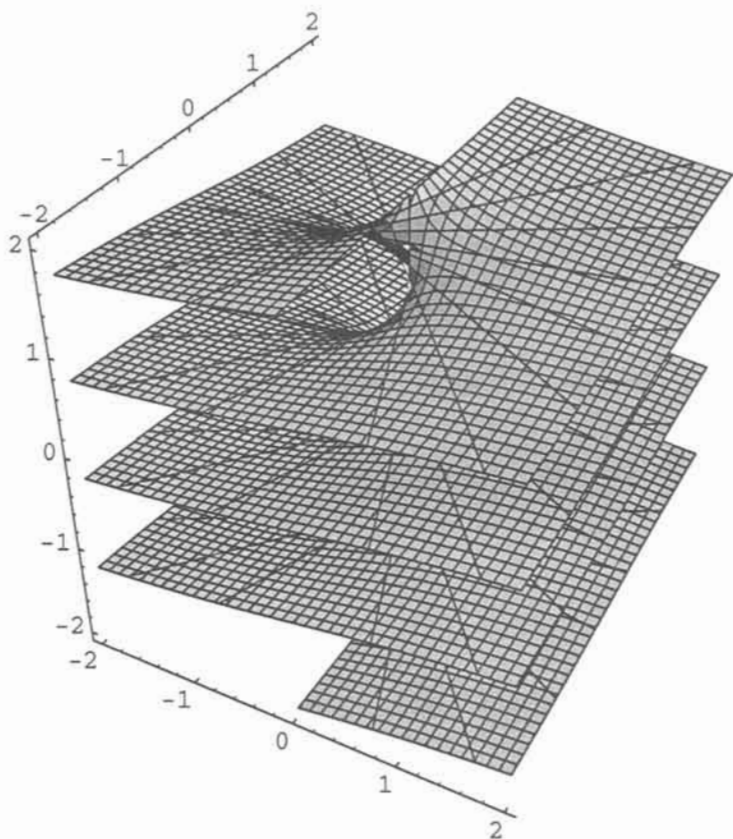


Fig. 5.1.7. The helicoid after equation 5.1.5.

The x and y planes are perpendicular in space. We can now systematically introduce more and more perpendicular planes and get multiple helicoids, as was done deriving the general expression for the tower surfaces [2]. We have above shown that the helicoid could be turned into a spiral using a cylinder operator. So we arrive at the complete equation in 5.1.6.

$$\left[\prod_{i=1}^{i=n} (x \cos(i\pi/n) + y \sin(i\pi/n)) \right] \cos \pi z$$

$$- \left[\prod_{i=1}^{i=n} (x \cos(i\pi/n + \pi/2n) + y \sin(i\pi/n + \pi/2n)) \right] \sin \pi z + p e^{x^2 + y^2} = C$$

5.1.6

With $p=0$ and $C=0$ we get intersecting surfaces for $n>1$. A constant $C=0.05$ is enough to make them non-intersecting. This is shown in figures 5.1.8 a, b, c. for the double helix case with $n=2$, $p=0$, $C=0$, and $n=2$, $p=0$, $C=0.05$ and finally $n=2$, $p=0.1$, $C=0$ respectively for the double spiral.

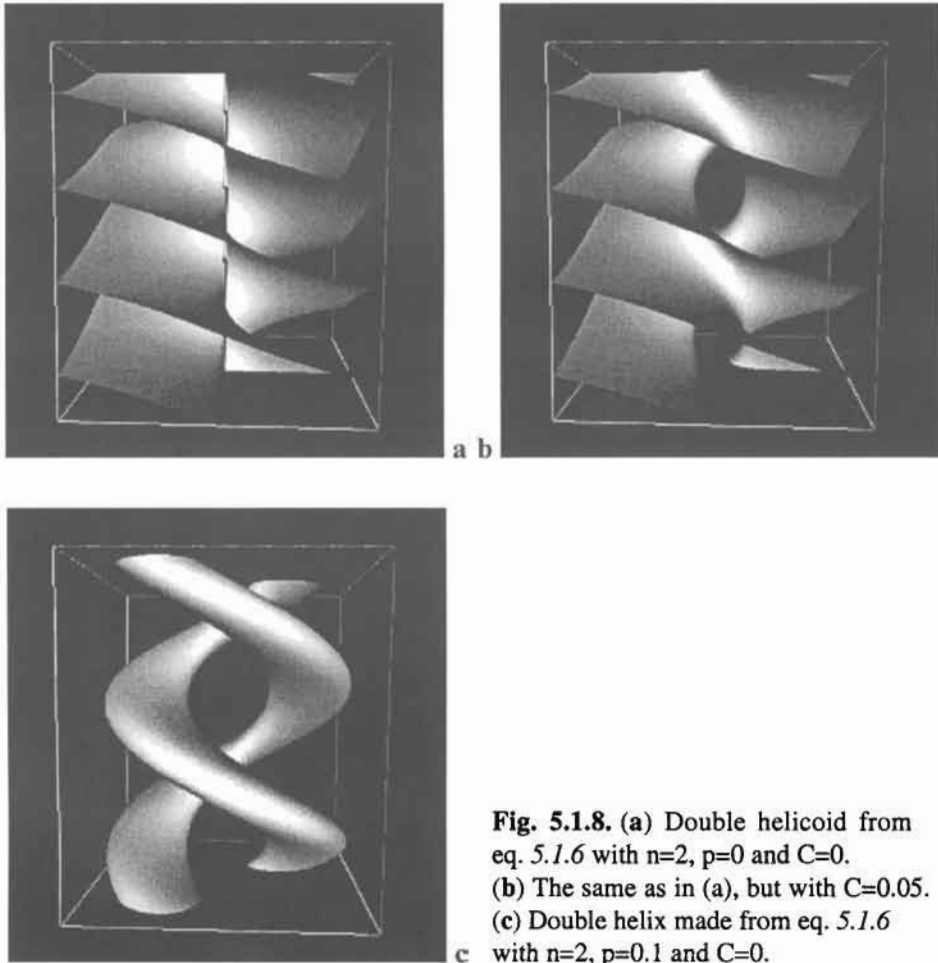
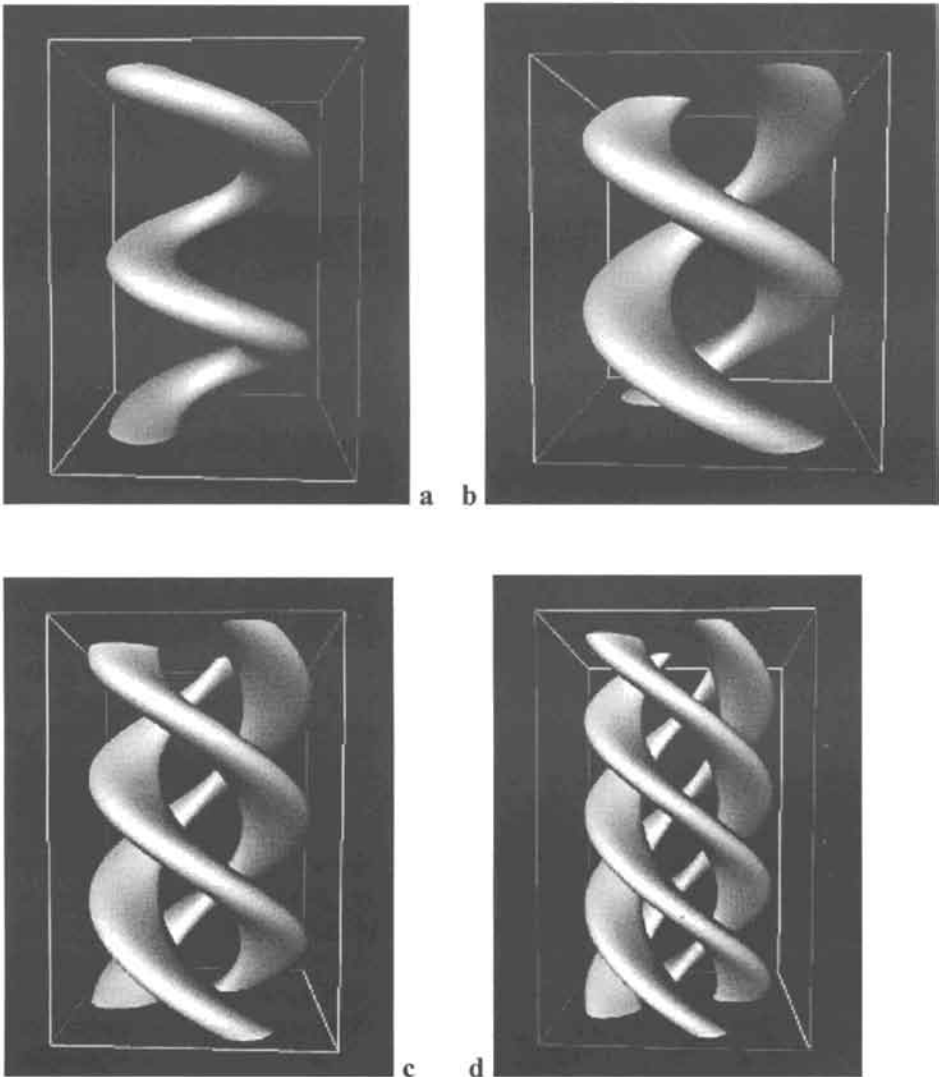


Fig. 5.1.8. (a) Double helicoid from eq. 5.1.6 with $n=2$, $p=0$ and $C=0$.
 (b) The same as in (a), but with $C=0.05$.
 (c) Double helix made from eq. 5.1.6 with $n=2$, $p=0.1$ and $C=0$.

Various multiple spirals are shown in figures 5.1.9 a-h, with the used constants as indicated. Here $n=2$ is a double helix, $n=3$ is a triple helix, $n=4$ quadruple helix etc. It is obvious from these studies why a rope with more than four strands needs a goke, from the cylindrical void in the centre.

Fig. 5.1.9:



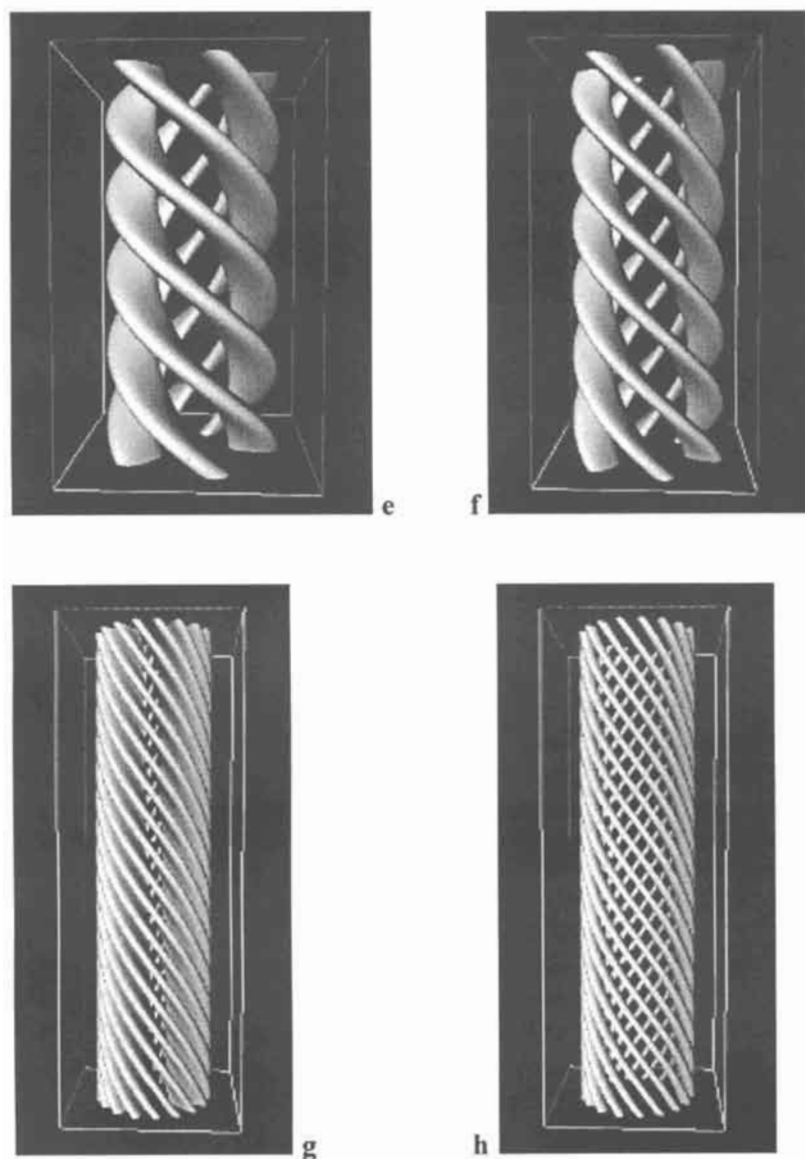


Fig. 5.1.9. Various multiple spirals from eq. 5.1.6. (a) Single helix with $n=1$, $p=0.3$, $C=0$ displayed in the region $-1.4 < x, y < 1.4$, $-2.0 < z < 2.0$. (b) Double helix with $n=2$, $p=0.1$, $C=0$, in the region $-1.7 < x, y < 1.7$, $-2.0 < z < 2.0$. (c) Triple helix, $n=3$, $p=0.05$, $C=0$, in the region $-2 < x, y < 2$, $-3 < z < 3$. (d) Tetragonal helix, $n=4$, $p=0.03$, $C=0$, $-2.5 < x, y < 2.5$, $-4.0 < z < 4.0$. (e) Pentagonal helix, $n=5$, $p=0.02$, $C=0$, $-3.0 < x, y < 3.0$, $-5.0 < z < 5.0$. (f) Hexagonal helix, $n=6$, $p=0.02$, $C=0$, $-3.0 < x, y < 3.0$, $-6.0 < z < 6.0$. (g) 17-fold helix, $n=17$, $p=0.008$, $C=0$, $-6.0 < x, y < 6.0$, $-17.0 < z < 17.0$. (h) Same as (g), but with $C=-10000$.

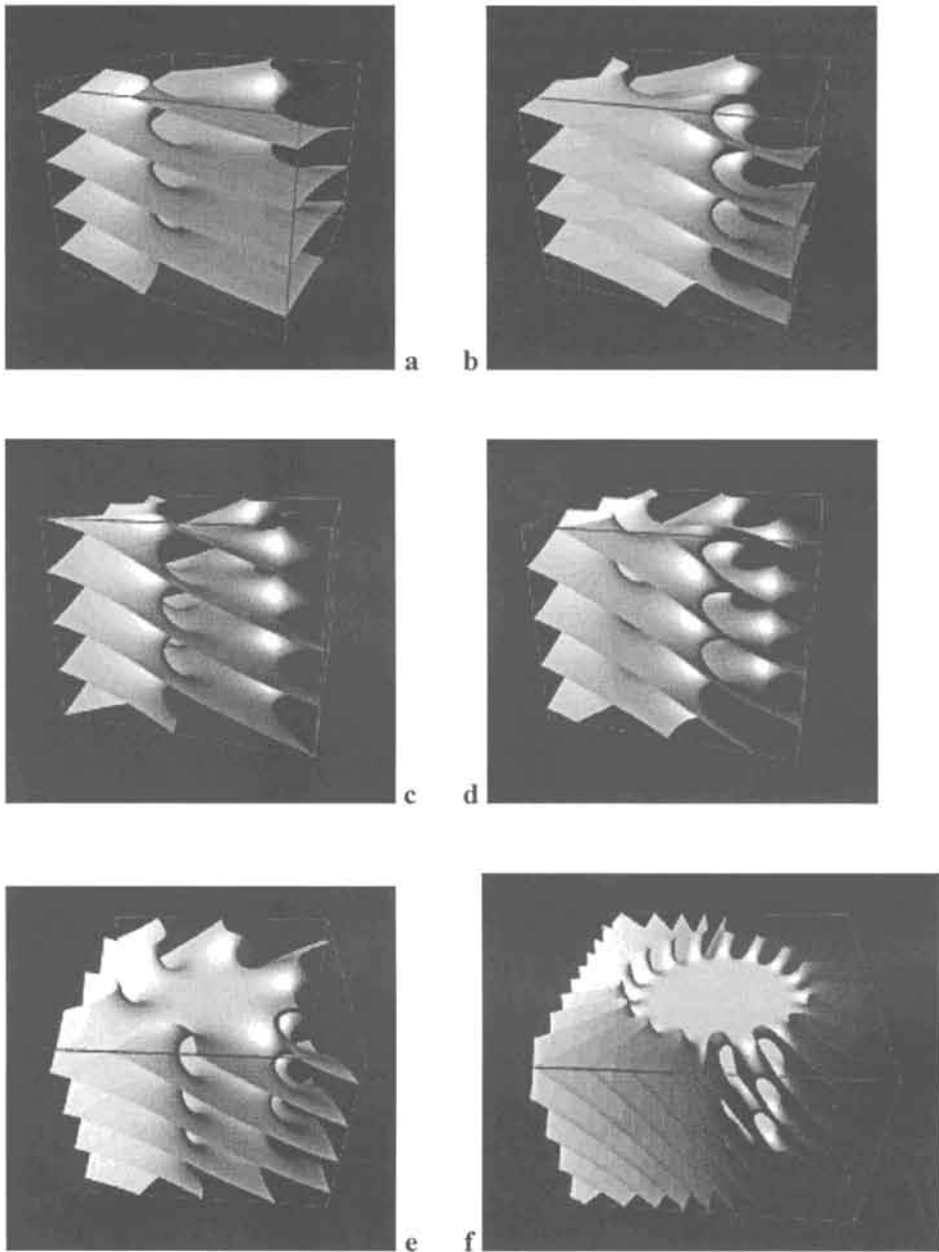


Fig 5.1.10. The helical saddle tower surfaces created with equation 5.1.7 and illustrated for different n -values. (a) Two-fold helical saddle tower with $n=2$, $p=q=\pi$ in the region $-2.5 < x, y < 2.5$, $-2 < z < 2$. (b) $n=3$, $p=q=\pi$, $-2.5 < x, y < 2.5$, $-2 < z < 2$. (c) $n=4$, $p=q=\pi$, $-2.5 < x, y < 2.5$, $-2 < z < 2$. (d) $n=5$, $p=q=\pi$, $-2.5 < x, y < 2.5$, $-2 < z < 2$. (e) $n=6$, $p=q=\pi$, $-2.5 < x, y < 2.5$, $-2 < z < 2$. (f) $n=17$, $p=q=\pi$, $-3 < x, y < 3$, $-2 < z < 2$.

The earlier described tower surfaces can be made into screws to obtain the helicoidal tower surfaces [2] with the equation 5.1.7.

$$\begin{aligned} & \cos(qz) \prod_{i=0}^{i<n} \left[x \cos\left(\frac{i\pi}{n}\right) + y \sin\left(\frac{i\pi}{n}\right) \right] \\ & - \sin(qz) \prod_{i=0}^{i<n} \left[x \cos\left(\frac{i\pi}{n} + \frac{\pi}{2n}\right) + y \sin\left(\frac{i\pi}{n} + \frac{\pi}{2n}\right) \right] - \cos(pz) = 0 \end{aligned} \quad 5.1.7$$

These beautiful surfaces are shown in figures 5.1.10 a-f. The q-value gives the pitch while p controls the distance between the saddles.

Squaring the equations for the building planes of the tower surfaces makes the saddles close up and give the so-called disc surfaces [3]. We give the simplest one in figure 5.1.11 with the equation:

$$x^2 y^2 - \cos z = 0 \quad 5.1.8$$

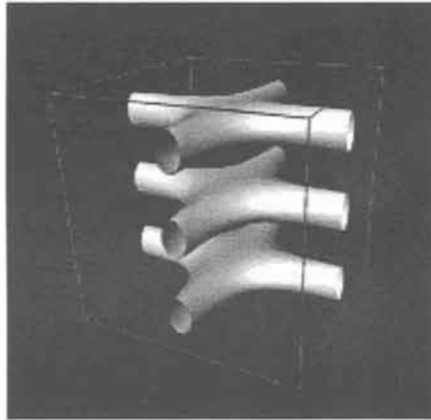


Fig 5.1.11. Tetragonal disc surface with equation $x^2 y^2 = \cos(\pi z)$ illustrated in the region $-3 < x, y, z < 3$.

All these families can be modulated via tilting the planes, and this means of course lowering the symmetry. Beautiful surfaces are obtained and we refer to the original reference for further studies.

These studies above stimulated to derive a mathematical function that describes the DNA spiral [2]. The equation is:

$$xy \cos\left(\frac{\pi z}{10}\right) + \frac{1}{2}(x^2 - y^2) \sin\left(\frac{\pi z}{10}\right) - \cos\left(\frac{\pi z}{2}\right) + \frac{3}{5}e^{(x^2+y^2)/10} = 0 \quad 5.1.9$$

Here a two-fold helical tower surface is used with ten bridging planes per helical pitch. By adding a cylinder exponentially, one side of the surface will close up and result in the structure of figure 5.1.12. This represents a DNA double-helix with ten base pairs per pitch, displaying also the bridging hydrogen bonds created by the saddles.

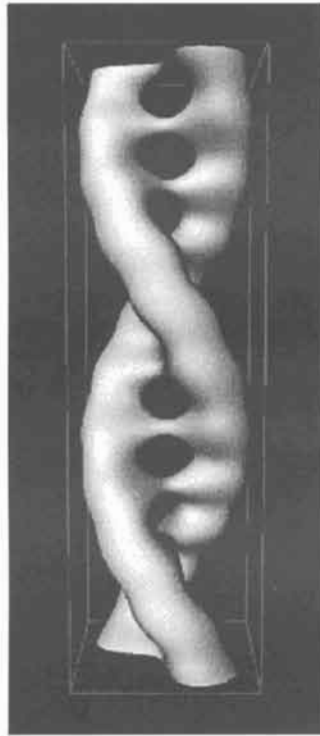


Fig 5.1.12. A function illustrating the DNA double helix chain with the bridging hydrogen bonds created from the two-fold helicoidal saddle tower surface with the addition of a cylinder on the exponential scale, eq. 5.1.9. The tower surface is constructed with ten bridges per pitch in order to model the DNA structure.

5.2 The Bending of a Helix

In the organisation of rods in space later on, rods meet (or touch) each other, and then pack. We just used the cylinder to make a helix above which means helices can pack in space like rods. We shall now bend a helix with the help of cylinders, and as this is a good example of how to work with the exponential scale, we shall carry out this to some detail.

We start making three cylinders with lids according to figs 5.2.1-3, and equations 5.2.1-3.

$$e^{-(x^2+y^2+e^{-z})} = 0.5 \tag{5.2.1}$$

$$e^{-(z^2+y^2+e^{-x}+e^{x-5})} = 0.5 \tag{5.2.2}$$

$$e^{-((x-5)^2+z^2+e^y)} = 0.5 \tag{5.2.3}$$

We add them together in the equation 5.2.4

$$e^{-(x^2+y^2+e^{-z})} + e^{-(z^2+y^2+e^{-x}+e^{x-5})} + e^{-((x-5)^2+z^2+e^y)} = 0.6 \tag{5.2.4}$$

and have the result in fig. 5.2.4 a and b in different projections.

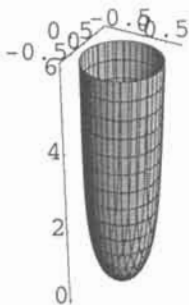


Fig. 5.2.1. Single closed cylinder after equation 5.2.1.

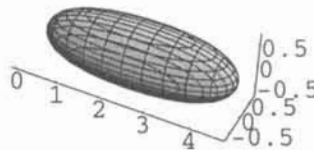


Fig. 5.2.2. Double closed cylinder after equation 5.2.2.

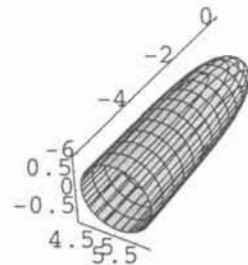


Fig. 5.2.3. Single closed cylinder after equation 5.2.3.

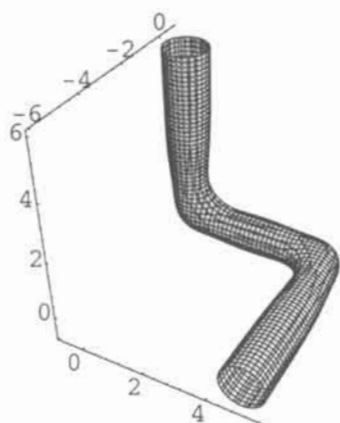


Fig. 5.2.4. a The three cylinders added together at closed ends after equation 5.2.4.

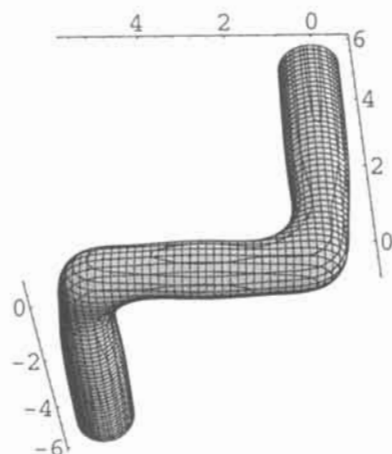


Fig. 5.2.4. b Different projection of a.

We show again how to make a helix out of a helicoid in fig. 5.2.5 after eq. 5.2.5, and we also put a lid on after eq. 5.2.6 to make the helix limited in extension, and form a snake's head as in fig. 5.2.6.

$$x \cos \pi z - y \sin \pi z + x^2 + y^2 = 0.25 \quad 5.2.5$$

$$x \cos \pi z - y \sin \pi z + x^2 + y^2 + e^z = 0.25 \quad 5.2.6$$

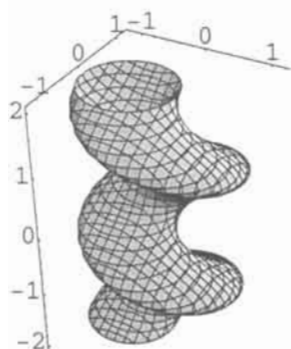


Fig. 5.2.5. The spiral surface again after equation 5.2.5.

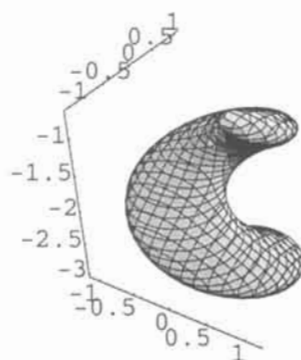


Fig. 5.2.6. A snakes head after equation 5.2.6.

We saw here that a negative constant makes the helix grow thicker - but we need thinner for the bending below, so we use positive constants.

In order to make two helices meet (at snake's heads) we formulate the equation below using eq. 5.2.4 and the exponential scale,

$$e^{-(y \cos \pi x - z \sin \pi x + z^2 + y^2 + e^{x-5} + 0.2)} + e^{-((x-5) \cos \pi y - z \sin \pi y + z^2 + (x-5)^2 + e^y + 0.2)} = 0.6 \quad 5.2.7$$

and the result is illustrated in fig. 5.2.7.

We may also change the periodicity in one of the helices, and also flatten the cylinder as in fig. 5.2.8 after equation 5.2.8. This is the way to change a helix into a loop or band.

$$e^{-(y \cos \pi x - z \sin \pi x + z^2 + y^2 + e^{x-5} + 0.25)} + e^{-((x-5) \cos 0.25 \pi y - z \sin 0.25 \pi y + 3z^2 + (x-5)^2 + e^{(y-0.75)} + 0.4)} = 0.6 \quad 5.2.8$$

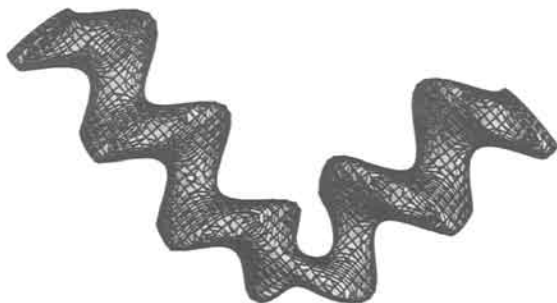


Fig. 5.2.7. Two of the cylinders above used to make two helices meet (at snake's heads) after equation 5.2.7.

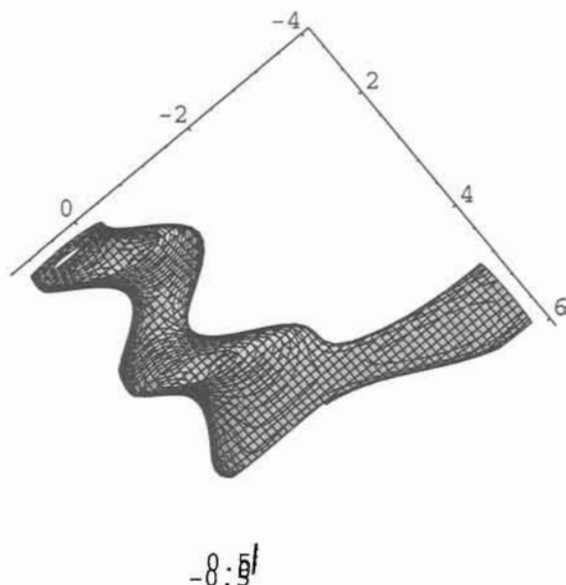


Fig. 5.2.8. A helix is changed into a band or sheet after equation 5.2.8.

The importance of the screw and helix is well known in science and technology - as one example we have just shown the mathematics for the double helix in form of the DNA molecule above [2]. The joining of two helices as in fig. 5.2.7 gives a loop via the snake-heads. The terms in the equation is organised to give a helix-turn-helix structure as it occurs in prokaryotic DNA binding proteins [4].

Obviously one can make bigger structures in this way. A small enzyme molecule like Myoglobine is possible to describe with one mathematical function with a resolution of the level of the experimental one. What requires for this is a big computer, a better graphic program, and plenty of patience.

5.3 Finite Periodicity - Molecules and the Larsson Cubosomes

The derivation of finite structures in two or three dimensions will be continued similarly. We may add spheres or cylinders or planes, as they are contained in a power expansion as shown below. We repeat the power expansions for cos and sin;

$$\cos x = 1 - \frac{x^2}{2!} + \frac{x^4}{4!} - \dots$$

and

$$\sin x = x - \frac{x^3}{3!} + \frac{x^5}{5!} - \dots$$

And rearrange

$$\cos x - 1 + \frac{x^2}{2!} = \frac{x^4}{4!} \quad 5.3.1$$

which in 3D we set

$$2 \cos \pi x + 2 \cos \pi y + 2 \cos \pi z + x^2 + y^2 + z^2 = 2 \quad 5.3.2$$

and is shown in fig. 5.3.1.

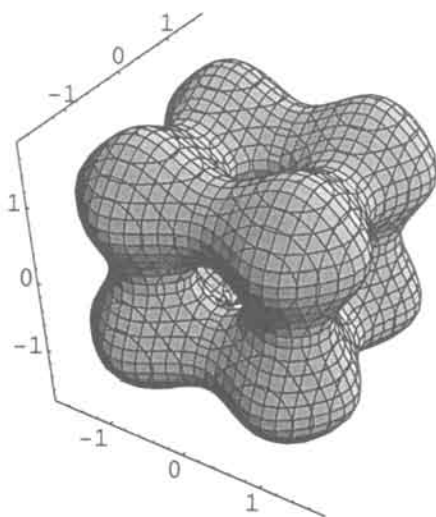


Fig. 5.3.1. Part of the power expansion of cos, after equation 5.3.2.

This part of the expansion of cosine is the ELF structure of the molecule B_6H_6 [7]. It is also the P-surface cut off by a sphere.

The corresponding equation for sine is

$$\sin \pi x + \sin \pi y + \sin \pi z - (x + y + z) = 0 \quad 5.3.3$$

and is shown in two projections in fig 5.3.2 and 5.3.3.

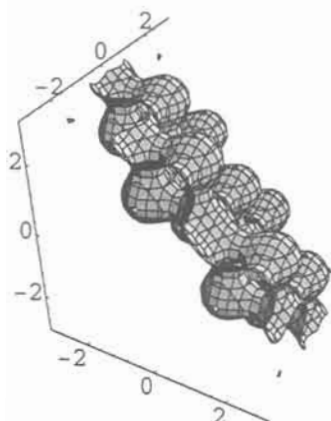


Fig. 5.3.2. Part of the power expansion of sine. After equation 5.3.3.

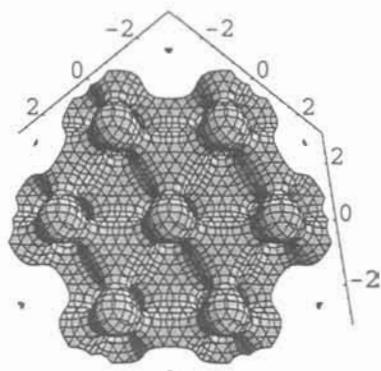


Fig. 5.3.3. Different projection of fig. 5.3.2.

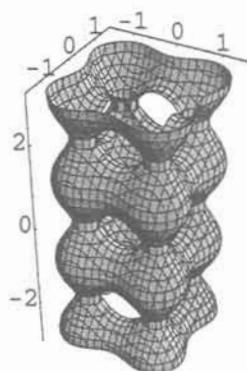


Fig. 5.3.4. Block structure after equation 5.3.4.

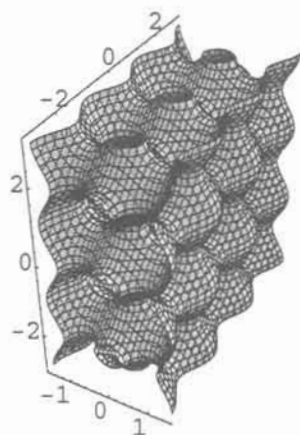


Fig. 5.3.5. Column structure after equation 5.3.5.

In the cosine case one may say we use a sphere, and in the sine case we use a plane. Like above using a cylinder to get a spiral from the helicoid. We add a cylinder to the P-surface, and also two planes in eq. 5.3.4 and 5.3.5, and the result is seen in figures 5.3.4 and 5.3.5.

$$\cos \pi x + \cos \pi y + \cos \pi z + x^2 + y^2 = 1 \quad 5.3.4$$

$$\cos \pi x + \cos \pi y + \cos \pi z + x^2 = 0.5 \quad 5.3.5$$

These three structures - the block (fig. 5.3.1), the column (5.3.4) and the layer (5.3.5) structures are the fundamentals for the building block principle in crystal structures [6,8].

We make more advanced cubosome structures by changing periodicities as in fig 5.3.6, after equation 5.3.6.

$$\cos 2\pi x + \cos 2\pi y + \cos 2\pi z + x^2 + y^2 + z^2 = 2 \quad 5.3.6$$

Slightly changing the equation as to 5.3.7 gives fig 5.3.7 where a number of bodies have condensed, or are just about to.

$$2 \cos 2\pi x + 2 \cos 2\pi y + 2 \cos 2\pi z + x^2 + y^2 + z^2 = 2 \quad 5.3.7$$

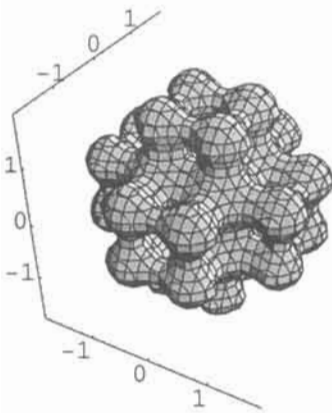


Fig. 5.3.6. A Larsson cubosome made after equation 5.3.6.

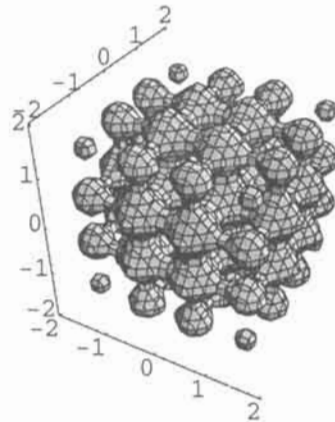


Fig. 5.3.7. Slight change to equation 5.3.7 make bodies land.

We have earlier found, by using similar functions, that we could describe small molecules, or the giant ones like the Larsson cubosomes [5,9,10,11]. We do this here by using the fundamental equation of symmetry and adding its complex exponential. We have then the complete description of a crystal, with its crystal structure and atomic positions from the complex exponential, and the outer shape and its symmetry from the natural exponential.

We add a cube as boundary after equation 5.3.8, which is shown in fig 5.3.8.

$$e^{\cos 3\pi x + \cos 3\pi y + \cos 3\pi z} + e^{x^2} + e^{y^2} + e^{z^2} = 8.7 \quad 5.3.8$$

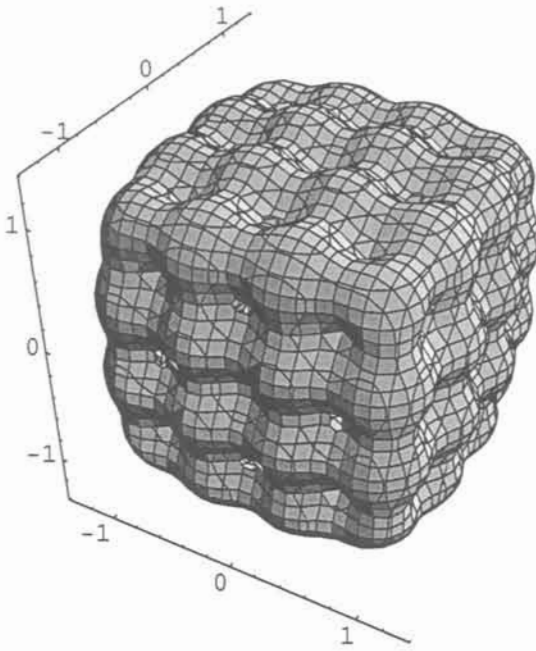


Fig. 5.3.8. A cube as boundary to the P surface after equation 5.3.8.

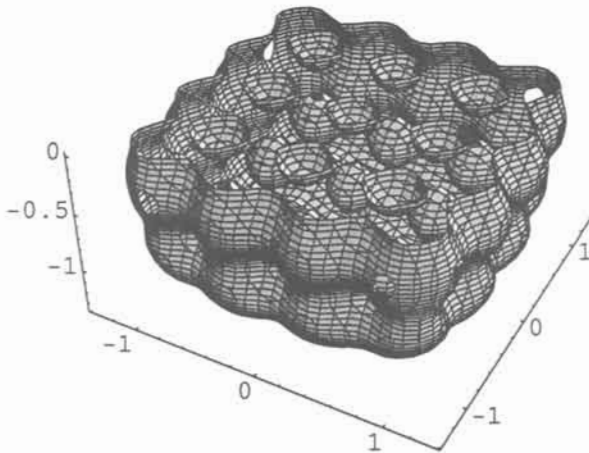


Fig. 5.3.9. A split of fig. 5.3.8.

In fig. 5.3.9 the above structure is shown as a split, revealing 27 atoms in the full cube.

And we make a tetrahedral crystal which is a small cubosome of D type, or of course a piece of diamond after equation 5.3.9, and shown in fig 5.3.10.

$$\begin{aligned}
 & e^{\operatorname{Re}(e^{\pi i(x+y+z)} + e^{\pi i(x-y-z)} + e^{\pi i(-x-y+z)} + e^{\pi i(-x+y-z)})} \\
 & \cdot e^{\operatorname{Im}(e^{\pi i(x+y+z)} + e^{\pi i(x-y-z)} + e^{\pi i(-x-y+z)} + e^{\pi i(-x+y-z)})} \\
 & + e^{x+y+z} + e^{x-y-z} + e^{-x-y+z} + e^{-x+y-z} = 11
 \end{aligned}
 \tag{5.3.9}$$

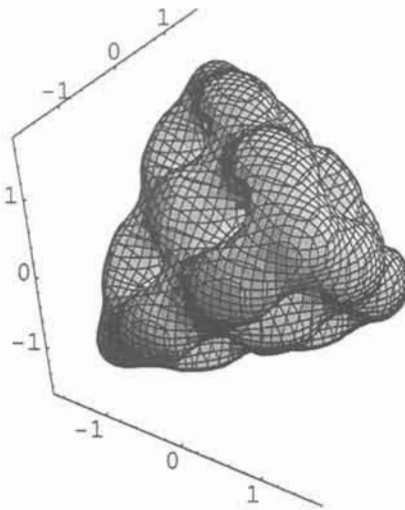


Fig. 5.3.10. A tetrahedron as boundary to the D surface after equation 5.3.9.

The two most common symmetries for the cubosomes are the diamond symmetry with a surface of D-type as above, or the bcc in form of the space group Ia3d, and the surface is then gyroid. So if the diamond surface in fig 5.3.10 represents a very small cubosome, the gyroid surface as seen in fig 5.3.11 is of 'normal' size. The boundary is a cube as in equation 5.3.10.

$$\begin{aligned}
 & e^{\operatorname{Im}(e^{4\pi i(x+y)} + e^{4\pi i(x-y)} + e^{4\pi i(x+z)} + e^{4\pi i(-x+z)} + e^{4\pi i(y+z)} + e^{4\pi i(y-z)})} \\
 & + e^{x^2} + e^{y^2} + e^{z^2} = 5.5
 \end{aligned}
 \tag{5.3.10}$$

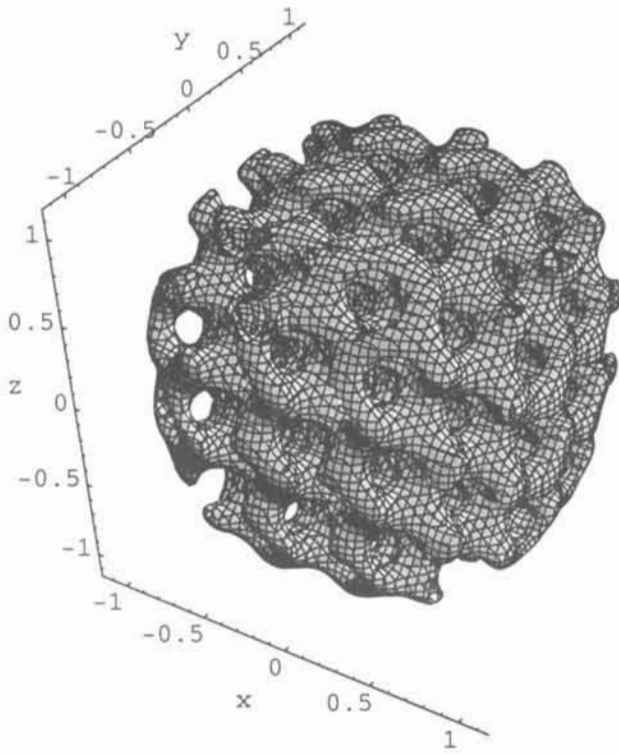


Fig. 5.3.11. A cube and the gyroid surface give a Larsson cubosome after equation 5.3.10.

Exercises 5

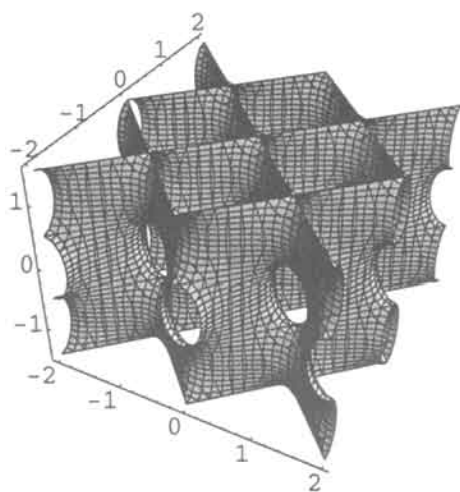
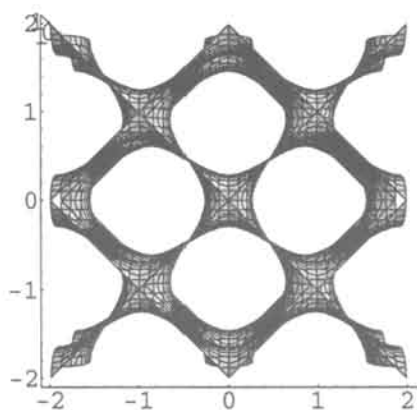
Exercise 5.1. The equation $\frac{\cos \pi y}{\cos \pi x} = e^{\frac{1}{2} \cos \pi z}$ is the nodal correspondence to the CLP minimal surface[12] and can easily be derived from a surface given earlier here. Find it and describe the relationships.

Exercise 5.2. In our lungs there is a multiple layer membrane of essential physiological importance. It has been found with electron microscopy that this layer has the topology of the CLP surface[13], but the boundaries correspond to a 45° rotation along c of the tetragonal coordinate system. Show a piece of this membrane.

Exercise 5.3. Use the simple formula in exercise 4.6 as obtained for the D-nodal surface to construct the smallest possible cubosome, which also is the ELF structure for molecule B_4H_4 .

Answer 5.1

The surface is Scherk's first surface $e^z \cos x = \cos y$, which also is a minimal surface, plotted in exercise 2.5, chapter 2. If made periodic in z it becomes the nodal correspondence of CLP. Below is plotted in two projections the tetragonal nodal surface of CLP from equation above in 5.1.

**Fig. 5.1. a****Fig. 5.1. b** Along the tetragonal axis.**Answer 5.2**

The equation is

$$\cos \frac{\pi}{4}(x-y)e^{\frac{1}{10} \cos \pi z} - \cos \frac{\pi}{4}(x+y) = 0$$

Answer 5.3

The equation and the molecule is below.

$$10^{\cos \pi x \cos \pi y \cos \pi z + \sin \pi x \sin \pi y \sin \pi z} + 10^{(x+y+z)} + 10^{(x-y-z)} + 10^{(-x-y+z)} + 10^{(y-z-x)} = 8$$

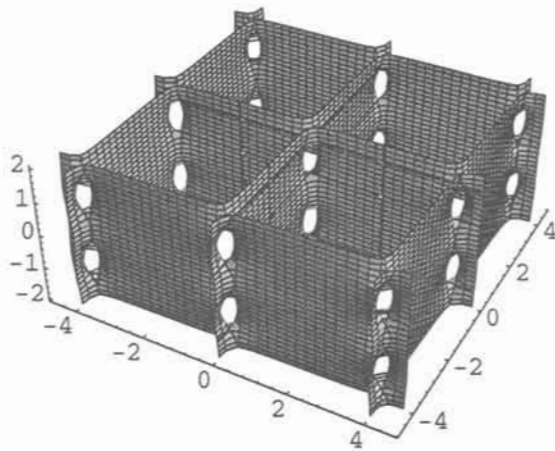


Fig. 5.2.



Fig. 5.3.

References 5

- 1 D. Hilbert and S. Cohn-Vossen, *GEOMETRY and the IMAGINATION*, Chelsea, New York, 1952, page 82.
- 2 Jacob, M, *J.Phys. II France* **7** (1997) 1035-1044.
- 3 U. Dierkes, S. Hildebrandt, A. Kuster and O. Wohlrab, *MINIMAL SURFACES 1 and 2*, Springer Verlag, Berlin, 1991.
- 4 C. Brändén and John Tooze, *INTRODUCTION TO PROTEIN STRUCTURE*, Garland, NewYork, 1991.
- 5 K. Larsson, *J. Phys. Chem.* **93**, 7304 (1989).
- 6 B.G. Hyde and S. Andersson, *INORGANIC CRYSTAL STRUCTURES*, Wiley, New York, 1988.
- 7 A. Burkhardt, U. Wedig, H. G. von Schnering and A. Savin, *Z. anorg. allg. Chem.* **619**, 437 (1993).
- 8 Andersson, S.; Jacob, M.: On the structure of mathematics and crystals, *Z. Kristallogr.* **212** (1997) 334-346.
- 9 S. Andersson, M. Jacob, K. Larsson and S. Lidin, *Z. Kristallogr.* **210** 315 (1995).
- 10 Larsson, K.; Jacob, M.; Andersson, S.: Lipid bilayer standing waves in cell membranes, *Z. Kristallogr.* **211** (1996) 875-878.
- 11 Jacob, M., Larsson, K. and Andersson, S.: Lipid bilayer standing wave conformations in aqueous cubic phases, *Z. Kristallogr.* **212** (1997) 5-8.
- 12 Andersson, S.; Hyde, S.T.; Larsson, K.; Lidin, S.: Minimal surfaces and structures: From inorganic and metal crystals to cell membranes and biopolymers. *Chemical Reviews*, **88** (1988) 221-242.
- 13 Larsson, K.; and Larsson, M.; Private communication.

6 Multiplication, Nets and Planar Groups

'makes it surprising that geometers have not explored this field during the past two thousand years' (Wells, Three dimensional nets and polyhedra [1]).

Here we go circular with the general saddle equation. We derive mathematical equations for nets and the planar square groups, and also the quasi-periodic symmetry. Extending to 3D we give the mathematics for some fundamental metal structure types like hcp, AlB_2 , CaZn_5 and CuAl_2 .

6.1 Lines and Saddles

In this chapter we go to multiplication, after addition and subtraction of the circular functions. We find a way to describe nets, and here we shall develop them in 2D and also go to 3D. We have earlier given some nets in 3D [2,3].

Nets in 2D have always fascinated mankind. Why is hard to understand, but perhaps it is the mysterious periodicity, and the property of symmetry, perhaps it is the applications in crystal chemistry, or in art as the Alhambra ornaments, or carpets or just wall paper.

The approach could be to go circular via the equation for polygons (eq. 3.1.11) or the finite products of the fundamental theorem of algebra (eq. 2.1.4 or 2.2.2). Or the multiple eigenvalues for a square membrane of eigenfunctions of type $\sin mx \sin my + \sin nx \sin my$, which give similar or identical results [10].

The approach we have taken is the saddle mathematics [4] where the products of equations of intersecting planes were used as in equation 2.3.5. We shall only use a few planes, up to five and the equations for these planes are:

$$xy = 0 \tag{6.1.1}$$

$$x\left(\frac{x}{2} + \frac{\sqrt{3}}{2}y\right)\left(-\frac{x}{2} + \frac{\sqrt{3}}{2}y\right) = 0 \tag{6.1.2}$$

$$xy(x+y)(x-y) = 0 \quad 6.1.3$$

$$x\left(\frac{\tau}{2}x + \frac{\sqrt{1+\tau^2}}{2\tau}y\right)\left(\frac{\tau-1}{2}x + \frac{\sqrt{1+\tau^2}}{2}\right) \quad 6.1.4$$

$$\cdot\left(-\frac{\tau-1}{2} + \frac{\sqrt{1+\tau^2}}{2}\right)\left(-\frac{\tau}{2}x + \frac{\sqrt{1+\tau^2}}{2\tau}\right) = 0$$

We give the corresponding figures in 6.1.1-4.

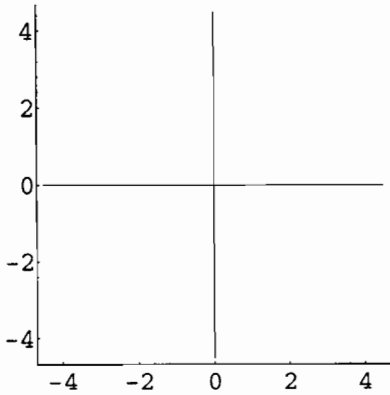


Fig. 6.1.1. After equation 6.1.1.

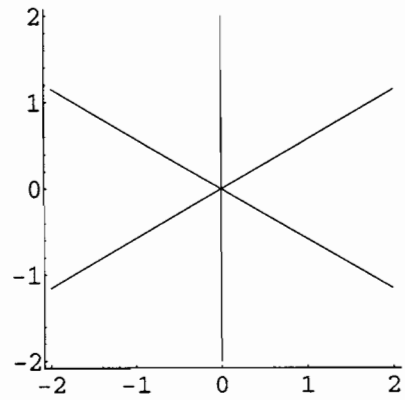


Fig. 6.1.2. After equation 6.1.2.

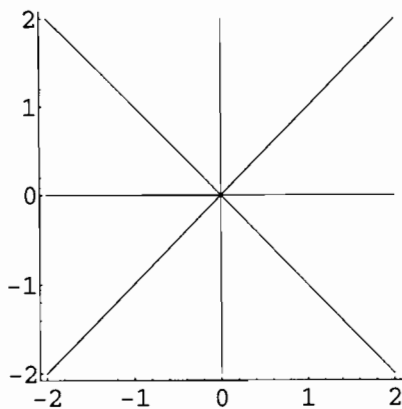


Fig. 6.1.3. After equation 6.1.3.

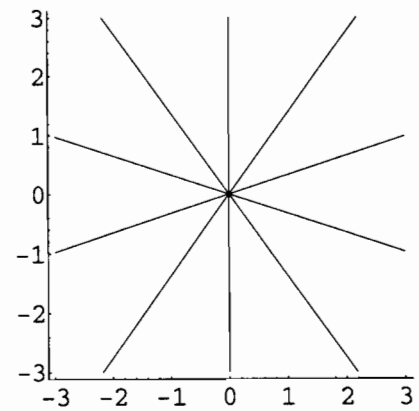


Fig. 6.1.4. After equation 6.1.4

6.2 Nets with Two Planes, and Variations

Multiplication of the type

$$\sin \pi x \sin \pi y = 0 \tag{6.2.1}$$

gives the saddle net repeated in fig. 6.2.1, and with a constant as in eq. 6.2.2 there is the structure in fig. 6.2.2.

$$\sin \pi x \sin \pi y = 0.8 \tag{6.2.2}$$

There are various ways to proceed and get beautiful nets and we restrict us to a simple one with equations of the type

$$\sin \pi x \sin \pi y + \sin n\pi x \sin n\pi y = C$$

For equations 6.2.3 and 6.2.4 there are the beautiful nets of figures 6.2.3 and 6.2.4.

$$\sin \pi x \sin \pi y + \sin 3\pi x \sin 3\pi y = 0.8 \tag{6.2.3}$$

$$\sin \pi x \sin \pi y + \sin 5\pi x \sin 5\pi y = 0.4 \tag{6.2.4}$$

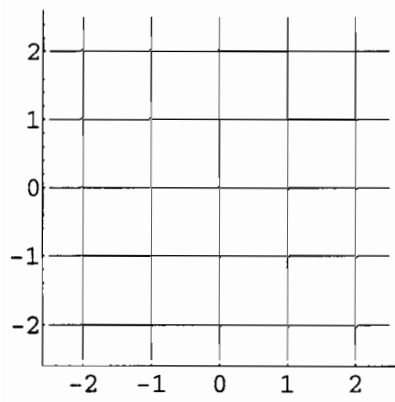


Fig. 6.2.1. After equation 6.2.1 with C=0.

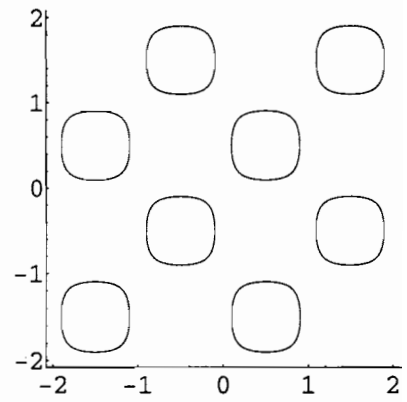


Fig. 6.2.2. C=0.8

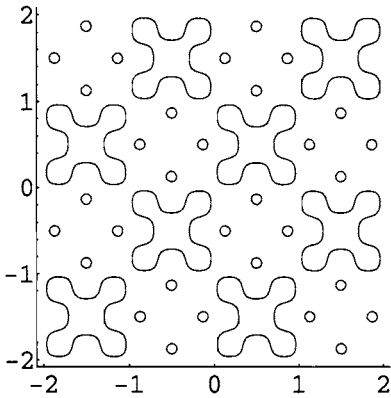


Fig. 6.2.3. After equation 6.2.3.

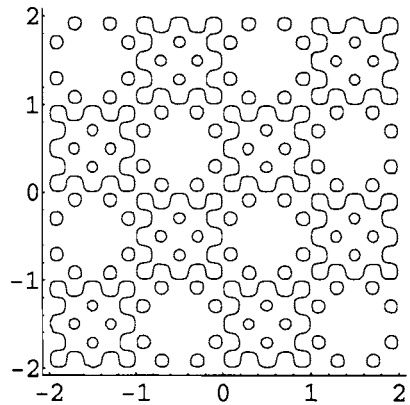


Fig. 6.2.4. After equation 6.2.4.

And for cosine there are the equations 6.2.5 and 6.2.6 and the nets in figs. 6.2.5 and 6.2.6.

$$\cos \pi x \cos \pi y + \cos 2\pi x \cos 2\pi y = 0.5 \quad 6.2.5$$

$$\cos \pi x \cos \pi y + \cos 4\pi x \cos 4\pi y = 0.8 \quad 6.2.6$$

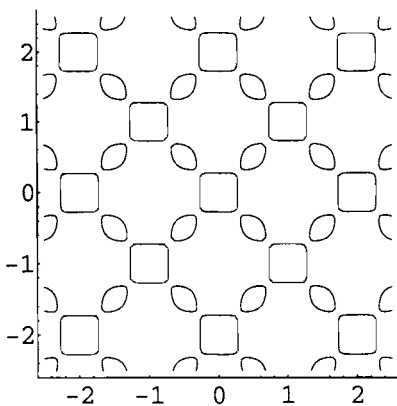


Fig. 6.2.5. After equation 6.2.5.

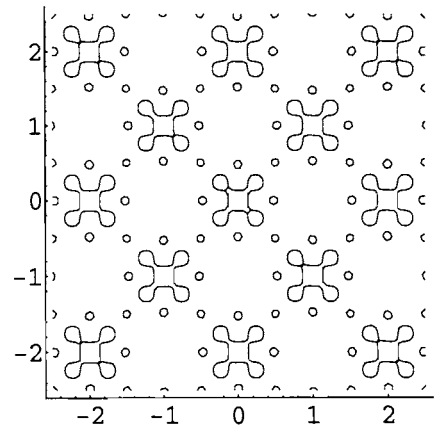


Fig. 6.2.6. After equation 6.2.6.

6.3 Nets with Three Planes, and Variations

Multiplication of the type

$$\sin \pi x \sin \pi \left(\frac{x}{2} + \frac{\sqrt{3}}{2} y \right) \sin \pi \left(-\frac{x}{2} + \frac{\sqrt{3}}{2} y \right) = 0 \tag{6.3.1}$$

$$\sin \pi x \sin \pi \left(\frac{x}{2} + \frac{\sqrt{3}}{2} y \right) \sin \pi \left(-\frac{x}{2} + \frac{\sqrt{3}}{2} y \right) = 0.1 \tag{6.3.2}$$

which gives intersecting lines in fig. 6.3.1, and with a constant of 0.1 we have a primitive trigonal structure as seen in fig. 6.3.2. We continue like above in the equations 6.3.3 and 4 which give the trigonal nets of figures 6.3.3 and 6.3.4.

$$\begin{aligned} &\sin \pi x \sin \pi \left(\frac{x}{2} + \frac{\sqrt{3}}{2} y \right) \sin \pi \left(-\frac{x}{2} + \frac{\sqrt{3}}{2} y \right) \\ &+ \sin 2\pi x \sin 2\pi \left(\frac{x}{2} + \frac{\sqrt{3}}{2} y \right) \sin 2\pi \left(-\frac{x}{2} + \frac{\sqrt{3}}{2} y \right) = 0.5 \end{aligned} \tag{6.3.3}$$

$$\begin{aligned} &\sin \pi x \sin \pi \left(\frac{x}{2} + \frac{\sqrt{3}}{2} y \right) \sin \pi \left(-\frac{x}{2} + \frac{\sqrt{3}}{2} y \right) \\ &+ \sin 3\pi x \sin 3\pi \left(\frac{x}{2} + \frac{\sqrt{3}}{2} y \right) \sin 3\pi \left(-\frac{x}{2} + \frac{\sqrt{3}}{2} y \right) = 0.4 \end{aligned} \tag{6.3.4}$$

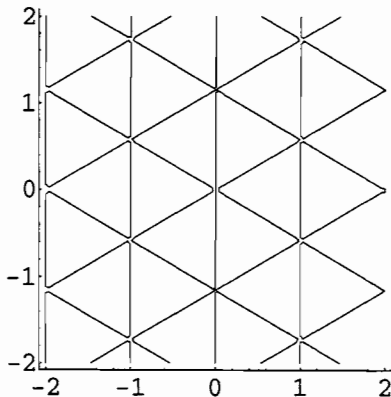


Fig. 6.3.1. After equation 6.3.1 with C=0.

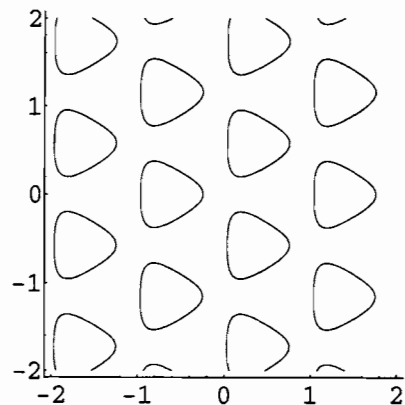


Fig. 6.3.2. As in fig. 6.3.1 but with C=0.1.

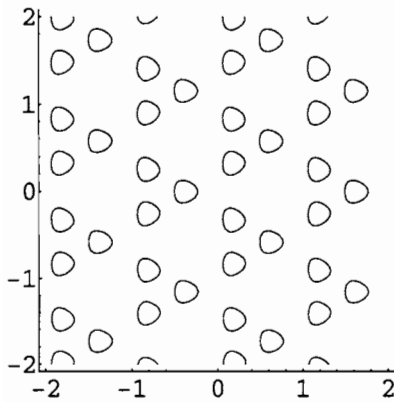


Fig. 6.3.3. After equation 6.3.3.

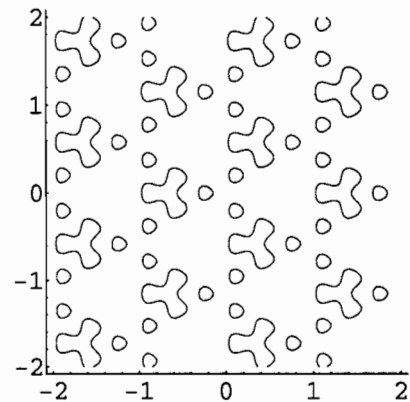


Fig. 6.3.4. After equation 6.3.4.

Multiplication of the type

$$\cos \pi x \cos \pi \left(\frac{x}{2} + \frac{\sqrt{3}}{2} y \right) \cos \pi \left(-\frac{x}{2} + \frac{\sqrt{3}}{2} y \right) = C \quad 6.3.5$$

gives the Kagomé in fig. 6.3.5, and with a constant of 0.3 we have a hexagonal structure, fig. 6.3.6. We continue like above in the equations 6.3.6 and 7 which give the hexagonal nets of figures 6.3.7 (eq. 6.3.6), 6.3.8 (eq. 6.3.7, $C=0.2$) and 6.3.9 (eq. 6.3.7, $C=0.8$), the last net very similar to the Apatite structure.

$$\begin{aligned} & \cos \pi x \cos \pi \left(\frac{x}{2} + \frac{\sqrt{3}}{2} y \right) \cos \pi \left(-\frac{x}{2} + \frac{\sqrt{3}}{2} y \right) \\ & + \cos 2\pi x \cos 2\pi \left(\frac{x}{2} + \frac{\sqrt{3}}{2} y \right) \cos 2\pi \left(-\frac{x}{2} + \frac{\sqrt{3}}{2} y \right) = 0.5 \end{aligned} \quad 6.3.6$$

$$\begin{aligned} & \cos \pi x \cos \pi \left(\frac{x}{2} + \frac{\sqrt{3}}{2} y \right) \cos \pi \left(-\frac{x}{2} + \frac{\sqrt{3}}{2} y \right) \\ & + \cos 3\pi x \cos 3\pi \left(\frac{x}{2} + \frac{\sqrt{3}}{2} y \right) \cos 3\pi \left(-\frac{x}{2} + \frac{\sqrt{3}}{2} y \right) = C \end{aligned} \quad 6.3.7$$

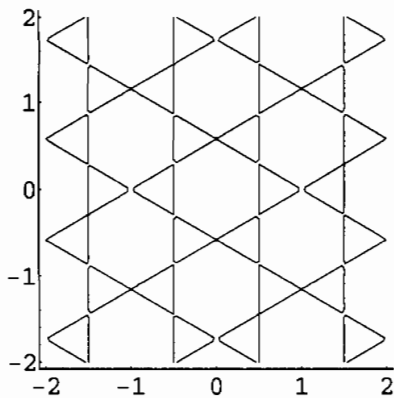


Fig. 6.3.5. After equation 6.3.5 with $C=0$.

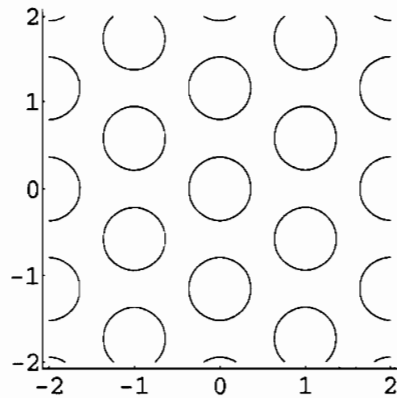


Fig. 6.3.6. As in fig. 6.3.5 but with $C=0.3$.

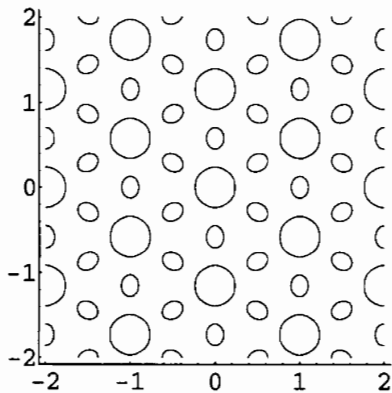


Fig. 6.3.7. After equation 6.3.6.

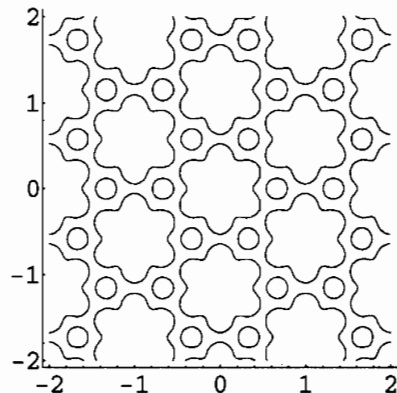


Fig. 6.3.8. After equation 6.3.7 with $C=0.2$.

These are well-known nets in the solid state science that represent crystal structures, and many more may be obtained by varying the equations. An example is in equation 6.3.8 below with multiplication of terms instead of addition and the result is a projection of the structure of the zeolite Gmelinite as shown in fig. 6.3.10.

$$\begin{aligned} & \sin \pi x \sin \pi \left(\frac{x}{2} + \frac{\sqrt{3}}{2} y \right) \sin \pi \left(-\frac{x}{2} + \frac{\sqrt{3}}{2} y \right) \\ & \cdot \sin 4\pi x \sin 4\pi \left(\frac{x}{2} + \frac{\sqrt{3}}{2} y \right) \sin 4\pi \left(-\frac{x}{2} + \frac{\sqrt{3}}{2} y \right) = 0.1 \end{aligned} \quad 6.3.8$$

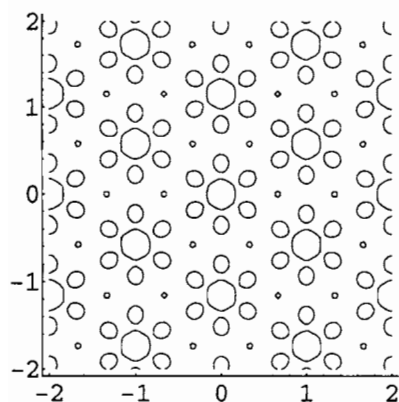


Fig. 6.3.9. After equation 6.3.7 with $C=0.8$.

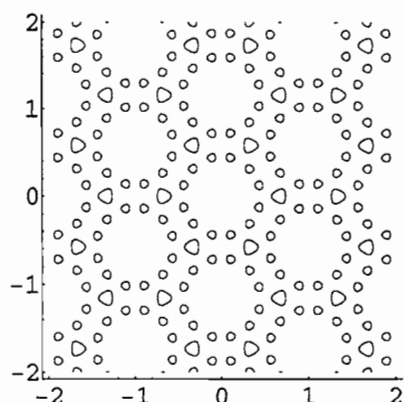


Fig. 6.3.10. After equation 6.3.8 the zeolite Gmelinite.

6.4 Nets with Four Planes, and Variations

We continue with four planes from the saddle equation, and eq. 6.4.1 gives the structure of CuAl_2 shown in fig. 6.4.1.

$$\sin \pi x \sin \pi y \sin \pi(x+y) \sin \pi(x-y) = 0.3 \quad 6.4.1$$

Cosine instead of sine as in eq. 6.4.2 gives a zeolite similar structure in fig. 6.4.2.

$$\cos \pi x \cos \pi y \cos \pi(x+y) \cos \pi(x-y) = 0.1 \quad 6.4.2$$

A simple phase shift as in eq. 6.4.3 gives for the two different constants, 0.3 and 0.1, the two figures 6.4.3 and 6.4.4.

$$\begin{aligned} &\sin \pi x \sin \pi y \sin \pi(x + y) \sin \pi(x - y) \\ &+ \cos \pi x \cos \pi y \cos \pi(x + y) \cos \pi(x - y) = C \end{aligned} \tag{6.4.3}$$

Interesting with these simple functions is that they describe the three square planar groups of crystallography [5]. The symmetries of the structures correspond to the groups **p4**, **p4m** and **p4g** (no 10, 11, and 12).

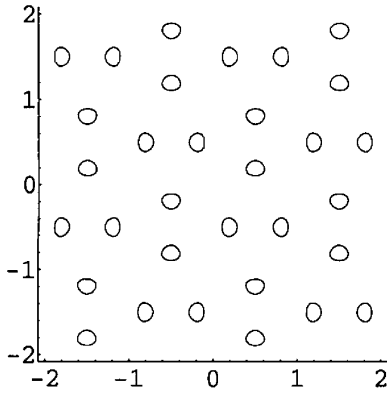


Fig. 6.4.1. After equation 6.4.1.

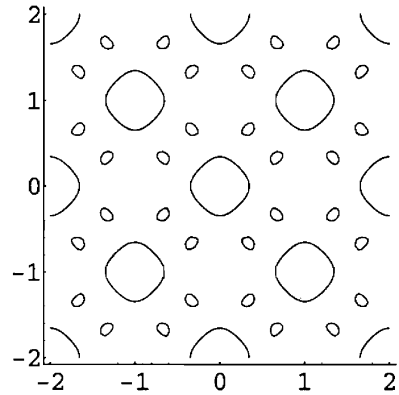


Fig. 6.4.2. After equation 6.4.2.

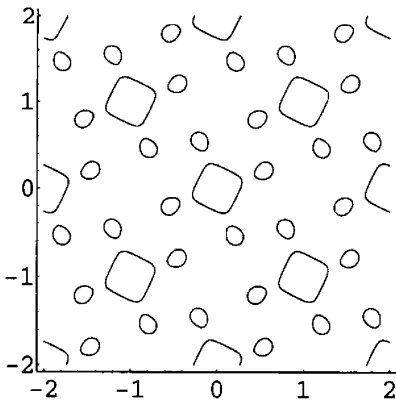


Fig. 6.4.3. After equation 6.4.3 with $C=0.3$.

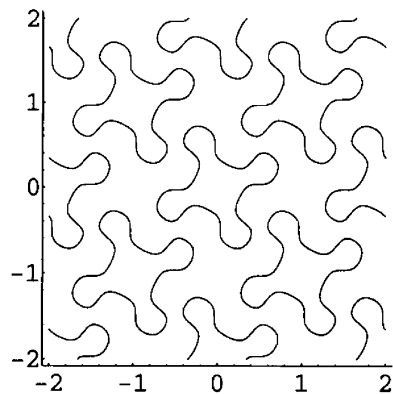


Fig. 6.4.4. After equation 6.4.3 with $C=0.1$.

6.5 Structures in 3D from the Nets

This is not a general study of nets in 3D - we have touched that before - 3D is a vast subject.

We continue on the approach above and an equation like $\sin x \cdot \sin y \cdot \sin z$ which we know gives intersecting planes in space. A non-zero constant gives a primitive structure of bodies (which joint with straight lines gives the simplest possible 3D net). The cosine addition in $\sin x \cdot \sin y \cdot \sin z + \cos x \cdot \cos y \cdot \cos z$ gives the diamond net and so on. This we also saw in chapter 2 in the study of the fundamental theorem of algebra in three dimensions.

We try below a somewhat different road going to 3D with the net functions of 2D just derived. Using the simple functions extended to 3D in a cubic way give the simple and fundamental structures described earlier in this book. As an example of the more complicated structures that quickly turn up at a systematic variation of equations we apply addition and multiplication and do permutations in space for a simple equation as below in 6.5.1. The structure of this is shown in fig. 6.5.1.

$$\begin{aligned} \sin \pi x \sin \pi y \sin 2\pi x \sin 2\pi y + \sin \pi x \sin \pi z \sin 2\pi x \sin 2\pi z \\ + \sin \pi z \sin \pi y \sin 2\pi z \sin 2\pi y = 0.6 \end{aligned} \quad 6.5.1$$

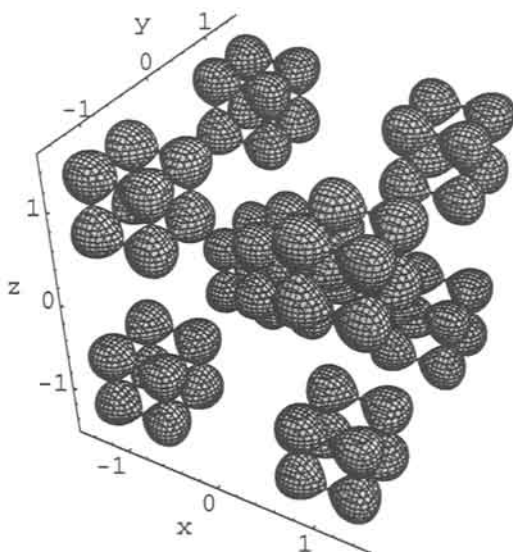


Fig. 6.5.1. A simple equation as in 6.5.1 gives this formidable structure in space.

Joining the centres of these bodies gives of course a bcc net.

For the hexagonal nets we use the simplest of the equations above and first we multiply with a z-term as in equations 6.5.2 and 6.5.3. In the corresponding figures 6.5.2 and 6.5.3 there are the structures of hexagonal close packing and AlB_2 resp. The small bodies are the boron atoms.

$$\sin 2\pi x \sin 2\pi \left(\frac{x}{2} + \frac{\sqrt{3}}{2} y \right) \sin 2\pi \left(-\frac{x}{2} + \frac{\sqrt{3}}{2} y \right) \sin 2\pi z = 0.1 \quad 6.5.2$$

$$\cos 2\pi x \cos 2\pi \left(\frac{x}{2} + \frac{\sqrt{3}}{2} y \right) \cos 2\pi \left(-\frac{x}{2} + \frac{\sqrt{3}}{2} y \right) \sin 3\pi z = 0.06 \quad 6.5.3$$

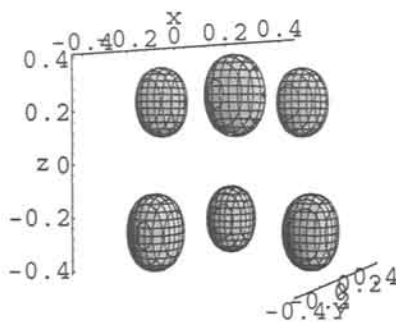


Fig. 6.5.2. Hcp structure after equation 6.5.2.

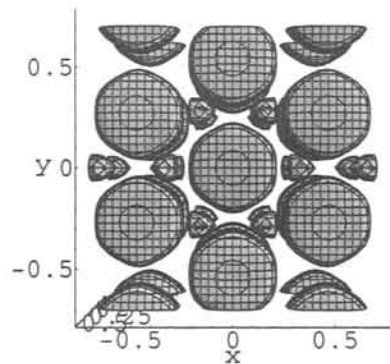


Fig. 6.5.3. AlB_2 structure after equation 6.5.3.

Addition and sine gives the H surface at zero constant by using eq. 6.5.4, which with the constant of 0.9 gives a polyhedral description of hcp, in form of trigonal bipyramids sharing corners as in fig. 6.5.4.

$$3 \sin 2\pi x \sin 2\pi \left(\frac{x}{2} + \frac{\sqrt{3}}{2} y \right) \sin 2\pi \left(-\frac{x}{2} + \frac{\sqrt{3}}{2} y \right) + \sin 3\pi z = C \quad 6.5.4$$

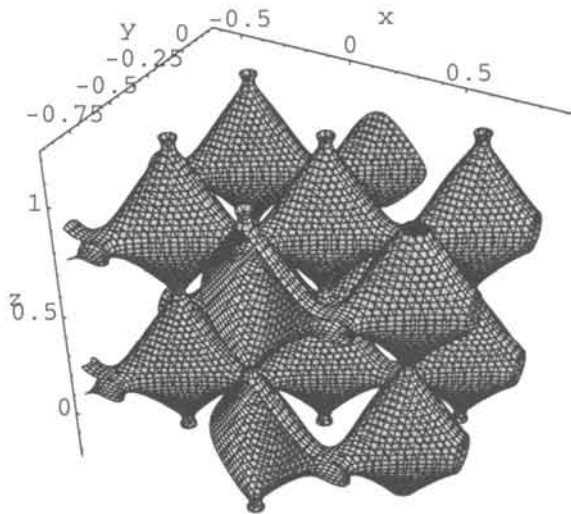


Fig. 6.5.4. Trigonal bipyramids describe the hcp structure after equation 6.5.4.

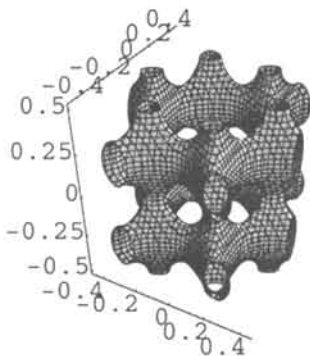


Fig. 6.5.5. Trigonal bipyramids describe the CaZn_5 structure after equation 6.5.5.

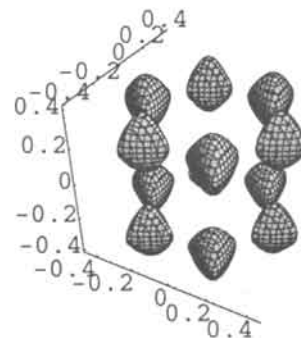


Fig. 6.5.6. Change of constant to 0.3 in 6.5.5 makes the Zn atoms show up.

Cosine as in eq. 6.5.5 below gives the surface of fig. 6.5.5 which is useful for the CaZn_5 structure. Adding a constant of 0.3 makes the Zn atoms show up in fig. 6.5.6.

$$3 \cos 2\pi x \cos 2\pi \left(\frac{x}{2} + \frac{\sqrt{3}}{2} y \right) \cos 2\pi \left(-\frac{x}{2} + \frac{\sqrt{3}}{2} y \right) + 0.25 \cos 4\pi z = 0 \quad 6.5.5$$

We go 3D with four planes adding a z-term after eq. 6.5.6.

$$6 \sin \pi x \sin \pi y \sin \pi(x+y) \sin \pi(x-y) + \sin 2\pi z = 0 \quad 6.5.6$$

A beautiful surface for the CuAl_2 structure is shown in fig. 6.5.7. In 6.5.8 we see the Al atoms of the crystal structure of CuAl_2 from multiplication with the z-term in equation 6.5.7.

$$6 \sin \pi x \sin \pi y \sin \pi(x+y) \sin \pi(x-y) \sin 2\pi z = 0.75 \quad 6.5.7$$

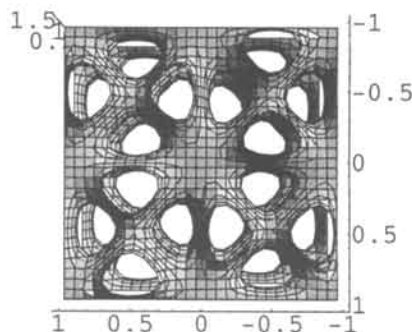


Fig. 6.5.7. A surface for the CuAl_2 structure after 6.5.6.

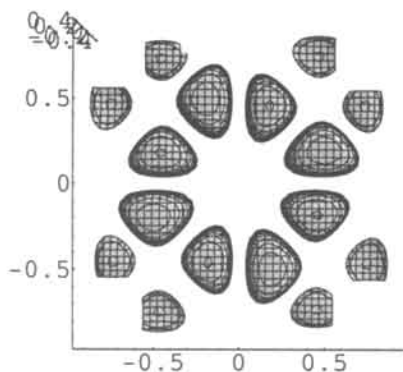


Fig. 6.5.8. The Al atoms in CuAl_2 show up after 6.5.7.

6.6 Quasi

This long-range order without periodic translation has recently been reviewed by one of us [6], and the structure of the icosahedral case has also been separately reported [7,8].

6.6.1 Four Planes and Quasi

With four planes or more, the use of irrational numbers in eq. 6.6.1 from the general saddle equation brings out quasi-periodic symmetry as shown in fig. 6.6.1 for a constant of 0.

$$\sin \pi x \sin \pi y \sin \left[\frac{\sqrt{2}}{2} \pi (x + y) \right] \sin \left[\frac{\sqrt{2}}{2} \pi (x - y) \right] = C \quad 6.6.1$$

The quasi symmetry is more obvious in fig. 6.6.2, calculated for a constant of 0.2.

The structure in fig. 6.6.2 can be understood as close to an interpenetrating fourling of the CuAl_2 structure.

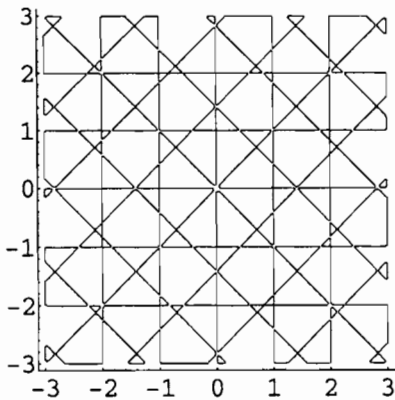


Fig. 6.6.1. After equation 6.6.1 with $C=0$.

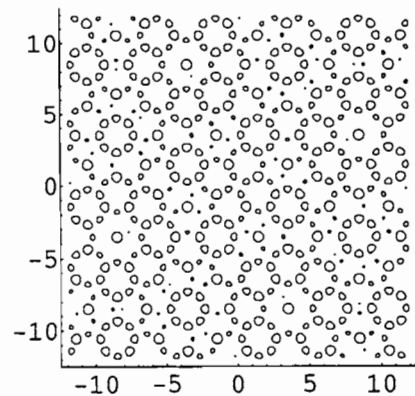


Fig. 6.6.2. After equation 6.6.1 with $C=0.2$.

6.6.2 Five Planes and Quasi

Five planes in the saddle way in eq. 6.6.2, and with sine and a constant of 0.31, shows a beautiful 5-fold quasi periodic symmetry in fig. 6.6.3, outside the origin. In analogy with observations above, this should be a structure, and it is remarkable how well it agrees with the quasi-structure model as derived [6,7,8]. Going cosine and a constant of 0.25 gives fig. 6.6.4, which looks exactly as the Fourier transform, or the commonly shown diffraction patterns of Al alloys.

$$\begin{aligned} & \sin 2\pi x \sin 2\pi \left(\frac{\tau}{2} x + \frac{\sqrt{1+\tau^2}}{2\tau} y \right) \sin 2\pi \left(\frac{\tau-1}{2} x + \frac{\sqrt{1+\tau^2}}{2} \right) \\ & \cdot \sin 2\pi \left(-\frac{\tau-1}{2} + \frac{\sqrt{1+\tau^2}}{2} \right) \sin 2\pi \left(-\frac{\tau}{2} x + \frac{\sqrt{1+\tau^2}}{2\tau} \right) = C \end{aligned} \tag{6.6.2}$$

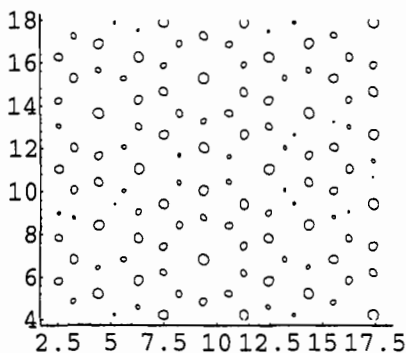


Fig. 6.6.3. After equation 6.6.2 with C=0.31.

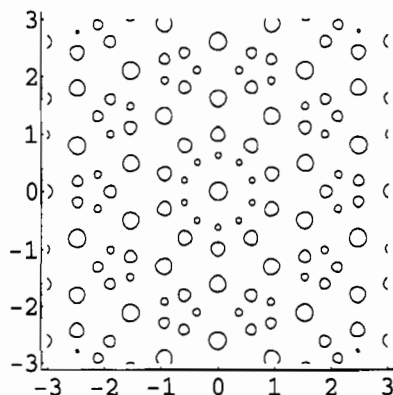


Fig. 6.6.4. After equation 6.6.2 with cosine and C=0.25.

A slight deviation from numbers containing τ (after eq. 6.6.3, with 0.8 instead of $\tau/2$ as an example) gives a beautiful structure of translational symmetry in fig. 6.6.5.

$$\begin{aligned} & \cos 2\pi x \cos 2\pi(0.8x + 0.6y) \cos 2\pi(0.3x + y) \\ & \cdot \cos 2\pi(-0.3090x + y) \cos 2\pi(-0.8x + 0.6y) = 0.5 \end{aligned} \tag{6.6.3}$$

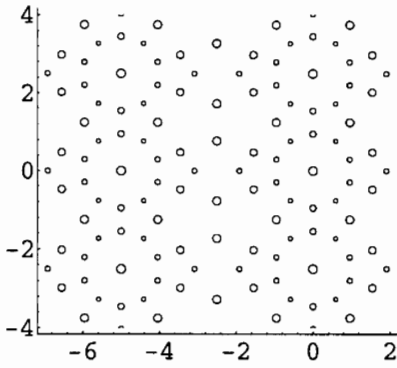


Fig. 6.6.5. Translational symmetry after equation 6.6.3.

Exercises 6

Exercise 6.1. Do four planes with cosine. Analyse!

Exercise 6.2. Go commensurate with sine and four planes, and show the relation to the CuAl_2 structure.

Exercise 6.3. Go commensurate with cosine and discuss the translational structure.

Exercise 6.4. Show the nets that build the structures for five, six, seven and ten planes (these are dilated variants of the circulants graphs as described by Skiena [11] - the vertices are pulled out to infinity).

Answer 6.1

The four planes build two identical square nets that interpenetrate to an incommensurate structure as in fig 6.1a. Notice the shift of centre compared to sine. A small constant shows the beautiful eight fold symmetry in 6.1b. The equation is as in 6.6.1 with constant of zero and 0.1 respectively, and cosine of course.

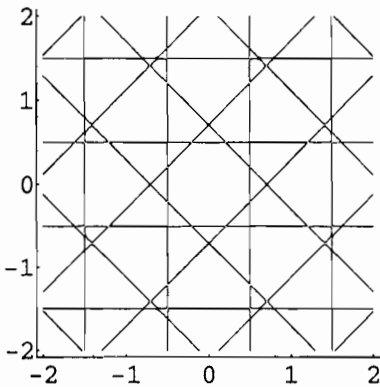


Fig. 6.1a.

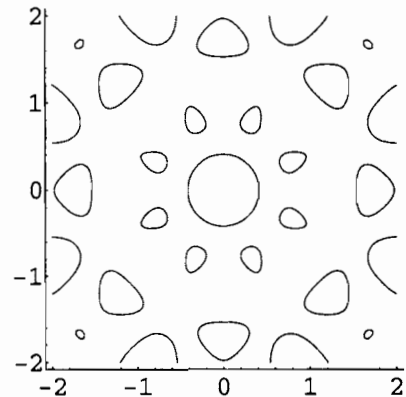


Fig. 6.1b.

Answer 6.2

The equation is

$$\sin \pi x \sin \pi y \sin \left[\frac{7}{10} \pi (x+y) \right] \sin \left[\frac{7}{10} \pi (x-y) \right] = 0.65$$

and the relation to CuAl_2 is obvious. The origin of the unit cell of the commensurate structure is from permutations of type 0,0; 0,10; etc.

Answer 6.3

The equation is

$$\cos \pi x \cos \pi y \cos \left[\frac{7}{10} \pi (x+y) \right] \cos \left[\frac{7}{10} \pi (x-y) \right] = 0.7$$

and the fourfold symmetry shows up beautifully in a zeolite like structure.

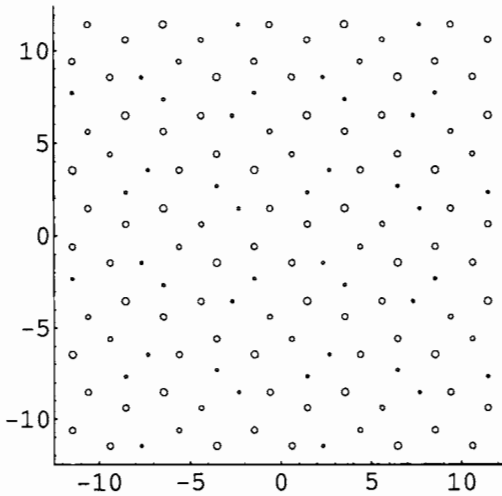


Fig. 6.2.

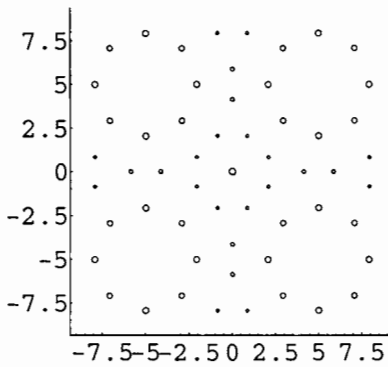


Fig. 6.3.

Answer 6.4

The term incommensurate was used already in the English translations of Euclid, *The Elements*, with reference to the discovery of the irrational as due to the Pythagoreans [9]. The incommensurate net in answer 6.1a, and its relation to the square commensurate nets as discussed above, was surely known to the Greeks. As well as what is given below.

Use the general saddle equation from 2.3.5 in 2D:

$$\prod_{i=0}^{i < n} [x \cos(\frac{i\pi}{n}) + y \sin(\frac{i\pi}{n})] = 0 \quad 6.4.a$$

We derive the equations and from the graphs below we conclude that in the description of the n -fold rotation symmetry the intersections-or the symmetries-are derived from the rotations of simple nets of translational periodicity. For n even there are always square nets, and for n odd there are always rhombic nets, with the rhombic angles directly related to the $n/2\pi$.

$$\begin{aligned} & \sin \pi x \sin \pi (x \cos \frac{\pi}{5} + y \sin \frac{\pi}{5}) \sin \pi (x \cos \frac{2\pi}{5} + y \sin \frac{2\pi}{5}) \\ & \cdot \sin \pi (x \cos \frac{3\pi}{5} + y \sin \frac{3\pi}{5}) \sin \pi (x \cos \frac{4\pi}{5} + y \sin \frac{4\pi}{5}) = 0 \end{aligned} \quad 6.4.b$$

$$\sin \pi (x \cos \frac{2\pi}{5} + y \sin \frac{2\pi}{5}) \sin \pi (x \cos \frac{4\pi}{5} + y \sin \frac{4\pi}{5}) = 0 \quad 6.4.c$$

$$\begin{aligned} & \sin \pi x \sin \pi (x \cos \frac{\pi}{6} + y \sin \frac{\pi}{6}) \sin \pi (x \cos \frac{2\pi}{6} + y \sin \frac{2\pi}{6}) \\ & \cdot \sin \pi (x \cos \frac{3\pi}{6} + y \sin \frac{3\pi}{6}) \sin \pi (x \cos \frac{4\pi}{6} + y \sin \frac{4\pi}{6}) \\ & \cdot \sin \pi (x \cos \frac{5\pi}{6} + y \sin \frac{5\pi}{6}) = 0 \end{aligned} \quad 6.4.d$$

$$\sin \pi (x \cos \frac{\pi}{6} + y \sin \frac{\pi}{6}) \sin \pi (x \cos \frac{4\pi}{6} + y \sin \frac{4\pi}{6}) = 0 \quad 6.4.e$$

$$\begin{aligned} & \sin \pi x \sin \pi (x \cos \frac{\pi}{7} + y \sin \frac{\pi}{7}) \sin \pi (x \cos \frac{2\pi}{7} + y \sin \frac{2\pi}{7}) \\ & \cdot \sin \pi (x \cos \frac{3\pi}{7} + y \sin \frac{3\pi}{7}) \sin \pi (x \cos \frac{4\pi}{7} + y \sin \frac{4\pi}{7}) \\ & \cdot \sin \pi (x \cos \frac{5\pi}{7} + y \sin \frac{5\pi}{7}) \sin \pi (x \cos \frac{6\pi}{7} + y \sin \frac{6\pi}{7}) = 0 \end{aligned} \quad 6.4.f$$

$$\sin \pi(x \cos \frac{\pi}{7} + y \sin \frac{\pi}{7}) \sin \pi(x \cos \frac{4\pi}{7} + y \sin \frac{4\pi}{7}) = 0 \tag{6.4.g}$$

$$\begin{aligned} &\sin \pi x \sin \pi(x \cos \frac{\pi}{10} + y \sin \frac{\pi}{10}) \\ &\cdot \sin \pi(x \cos \frac{2\pi}{10} + y \sin \frac{2\pi}{10}) \sin \pi(x \cos \frac{3\pi}{10} + y \sin \frac{3\pi}{10}) \\ &\cdot \sin \pi(x \cos \frac{4\pi}{10} + y \sin \frac{4\pi}{10}) \sin \pi(x \cos \frac{5\pi}{10} + y \sin \frac{5\pi}{10}) \\ &\cdot \sin \pi(x \cos \frac{6\pi}{10} + y \sin \frac{6\pi}{10}) \sin \pi(x \cos \frac{7\pi}{10} + y \sin \frac{7\pi}{10}) \\ &\cdot \sin \pi(x \cos \frac{8\pi}{10} + y \sin \frac{8\pi}{10}) \sin \pi(x \cos \frac{9\pi}{10} + y \sin \frac{9\pi}{10}) = 0 \end{aligned} \tag{6.4.h}$$

$$\sin \pi x \sin \pi(x \cos \frac{5\pi}{10} + y \sin \frac{5\pi}{10}) = 0 \tag{6.4.i}$$

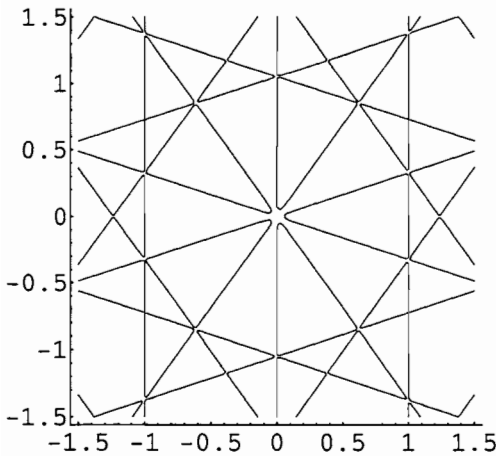


Fig. 6.4. a.

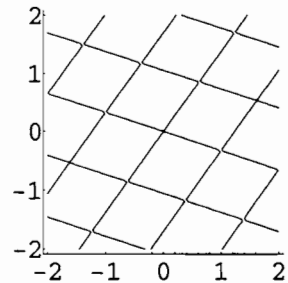


Fig. 6.4. b.

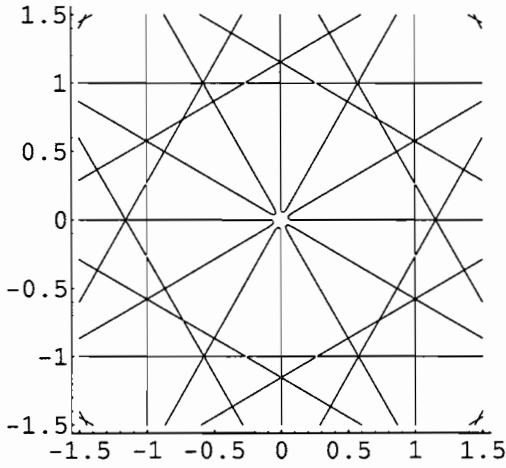


Fig. 6.4. c.

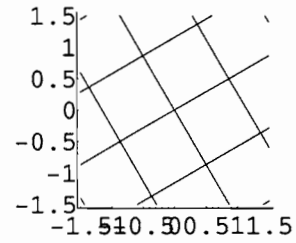


Fig. 6.4. d.

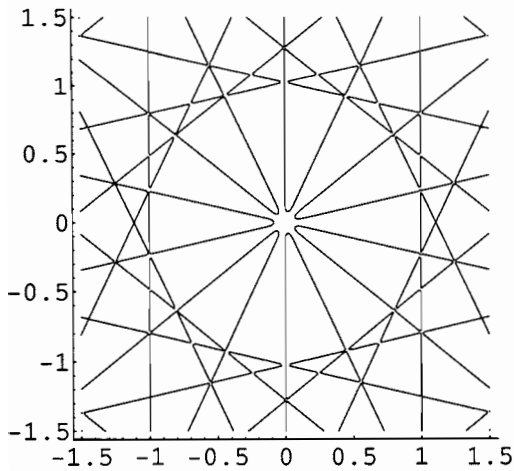


Fig. 6.4. e.

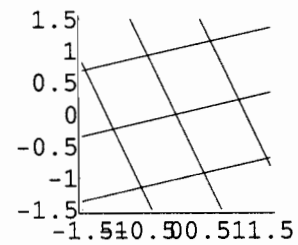


Fig. 6.4. f.

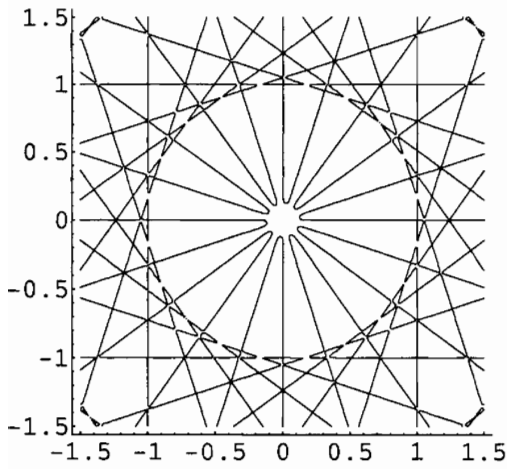


Fig. 6.4. g.

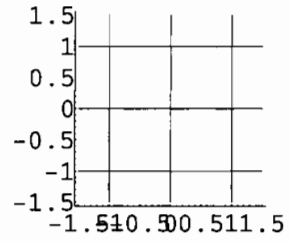


Fig. 6.4. h.

References 6

- 1 A.F. Wells, *THREE-DIMENSIONAL NETS AND POLYHEDRA*, Wiley, New York, 1977, page vii.
- 2 S. Andersson and M. Jacob, *THE MATHEMATICS OF STRUCTURES - THE EXPONENTIAL SCALE*, Oldenbourg, München, 1997.
- 3 Andersson, S., Jacob, M., Lidin, S., *Z.Kristallogr.* **210** (1995) 826-831.
- 4 Jacob, M., *J.Phys. II France* **7** (1997) 1035-1044.
- 5 Grin Y., Jacob M, Andersson S.: To be published.
- 6 Jacob, M., *Order, disorder and new order in solid state*. Thesis, Lund, 1994.
- 7 Jacob M., A routine for generating the structure of an icosahedral quasicrystal, *Z. Kristallogr.* **209** 925 (1994).
- 8 Jacob M., Lidin S., Andersson S.: On the Icosahedral Quasicrystal Structure, *Z. anorg. allg. Chem.* **619** (1993) 1721.
- 9 *EUCLID'S ELEMENTS*, Dover Publications, Inc. New York 1956. Book 1, p 351, or Book X, p 1.
- 10 Courant & Hilbert, *Methods of Mathematical Physics, Volume 1*, Wiley, New York, 1953, p 300.
- 11 Skiena, S., *Implementing Discrete Mathematics*, Addison-Wesley, CA 94065, 1990 p 98.

7 The Gauss Distribution Function

'Good work is not done by 'humble' men' [1].

Here we describe the remarkable properties of the Gauss distribution (GD) function, and use it to describe finite periodicity and the geometry of molecules, small ones or large ones, as cubosomes. Models for defects in crystals are also given. The broken symmetry in DNA and the possibility of a mathematical code matching this is sketched. A model for different grooves in DNA is also given. By mixing phases the outer shape of a crystal can be varied. Non convex polyhedra are shown. A structure of dilatation symmetry is given. The link to cosine is shown. The shape of several radiolarian creatures are derived.

7.1 The GD Function and Periodicity

Infinite and regular periodicity is not the normal case in Nature, since crystals are finite and also contain defects, often planar. The giant DNA molecule is certainly finite, and the double spiral has deviations - giving the genetic code - from the ideal wavy periodicity. Nevertheless, the circular functions are used and said to describe these structures of crystals or molecules, and some of their properties.

The periodicity of the circular functions was made finite above with a special parametrisation, and was found useful in the description of crystals and molecules, small or large.

One definition of a circular function is via the infinite products of roots. In chapter 2 we used some first few terms in such a product, which is a polynomial from the fundamental theorem of algebra. This was found useful in the description of defect crystals as well as symmetry of dilatation.

We have found that periodicity can be constructed from the GD function which to its nature is finite [2]. We shall give a detailed description of this.

The GD function

$$e^{-x^2} = C$$

7.1.1

has two lines (or points) - the roots of the function. These go apart for small constants, as in fig 7.1.1 (C=0.2), and disappear when the constant approach unity as in 7.1.2.

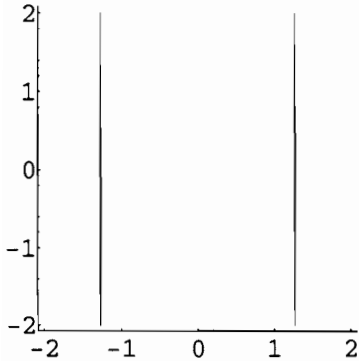


Fig. 7.1.1. After equation 7.1.1 with C=0.2.

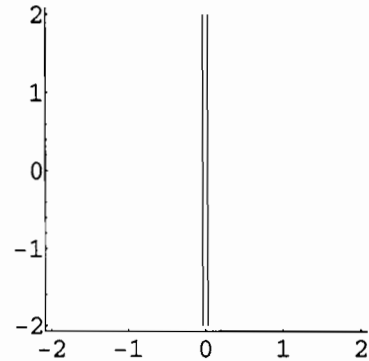


Fig. 7.1.2. After equation 7.1.1 with C=0.999.

We now introduce some periodicity as we did with the polynomials;

$$\begin{aligned}
 &e^{-x^2} + e^{-(x-2)^2} + e^{-(x-4)^2} + e^{-(x-6)^2} + e^{-(x-8)^2} \\
 &+ e^{-(x-10)^2} + e^{-(x-12)^2} + e^{-(x-14)^2} + e^{-(x-16)^2} \\
 &+ e^{-(x-18)^2} + e^{-(x-20)^2} + e^{-(x-22)^2} = C
 \end{aligned}
 \tag{7.1.2}$$

The function 7.1.2 is positive so we use a constant as shown in fig 7.1.3, and it seems to be identical with cosine, or rather its square.

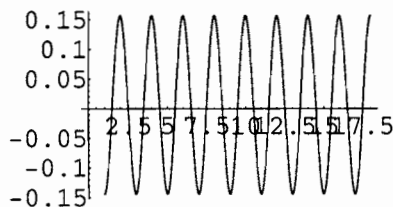


Fig 7.1.3. After equation 7.1.2 with C=0.88.

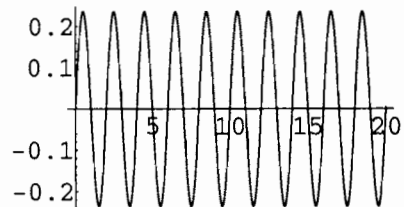


Fig. 7.1.4. After equation 7.1.3 with C=0.

We make the GD function oscillate around zero just like a circular function by using equation 7.1.3, which is shown in fig. 7.1.4. As this function is built up term by term, it is possible to go into the function and ‘disturb’ the periodicity. This can be done by a small coordinate, or phase, shift, or also just by changing the base in one term. The base is changed from e to 2.5 in eq. 7.1.4, and the effect is shown in fig. 7.1.5.

$$\begin{aligned}
 &(x+2)e^{-(x+2)^2} + xe^{-x^2} + (x-2)e^{-(x-2)^2} + (x-4)e^{-(x-4)^2} \\
 &+(x-6)e^{-(x-6)^2} + (x-8)e^{-(x-8)^2} + (x-10)e^{-(x-10)^2} \\
 &+(x-12)e^{-(x-12)^2} + (x-14)e^{-(x-14)^2} + (x-16)e^{-(x-16)^2} \\
 &+(x-18)e^{-(x-18)^2} + (x-20)e^{-(x-20)^2} + (x-22)e^{-(x-22)^2} = C
 \end{aligned}
 \tag{7.1.3}$$

$$\begin{aligned}
 &(x+2)e^{-(x+2)^2} + xe^{-x^2} + (x-2)e^{-(x-2)^2} + (x-4)e^{-(x-4)^2} \\
 &+(x-6)e^{-(x-6)^2} + (x-8)e^{-(x-8)^2} + (x-10)(2.5)^{-(x-10)^2} \\
 &+(x-12)e^{-(x-12)^2} + (x-14)e^{-(x-14)^2} + (x-16)e^{-(x-16)^2} \\
 &+(x-18)e^{-(x-18)^2} + (x-20)e^{-(x-20)^2} + (x-22)e^{-(x-22)^2} = C
 \end{aligned}
 \tag{7.1.4}$$

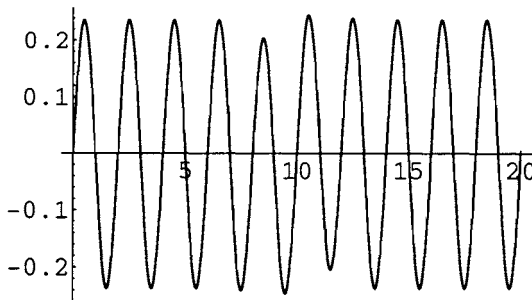


Fig. 7.1.5. After equation 7.1.4 with C=0.

Before we go 2D we shall show applications of this type of function and we do two helicoids. First is the traditional one,

$$x \sin \pi z + y \cos \pi z = 0
 \tag{7.1.5}$$

which is shown in fig 7.1.6. In equation 7.1.6 there is now the periodic GD function instead of the circular, and the result in fig 7.1.7 which seems to be identical with 7.1.6.

$$\begin{aligned}
 & x[ze^{-z^2} + (z-2)e^{-(z-2)^2} + (z-4)e^{-(z-4)^2} \\
 & + (z+2)e^{-(z+2)^2} + (z+4)e^{-(z+4)^2}] \\
 & + y[(z+.5)e^{-(z+.5)^2} + (z+2.5)e^{-(z+2.5)^2} \\
 & + (z-1.5)e^{-(z-1.5)^2} + (z-3.5)e^{-(z-3.5)^2}] = 0
 \end{aligned}
 \tag{7.1.6}$$

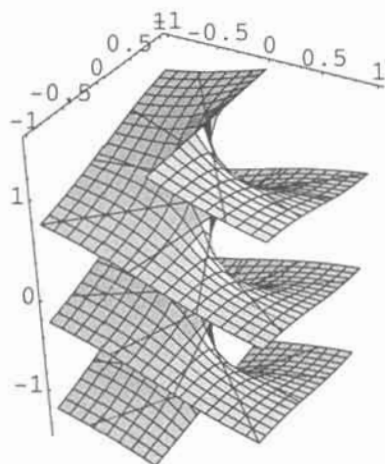


Fig. 7.1.6. After circular equation 7.1.5 with $C=0$.

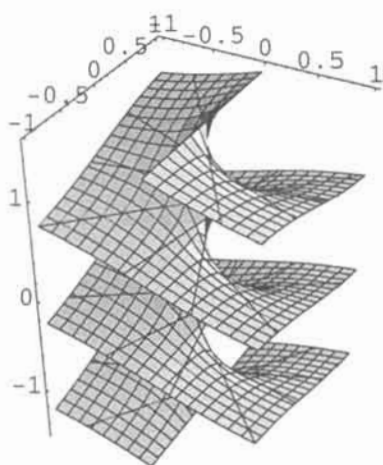


Fig. 7.1.7. After GD equation 7.1.6 with $C=0$.

One of us [3] has earlier given the topology for the DNA molecule in form of an equation. As the molecule in reality is not exactly a double spiral, the change to the mathematics which would match the structure of coding has to be found. We propose a possible path via a slight phase change as done on the coordinate of $x=6$. This gives a topological change in the corresponding catenoid in equation 7.1.7. In eq. 7.1.8 there is the undistorted version. The corresponding figures for these equations are in pictures 7.1.8 and 7.1.9.

$$\begin{aligned}
 & e^{(x^2+y^2)/10} + xy \cos\left(\frac{pz}{10}\right) + \frac{1}{2}(x^2 - y^2) \sin\left(\frac{pz}{10}\right) + (z+2)e^{-(z+2)^2} \\
 & + ze^{-z^2} + (z-2)e^{-(z-2)^2} + (z-4)e^{-(z-4)^2} + (z-6.2)e^{-(z-6.2)^2} \quad 7.1.7 \\
 & + (z-8)e^{-(z-8)^2} + (z-10)e^{-(z-10)^2} + (z-12)e^{-(z-12)^2} = 1
 \end{aligned}$$

$$\begin{aligned}
 & e^{(x^2+y^2)/10} + xy \cos\left(\frac{\pi z}{10}\right) + \frac{1}{2}(x^2 - y^2) \sin\left(\frac{\pi z}{10}\right) + (z+2)e^{-(z+2)^2} \\
 & + ze^{-z^2} + (z-2)e^{-(z-2)^2} + (z-4)e^{-(z-4)^2} + (z-6)e^{-(z-6)^2} \quad 7.1.8 \\
 & + (z-8)e^{-(z-8)^2} + (z-10)e^{-(z-10)^2} + (z-12)e^{-(z-12)^2} = 1
 \end{aligned}$$

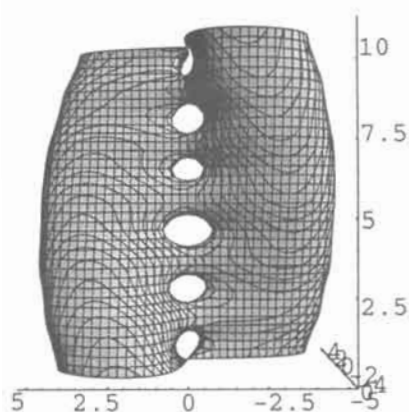


Fig. 7.1.8. Distorted DNA after equation 7.1.7 with C=1.

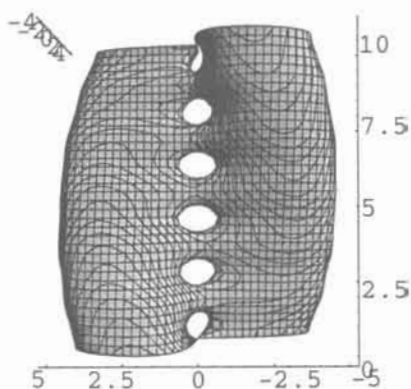


Fig. 7.1.9. Regular DNA after equation 7.1.8 with C=1.

In the DNA molecule the two spirals are not separated by a simple translation. There are two different distances between them, one is moved along the spiral axis with respect to the other. In order to find the mathematics we must have two functions different in phase, which we separate with the exponential scale as in eq. 7.1.9 and showed in fig 7.1.10.

$$\frac{1}{e^5}(x^2+y^2) + e^{(y \cos \frac{\pi}{2} z + x \sin \frac{\pi}{2} z)} + e^{(y \cos \frac{\pi}{2} (z+2) + x \sin \frac{\pi}{2} (z+2))} = 3.5 \quad 7.1.9$$

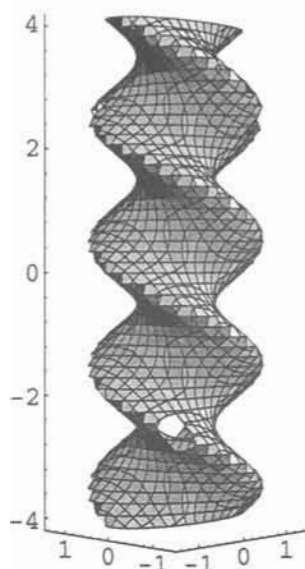


Fig. 7.1.10. DNA after equation 7.1.9 with $C=3.5$.

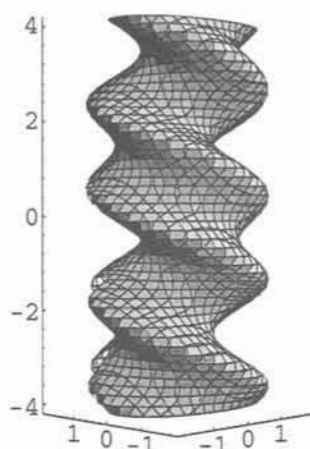


Fig. 7.1.11. DNA after equation 7.1.10 with $C=3.5$ showing different grooves.

Changing the weight of one of the spirals is a simple way to have the spirals non-equidistant, as in eq. 7.1.10 and shown in fig 7.1.11. We have chosen this topology instead of separated spirals in order to demonstrate the different grooves. It is remarkable how similar this picture is to the common ball and stick models of B-DNA.

$$e^{\frac{1}{5}(x^2+y^2)} + e^{y \cos \frac{\pi}{2} z + x \sin \frac{\pi}{2} z} + \frac{1}{2} e^{y \cos \frac{\pi}{2} (z+2) + x \sin \frac{\pi}{2} (z+2)} = 3.5 \quad 7.1.10$$

Changing the available constants give a great variety of topologies - the pitch is of course the same. One example with even more marked difference in grooves is shown in equation 7.1.11 and the picture in 7.1.12.

$$e^{0.16(z^2+y^2)} + e^{y \cos \frac{\pi}{2} x + z \sin \frac{\pi}{2} x} + \frac{1}{2} e^{y \cos \frac{\pi}{2} (x+2) + z \sin \frac{\pi}{2} (x+2)} = 2.55$$

7.1.11



Fig. 7.1.12. DNA after equation 7.1.11 with $C=2.55$.

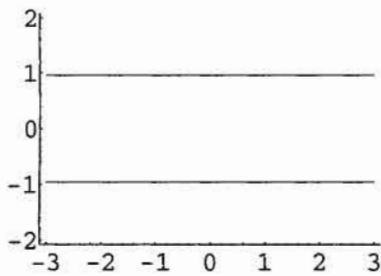


Fig. 7.1.13. After equation 7.1.12 with $C=0.4$.

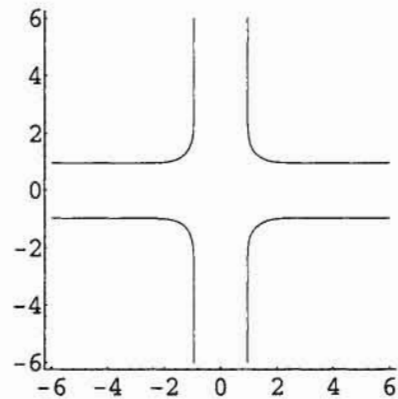


Fig. 7.1.14. After equation 7.1.13 with $C=0.4$.

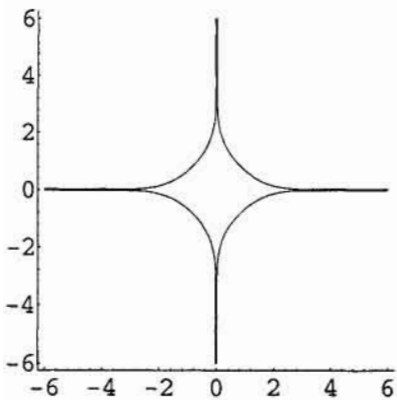


Fig. 7.1.15. After equation 7.1.13 with $C=0.9995$.

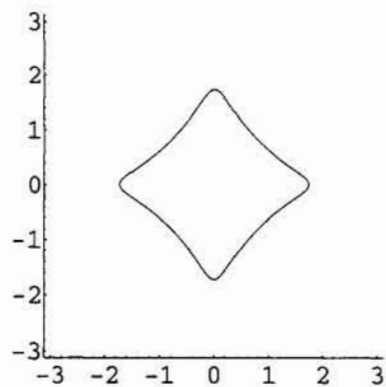


Fig. 7.1.16. After equation 7.1.13 with $C=1.05$.

Going 2D, we start with the lines in eq. 7.1.12, shown in fig 7.1.13, which together with the lines from eq. 7.1.1 form equation 7.1.13, and figure 7.1.14. Continuing changing the constant gives the development in the following figures. Via hyperbolic geometry the lines switch over to the diagonal type, to form a circle like closed curve at the end.

$$e^{-y^2} = 0.4 \tag{7.1.12}$$

$$e^{-x^2} + e^{-y^2} = C \tag{7.1.13}$$

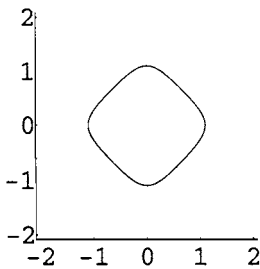


Fig. 7.1.17. After equation 7.1.13 with C=1.3.

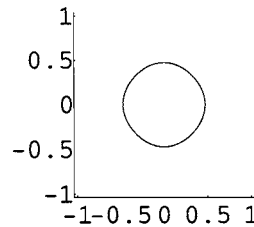


Fig. 7.1.18. After equation 7.1.13 with C=1.8.

We use more terms to show the periodicity as in eq. 7.1.14, shown in fig 7.1.19.

$$\begin{aligned} &e^{-x^2} + e^{-y^2} + e^{-(x-2)^2} + e^{-(y-2)^2} \\ &+ e^{-(x-4)^2} + e^{-(y-4)^2} + e^{-(x-6)^2} + e^{-(y-6)^2} \\ &+ e^{-(x-8)^2} + e^{-(y-8)^2} + e^{-(x-10)^2} + e^{-(y-10)^2} \\ &+ e^{-(x-12)^2} + e^{-(y-12)^2} + e^{-(x-14)^2} + e^{-(y-14)^2} \\ &+ e^{-(x-16)^2} + e^{-(y-16)^2} = C \end{aligned} \tag{7.1.14}$$

In fig 7.1.20 we have taken away two planes and have a structure with planar defects.

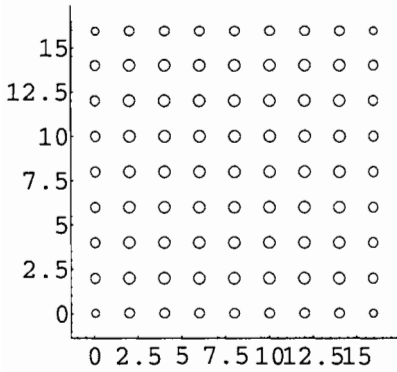


Fig. 7.1.19. After equation 7.1.14 with C=2.

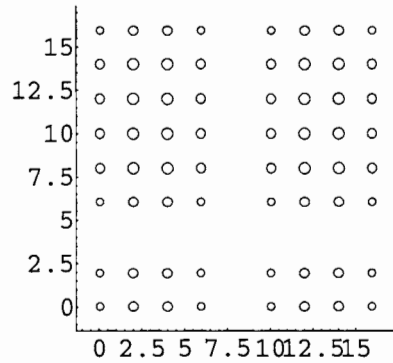


Fig. 7.1.20. After equation 7.1.14 but with two terms or planes missing.

7.1.1 Handmade Periodicity

With the GD function a plane can be moved and put anywhere, and we do the same with the circle below in fig 7.1.21:

$$e^{-(x^2+y^2)} = 0.9 \tag{7.1.15}$$

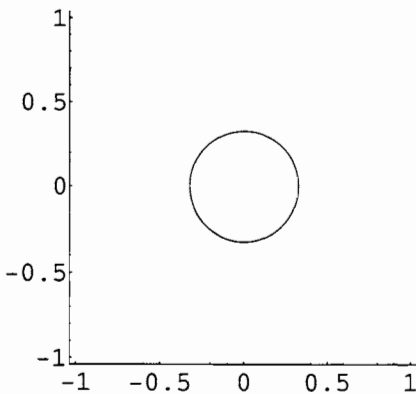


Fig. 7.1.21. After equation 7.1.15.

We add more circles after eq. 7.1.16 and show this in fig 7.1.22.

$$\begin{aligned}
 &e^{-(x^2+y^2)} + e^{-((x-2)^2+y^2)} + e^{-((x-4)^2+y^2)} \\
 &+ e^{-(x^2+(y-2)^2)} + e^{-(x^2+(y-4)^2)} = 0.9
 \end{aligned}
 \tag{7.1.16}$$

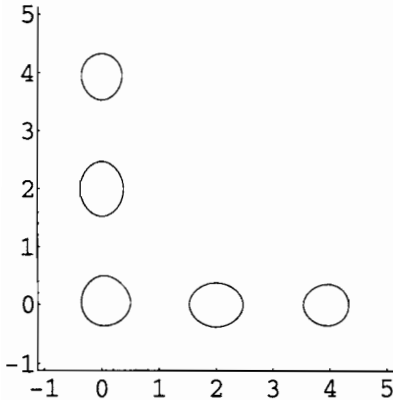


Fig. 7.1.22. After equation 7.1.16.

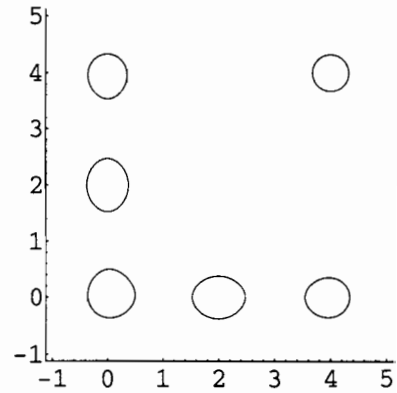


Fig. 7.1.23. After equation 7.1.17.

This time there is no periodicity - the circle is a closed function. There are no lines to collaborate in space to give true periodicity. But we can still build a structure by putting out the figures one by one, as we have done in eq. 7.1.17 and shown in fig 7.1.23. We call this handmade periodicity, which also is useful and will be developed in next chapter.

$$\begin{aligned}
 &e^{-(x^2+y^2)} + e^{-((x-2)^2+y^2)} + e^{-((x-4)^2+y^2)} + e^{-(x^2+(y-2)^2)} \\
 &+ e^{-(x^2+(y-4)^2)} + e^{-((x-4)^2+(y-4)^2)} = 0.9
 \end{aligned}
 \tag{7.1.17}$$

7.2 The GD Function and Periodicity in 3D

The general natural exponential in eq. 7.2.1, here called the equation of symmetry, is particular useful for describing shapes and forms of polyhedra, and also for giving finite periodicity to the circular functions.

$$\begin{aligned}
 & e^{(x+y+z)^n} + e^{(-x+y+z)^n} + e^{(x+y-z)^n} + e^{(x-y+z)^n} \\
 & + e^{(x+y)^m} + e^{(-x+y)^m} + e^{(z+x)^m} + e^{(z-x)^m} + e^{(y+z)^m} + e^{(y-z)^m} \\
 & + e^{(x)^p} + e^{(y)^p} + e^{(z)^p} = C
 \end{aligned} \tag{7.2.1}$$

Multiplication with i as in eq. 7.2.2 gives the general complex exponential for $n,m,p=1$.

$$\begin{aligned}
 & e^{[i(x+y+z)]^n} + e^{[i(-x+y+z)]^n} + e^{[i(x+y-z)]^n} + e^{[i(x-y+z)]^n} \\
 & + e^{[i(x+y)]^m} + e^{[i(-x+y)]^m} + e^{[i(z+x)]^m} \\
 & + e^{[i(z-x)]^m} + e^{[i(y+z)]^m} + e^{[i(y-z)]^m} \\
 & + e^{[i(x)]^p} + e^{[i(y)]^p} + e^{[i(z)]^p} = 0
 \end{aligned} \tag{7.2.2}$$

For a value $n,m,p=2$ we have the general GD function in three dimensions, and for $n,m=0$ and $p=2$ we have the simple GD function in 3D.

$$e^{-x^2} + e^{-y^2} + e^{-z^2} = C \tag{7.2.3}$$

The three dimensional Gauss distribution in eq. 7.2.3 has a remarkable development with the constant. From an anti-cube composed of six planes in fig. 7.2.1 at a constant of 0.1, it forms via fig. 7.2.2 at $C=1$ an open octahedron at $C=1.8$, composed of the intersection of six rods in fig 7.2.3. Finally at $C=2.5$ there is a body - an octahedrally distorted sphere - in fig. 7.2.4.

The equation 7.2.4,

$$e^{-x^2} + e^{-y^2} + e^{-z^2} + e^{-(x-2)^2} + e^{-(y-2)^2} + e^{-(z-2)^2} = C \tag{7.2.4}$$

which is a simple translational extension of eq. 7.2.3, gives a similar pattern, and in figures 7.2.5-7 we see that periodicity starts to emerge.

Equation

$$\begin{aligned}
 & e^{-x^2} + e^{-y^2} + e^{-z^2} + e^{-(x-2)^2} + e^{-(y-2)^2} + e^{-(z-2)^2} \\
 & + e^{-(x-4)^2} + e^{-(y-4)^2} + e^{-(z-4)^2} = C
 \end{aligned} \tag{7.2.5}$$

gives fig. 7.2.8, which shows how six bundles of rods meet to form a nodal surface of P-type in the centre at a const of 1.8, and in fig. 7.2.9 the complete primitive structure is shown.

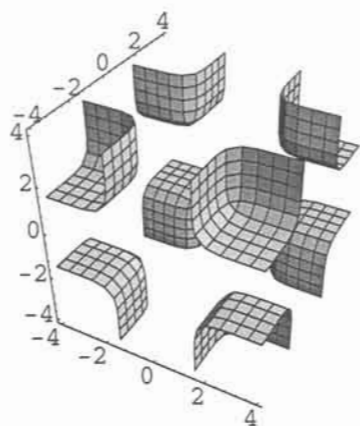


Fig. 7.2.1. After equation 7.2.3 with $C=0.1$.

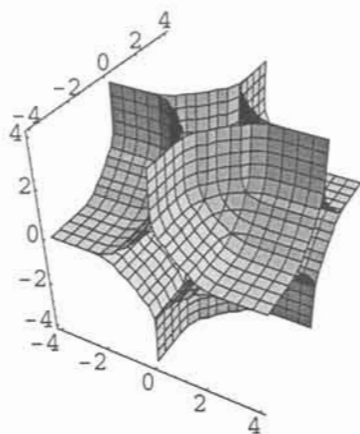


Fig. 7.2.2. After equation 7.2.3 with $C=1$.

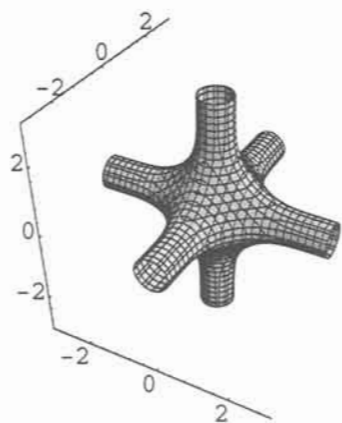


Fig. 7.2.3. After equation 7.2.3 with $C=1.8$.

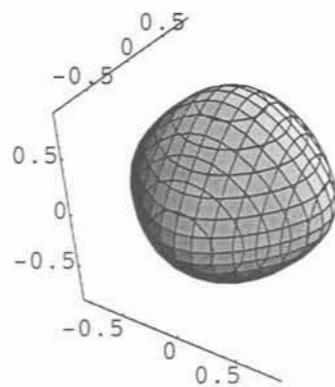


Fig. 7.2.4. After equation 7.2.3 with $C=2.5$.

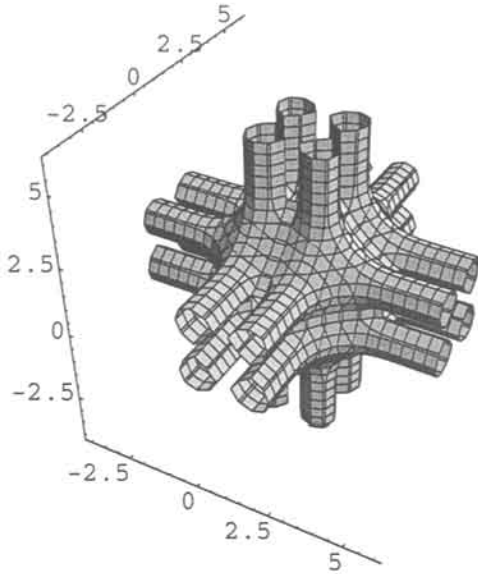


Fig. 7.2.5. After equation 7.2.4 with $C=1.8$.

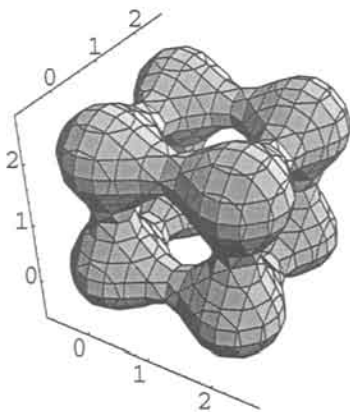


Fig. 7.2.6. After equation 7.2.4 with $C=2.7$.

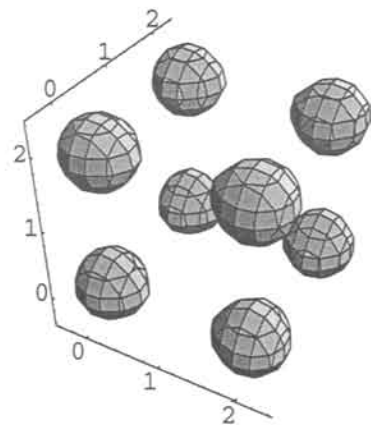


Fig. 7.2.7 After equation 7.2.4 with $C=2.9$.

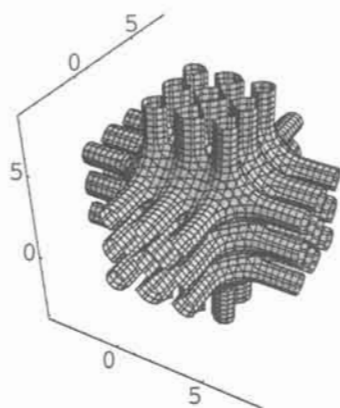


Fig. 7.2.8. After equation 7.2.5 with $C=1.8$.

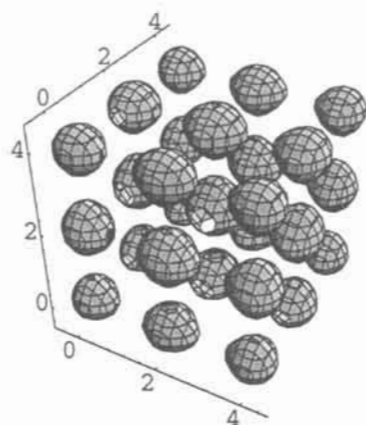


Fig. 7.2.9. After equation 7.2.5 with $C=2.85$.

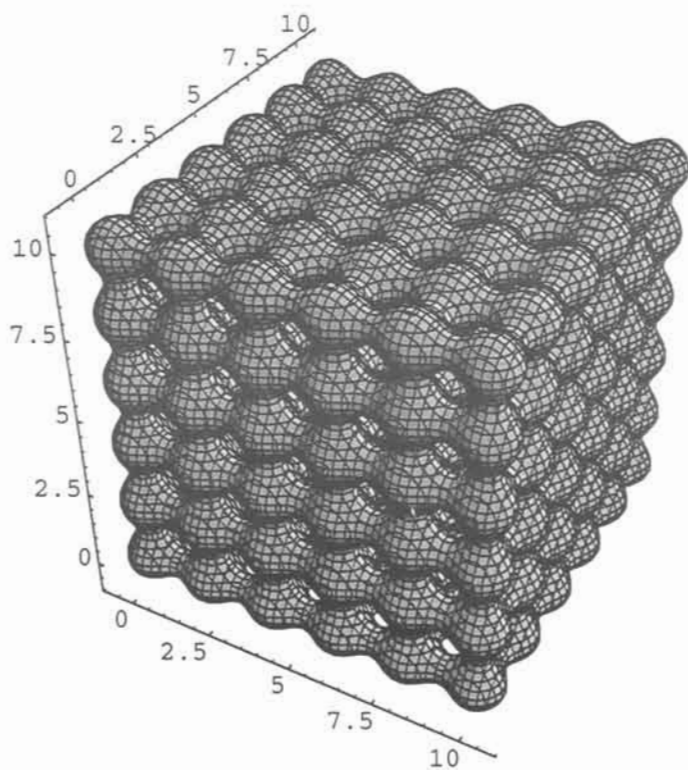


Fig. 7.2.10. Large crystal or cubosome after equation 7.2.6.

Next could be a picture of a big zeolite crystal, such as Linde A, or a Larsson-cubosome in fig. 7.2.10, from equation 7.2.6.

$$\begin{aligned}
 & e^{-x^2} + e^{-y^2} + e^{-z^2} + e^{-(x-2)^2} + e^{-(y-2)^2} + e^{-(z-2)^2} \\
 & + e^{-(x-4)^2} + e^{-(y-4)^2} + e^{-(z-4)^2} + e^{-(x-6)^2} + e^{-(y-6)^2} + e^{-(z-6)^2} \\
 & + e^{-(x-8)^2} + e^{-(y-8)^2} + e^{-(z-8)^2} \\
 & + e^{-(x-10)^2} + e^{-(y-10)^2} + e^{-(z-10)^2} = 2.65
 \end{aligned} \tag{7.2.6}$$

7.3 The BCC and Diamond Symmetries

More symmetry groups in space are obtained via the permutation of the variables, using the GD function.

In order to get the IWP and gyroid surfaces for comparison, we use the real respectively imaginary part of function 7.3.1 below.

$$i^{(x+y)} + i^{(x-y)} + i^{(x+z)} + i^{-(y+z)} + i^{-(x+z)} + i^{-(y-z)} = C \tag{7.3.1}$$

Eq. 7.3.2 gives planes, in this case two as in fig. 7.3.1.

$$e^{-(x+y)^2} = 0.8 \tag{7.3.2}$$

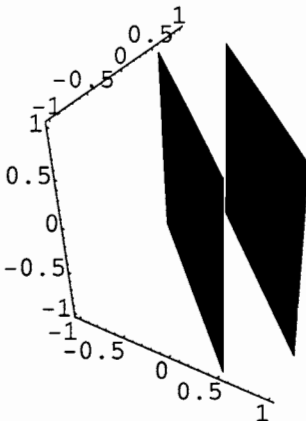


Fig. 7.3.1. After equation 7.3.2.

The prehistory is complicated, so we directly show the equation for the gyroid surface as shown in 7.3.3.

$$\begin{aligned}
 & e^{-(x+y-0.5)^2} + e^{-(x-y-0.5)^2} + e^{-(x+z-0.5)^2} + e^{-(y+z-0.5)^2} \\
 & + e^{-(x+z-0.5)^2} + e^{-(y-z-0.5)^2} + e^{-(x+y-2.5)^2} + e^{-(x-y-2.5)^2} \\
 & + e^{-(x+z-2.5)^2} + e^{-(y+z-2.5)^2} + e^{-(x+z-2.5)^2} + e^{-(y-z-2.5)^2} \\
 & + e^{-(x+y-4.5)^2} + e^{-(x-y-4.5)^2} + e^{-(x+z-4.5)^2} + e^{-(y+z-4.5)^2} \\
 & + e^{-(x+z-4.5)^2} + e^{-(y-z-4.5)^2} + e^{-(x+y+1.5)^2} + e^{-(x-y+1.5)^2} \\
 & + e^{-(x+z+1.5)^2} + e^{-(y+z+1.5)^2} + e^{-(x+z+1.5)^2} + e^{-(y-z+1.5)^2} \\
 & + e^{-(x+y+3.5)^2} + e^{-(x-y+3.5)^2} + e^{-(x+z+3.5)^2} + e^{-(y+z+3.5)^2} \\
 & + e^{-(x+z+3.5)^2} + e^{-(y-z+3.5)^2} + e^{-(x+y+5.5)^2} + e^{-(x-y+5.5)^2} \\
 & + e^{-(x+z+5.5)^2} + e^{-(y+z+5.5)^2} + e^{-(x+z+5.5)^2} + e^{-(y-z+5.5)^2} = 5.3
 \end{aligned} \tag{7.3.3}$$

The gyroid calculated in this way is shown in fig. 7.3.2, and the corresponding surface, as calculated with the Im part of the complex exponential in eq. 7.3.1, is shown in fig. 7.3.3. The complete surface as obtained from eq. 7.3.3 with larger boundaries is shown in 7.3.4. The boundary properties of the finite periodical function closes the surface and forms the particle. This is again a possible Larsson cubosome of the G type, or also a crystal of with the structure of garnet. The outer shape is that of a rhombic dodecahedron.

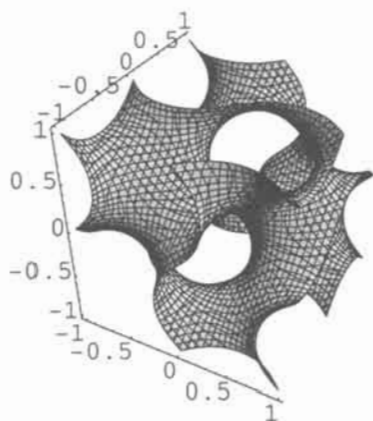


Fig. 7.3.2. The gyroid surface from equation 7.3.3.

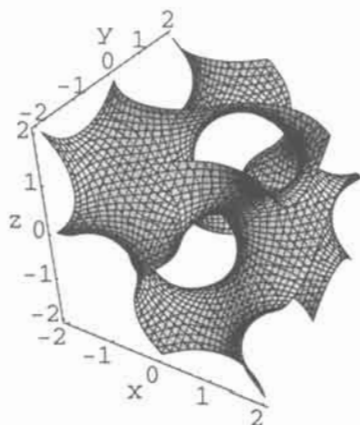


Fig. 7.3.3. The nodal gyroid surface from equation 7.3.1.

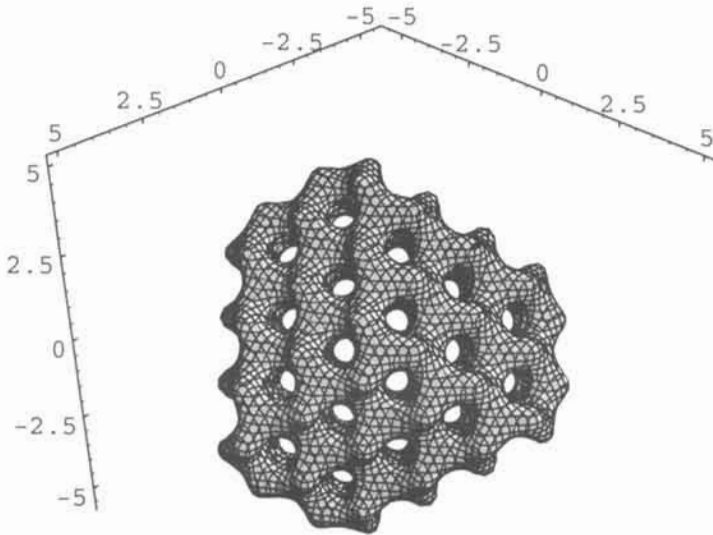


Fig. 7.3.4. The complete gyroid surface from equation 7.3.3 from larger boundaries.

A smaller cubosome-like gyroid surface is shown along the three fold axis in fig. 7.3.5 and the equation is 7.3.4.

$$\begin{aligned}
 & e^{-(x+y-0.5)^2} + e^{-(x-y-0.5)^2} + e^{-(x+z-0.5)^2} + e^{-(y+z-0.5)^2} + \\
 & + e^{-(x+z-0.5)^2} + e^{-(y-z-0.5)^2} + e^{-(x+y-2.5)^2} + e^{-(x-y-2.5)^2} + \\
 & + e^{-(x+z-2.5)^2} + e^{-(y+z-2.5)^2} + e^{-(x+z-2.5)^2} + e^{-(y-z-2.5)^2} + \quad 7.3.4 \\
 & + e^{-(x+y+1.5)^2} + e^{-(x-y+1.5)^2} + e^{-(x+z+1.5)^2} + e^{-(y+z+1.5)^2} + \\
 & + e^{-(x+z+1.5)^2} + e^{-(y-z+1.5)^2} = 5.3
 \end{aligned}$$

The real part of the complex exponential in eq. 7.3.1 gives the IWP nodal surface. The corresponding symmetry for the exponential function is developed with translations of 2, 4, 6 in eq. 7.3.5, and give the IWP surface

in fig. 7.3.6, and also the body centred packing of bodies as isosurfaces. And the inside is in fig. 7.3.7.

$$\begin{aligned}
 & e^{-(x+y)^2} + e^{-(x-y)^2} + e^{-(x+z)^2} + e^{-(y+z)^2} + e^{-(x+z)^2} + e^{-(y-z)^2} \\
 & + e^{-(x+y-2)^2} + e^{-(x-y-2)^2} + e^{-(x+z-2)^2} + e^{-(y+z-2)^2} \\
 & + e^{-(x+z-2)^2} + e^{-(y-z-2)^2} + e^{-(x+y-4)^2} + e^{-(x-y-4)^2} \\
 & + e^{-(x+z-4)^2} + e^{-(y+z-4)^2} + e^{-(x+z-4)^2} + e^{-(y-z-4)^2} \\
 & + e^{-(x+y+2)^2} + e^{-(x-y+2)^2} + e^{-(x+z+2)^2} + e^{-(y+z+2)^2} \\
 & + e^{-(x+z+2)^2} + e^{-(y-z+2)^2} + e^{-(x+y+4)^2} + e^{-(x-y+4)^2} \\
 & + e^{-(x+z+4)^2} + e^{-(y+z+4)^2} + e^{-(x+z+4)^2} + e^{-(y-z+4)^2} \\
 & + e^{-(x+y+6)^2} + e^{-(x-y+6)^2} + e^{-(x+z+6)^2} + e^{-(y+z+6)^2} \\
 & + e^{-(x+z+6)^2} + e^{-(y-z+6)^2} = 5.2
 \end{aligned}
 \tag{7.3.5}$$

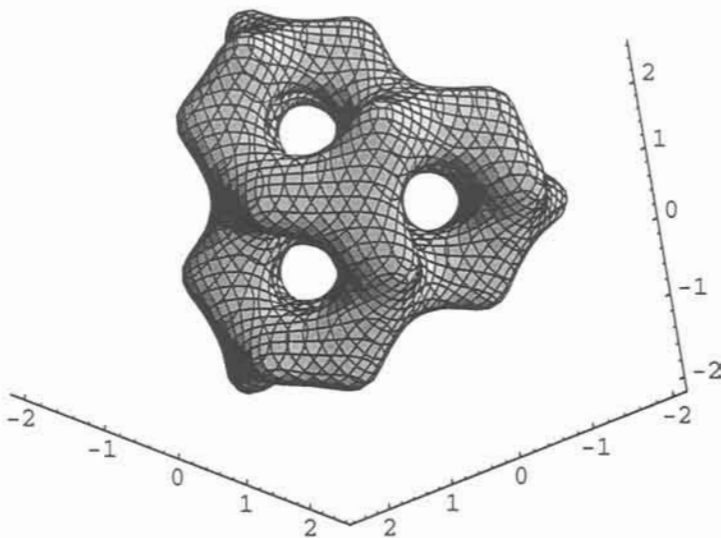


Fig. 7.3.5. Smaller part of the gyroid surface after equation 7.3.4.

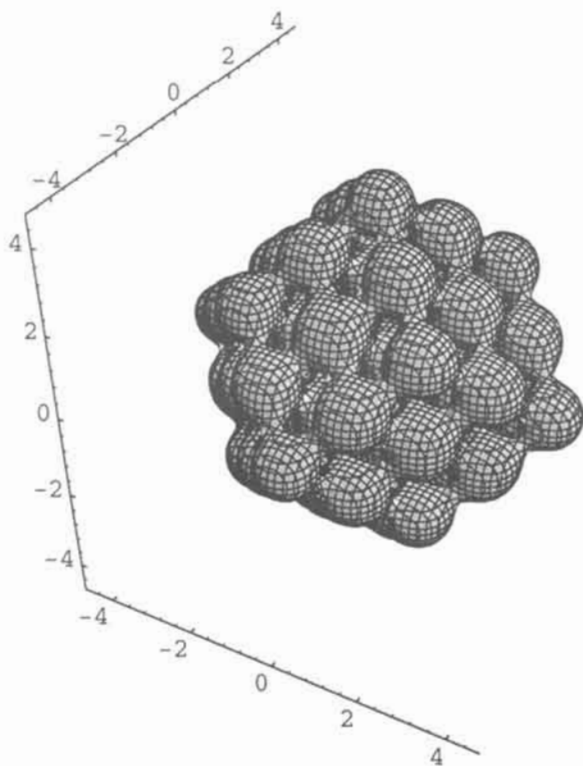


Fig. 7.3.6. Bcc arrangement of bodies after equation 7.3.5.

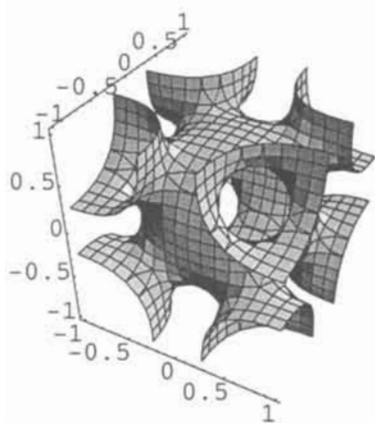


Fig. 7.3.7. Inside of fig. 7.3.6.

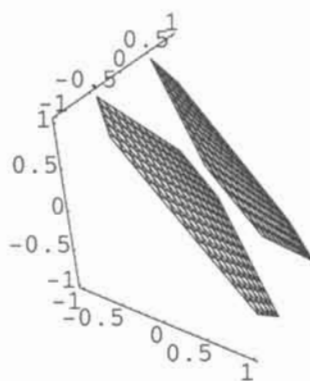


Fig. 7.3.8. After equation 7.3.6.

In the last set of GD functions the translation shift corresponds to ordinary sine. One term gives planes, in this case two as in fig. 7.3.8 after eq. 7.3.6.

$$e^{-(x+y+z)^2} = -0.8 \quad 7.3.6$$

The first permutation is in equation 7.3.7:

$$\begin{aligned} e^{-(x+y+z+0.5)^2} + e^{-(x-y+z+0.5)^2} \\ + e^{-(x+y-z+0.5)^2} + e^{-(x-y+z+0.5)^2} = C \end{aligned} \quad 7.3.7$$

In fig. 7.3.9 the constant is 1.8 and the prehistory is as earlier. At $C=2.3$ in fig. 7.3.10 the structure describes a C_4H_4 molecule.

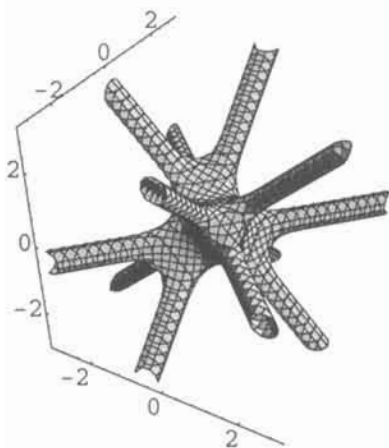


Fig. 7.3.9. After equation 7.3.7 with $C=1.8$.

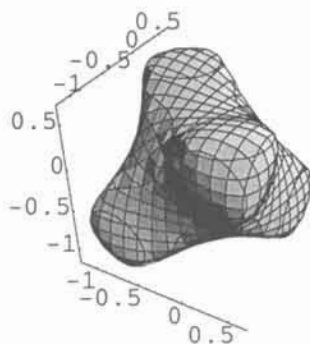


Fig. 7.3.10. After equation 7.3.7 with $C=2.3$.

One more set of terms in the summation gives the following equation:

$$\begin{aligned} e^{-(x+y+z+0.5)^2} + e^{-(x-y+z+0.5)^2} + e^{-(x+y-z+0.5)^2} \\ + e^{-(x-y+z-0.5)^2} + e^{-(x+y+z-1.5)^2} + e^{-(x-y+z-1.5)^2} \\ + e^{-(x+y-z-1.5)^2} + e^{-(x-y+z-1.5)^2} = 3.7 \end{aligned} \quad 7.3.8$$

The prehistory is again bundles of rods that this time intersect to a structure describing the adamantane molecule in fig. 7.3.11, which really is a part of the diamond structure. A larger part of this structure, which of course starts to look like a cubosome, is shown in fig. 7.3.12, and the equation is in 7.3.9.

$$\begin{aligned}
 & e^{-(x+y+z+0.5)^2} + e^{-(x-y+z+0.5)^2} + e^{-(x+y-z+0.5)^2} \\
 & + e^{-(-x+y+z+0.5)^2} + e^{-(x+y+z-1.5)^2} + e^{-(x-y+z-1.5)^2} \\
 & + e^{-(x+y-z-1.5)^2} + e^{-(-x+y+z-1.5)^2} + e^{-(x+y+z+2.5)^2} \\
 & + e^{-(x-y+z+2.5)^2} + e^{-(x+y-z+2.5)^2} + e^{-(-x+y+z+2.5)^2} = 3.7
 \end{aligned} \tag{7.3.9}$$

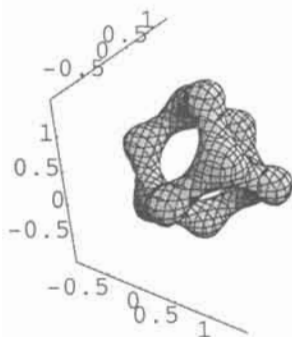


Fig. 7.3.11. Adamantane molecule after 7.3.8.

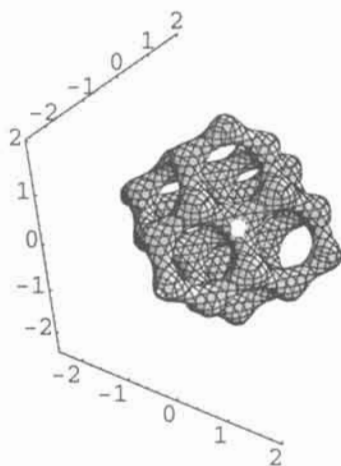


Fig. 7.3.12. Piece of diamond after 7.3.9.

A summation with only negative phase shifts as eq. 7.3.10 gives the structure of the methane molecule (CH_4) as shown in fig. 7.3.13.

$$\begin{aligned}
 & e^{-(x+y+z+0.5)^2} + e^{-(x-y+z+0.5)^2} + e^{-(x+y-z+0.5)^2} \\
 & + e^{-(-x+y+z+0.5)^2} + e^{-(x+y+z+2.5)^2} + e^{-(x-y+z+2.5)^2} \\
 & + e^{-(x+y-z+2.5)^2} + e^{-(-x+y+z+2.5)^2} = 3.7
 \end{aligned} \tag{7.3.10}$$

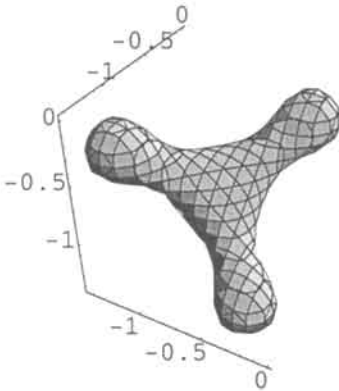


Fig. 7.3.13. After equation 7.3.10.

We have obviously derived the exponential mathematics for the so called D-nodal surface, and the summation in eq. 7.3.11 gives the surface in 7.3.14.

$$\begin{aligned}
 & e^{-(x+y+z+0.5)^2} + e^{-(x-y+z+0.5)^2} + e^{-(x+y-z+0.5)^2} \\
 & + e^{-(-x+y+z+0.5)^2} + e^{-(x+y+z-1.5)^2} + e^{-(x-y+z-1.5)^2} \\
 & + e^{-(x+y-z-1.5)^2} + e^{-(-x+y+z-1.5)^2} + e^{-(x+y+z+2.5)^2} \\
 & + e^{-(x-y+z+2.5)^2} + e^{-(x+y-z+2.5)^2} + e^{-(-x+y+z+2.5)^2} \\
 & + e^{-(x+y+z-3.5)^2} + e^{-(x-y+z-3.5)^2} + e^{-(x+y-z-3.5)^2} \\
 & + e^{-(-x+y+z-3.5)^2} + e^{-(x+y+z+4.5)^2} + e^{-(x-y+z+4.5)^2} \\
 & + e^{-(x+y-z+4.5)^2} + e^{-(-x+y+z+4.5)^2} = 3.5
 \end{aligned} \tag{7.3.11}$$

The corresponding equation for the classical nodal D surface is

$$\text{Im} [i^{x+y+z} + i^{x-y+z} + i^{x+y-z} + i^{-x+y+z}] = 0 \tag{7.3.12}$$

which we show in fig. 7.3.15 for comparison.

The complete surface for equation 7.3.11 is given in fig. 7.3.16, and its projection shown in fig. 7.3.17. The shape is octahedral.

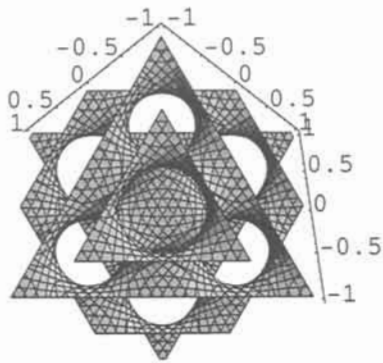


Fig. 7.3.14. GD mathematics after equation 7.3.11.

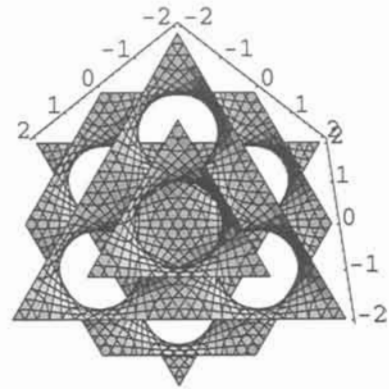


Fig. 7.3.15. Complex exponential after equation 7.3.12.

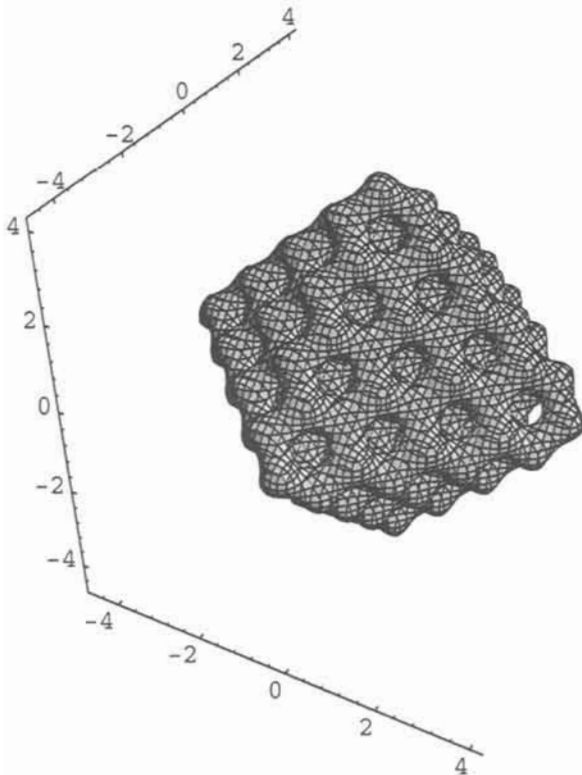


Fig. 7.3.16. Larsson cubosome D after equation 7.3.11.

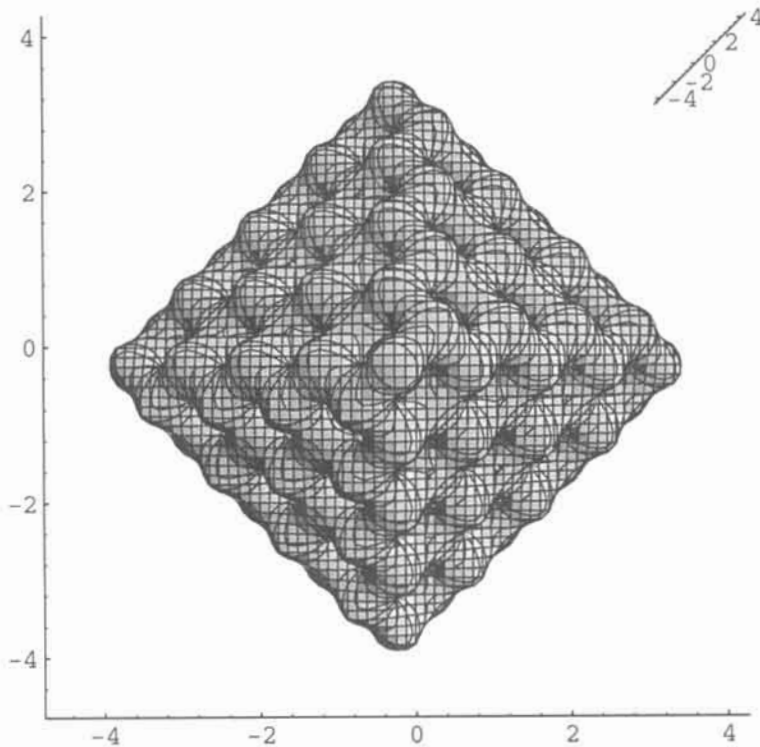


Fig. 7.3.17. Projection of the octahedron in fig 7.3.16.

By using only positive 'phase shift' or translations 7.3.13, the outer shape is the tetrahedron shown in fig. 7.3.18.

$$\begin{aligned}
 & e^{-(x+y+z+0.5)^2} + e^{-(x-y+z+0.5)^2} + e^{-(x+y-z+0.5)^2} \\
 & + e^{-(-x+y+z+0.5)^2} + e^{-(x+y+z+2.5)^2} + e^{-(x-y+z+2.5)^2} \\
 & + e^{-(x+y-z+2.5)^2} + e^{-(-x+y+z+2.5)^2} + e^{-(x+y+z+4.5)^2} \\
 & + e^{-(x-y+z+4.5)^2} + e^{-(x+y-z+4.5)^2} + e^{-(-x+y+z+4.5)^2} \\
 & + e^{-(x+y+z+6.5)^2} + e^{-(x-y+z+6.5)^2} + e^{-(x+y-z+6.5)^2} \\
 & + e^{-(-x+y+z+6.5)^2} + e^{-(x+y+z+8.5)^2} + e^{-(x-y+z+8.5)^2} \\
 & + e^{-(x+y-z+8.5)^2} + e^{-(-x+y+z+8.5)^2} = 3.5
 \end{aligned}
 \tag{7.3.13}$$

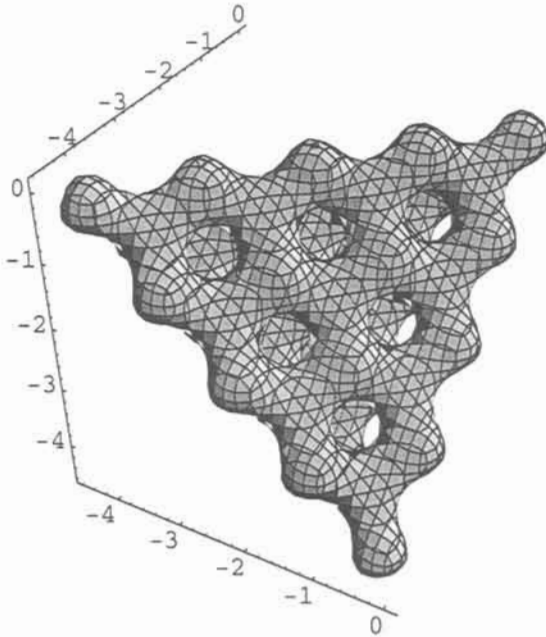


Fig. 7.3.18. A tetrahedron after equation 7.3.13, and still the D-surface.

Only using negative phases in eq. 7.3.13 gives the dual tetrahedron. By truncating eq. 7.3.11, or mixing the ‘phases’ as in eq. 7.3.14, we get a somewhat irregular outer shape that still has perfect ordered inside, as in fig. 7.3.19.

$$\begin{aligned}
 & e^{-(x+y+z+0.5)^2} + e^{-(x-y+z+0.5)^2} + e^{-(x+y-z+0.5)^2} \\
 & + e^{-(x+y+z+1.5)^2} + e^{-(x-y+z+1.5)^2} + e^{-(x+y-z+1.5)^2} \\
 & + e^{-(x+y+z+2.5)^2} + e^{-(x-y+z+2.5)^2} + e^{-(x+y-z+2.5)^2} \\
 & + e^{-(x+y+z+3.5)^2} + e^{-(x-y+z+3.5)^2} + e^{-(x+y-z+3.5)^2} \\
 & + e^{-(x+y+z+4.5)^2} = 3.5
 \end{aligned}
 \tag{7.3.14}$$

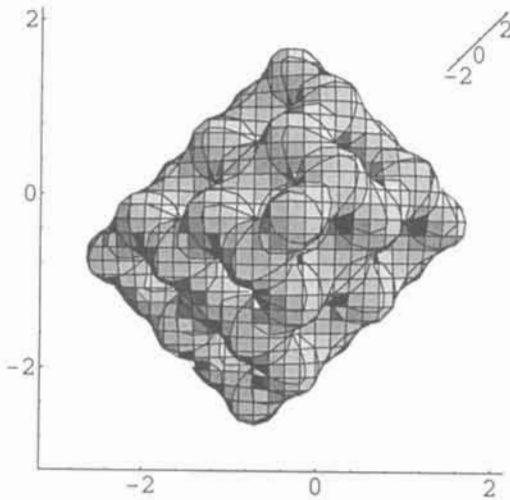


Fig. 7.3.19. Still the D- surface but with different outer crystal shape, after equation 7.3.14.

It is clear that the changes of phases causes dramatic changes of shapes, so this is of course a way to mimic the various shapes crystals take.

Introducing a real defect in the phases as in eq. 7.3.15 - actually breaking the regularity, or symmetry - is shown in fig. 7.3.20.

$$\begin{aligned}
 & e^{-(x+y+z-0.5)^2} + e^{-(x-y+z-0.5)^2} + e^{-(x+y-z-0.5)^2} \\
 & + e^{-(x+y+z-2.5)^2} + e^{-(x-y+z-2.5)^2} + e^{-(x+y-z-2.5)^2} \\
 & + e^{-(x+y+z-4.5)^2} + e^{-(x-y+z-4.5)^2} + e^{-(x+y-z-4.5)^2} \\
 & + e^{-(x+y+z-6.5)^2} + e^{-(x-y+z-6.5)^2} + e^{-(x+y-z-6.5)^2} \\
 & + e^{-(x+y+z+0.5)^2} + e^{-(x-y+z+0.5)^2} + e^{-(x+y-z+0.5)^2} \\
 & + e^{-(x+y+z+2.5)^2} + e^{-(x-y+z+2.5)^2} + e^{-(x+y-z+2.5)^2} \\
 & + e^{-(x+y+z+4.5)^2} + e^{-(x-y+z+4.5)^2} + e^{-(x+y-z+4.5)^2} \\
 & + e^{-(x+y+z+6.5)^2} + e^{-(x-y+z+6.5)^2} + e^{-(x+y-z+6.5)^2} \\
 & + e^{-(x+y+z+6.5)^2} + e^{-(x-y+z+6.5)^2} = 4.15
 \end{aligned}
 \tag{7.3.15}$$

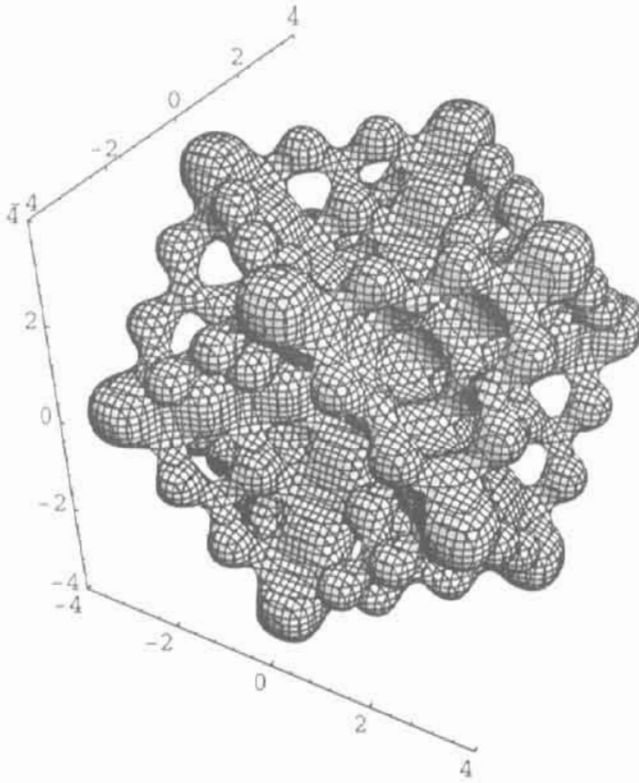


Fig. 7.3.20. After equation 7.3.15 - the octahemioctahedron.

Similarly we construct the equation 7.3.16

$$\begin{aligned}
 & e^{-x^2} + e^{-y^2} + e^{-z^2} + e^{-(x-2)^2} + e^{-(y-2)^2} + e^{-(z-2)^2} \\
 & + e^{-(x-4)^2} + e^{-(y-4)^2} + e^{-(z-4)^2} + e^{-(x-6)^2} + e^{-(y-6)^2} + e^{-(z-6)^2} \\
 & + e^{-(x-8)^2} + e^{-(y-8)^2} + e^{-(z-8)^2} + e^{-(x+1)^2} + e^{-(y+1)^2} + e^{-(z+1)^2} \\
 & + e^{-(x+3)^2} + e^{-(y+3)^2} + e^{-(z+3)^2} + e^{-(x+5)^2} + e^{-(y+5)^2} + e^{-(z+5)^2} \\
 & + e^{-(x+7)^2} + e^{-(y+7)^2} + e^{-(z+7)^2} + e^{-(x+9)^2} + e^{-(y+9)^2} + e^{-(z+9)^2} = 3.1
 \end{aligned}$$

7.3.16

which gives fig. 7.3.21.

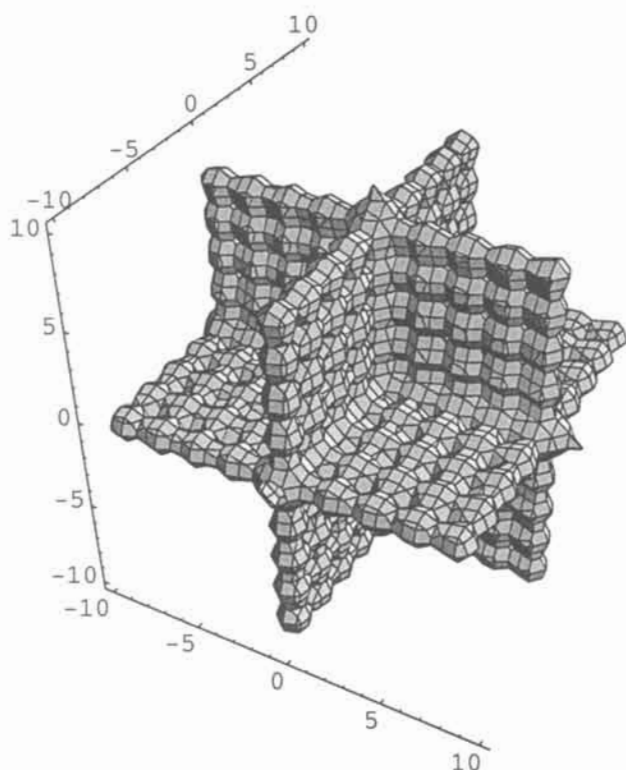


Fig. 7.3.21. After equation 7.3.16 - tetrahemihexahedron.

These two surfaces are remarkable - they are very similar to the non convex polyhedra, and the octahemioctahedron and tetrahemihexahedron. Like these polyhedra, the surfaces are built of four equatorial hexagons and three perpendicular squares, which lie in planes which are described above to generate periodicity. These planes may also be regarded as twin planes, and as such these generate unique structures.

The real term of eq. 7.3.17 gives intersecting planes as a nodal surface, shown in fig. 7.3.22.

$$\text{Re}[i^{x+y+z} + i^{x-y+z} + i^{x+y-z} + i^{-x+y+z}] = 0 \quad 7.3.17$$

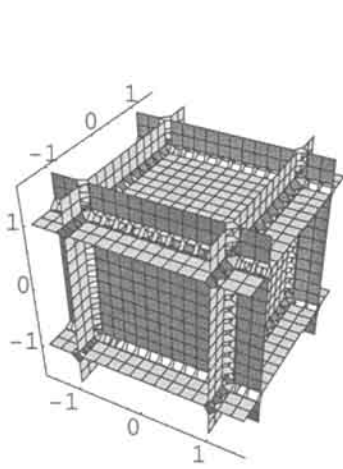


Fig. 7.3.22. After equation 7.3.17.

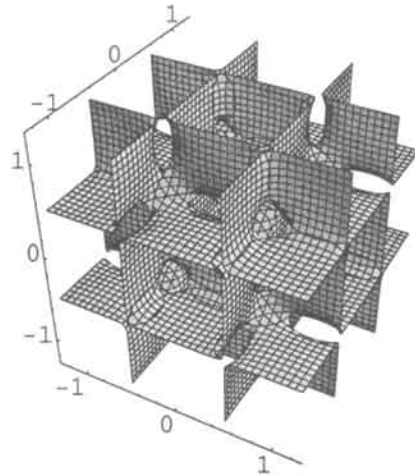


Fig. 7.3.23. After equation 7.3.18 - a FRD related surface.

With the GD function developed with translations of 2, 4, 6 in eq. 7.3.18, which corresponds to cosine in terms of the circular functions, we have a surface related to the FRD as shown in fig. 7.3.23. This surface is a beautiful demonstration of how perpendicular planes continuously can go through each other without intersections.

$$\begin{aligned}
 &10^{-(x+y+z)^2} + 10^{-(x-y+z)^2} + 10^{-(x+y-z)^2} + 10^{-(x+y+z)^2} \\
 &+ 10^{-(x+y+z+2)^2} + 10^{-(x-y+z+2)^2} + 10^{-(x+y-z+2)^2} + 10^{-(x+y+z+2)^2} \\
 &+ 10^{-(x+y+z+4)^2} + 10^{-(x-y+z+4)^2} + 10^{-(x+y-z+4)^2} + 10^{-(x+y+z+4)^2} \\
 &+ 10^{-(x+y+z+6)^2} + 10^{-(x-y+z+6)^2} + 10^{-(x+y-z+6)^2} + 10^{-(x+y+z+6)^2} \\
 &+ 10^{-(x+y+z-2)^2} + 10^{-(x-y+z-2)^2} + 10^{-(x+y-z-2)^2} + 10^{-(x+y+z-2)^2} \\
 &+ 10^{-(x+y+z-4)^2} + 10^{-(x-y+z-4)^2} + 10^{-(x+y-z-4)^2} + 10^{-(x+y+z-4)^2} \\
 &+ 10^{-(x+y+z-6)^2} + 10^{-(x-y+z-6)^2} + 10^{-(x+y-z-6)^2} + 10^{-(x+y+z-6)^2} = 2.33
 \end{aligned}
 \tag{7.3.18}$$

Any degree of irregular structures may of course be designed in 3D, as was done in 2D. The obvious application is functions of dilatation symmetry. In eq. 7.3.19 we have formulated a function which indeed gives the remarkable structure of a 3D Fibonacci periodicity, illustrated in fig. 7.3.24. The structure is a dilated P-surface, or dilated primitive packing of bodies.

In fig. 7.3.25 we give a larger region of this beautiful symmetry as the corresponding 2D plot, at a constant of 1.9.

$$\begin{aligned}
 & e^{-(x-3)^2} + e^{-(y-3)^2} + e^{-(z-3)^2} + e^{-(x-5)^2} + e^{-(y-5)^2} + e^{-(z-5)^2} \\
 & + e^{-(x-8)^2} + e^{-(y-8)^2} + e^{-(z-8)^2} + e^{-(x-13)^2} + e^{-(y-13)^2} + e^{-(z-13)^2} \\
 & + e^{-(x-21)^2} + e^{-(y-21)^2} + e^{-(z-21)^2} \\
 & + e^{-(x-34)^2} + e^{-(y-34)^2} + e^{-(z-34)^2} = 2.5
 \end{aligned}$$

7.3.19

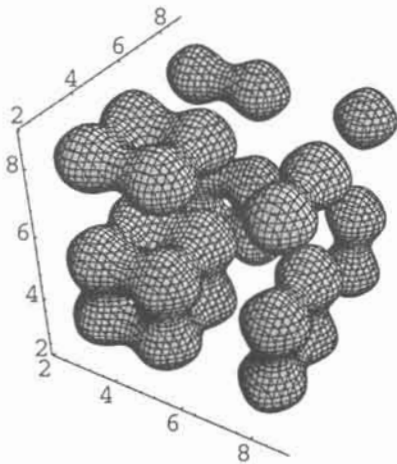


Fig. 7.3.24. 3D Fibonacci periodicity after 7.3.19.

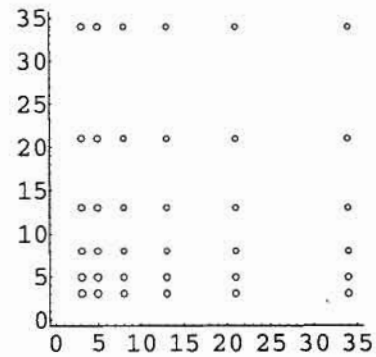


Fig. 7.3.25. 2D Fibonacci periodicity.

7.4 The Link to Cosine

For a constant of 2 according to eq. 7.4.1,

$$e^{-x^2} + e^{-y^2} + e^{-z^2} = 2$$

7.4.1

there is the remarkable octahedron in fig. 7.4.1.

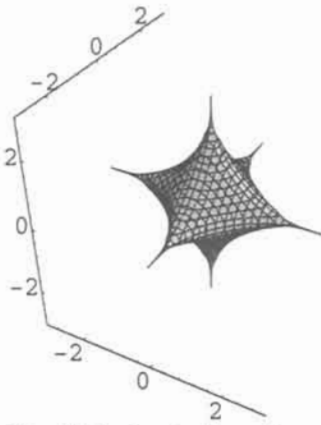


Fig. 7.4.1. Octahedron after equation 7.4.1.

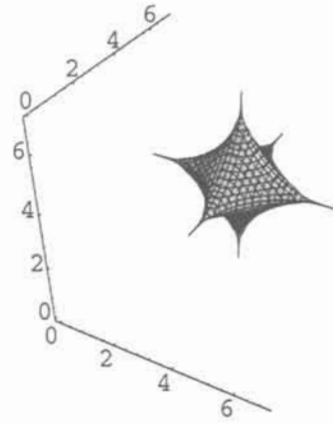


Fig. 7.4.2. Octahedron shifted after equation 7.4.2.

This octahedron may be shifted after eq. 7.4.2

$$e^{-(x-4)^2} + e^{-(y-4)^2} + e^{-(z-4)^2} = 2 \tag{7.4.2}$$

which gives fig. 7.4.2.

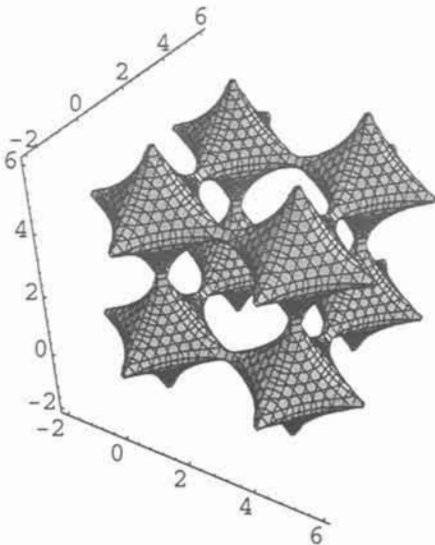


Fig. 7.4.3. Adding the two octahedra gives eight after equation 7.4.3.

By adding the two octahedra after eq. 7.4.3 we get eight as in fig 7.4.3, which means beginning of periodicity.

$$e^{-x^2} + e^{-y^2} + e^{-z^2} + e^{-(x-4)^2} + e^{-(y-4)^2} + e^{-(z-4)^2} = 2 \quad 7.4.3$$

We take the octahedra apart as in figures 7.4.4 and 7.4.5 after equations 7.4.4 and 7.4.5 respectively.

$$e^{-x^2} + e^{-y^2} + e^{-z^2} + e^{-(x-6)^2} + e^{-(y-6)^2} + e^{-(z-6)^2} = 2 \quad 7.4.4$$

$$e^{-x^2} + e^{-y^2} + e^{-z^2} + e^{-(x-8)^2} + e^{-(y-8)^2} + e^{-(z-8)^2} = 2 \quad 7.4.5$$

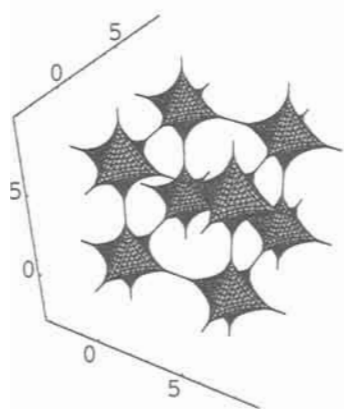


Fig. 7.4.4. After equation 7.4.4.

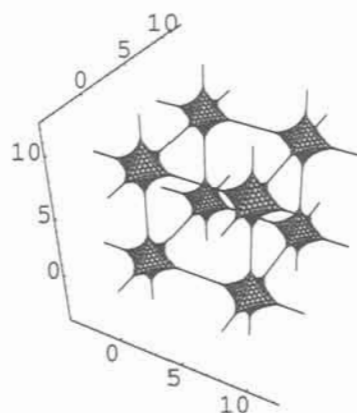


Fig. 7.4.5. After equation 7.4.5.

The surfaces of the circular equations from chapter 4,

$$(\cos x)^2 + (\cos y)^2 + (\cos z)^2 = 2 \quad 7.4.6$$

$$(\cos x)^4 + (\cos y)^4 + (\cos z)^4 = 2 \quad 7.4.7$$

$$(\cos x)^6 + (\cos y)^6 + (\cos z)^6 = 2 \quad 7.4.8$$

are very similar to figures 7.4.3-5. Especially is this the case for the figures 4.3.3 and 7.4.5 - to the eye they look identical.

Note that the constant is always 2 whichever we use, the GD function or cosine function. From these observations it is obvious that there must be a link between the GD-function and the circular functions.

The GD function is very famous for its applications:

$$y = e^{-x^2} \tag{7.4.9}$$

The function is the fundamental solution to the diffusion equation [4],

$$\frac{\partial u}{\partial t} - \frac{\partial^2 u}{\partial x^2} = 0 \tag{7.4.10}$$

and its solution with time.

$$u(x, t) = \frac{1}{\sqrt{4pt}} e^{-\frac{x^2}{4t}} \tag{7.4.11}$$

For a constant time we have the so called GD function below in fig. 7.4.6, which is plotted after eq. 7.4.9.

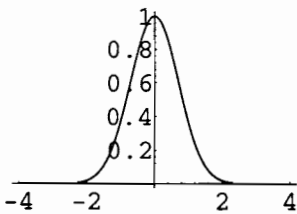


Fig. 7.4.6. Gauss-distribution (GD) function after equation 7.4.9.

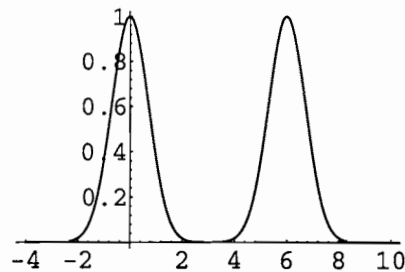


Fig. 7.4.7. Handmade periodicity with GD function after equation 7.4.12.

With a shift as

$$y = e^{-x^2} + e^{-(x-6)^2} \tag{7.4.12}$$

we can build a handmade periodicity as in fig 7.4.7.

We do the expansions

$$e^{-x^2} = 1 - x^2 + 0.5x^4 - 0.16667x^6 + 0.041667x^8 \dots \quad 7.4.13$$

$$\cos x = 1 - 0.5x^2 + 0.041667x^4 \dots \quad 7.4.14$$

$$\cos^2 x = 1 - x^2 + 0.333x^4 \dots \quad 7.4.15$$

and see already by squaring $\cos x$ and expanding that there are similarities to the GD function, which is the background to the 3D pictures above.

After some trials we found the function

$$\cos^{2n} \frac{x}{\sqrt{n}} \Rightarrow e^{-x^2}, n \rightarrow \infty \quad 7.4.16$$

and its convergence is shown below. Compare

$$e^{-x^2} = 1 - x^2 + 0.5x^4 - 0.16667x^6 + 0.041667x^8 \dots \quad 7.4.17$$

with

$$\cos^{800} x \sqrt{\frac{1}{400}} = 1 - x^2 + 0.49958x^4 - 0.16625x^6 + 0.041459x^8 \dots \quad 7.4.18$$

and

$$\cos^{20000} x/100 = 1 - x^2 + 0.49998x^4 - 0.16665x^6 + 0.041658x^8 \quad 7.4.19$$

The function for $n=10$, or $y = \cos^{20} \frac{x}{\sqrt{10}}$ is compared with $\cos x$ in fig.

7.4.8 and we see that the periodicity is increasing with n .

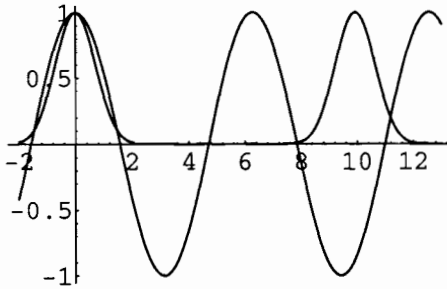


Fig. 7.4.8. $n=10$ in equation 7.4.16 as compared with $\cos x$.

The typical GD similar shapes are separated and very flat, or close to 0, between the peaks, and we continue with the cosine function for $n=200$ in figures 7.4.9 and 7.4.10.

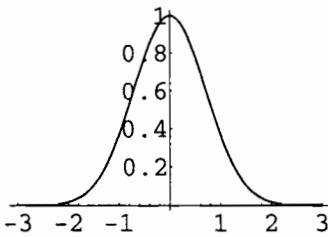


Fig. 7.4.9. $n=200$ in equation 7.4.16 and the first peak.

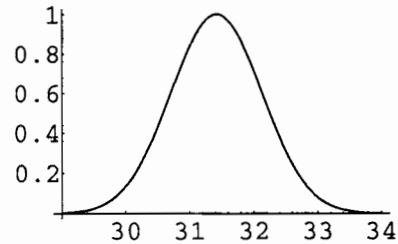


Fig. 7.4.10. $n=200$ in equation 7.4.16 and the second peak.

To left there is the shape around $x=0$ in fig 7.4.9, and after that the function is flat all the way until x is about 31.5, in fig. 7.4.10, where it repeats again for the first time.

Of course it is not possible to distinguish the plots of the GD function and this cosine function for this value of n . We have to go back to a value of $n=20$ to see any difference of the two functions as they are plotted in figure 7.4.11.

Is there any use for this function? In the precipitation of crystals, or particles, from a solid or a liquid, there should be a concentration gradient with a shape such as that of this new function. And of course the concentration is constant, or flat, between the crystals. Indeed the precipitation phenomena may be periodic which also has been reported by

Terasaki [5]. He also points out the relevance for the Liesegang rings as a periodic precipitation.

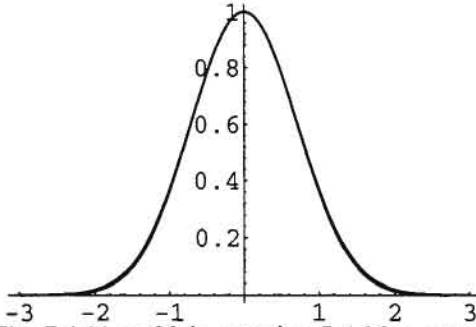


Fig. 7.4.11. $n=20$ in equation 7.4.16 as compared with the GD function.

More examples come from the general permutations in space as in equations 7.4.20 and 7.4.21, which are shown in figures 7.4.12 and 7.4.13 respectively.

$$\begin{aligned} &(\cos(x+y+z))^8 + (\cos(x-y-z))^8 \\ &+ (\cos(-x-y+z))^8 + (\cos(-x+y-z))^8 = 2 \end{aligned} \quad 7.4.20$$

$$e^{-(x+y+z)^2} + e^{-(x-y-z)^2} + e^{-(x+y-z)^2} + e^{-(x-y+z)^2} = 2 \quad 7.4.21$$

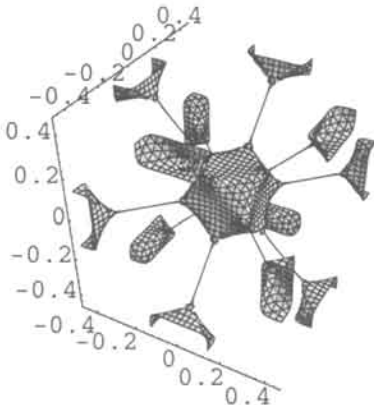


Fig. 7.4.12. After equation 7.4.20.

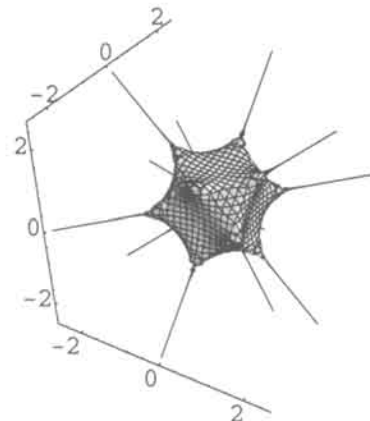


Fig. 7.4.13. After equation 7.4.21.

And also the permutations:

$$\begin{aligned} & \cos \pi(x+y)^8 + \cos \pi(x-y)^8 + \cos \pi(x+z)^8 \\ & + \cos \pi(z-x)^8 + \cos \pi(y+z)^8 + \cos \pi(y-z)^8 = C \end{aligned} \quad 7.4.22$$

$$\begin{aligned} & e^{-(x+y)^2} + e^{-(-x+y)^2} + e^{-(y+z)^2} \\ & + e^{-(-y+z)^2} + e^{-(x+z)^2} + e^{-(-x+z)^2} = C \end{aligned} \quad 7.4.23$$

Fig 7.4.14 shows the cos function, and 7.4.15 the GD function, both for a constant $C=2$, which is the limit for the extremely thin catenoids running out from the cube faces, of octahedral symmetry.

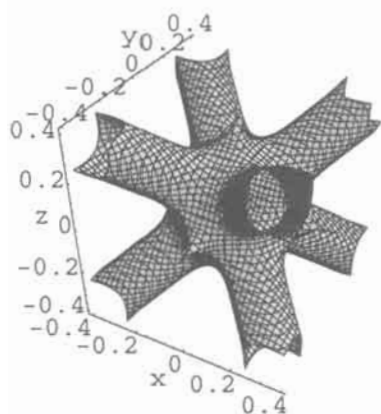


Fig. 7.4.14. After equation 7.4.22 for $C=2$.

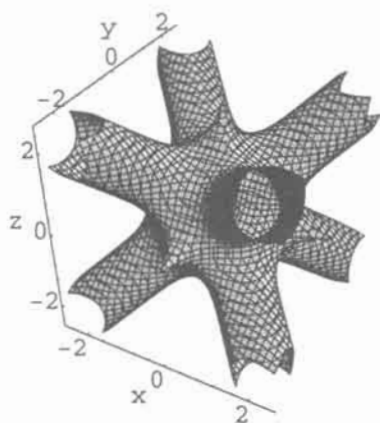


Fig. 7.4.15. After equation 7.4.23 for $C=2$.

Going to a constant $C=3$, the catenoids are extremely thin so we show figs 7.4.16 and 7.4.17, both calculated for a constant of 2.99 from equations 7.4.22 and 7.4.23 respectively.

The remarkable shapes above are descriptions of some strange creatures, the radiolarians.

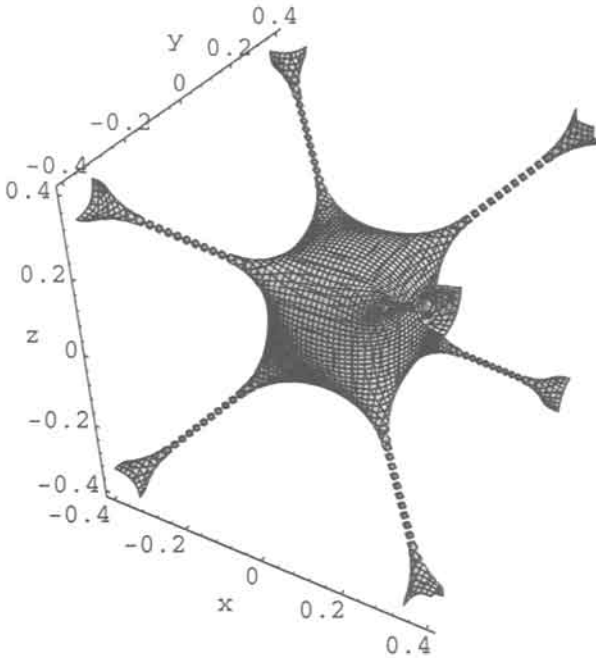


Fig. 7.4.16. After equation 7.4.22 for $C=2.99$.

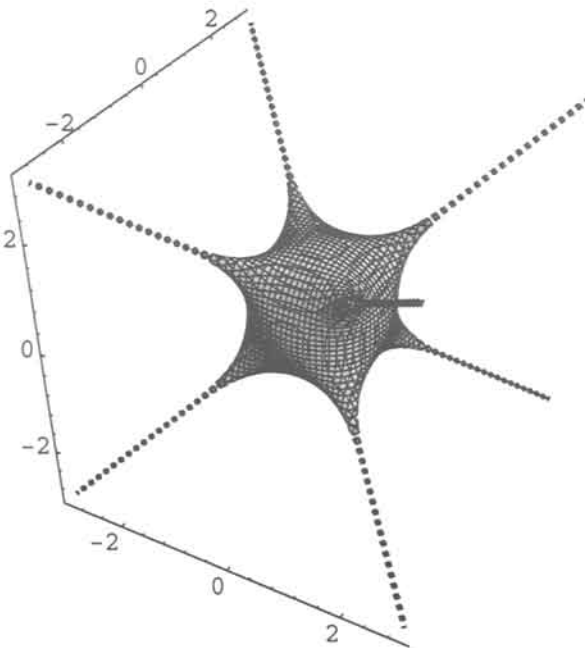


Fig. 7.4.17. After equation 7.4.23 for $C=2.99$.

The science of the shape of these organisms is enormously rich, and we will make no attempt to describe it here. But we would like to point out the extraordinary similarity in the discussion of their formation and the recently discovered so-called giant zeolites. It is enough to quote d'Arcy Thompson [6, page 723] 'skeletons are formed --- by surface action --- by the adsorptive deposition of silica in walls and wedges, corresponding to the manifold surfaces and interfaces of the system. --- the skeletons consists (1) of radiating spicular rods, definite in number and position, and (2) of interconnecting rods or plates, tangential to --- that of a geometric, polyhedral solid.' These creatures are obviously grown by a chemical transport reaction, controlled by diffusion which is in perfect agreement with our models above as fundamental solutions they are to the diffusion equation.

Exercises 7

Exercise 7.1. Plot the GD function and the new cosine function for $n=100$. Do the numerical integration for both, with suitable boundaries and show the difference. (Hint: Use Mathematica's NIntegrate function).

Exercise 7.2. Show which curve is which in fig 7.4.11.

Exercise 7.3. Do the planar square group p4g as in chapter 6, but with the fundamental theorem of algebra.

Exercise 7.4. Do the equation for fig 7.1.20.

Exercise 7.5. Compare a GD function like xe^{-x^2} with sine.

Answer 7.1

```
NIntegrate[E^(-x^2), {x,-3,3}]
1.77241
NIntegrate[Cos[(2/100)^.5x]^100, {x,-3,3}]
1.768
dev .25%
```

Or just

```
Integrate[Cos[(2/100)^.5x]^100, {x,-3,3}]
1.768
```

```
Plot[Cos[(2/100)^.5x]^100, {x,-3,3} in 7.1a,
Plot[E^(-x^2), {x,-3,3} in 7.1b,
PlotPoints->400, Axes->True] PlotPoints->400, Axes->True]
```

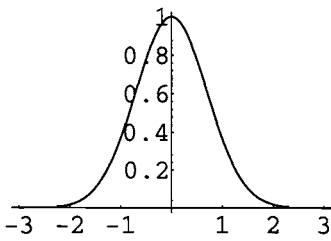


Fig. 7.1a

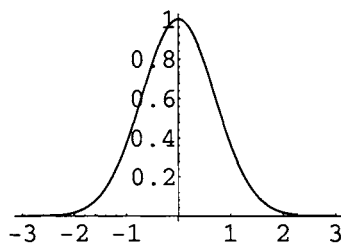


Fig. 7.1b

Answer 7.2

Use smaller boundaries doing the NIntegrate and you will see.

Answer 7.3

```
ImplicitPlot[
x(x-1)(x-2)(x-3)(x-4)(x-5)(x-6)(x-7)(x-8)(x+y)(x+y-1)(x+y-2)
(x+y-3)(x+y-4)(x+y-5)(x+y-6)(x+y-7)(x+y-8)
y(y-1)(y-2)(y-3)(y-4)(y-5)(y-6)(y-7)(y-8)(x-y)(x-y-1)(x-y-2)
(x-y-3)(x-y-4)(x-y-5)(x-y-6)(x-y-7)(x-y-8)==1000000000,
{x,2,6},{y,-.5,3.5},PlotPoints->100]
```

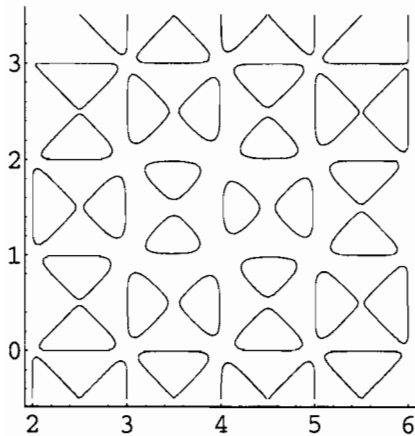



Fig. 7.3

Answer 7.4

$$\begin{aligned}
 & e^{-x^2} + e^{-y^2} + e^{-(x-2)^2} + e^{-(y-2)^2} + e^{-(x-4)^2} + e^{-(x-6)^2} + e^{-(y-6)^2} \\
 & + e^{-(y-8)^2} + e^{-(x-10)^2} + e^{-(y-10)^2} + e^{-(x-12)^2} + e^{-(y-12)^2} + e^{-(x-14)^2} \\
 & + e^{-(y-14)^2} + e^{-(x-16)^2} + e^{-(y-16)^2} = C
 \end{aligned}$$

Answer 7.5

```

Plot[
{(x+2) E^-(x+2)^2+x E^-(x)^2+(x-2)E^-(x-2)^2+
(x-4)E^-(x-4)^2+(x-6)E^-(x-6)^2+(x-8)E^-(x-8)^2+
(x-10)(E^-(x-10)^2+(x-12)E^-(x-12)^2+
(x-14)E^-(x-14)^2+(x-16)E^-(x-16)^2+
(x-18)E^-(x-18)^2+(x-20)E^-(x-20)^2+
(x-22)E^-(x-22)^2, 0.236 Sin[Pi x]}, {x,0,20},
PlotPoints->400, Axes->True]

```

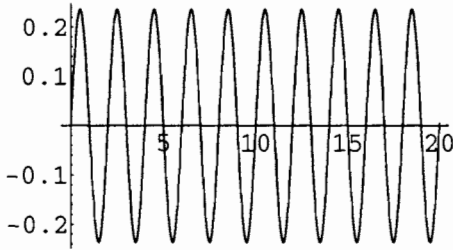


Fig. 7.5a

Plot as above but with the boundaries $\{x,6,7\}$,
PlotPoints->400,Axes->True]

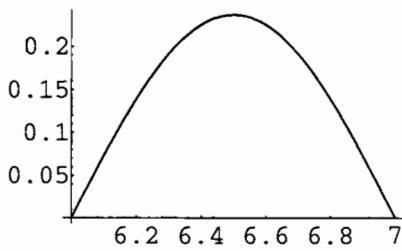


Fig. 7.5b

References 7

- 1 G.H. Hardy; A MATHEMATICIAN'S APOLOGY, Cambridge University press, 1976, page 66.
- 2 Jacob, M. and Andersson, S.; Z. Kristallogr. **212** (1997) 486-492.
- 3 M. Jacob; J. Phys. II France **7** (1997) 1035-1044.
- 4 D. Vvedensky; PARTIAL DIFFERENTIAL EQUATIONS, Addison-Wesley, 1992.
- 5 Terasaki, Osamu. Acta Chem. Scand. **45** (1991) 785.
- 6 D'Arcy Wentworth Thompson, ON GROWTH AND FORM, Cambridge University press, 1942.

8 Handmade Structures and Periodicity

There is no business like show business (origin unknown).

Here we continue to use the exponential scale and the GD function to build constructions of different kinds. We do some classic geometry. We see repulsion and also the hanging drop.

We see the hyperbolic plane and use it to revisit the radiolarians.

In chapter 7 we added planes - here we add closed bodies, one by one, to periodic structures.

We derive surfaces from structures by making spheres meet in space. We analyse the topology of the surfaces created. We find that a periodic structure has a dual. We describe some fundamental oxide chemistry.

We make closed bodies, like tetrahedra and octahedra, meet in space and show in that way how mathematical functions describe crystal structures.

8.1 Prelude

Handmade constructions have been touched earlier in the section for hierarchical growth, and described in the last chapter. Here we shall start from scratch and develop it.

We showed earlier that it was necessary to go higher up in the exponential scale, in order to keep the original characters of the units we put together into a continuous function. This is more pronounced the higher up you are on the scale, and with the scale we mean as before:

$$e^x; e^{e^x}; e^{e^{e^x}}$$

In chapter 7 we used planes or lines in GD functions and had real periodicity after our definition. Now we use closed bodies like spheres or polyhedra, and build them one by one to a periodic structure. We shall first give a short study of spheres, cylinders and planes, as a preparation before we start with the GD functions.

We said it before, cylinders and spheres consist of collaborating planes. We start with the cylinder;

$$x^2 + y^2 = 1$$

$x^2 = 1$ is two planes as in figure 8.1.1, and so is $y^2 = 1$. The four planes collaborate and form the cylinder of equation 8.1.1.

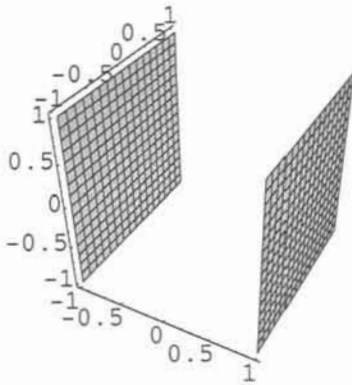


Fig. 8.1.1. Two planes after $x^2 = 1$.

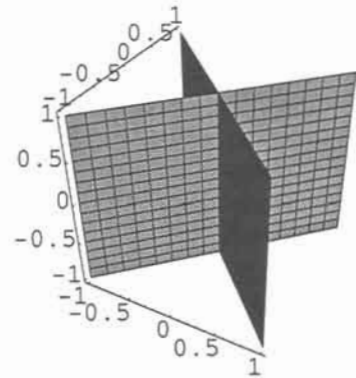


Fig. 8.1.2. Two intersecting planes after equation 8.1.2.

For

$$x^2 - y^2 = 0 \quad 8.1.2$$

there are two intersecting planes. It is important to note that the function can be written as $(x-y)(x+y)$ which are the planes in fig. 8.1.2.

For

$$x^2 - y^2 = 0.05 \quad 8.1.3$$

there is fig. 8.1.3, and for

$$x^2 - y^2 = -0.05 \quad 8.1.4$$

fig. 8.1.4.

And for

$$x^2 + y^2 + z^2 = 1$$

there are six planes in space that collaborate to form a sphere.

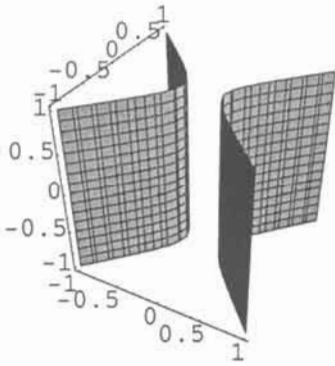


Fig. 8.1.3. After equation 8.1.3.

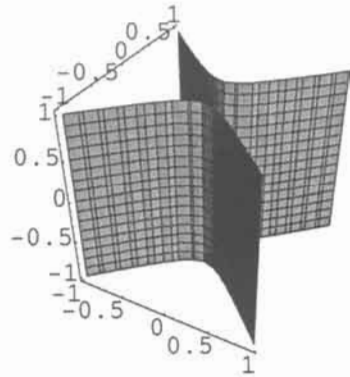


Fig. 8.1.4. After equation 8.1.4.

The equation

$$x^2 + y^2 - z^2 = 0 \quad 8.1.5$$

is a double cone as in fig 8.1.5. Adding a constant,

$$x^2 + y^2 - z^2 = 1 \quad 8.1.6$$

gives a catenoid structure as in fig 8.1.6, while subtraction gives parabolic geometry. We can also say that we opened up a sphere by making one of its terms negative. Or that the addition of two planes to the cylinder makes it spherical.

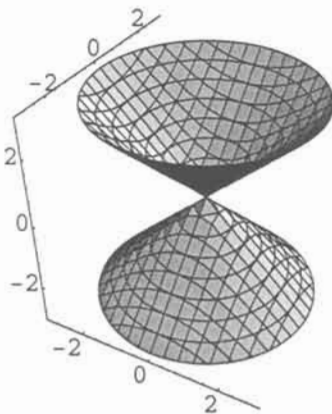


Fig. 8.1.5. After equation 8.1.5.

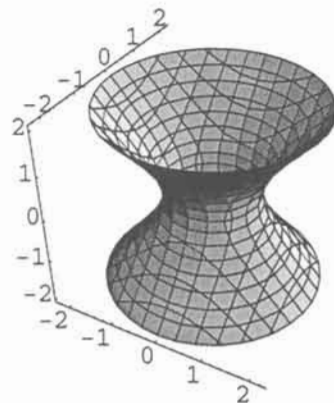


Fig. 8.1.6. After equation 8.1.6.

Adding two spheres like in

$$x^2 + y^2 + z^2 + x^2 + y^2 + (z-2)^2 = 10 \quad 8.1.7$$

gives one sphere but with shifted centre, illustrated in fig. 8.1.7.

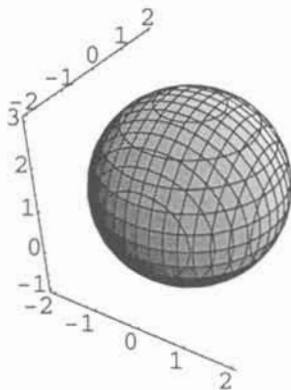


Fig. 8.1.7. After equation 8.1.7.

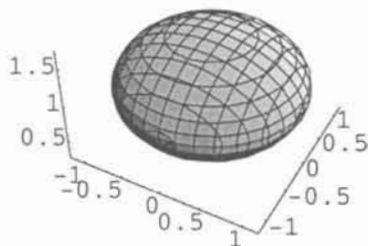


Fig. 8.1.8. After equation 8.1.8.

Going to the exponential scale and adding the same two spheres with different centres with equation 8.1.8, gives again complete fusion as in fig. 8.1.8. From the shape it is obvious that the origin is two spheres.

$$e^{x^2+y^2+z^2} + e^{x^2+y^2+(z-2)^2} = 20 \quad 8.1.8$$

Going to negative scale, or GD similar functions, helps. We see drastically increased resolution and two different spheres as in eq. 8.1.9 and fig. 8.1.9. It is possible to build things from several parts.

$$e^{-(x^2+y^2+z^2)} + e^{-(x^2+y^2+(z-2)^2)} = 0.8 \quad 8.1.9$$

We have shown earlier that two different functions can be added on the exponential scale so that the sum function is continuous and the properties of the original functions are kept. A centaur function is a good name - the man and his horse are intergrown via a catenoid - there is negative curvature. A change of coordinates, or change of constant, makes the bodies in fig. 8.1.9 approach and form a catenoid - negative curvature as in fig. 8.1.10. And an example of a centaur function is the cylinder and sphere grown together - the hanging drop - in fig. 8.1.11 after eq. 8.1.10.

$$e^{-(x^2+y^2+z^2)} + e^{-(x^2+(z-1.9)^2)} = 0.8$$

8.1.10

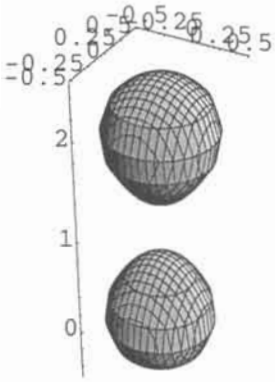


Fig. 8.1.9. After equation 8.1.9.

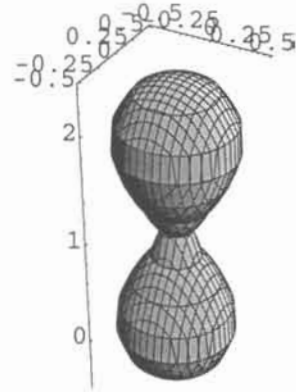
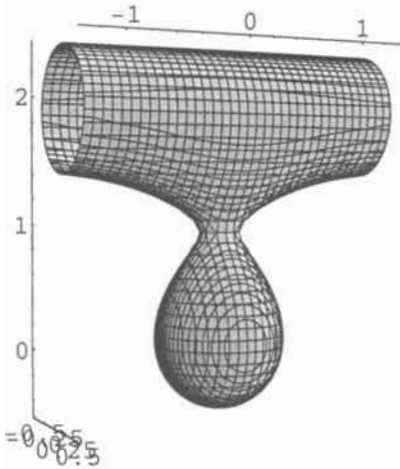
Fig. 8.1.10. After equation 8.1.9 but with $z=1.9$.

Fig. 8.1.11. Hanging drop after equation 8.1.10.

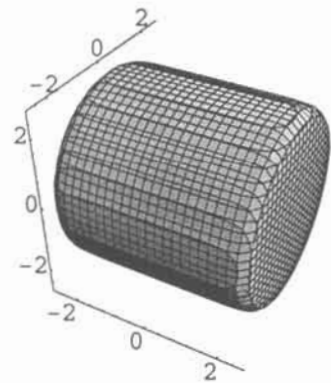


Fig. 8.1.12. Almost a sphere after equation 8.1.11.

We said that the sphere consists of six planes, and in equation 8.1.11 we have separated two of them using the exponential scale as seen in fig. 8.1.12. The operation left us with a cylinder, with two lids as given by the two planes.

$$e^{x^2} + e^{y^2+z^2} = 1000 \quad 8.1.11$$

Using the GD function gives beautiful geometry. We start with the analogous equation in 8.1.12 as shown in fig. 8.1.13. The picture talks for itself. We note again that with the normal exponential scale things are added, and positive Gaussian curvature is kept as above. Using the GD function instead gives negative curvature as below.

$$e^{-x^2} + e^{-(y^2+z^2)} = 0.5 \quad 8.1.12$$

Increasing the constant towards unity makes the planes come together and the geometry is approaching the topology for the pseudosphere, famous for having constant negative Gaussian curvature. With one plane as in eq. 8.1.13 and with a constant close to unity the surface is pulled out from the plane, as shown in fig. 8.1.14.

$$e^{-z} + e^{-(x^2+y^2)} = 0.99 \quad 8.1.13$$

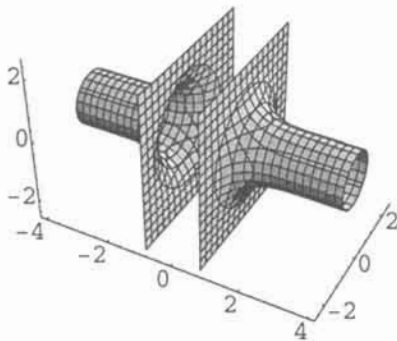


Fig. 8.1.13. Two GD planes open a cylinder.

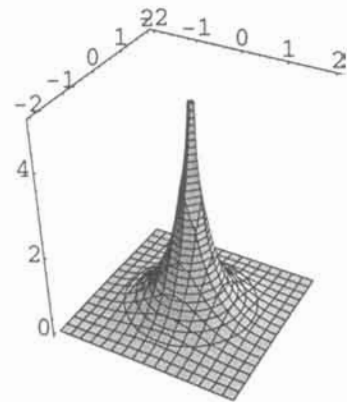


Fig. 8.1.14. With C close to 1 a 'pseudosphere' is pulled out of the plane.

With eq. 8.1.14 we pull ‘pseudospheres’ out from a sphere as well, as shown in fig. 8.1.15.

$$e^{-(x^2+y^2+z^2)} + e^{-(y^2+z^2)} = 1 \quad 8.1.14$$

In fig. 8.1.16 there are two cylinders after eq. 8.1.15.

$$e^{-(x^2+y^2+z^2)} + e^{-(y^2+z^2)} + e^{-(x^2+z^2)} = 1 \quad 8.1.15$$

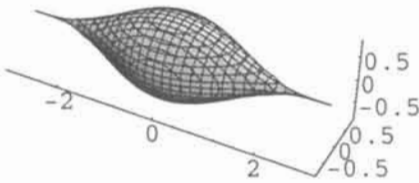


Fig. 8.1.15. Two ‘pseudospheres’ are pulled out of the sphere after equation 8.1.14.

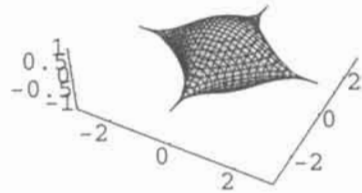


Fig. 8.1.16. Four ‘pseudospheres’ are pulled out of the sphere.

These two cylinders are after two unit cube axes, and in fig. 8.1.17 we have also added a cylinder which is a space diagonal in the cube. The equation for that cylinder in eq. 8.1.16 is from the next chapter.

$$e^{-(x^2+y^2+z^2)} + e^{-(y^2+z^2)} + e^{-(x^2+z^2)} + e^{-((x+z)^2+(x-y)^2+(y+z)^2)} = 1 \quad 8.1.16$$

This is a powerful method for making radiolarians by just using the cylinder approach from next chapter. This topology shows that many structures in Nature might well be built with constant negative curvature. The mathematics of the hyperbolic plane is difficult, and not possible to use directly. It has been pointed out before that the geometry of many leaves, in particular the holly ones, are related to the hyperbolic plane [1] and the structure of water [2]. Perhaps the development of this topology in Nature is favoured by the finite growth, which the GD functions indeed can offer. The deviations from the real hyperbolic plane are certainly small.

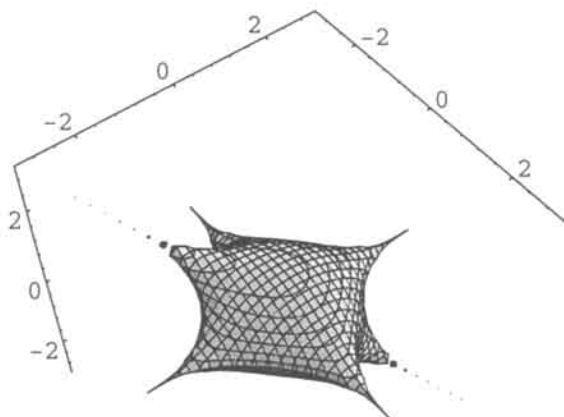


Fig. 8.1.17. Three 'pseudospheres' are pulled out of the sphere after equation 8.1.16.

Subtracting two planes from the sphere gave the double cone above. Using the scale or the GD function give similar results. Subtracting more planes as in eq. 8.1.17, give a number of bodies or particles between the cones, as shown in figure 8.1.18.

$$e^{-x^2} - e^{-(y^2+z^2)} + e^{-(x-2)^2} + e^{-(x-4)^2} = 0 \quad 8.1.17$$

With the square of functions we get concentric structures as in figures 8.1.19 and 8.1.20.

$$(x^2 + y^2 + z^2 - 2)^2 = 0.5 \quad 8.1.18$$

$$(x^2 + y^2 - 1)^2 = 0.5 \quad 8.1.19$$

With the sphere, pairs are added to a remarkable concentric structure as in eq. 8.1.20 and fig. 8.1.21, which is the topology of s-electron shells of the structure of an atom..

$$e^{-(x^2+y^2+z^2-2)^2} + e^{-(x^2+y^2+z^2-4)^2} + e^{-(x^2+y^2+z^2-6)^2} = 0.8 \quad 8.1.20$$

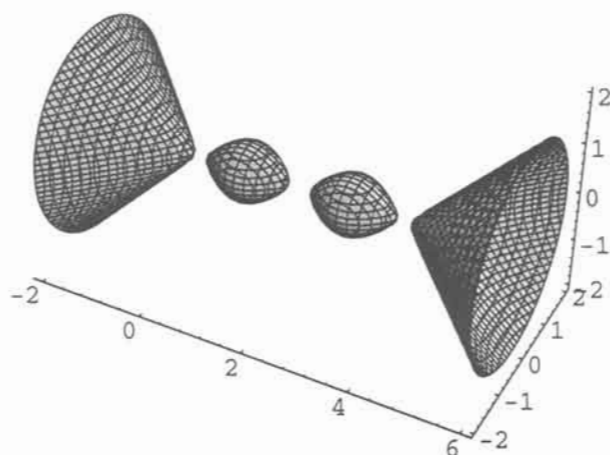


Fig. 8.1.18. A cylinder and two planes subtracted give a double cone and two added 'concentrations' give two extra bodies, after equation 8.1.17.

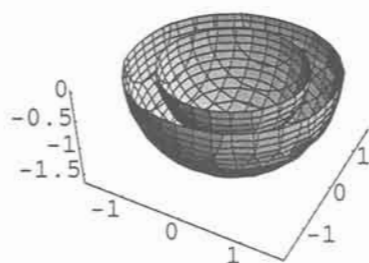


Fig. 8.1.19. Concentric spheres are obtained by squaring.

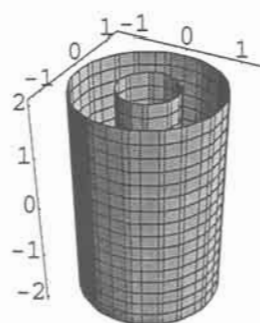


Fig. 8.1.20. After equation 8.1.19.

We add 2 spheres by coordinate shift, with the individual radii in the exponent, which generates the 'double' structure as in eq. 8.1.21, illustrated in fig. 8.1.22.

$$e^{-(x^2+(y+1)^2+z^2-0.5)^2} + e^{-(x^2+(y-1)^2+z^2-0.5)^2} = 0.9 \quad 8.1.21$$

We make the bodies approach by a small shift in y , and during the resulting fusion the inner spheres are distorted as if they repel each other, as in eq. 8.1.22 and fig. 8.1.23.

$$e^{-(x^2+(y+0.9)^2+z^2-0.5)^2} + e^{-(x^2+(y-0.9)^2+z^2-0.5)^2} = 0.9 \quad 8.1.22$$

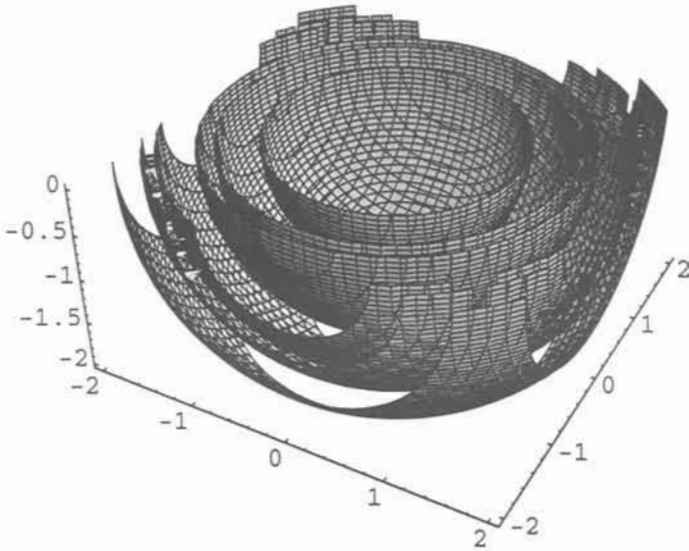


Fig. 8.1.21. After equation 8.1.20.

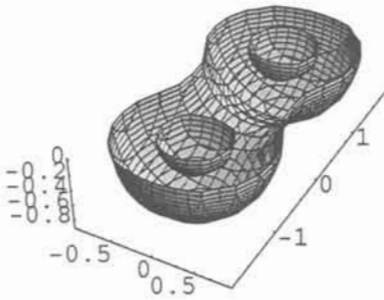


Fig. 8.1.22. Two spheres added by coordinate shifts and squared give 'double' structure after equation 8.1.21.

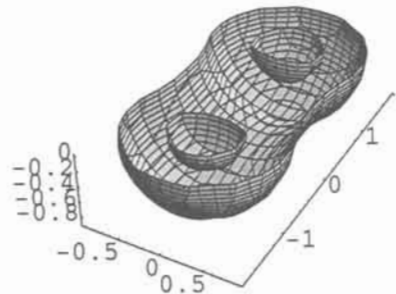


Fig. 8.1.23. The spheres are made to approach, and the inner spheres distort as after repulsion. After equation 8.1.22.

8.2 Simplest of Periodic Structures

We continue to structures of some extension in space. First we give coordinates for eight atoms, and put them together in the GD function in eq. 8.2.1. The structure is illustrated in figure 8.2.1.

$$\begin{aligned}
 & e^{-(x^2+y^2+z^2)} + e^{-((x-2)^2+y^2+z^2)} + e^{-(x^2+(y-2)^2+z^2)} \\
 & + e^{-(x^2+y^2+(z-2)^2)} + e^{-((x-2)^2+y^2+(z-2)^2)} \\
 & + e^{-(x^2+(y-2)^2+(z-2)^2)} + e^{-((x-2)^2+(y-2)^2+z^2)} \\
 & + e^{-((x-2)^2+(y-2)^2+(z-2)^2)} = 0.8
 \end{aligned} \tag{8.2.1}$$

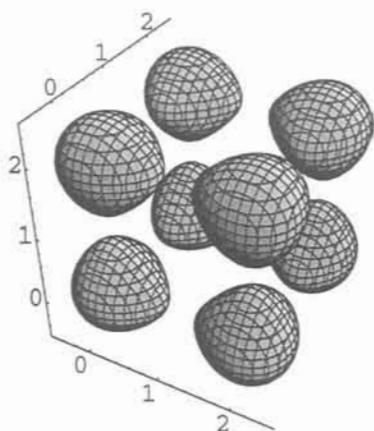


Fig. 8.2.1. Structure after equation 8.2.1.

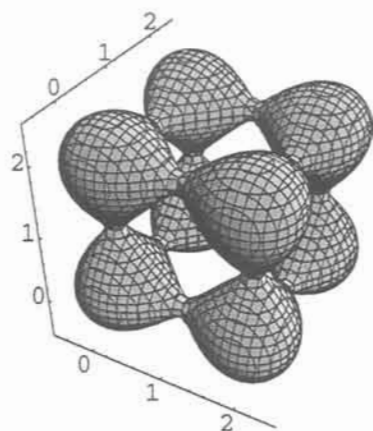


Fig. 8.2.2. After equation 8.2.2.

Using circular periodic functions we changed size of bodies by changing constant, and could make them approach each others. We may do that as well here, but we can also change distances between bodies - actually move them as in eq. 8.2.2 with the result displayed in fig. 8.2.2.

$$\begin{aligned}
 & e^{-(x^2+y^2+z^2)} + e^{-((x-1.95)^2+y^2+z^2)} + e^{-(x^2+(y-1.95)^2+z^2)} \\
 & + e^{-(x^2+y^2+(z-1.95)^2)} + e^{-((x-1.95)^2+y^2+(z-1.95)^2)} \\
 & + e^{-(x^2+(y-1.95)^2+(z-1.95)^2)} + e^{-((x-1.95)^2+(y-1.95)^2+z^2)} \\
 & + e^{-((x-1.95)^2+(y-1.95)^2+(z-1.95)^2)} = 0.8
 \end{aligned} \tag{8.2.2}$$

We have continued with equation 8.2.3 and this is shown in fig. 8.2.3.

$$\begin{aligned}
 & e^{-(x^2+y^2+z^2)} + e^{-((x-1.9)^2+y^2+z^2)} + e^{-(x^2+(y-1.9)^2+z^2)} \\
 & + e^{-(x^2+y^2+(z-1.9)^2)} + e^{-((x-1.9)^2+y^2+(z-1.9)^2)} \\
 & + e^{-(x^2+(y-1.9)^2+(z-1.9)^2)} + e^{-((x-1.9)^2+(y-1.9)^2+z^2)} \\
 & + e^{-((x-1.9)^2+(y-1.9)^2+(z-1.9)^2)} = 0.8
 \end{aligned}
 \tag{8.2.3}$$

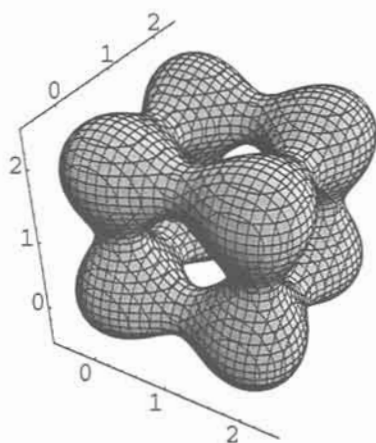


Fig. 8.2.3. After equation 8.2.3.

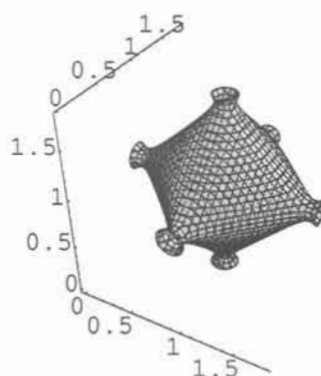


Fig. 8.2.4. Inside of fig 8.2.3 shows the dual.

When bodies still come closer together -1.82 instead of -1.9 in eq. 8.2.3 - the octahedral body of dual shape is more pronounced with proper boundaries as shown in fig. 8.2.4. If this is the B_6H_6 octahedron, the dual shape in fig. 8.2.3 is then the Savin-ELF structure of the molecule. This dual relation was pointed out by von Schnering et al. in their study of the electronic structure of boron hydrides [3].

Finally the octahedral dual structure - which of course is a part of the spheres that were made to approach each other - is reduced to a small particle at a distance of 1.76 in fig. 8.2.5.

We may disorder as in eq. 8.2.4, which gives fig. 8.2.6.

$$\begin{aligned}
 & e^{-(x^2+y^2+z^2)} + e^{-((x-2.2)^2+y^2+z^2)} + e^{-(x^2+(y-1.95)^2+z^2)} \\
 & + e^{-((x+0.2)^2+(y+0.2)^2+(z-2.5)^2)} + e^{-((x-2.3)^2+y^2+(z-2.1)^2)} \\
 & + e^{-(x^2+(y-1.95)^2+(z-1.9)^2)} + e^{-((x-2.3)^2+(y-2.3)^2+z^2)} \\
 & + e^{-((x-2.5)^2+(y-2.5)^2+(z-2.5)^2)} = 0.8
 \end{aligned}
 \tag{8.2.4}$$

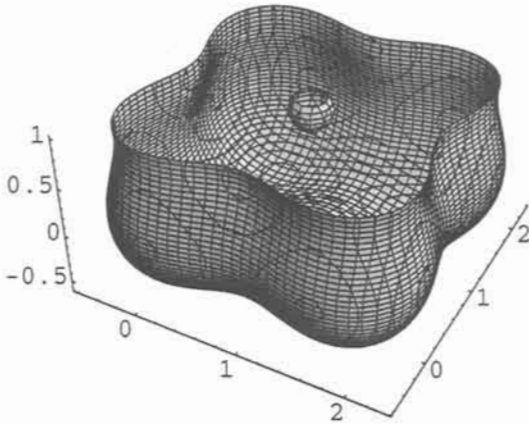


Fig. 8.2.5. After equation 8.2.3 with coordinate shift of 1.76 instead of 1.9.

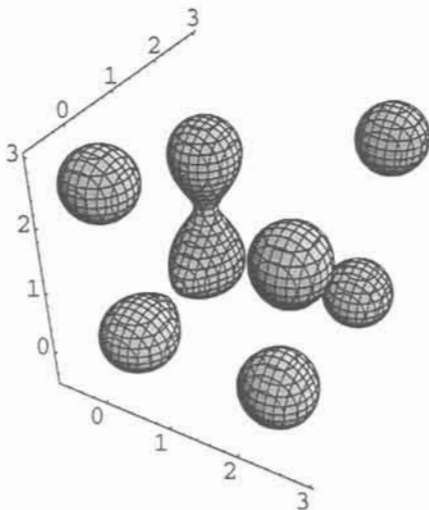


Fig. 8.2.6. Disordered structure after equation 8.2.4.

In order to prepare us for the next section, we go back to the cube of bodies and put an extra body, an interstitial atom, in the cube with eq. 8.2.5. In order to keep the same coordinates and resolution we have gone up in scale. The ordinary scale would mean fusion of the small sphere with the bigger. We take advantage of these special mathematics, and take off a corner atom so you can see better. The corner atom we put on the desk to the right, so it can be put back when needed. Figure 8.2.7 describes the whole thing and is given by eq. 8.2.5.

$$\begin{aligned}
 & e^{-e^{x^2+y^2+z^2}} + e^{-e^{(x-2)^2+y^2+z^2}} + e^{-e^{x^2+(y-2)^2+z^2}} \\
 & + e^{-e^{x^2+y^2+(z-2)^2}} + e^{-e^{(x-2)^2+(y-2)^2+z^2}} \\
 & + e^{-e^{x^2+(y-2)^2+(z-2)^2}} + e^{-e^{(x-2)^2+(y-2)^2+(z-2)^2}} \\
 & + e^{-e^{2((x-1)^2+(y-1)^2+(z-1)^2)}} + e^{-e^{(x-5)^2+y^2+z^2}} = 0.1
 \end{aligned}
 \tag{8.2.5}$$

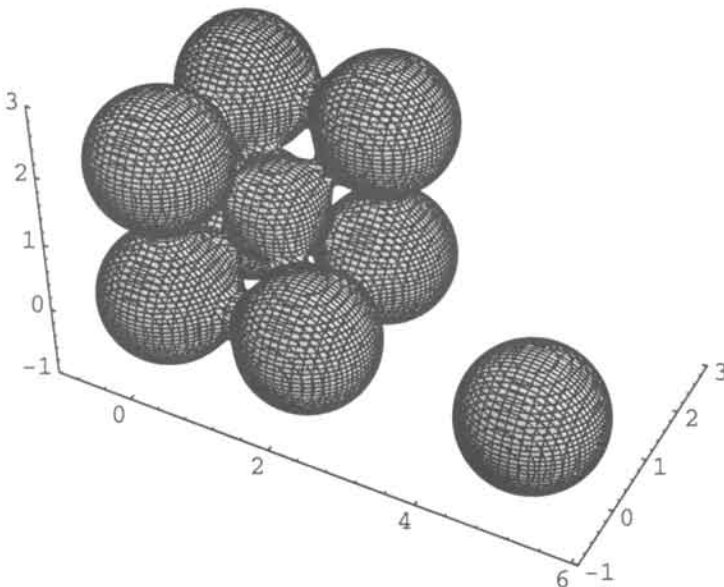


Fig. 8.2.7. A smaller interstitial body in the centre of eight bodies of a primitive cube. One of the corner bodies is taken off and put on the desk to right. The whole thing after equation 8.2.5.

8.3 Contact of Spheres in Space - Structures and Surfaces

Earlier we used surfaces to derive structures [4,5,6,7], and now we shall do the reverse - we use structures to derive surfaces. The structures here are spheres placed in space after a certain pattern we choose from structural chemistry. The jargon is that we say the spheres are organised in primitive packing (pc) above in fig 8.2.1, 8.3.1 and 8.3.6, in body centred packing (bcc) in fig. 8.3.8, in cubic close packing (ccp) in fig. 8.3.16, in diamond packing (D) in fig. 8.3.23, the G-packing (G) in 8.3.27 and finally hexagonal close packing (hcp) in fig. 8.3.29. These structures are described in terms of neighbours - in ccp and hcp each body has 12 neighbours, in bcc there are 6+8, in pc 6, in D 4 and in G only 3. What about 2? It is not trivial, but it occurs in ordinary structural chemistry, and is much more important in biology.

With the spheres spread out in these various packings, we shall make the spheres move against each other so that catenoids develop between them, just as above, or in soap water chemistry, or in the mathematics of the minimal surfaces. To some surprise we get the topology of just the famous minimal surfaces one by one, or the nowadays equally famous nodal surfaces [8,9]. As shown below.

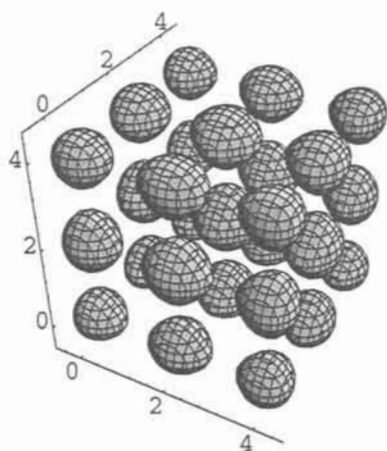


Fig. 8.3.1. 27 spheres in pc arrangement after equation 8.3.1 with $C=0.83$.

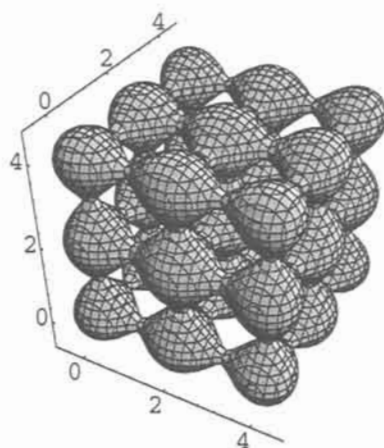


Fig. 8.3.2. After equation 8.3.1 with $C=0.75$.

In fig. 8.3.1 we have 27 spheres after eq. 8.3.1 and a constant of 0.83. By decreasing the constant to 0.75, the spheres expand and catenoids are formed as in fig. 8.2.2. But normalisation to constant sizes of spheres means that the whole structure shrinks. The auxiliary parameter - the constant - is physically the temperature, or the reverse of pressure.

$$\begin{aligned}
& e^{-(x^2+y^2+z^2)} + e^{-((x-2)^2+y^2+z^2)} + e^{-(x^2+(y-2)^2+z^2)} \\
& + e^{-(x^2+y^2+(z-2)^2)} + e^{-((x-2)^2+y^2+(z-2)^2)} \\
& + e^{-(x^2+(y-2)^2+(z-2)^2)} + e^{-((x-2)^2+(y-2)^2+z^2)} \\
& + e^{-((x-2)^2+(y-2)^2+(z-2)^2)} + e^{-((x-4)^2+y^2+z^2)} + \\
& + e^{-(x^2+(y-4)^2+z^2)} + e^{-(x^2+y^2+(z-4)^2)} + e^{-((x-4)^2+y^2+(z-2)^2)} \\
& + e^{-(x^2+(y-2)^2+(z-4)^2)} + e^{-((x-4)^2+(y-2)^2+z^2)} \\
& + e^{-((x-2)^2+y^2+(z-4)^2)} + e^{-(x^2+(y-4)^2+(z-2)^2)} \\
& + e^{-((x-2)^2+(y-4)^2+z^2)} + e^{-((x-4)^2+(y-2)^2+(z-2)^2)} \\
& + e^{-((x-2)^2+(y-2)^2+(z-4)^2)} + e^{-((x-2)^2+(y-4)^2+(z-2)^2)} \\
& + e^{-((x-4)^2+(y-2)^2+(z-4)^2)} + e^{-((x-4)^2+(y-4)^2+(z-2)^2)} \\
& + e^{-((x-2)^2+(y-4)^2+(z-4)^2)} + e^{-((x-4)^2+y^2+(z-4)^2)} \\
& + e^{-(x^2+(y-4)^2+(z-4)^2)} + e^{-((x-4)^2+(y-4)^2+z^2)} \\
& + e^{-((x-4)^2+(y-4)^2+(z-4)^2)} = 0.83
\end{aligned} \tag{8.3.1}$$

We change the constant to 0.68 and in fig. 8.3.3 we see the great similarity with the P surface with the boundaries used. The circles are even slightly square.

A constant of 0.58 gives fig. 8.3.4 and 0.50 gives 8.3.5.

In equation 8.3.2 we have added 27 spheres on the double exponential scale, and in fig. 8.3.6 we see the result. The spheres are almost undistorted, but still connected via catenoids.

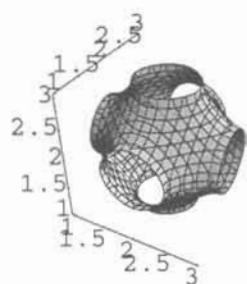


Fig. 8.3.3. After equation 8.3.1 with $C=0.68$ the inside shows the P surface.

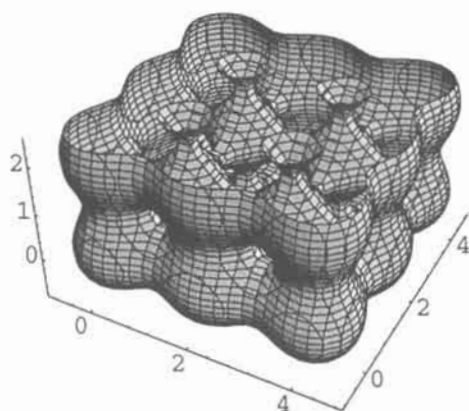


Fig. 8.3.4. $C=0.58$

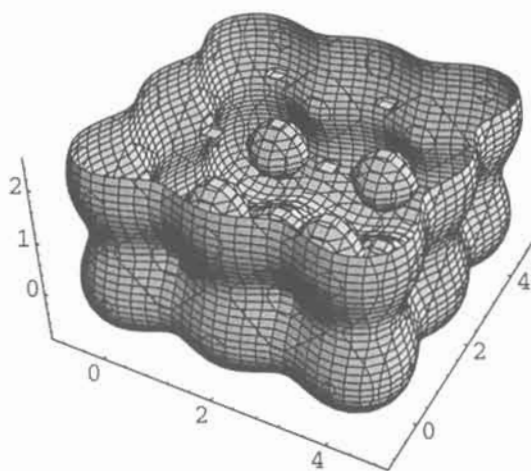


Fig. 8.3.5. $C=0.5$

$$\begin{aligned}
& e^{-e^{x^2+y^2+z^2}} + e^{-e^{(x-2)^2+y^2+z^2}} + e^{-e^{x^2+(y-2)^2+z^2}} + e^{-e^{x^2+y^2+(z-2)^2}} \\
& + e^{-e^{(x-2)^2+(y-2)^2+z^2}} + e^{-e^{(x-2)^2+y^2+(z-2)^2}} + e^{-e^{x^2+(y-2)^2+(z-2)^2}} \\
& + e^{-e^{(x-2)^2+(y-2)^2+(z-2)^2}} + e^{-e^{(x-4)^2+y^2+z^2}} + e^{-e^{x^2+(y-4)^2+z^2}} \\
& + e^{-e^{x^2+y^2+(z-4)^2}} + e^{-e^{(x-4)^2+(y-2)^2+z^2}} + e^{-e^{(x-4)^2+y^2+(z-2)^2}} \\
& + e^{-e^{x^2+(y-2)^2+(z-4)^2}} + e^{-e^{(x-2)^2+(y-4)^2+z^2}} + e^{-e^{(x-2)^2+y^2+(z-4)^2}} \\
& + e^{-e^{x^2+(y-4)^2+(z-2)^2}} + e^{-e^{(x-4)^2+(y-2)^2+(z-2)^2}} \\
& + e^{-e^{(x-2)^2+(y-2)^2+(z-4)^2}} + e^{-e^{(x-2)^2+(y-4)^2+(z-2)^2}} \\
& + e^{-e^{(x-4)^2+(y-2)^2+(z-4)^2}} + e^{-e^{(x-4)^2+(y-4)^2+(z-2)^2}} \\
& + e^{-e^{(x-2)^2+(y-4)^2+(z-4)^2}} + e^{-e^{(x-4)^2+y^2+(z-4)^2}} + e^{-e^{(x-4)^2+(y-4)^2+z^2}} \\
& + e^{-e^{x^2+(y-4)^2+(z-4)^2}} + e^{-e^{(x-4)^2+(y-4)^2+(z-4)^2}} = 0.075
\end{aligned}$$

8.3.2

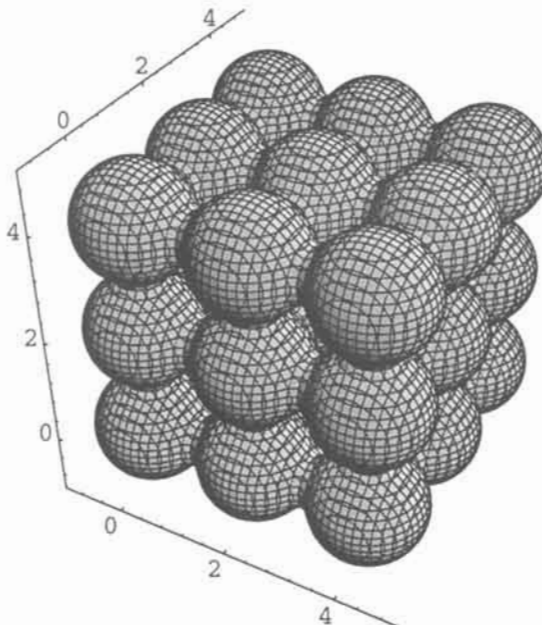


Fig. 8.3.6. The double exponential scale as in equation 8.3.2 gives more spherical bodies.

We are now ready for a denser combination of spheres, the so called bcc or body centred cubic packing. This is a structure very common in Nature, for example in many metals or alloys, like stainless steel. Figure 8.3.7 shows a small unit for this packing from eq. 8.3.3, and it is clear that the central atom pushes the corner atoms so they loose contact with each other. Instead, catenoids along the space diagonals are generated.

$$\begin{aligned}
 & e^{-(x^2+y^2+z^2)} + e^{-((x-3)^2+y^2+z^2)} + e^{-(x^2+(y-3)^2+z^2)} \\
 & + e^{-(x^2+y^2+(z-3)^2)} + e^{-((x-3)^2+y^2+(z-3)^2)} \\
 & + e^{-(x^2+(y-3)^2+(z-3)^2)} + e^{-((x-3)^2+(y-3)^2+z^2)} \\
 & + e^{-((x-3)^2+(y-3)^2+(z-3)^2)} + e^{-((x-1.5)^2+(y-1.5)^2+(z-1.5)^2)} = 0.3
 \end{aligned}
 \tag{8.3.3}$$

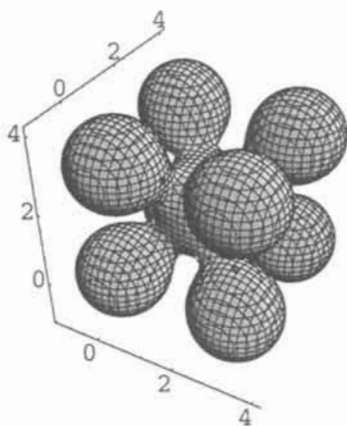


Fig. 8.3.7. Bcc arrangement of bodies after equation 8.3.3.

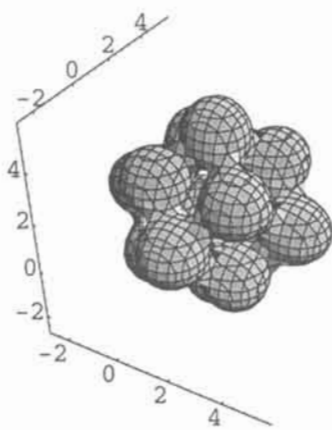


Fig. 8.3.8. The centres of 14 bodies in bcc form a rhombic dodecahedron. After equation 8.3.4.

In fig. 8.3.8 there are six more atoms after eq. 8.3.4, still with the same constant of 0.3, and the bodies form the corners of a polyhedron, the rhombic dodecahedron, which is characteristic for this geometry. The central atom is surrounded by 6+8 others and is the commencement of a surface called IWP, as shown in fig. 8.3.9.

$$\begin{aligned}
& e^{-(x^2+y^2+z^2)} + e^{-((x-3)^2+y^2+z^2)} + e^{-(x^2+(y-3)^2+z^2)} \\
& + e^{-(x^2+y^2+(z-3)^2)} + e^{-((x-3)^2+y^2+(z-3)^2)} + e^{-(x^2+(y-3)^2+(z-3)^2)} \\
& + e^{-((x-3)^2+(y-3)^2+z^2)} + e^{-((x-3)^2+(y-3)^2+(z-3)^2)} \\
& + e^{-((x-1.5)^2+(y-1.5)^2+(z-1.5)^2)} + e^{-((x-4.5)^2+(y-1.5)^2+(z-1.5)^2)} \\
& + e^{-((x-1.5)^2+(y-4.5)^2+(z-1.5)^2)} + e^{-((x-1.5)^2+(y-1.5)^2+(z-4.5)^2)} \\
& + e^{-((x+1.5)^2+(y-1.5)^2+(z-1.5)^2)} + e^{-((x-1.5)^2+(y+1.5)^2+(z-1.5)^2)} \\
& + e^{-((x-1.5)^2+(y-1.5)^2+(z+1.5)^2)} = 0.3
\end{aligned} \tag{8.3.4}$$

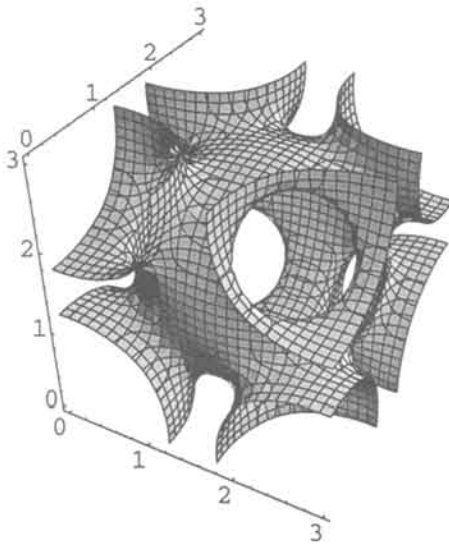


Fig. 8.3.9. Catenoids around the central body reveal the commencement of the IWP surface. After equation 8.3.4.

In order to make all atoms touch each other in bcc, every second atom has to be smaller, which is the case in fig. 8.3.10. In 8.3.11 the central part is shown with 6+8 catenoids to its neighbours, and a surface better suited for bcc. The equation for all this is 8.3.5 and we went to double exponential to get better resolution. The topology of the surface is O,C-TO after Schoen.

$$\begin{aligned}
& e^{-e^{(x^2+y^2+z^2)}} + e^{-e^{((x-2)^2+y^2+z^2)}} + e^{-e^{(x^2+(y+2)^2+z^2)}} \\
& + e^{-e^{(x^2+y^2+(z-2)^2)}} + e^{-e^{((x+2)^2+y^2+z^2)}} + e^{-e^{(x^2+(y-2)^2+z^2)}} \\
& + e^{-e^{((x)^2+y^2+(z+2)^2)}} + e^{-e^{1.5((x-1)^2+(y-1)^2+(z-1)^2)}} \\
& + e^{-e^{1.5((x+1)^2+(y-1)^2+(z-1)^2)}} + e^{-e^{1.5((x-1)^2+(y+1)^2+(z-1)^2)}} \\
& + e^{-e^{1.5((x-1)^2+(y-1)^2+(z+1)^2)}} + e^{-e^{1.5((x+1)^2+(y+1)^2+(z+1)^2)}} \\
& + e^{-e^{1.5((x-1)^2+(y+1)^2+(z+1)^2)}} + e^{-e^{1.5((x+1)^2+(y-1)^2+(z+1)^2)}} \\
& + e^{-e^{1.5((x+1)^2+(y+1)^2+(z-1)^2)}} = 0.12
\end{aligned} \tag{8.3.5}$$

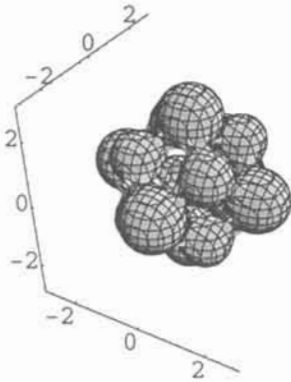


Fig. 8.3.10. Sizes of bodies changed so all touch each other. After equation 8.3.5.

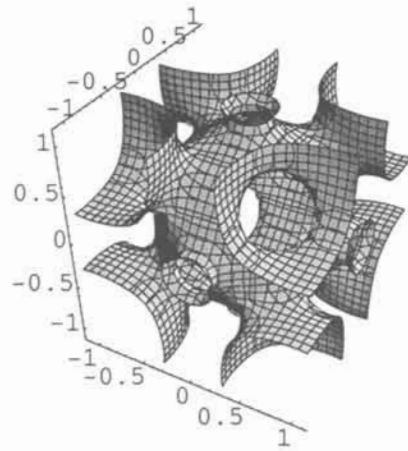


Fig. 8.3.11. Catenoids around the central body reveal the commencement of the O,C-TO surface. After equation 8.3.5.

In the close packing of spheres, cubic or hexagonal, the tetrahedron and the octahedron are essential parts. So we make the tetrahedron with four spheres in eq. 8.3.6, and for a constant of 0.16 they fuse together via catenoids in fig. 8.3.12. In the centre there is a tetrahedron of reverse orientation, the dual, which is a result of the catenoid openings between the spheres. For $C=0.15$ the tetrahedron is small and isolated, illustrated in fig 8.3.13.

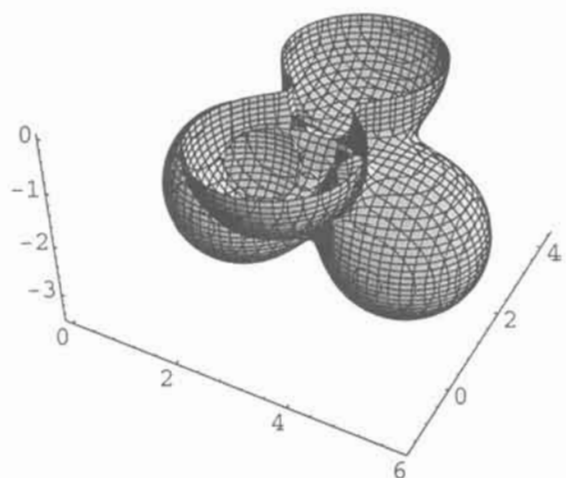


Fig. 8.3.12. Four bodies fused together tetrahedrally. After equation 8.3.6 and $C=0.16$.

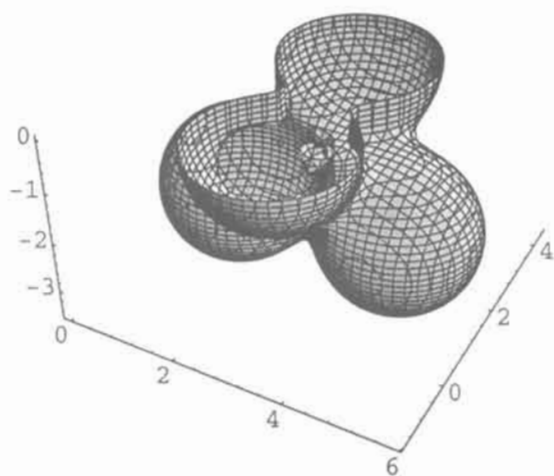


Fig. 8.3.13. After equation 8.3.6 and $C=0.15$.

$$\begin{aligned}
& e^{-((x-3)^2+y^2+z^2)} + e^{-((x-3)^2+(y-3)^2+z^2)} \\
& + e^{-((x-1.5)^2+(y-1.5)^2+(z+2.121)^2)} \\
& + e^{-((x-4.5)^2+(y-4.5)^2+(z+2.121)^2)} = C
\end{aligned} \tag{8.3.6}$$

We propose here that the dual relation between a molecule and its ELF structure [3] has a correspondence in a crystal of an ionic or metal infinite structure. A simple example is the classic solid Perovskite, CaTiO_3 , in which the negative TiO_3 part consists of TiO_6 octahedra sharing corners and exists as one isosurface as in fig. 8.3.4, while the dual, the positive Ca part, exists as bodies for another constant as in fig. 8.3.1 or 8.3.2.

The dual behaviours as also seen above in figures 8.2.3 and 8.2.4, and here in figures 8.3.12 and 8.3.13, correspond to the molecules B_6H_6 and B_4H_4 and their dual ELF structures. So we show here that the atoms in the molecule, as well as their dual electron structure, is described in one continuous and closed function. We also show a mechanism of formation by letting spheres interact in space. We continue with the octahedron by letting six equidistant spheres approach each other in space as in fig. 8.3.14, after eq. 8.3.7. The split is shown in fig. 8.3.15, and reveals the dual cube that corresponds to a molecule B_8H_8 .

$$\begin{aligned}
& e^{-(x^2+y^2+z^2)} + e^{-(x^2+(y-3)^2+z^2)} \\
& + e^{-((x-1.5)^2+(y-1.5)^2+(z-2.12)^2)} + e^{-((x-3)^2+y^2+z^2)} \\
& + e^{-((x-3)^2+(y-3)^2+z^2)} + e^{-((x-1.5)^2+(y-1.5)^2+(z+2.12)^2)} = 0.16
\end{aligned} \tag{8.3.7}$$

In fig. 8.3.16 there is a structure of two edge sharing octahedra - into the bargain comes tetrahedral interstices between the octahedra - and in the split in 8.3.17 we see the dual structure of a string of corner sharing cubes and tetrahedra. The edge sharing of octahedra is a fundamental building unit in solid state chemistry - one example is the Rutile structure which contains just such chains of edge sharing octahedra. VO_2 is one of the many compounds that have this structure, and the chains are used to explain the drastic changes of electric conductivity that occurs with temperature for crystals of this material [10]. We propose that the dual structure could be a picture of this phenomenon - the structure of fig. 8.3.17 would correspond to the metal conducting form, while the change of constant that gives isolated cubes would give the structure of the oxide insulator.

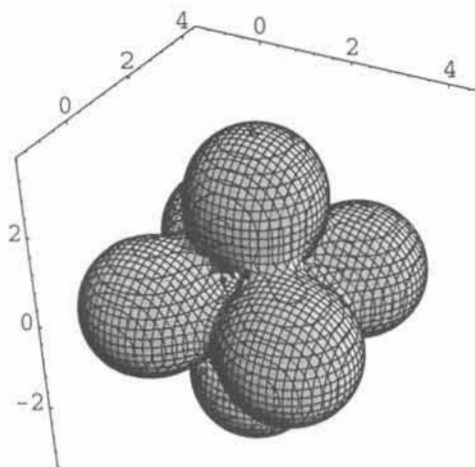


Fig. 8.3.14. Octahedron after equation 8.3.7.

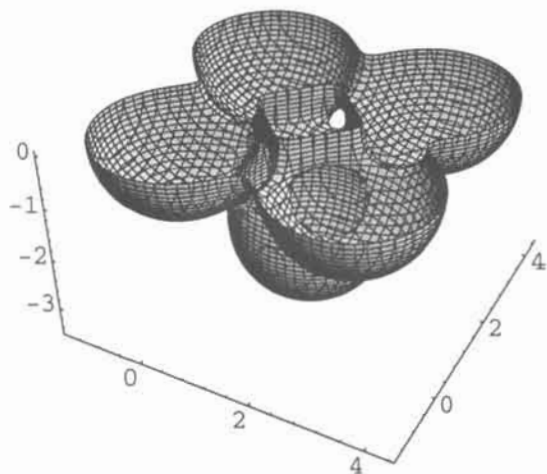


Fig. 8.3.15. Split of octahedron reveals the dual cube.

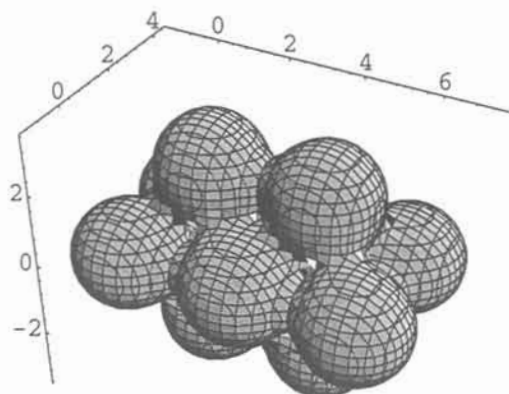


Fig. 8.3.16. Two edge sharing octahedra as in the structure of Rutile

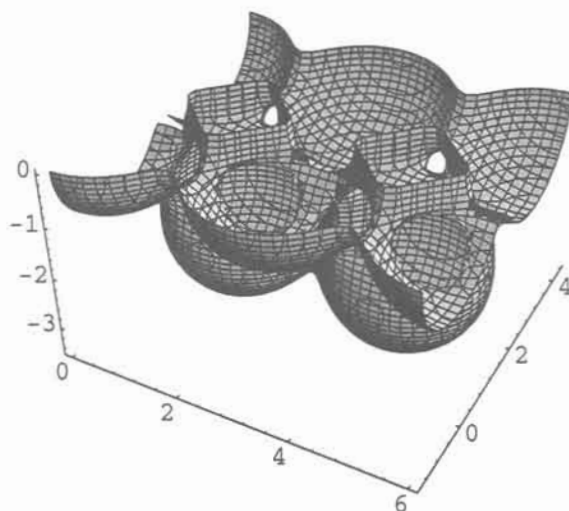


Fig. 8.3.17. Split of octahedron reveals a dual structure of corner connected cubes and tetrahedra.

We are now ready for a more complete piece of cubic close packing of bodies, and in fig. 8.3.18 we see eight tetrahedra sitting on one octahedron, and it is called after its inventor, Kepler's stella octangula. The split in fig. 8.3.19 shows the dual structure, one cube, sharing corners with eight

tetrahedra, and its equation is in 8.3.8. This structure is a model for several clusters in chemistry, and we just mention the celebrated Mo_6Cl_8 and point out that it was discovered by W. Klemm. The octahedron has six molybdenum atoms and the chlorine atoms form the outer tips of the tetrahedra.

$$\begin{aligned}
 & e^{-(x^2+y^2+z^2)} + e^{-(x^2+(y-3)^2+z^2)} + e^{-((x-1.5)^2+(y-1.5)^2+(z-2.12)^2)} \\
 & + e^{-((x-3)^2+y^2+z^2)} + e^{-((x-3)^2+(y-3)^2+z^2)} \\
 & + e^{-((x-1.5)^2+(y-1.5)^2+(z+2.12)^2)} + e^{-((x-4.5)^2+(y-1.5)^2+(z-2.12)^2)} \\
 & + e^{-((x-4.5)^2+(y-1.5)^2+(z+2.12)^2)} + e^{-((x-1.5)^2+(y+1.5)^2+(z-2.12)^2)} \\
 & + e^{-((x-1.5)^2+(y+1.5)^2+(z+2.12)^2)} + e^{-((x-1.5)^2+(y-4.5)^2+(z-2.12)^2)} \\
 & + e^{-((x-1.5)^2+(y-4.5)^2+(z+2.12)^2)} + e^{-((x+1.5)^2+(y-1.5)^2+(z-2.12)^2)} \\
 & + e^{-((x+1.5)^2+(y-1.5)^2+(z+2.12)^2)} = 0.161
 \end{aligned}$$

8.3.8

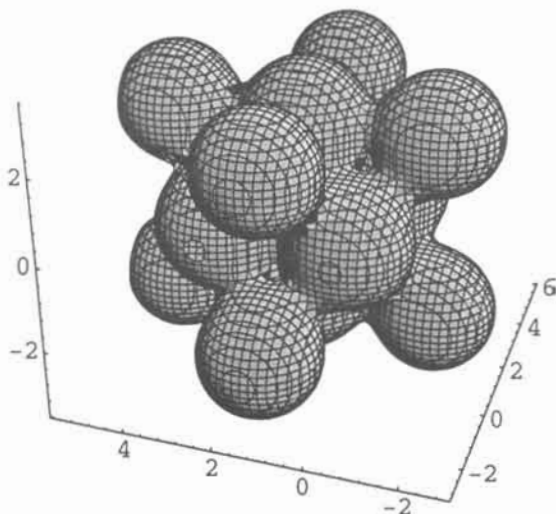


Fig. 8.3.18. Kepler's stella octangula, or Mo_6Cl_8 in chemistry. After equation 8.3.8.

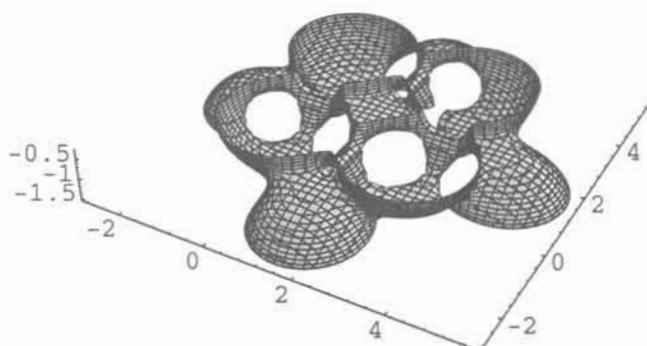


Fig. 8.3.19. Split of fig 8.3.18 reveals a dual structure of a cube corner connected with eight tetrahedra.

In cubic close packing (ccp) each atom has 12 neighbours at the corners of a cube octahedron as in fig. 8.3.20, and we can get the corresponding surface in fig. 8.3.21 by letting 12 such spheres approach a central one. This is the commencement of a surface related to the so called F-RD, also one of the minimal surfaces of Schoen. The equation is in 8.3.9.

$$\begin{aligned}
 & e^{-(x^2+y^2+z^2)} + e^{-((x-3)^2+y^2+z^2)} \\
 & + e^{-(x^2+(y-3)^2+z^2)} + e^{-((x-1.5)^2+(y-1.5)^2+(z-2.121)^2)} \\
 & + e^{-((x-3)^2+(y-3)^2+z^2)} + e^{-((x-4.5)^2+(y-1.5)^2+(z-2.121)^2)} \\
 & + e^{-((x+1.5)^2+(y-1.5)^2+(z-2.121)^2)} = 0.2
 \end{aligned}
 \tag{8.3.9}$$

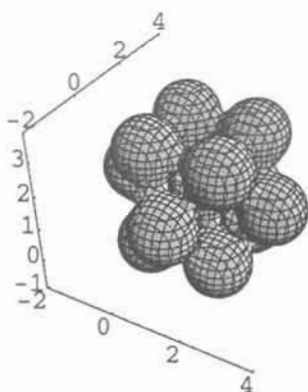


Fig. 8.3.20. Twelve bodies in ccp. After equation 8.3.9.

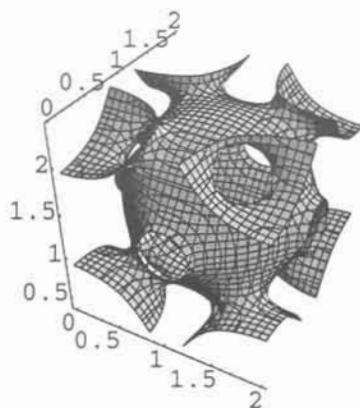


Fig. 8.3.21. The FRD surface. After equation 8.3.9.

In ccp there are octahedral interstices as shown in fig. 8.3.22 with a smaller body in the centre of the octahedron. One atom of the bigger is then surrounded by 12+6 catenoids connecting to other atoms in the packing, and the equation is below in 8.3.10.

$$\begin{aligned}
 & e^{-e^{(x^2+y^2+z^2)}} + e^{-e^{((x-2)^2+y^2+z^2)}} + e^{-e^{(x^2+(y-2)^2+z^2)}} \\
 & + e^{-e^{((x-2)^2+(y-2)^2+z^2)}} + e^{-e^{((x-1)^2+(y-1)^2+(z-1.414)^2)}} \\
 & + e^{-e^{((x-1)^2+(y-1)^2+(z+1.414)^2)}} + e^{-e^{6((x-1)^2+(y-1)^2+z^2)}} = 0.1
 \end{aligned} \tag{8.3.10}$$

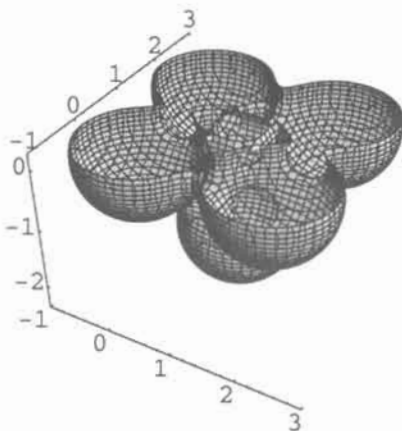


Fig. 8.3.22. Split of an octahedron with a small interstitial body. After equation 8.3.10.

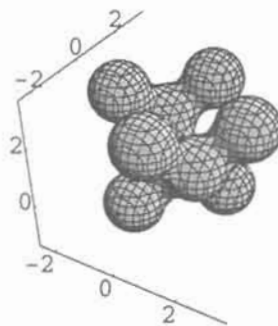


Fig. 8.3.23. Diamond. After equation 8.3.11.

We take out every second atom from ccp and get the diamond structure in fig. 8.3.23, which is the well known D-surface, and the equation is in 8.3.11.

$$\begin{aligned}
 & e^{-e^{(x-0.5)^2+(y-0.5)^2+(z-0.5)^2}} + e^{-e^{(x+0.5)^2+(y+0.5)^2+(z+0.5)^2}} \\
 & + e^{-e^{(x+0.5)^2+(y-1.5)^2+(z-1.5)^2}} + e^{-e^{(x-1.5)^2+(y+0.5)^2+(z-1.5)^2}} \\
 & + e^{-e^{(x-0.5)^2+(y-2.5)^2+(z-2.5)^2}} + e^{-e^{(x-2.5)^2+(y-0.5)^2+(z-2.5)^2}} \\
 & + e^{-e^{(x+1.5)^2+(y-0.5)^2+(z-2.5)^2}} + e^{-e^{(x-0.5)^2+(y+1.5)^2+(z-2.5)^2}} \\
 & + e^{-e^{(x-1.5)^2+(y-1.5)^2+(z+0.5)^2}} = 0.1
 \end{aligned} \tag{8.3.11}$$

In fig. 8.3.23 each sphere is a silicon atom, the catenoids oxygen atoms, and we have a part of the cristobalite structure, which is more clearly shown in fig 8.3.24. The equation is 8.3.12 with a constant of 0.08. The smaller spheres are now the Si atoms, which have the weight 1.5 in the two last terms, and the larger are the oxygen atoms. We need to go to the double scale to resolve the smaller atoms. The composition is Si_2O_7 .

$$\begin{aligned}
 & e^{-e^{x^2+y^2+z^2}} + e^{-e^{(x-2)^2+(y-2)^2+z^2}} + e^{-e^{(x+2)^2+(y+2)^2+z^2}} \\
 & + e^{-e^{x^2+(y-2)^2+(z-2)^2}} + e^{-e^{x^2+(y+2)^2+(z+2)^2}} \\
 & + e^{-e^{(x-2)^2+y^2+(z-2)^2}} + e^{-e^{(x+2)^2+y^2+(z+2)^2}} \\
 & + e^{-e^{1.5((x-1)^2+(y-1)^2+(z-1)^2)}} + e^{-e^{1.5((x+1)^2+(y+1)^2+(z+1)^2)}} = 0.08
 \end{aligned}
 \tag{8.3.12}$$

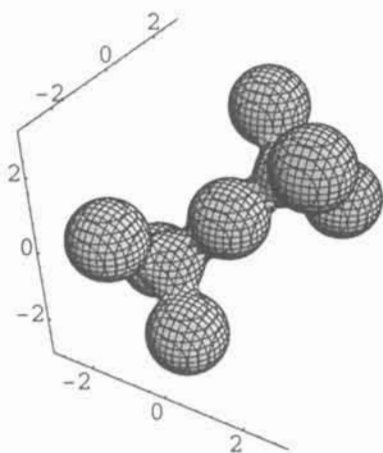


Fig. 8.3.24. A piece of the cristobalite structure. After equation 8.3.12.

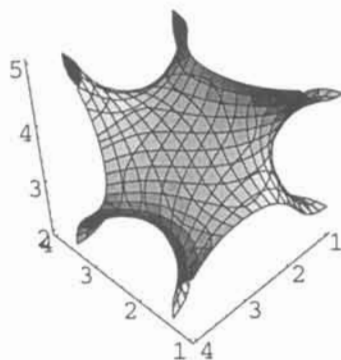


Fig. 8.3.25. A three-connector net is described by equation 8.3.13, and its surface centre is a monkey saddle of the gyroid type.

Next arrangement of spheres is somewhat special. We have seen space nets as mathematical functions, with spheres that move towards each other giving 14, 12, 8, 6, and 4 neighbours to a central body. The latter was the diamond arrangement. The next is the simplest, a cubic three-connector that has been described by Wells [11], and which we shall study. As we focus on the net we use the ordinary scale. Wells' net has got eight points in the cubic unit cell:

$$\left(\frac{111}{888}\right), \left(\frac{537}{888}\right), \left(\frac{753}{888}\right), \left(\frac{375}{888}\right), \left(\frac{555}{888}\right), \left(\frac{173}{888}\right), \left(\frac{317}{888}\right), \left(\frac{731}{888}\right)$$

$$\begin{aligned} & e^{-((x+0.5)^2+(y-0.5)^2+(z-0.5)^2)} + e^{-((x-0.5)^2+(y-0.5)^2+(z-1.5)^2} \\ & + e^{-((x-0.5)^2+(y+0.5)^2+(z-2.5)^2} + e^{-((x+0.5)^2+(y+0.5)^2+(z-3.5)^2} \\ & + e^{-((x+0.5)^2+(y-4.5)^2+(z-0.5)^2} + e^{-((x+0.5)^2+(y-3.5)^2+(z-3.5)^2} \\ & + e^{-((x-0.5)^2+(y-3.5)^2+(z-2.5)^2} + e^{-((x-0.5)^2+(y-4.5)^2+(z-1.5)^2} \\ & + e^{-((x-3.5)^2+(y-3.5)^2+(z-3.5)^2} + e^{-((x-3.5)^2+(y-4.5)^2+(z-0.5)^2} \\ & + e^{-((x-4.5)^2+(y-4.5)^2+(z-1.5)^2} + e^{-((x-1.5)^2+(y-1.5)^2+(z-1.5)^2} \\ & + e^{-((x-1.5)^2+(y-2.5)^2+(z-2.5)^2} + e^{-((x-2.5)^2+(y-2.5)^2+(z-3.5)^2} \\ & + e^{-((x-2.5)^2+(y-1.5)^2+(z-.5)^2} + e^{-((x-4.5)^2+(y-3.5)^2+(z-2.5)^2} \\ & + e^{-((x-3.5)^2+(y-0.5)^2+(z-0.5)^2} + e^{-((x-4.5)^2+(y-0.5)^2+(z-1.5)^2} \\ & + e^{-((x-3.5)^2+(y+0.5)^2+(z-3.5)^2} + e^{-((x-4.5)^2+(y+0.5)^2+(z-2.5)^2} \\ & + e^{-((x+0.5)^2+(y-0.5)^2+(z-4.5)^2} + e^{-((x-0.5)^2+(y-0.5)^2+(z-5.5)^2} \\ & + e^{-((x-0.5)^2+(y+0.5)^2+(z-6.5)^2} + e^{-((x+0.5)^2+(y+0.5)^2+(z-7.5)^2} \\ & + e^{-((x+.5)^2+(y-4.5)^2+(z-4.5)^2} + e^{-((x+.5)^2+(y-3.5)^2+(z-7.5)^2} \\ & + e^{-((x-0.5)^2+(y-3.5)^2+(z-6.5)^2} + e^{-((x-0.5)^2+(y-4.5)^2+(z-5.5)^2} \\ & + e^{-((x-1.5)^2+(y-1.5)^2+(z-5.5)^2} + e^{-((x-1.5)^2+(y-2.5)^2+(z-6.5)^2} \\ & + e^{-((x-2.5)^2+(y-2.5)^2+(z-7.5)^2} + e^{-((x-2.5)^2+(y-1.5)^2+(z-4.5)^2} \\ & + e^{-((x-3.5)^2+(y-4.5)^2+(z-4.5)^2} + e^{-((x-4.5)^2+(y-4.5)^2+(z-5.5)^2} \\ & + e^{-((x-3.5)^2+(y-3.5)^2+(z-7.5)^2} + e^{-((x-4.5)^2+(y-3.5)^2+(z-6.5)^2} \\ & + e^{-((x-3.5)^2+(y-0.5)^2+(z-4.5)^2} + e^{-((x-4.5)^2+(y-0.5)^2+(z-5.5)^2} \\ & + e^{-((x-3.5)^2+(y+0.5)^2+(z-7.5)^2} + e^{-((x-4.5)^2+(y+0.5)^2+(z-6.5)^2} = 0.9 \end{aligned}$$

8.3.13

We derive centres for 28 spheres after eq. 8.3.13, and each sphere has three neighbours.

By starting to vary the constant we get the gyroid surface with the typical monkey saddle in fig. 8.3.25, as calculated from eq. 8.3.13 with a constant of 0.65 instead of 0.9. The boundaries given show the central part of the surface.

Wells also showed that it is possible to make a racemate consisting of two interpenetrating nets of this kind, one D and one L. This is shown in fig. 8.3.26 for two interpenetrating gyroid nets after equation 8.3.14 [4], which clearly shows the three connectors. Another way to do this was shown earlier in fig. 4.2.10.

$$e^{\cos \pi x \sin \pi z + \cos \pi y \sin \pi x + \cos \pi z \sin \pi y} + e^{-(\cos \pi x \sin \pi z + \cos \pi y \sin \pi x + \cos \pi z \sin \pi y)} = 3.9 \quad 8.3.14$$

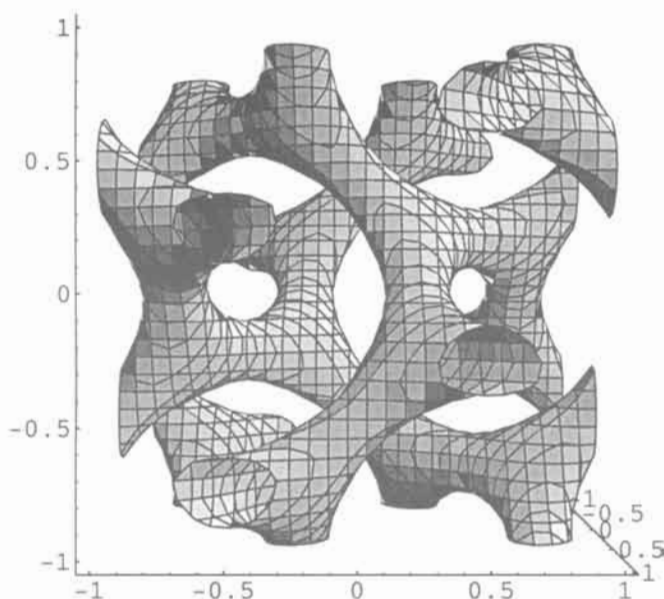


Fig. 8.3.26. Two interpenetrating gyroid nets, three connecting, after equation 8.3.14.

Going back to equation 8.3.13, we now use the constant 0.9 and get then the original net by Wells as shown in figures 8.3.27 and 8.3.28, the latter projected along the cube-axes of the used boundaries. This is surely an alternative to derive a cubosome shape for the gyroid. To this structure could be added another interpenetrating structure like in fig. 8.3.26, using double as many spheres in the equation above. The resulting total structure would be two interpenetrating structures, separate and closed, one left-handed and the other right-handed!

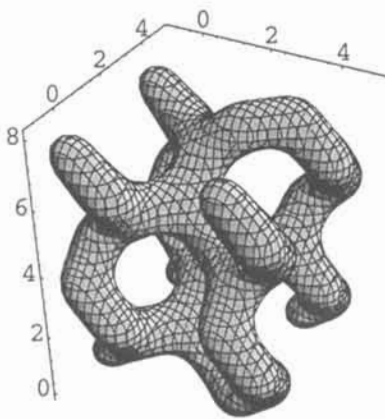


Fig. 8.3.27. Finite gyroid net, three connecting, after equation 8.3.13.

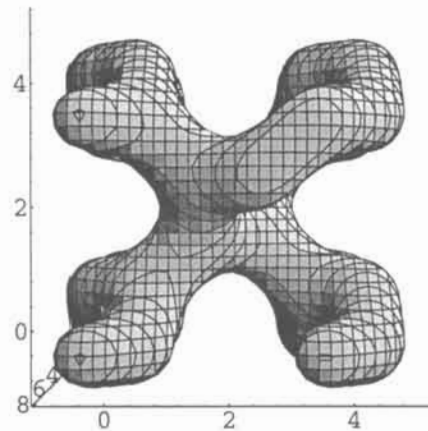


Fig. 8.3.28. Projection of fig. 8.3.27.

In fig. 8.3.29 we show the hexagonal correspondence to the cubeoctahedron with thirteen spheres in hexagonal close packing, and they are brought close to each other via eq. 8.3.14 to develop catenoids. The central part of the surface for hexagonal close packing is shown in fig. 8.3.30.

$$\begin{aligned}
& e^{-e(x^2+y^2+z^2)} + e^{-e((x-2)^2+y^2+z^2)} + e^{-e((x-1)^2+(y-1.732)^2+z^2)} \\
& + e^{-e((x-1)^2+(y-.577)^2+(z-1.633)^2)} + e^{-e((x-2)^2+(y-2.309)^2+(z-1.633)^2)} \\
& + e^{-e(x^2+(y-2.309)^2+(z-1.633)^2)} + e^{-e((x-2)^2+(y+1.155)^2+(z-1.633)^2)} \\
& + e^{-e(x^2+(y+1.155)^2+(z-1.633)^2)} + e^{-e((x-3)^2+(y-.577)^2+(z-1.633)^2)} \\
& + e^{-e((x+1)^2+(y-.577)^2+(z-1.633)^2)} + e^{-e((x-2)^2+y^2+(z-3.27)^2)} \\
& + e^{-e((x-1)^2+(y-1.732)^2+(z-3.27)^2)} + e^{-e(x^2+y^2+(z-3.27)^2)} = 0.11
\end{aligned}$$

8.3.14

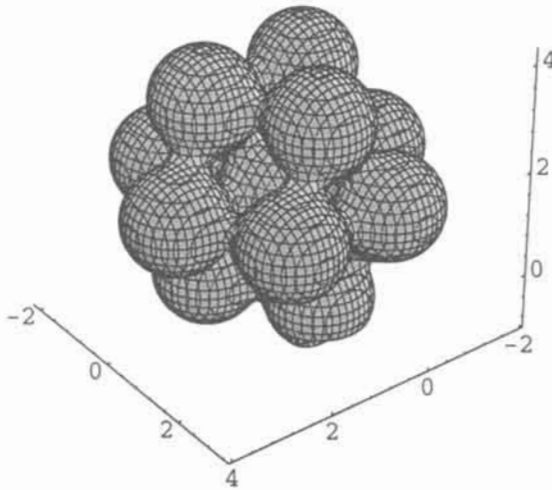


Fig. 8.3.29. Hexagonal close packing of bodies after equation 8.3.14.

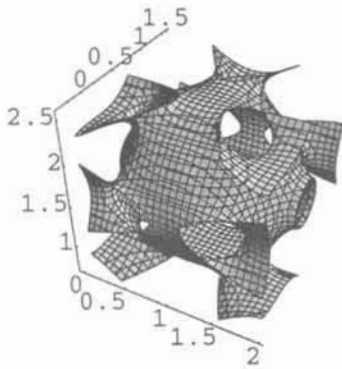


Fig. 8.3.30. The central part of fig. 8.3.29.

Similarly we can derive a surface for tridymite or ice, the hexagonal correspondence to the D surface, by using a part of the structure as shown in fig. 8.3.31.

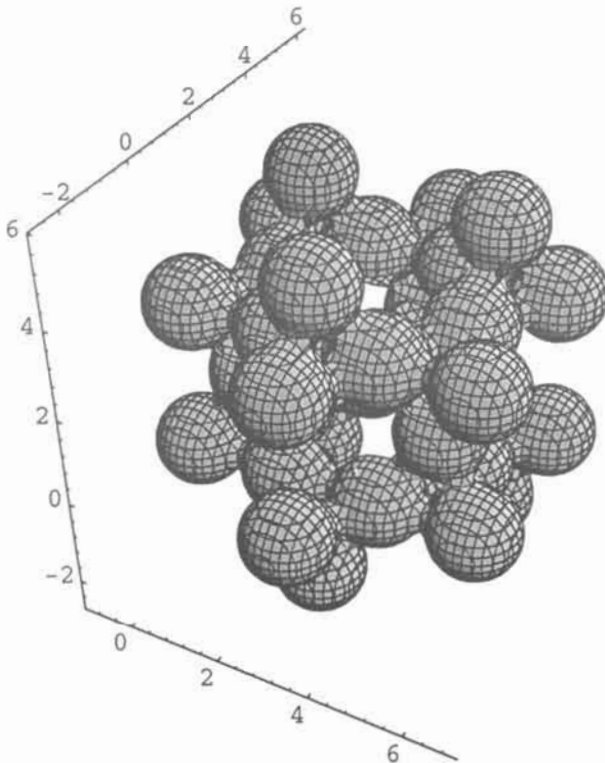


Fig. 8.3.31. A piece of the ice, or tridymite, structure.

Finally there is the simple triangle arrangement of spheres in space, or for a chemist the structure of primitive hexagonal packing (the structure of W in WC). In fig. 8.3.32 there are six spheres at the corners of a trigonal prism, using only the six first terms of eq. 8.3.15. The dual structure is a trigonal bipyramid, and in fig 8.3.33 all the spheres from eq. 8.3.15 are included to show the CaZn_5 arrangement (without Ca) as the dual structure of a primitive hexagonal arrangement of bodies.

$$\begin{aligned}
 & e^{-(x^2+y^2+z^2)} + e^{-((x-3)^2+y^2+z^2)} + e^{-((x-1.5)^2+(y-2.6)^2+(z)^2)} \\
 & + e^{-((x-3)^2+(y)^2+(z-2)^2)} + e^{-((x-1.5)^2+(y-2.6)^2+(z-2)^2)} \\
 & + e^{-((x)^2+(y)^2+(z-2)^2)} + e^{-((x+1.5)^2+(y-2.6)^2+(z-2)^2)} \\
 & + e^{-((x+1.5)^2+(y-2.6)^2+(z)^2)} + e^{-((x-3)^2+(y)^2+(z+2)^2)} \\
 & + e^{-((x-1.5)^2+(y-2.6)^2+(z+2)^2)} + e^{-((x)^2+(y)^2+(z+2)^2)} \\
 & + e^{-((x+1.5)^2+(y-2.6)^2+(z+2)^2)} = 0.17
 \end{aligned}$$

8.3.15

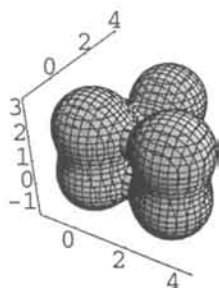


Fig. 8.3.32. Primitive hexagonal packing of bodies after equation 8.3.15 only using six terms.

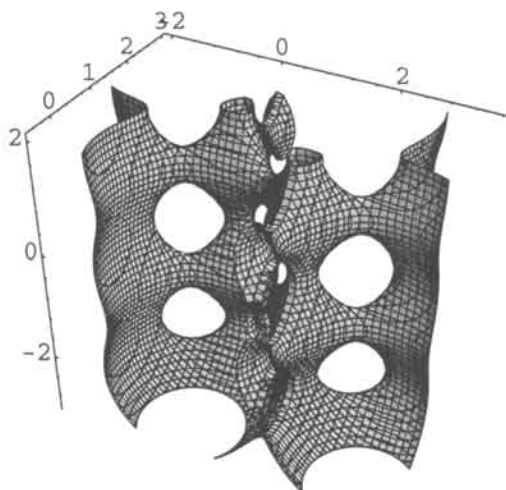


Fig. 8.3.33. The dual structure of fig 8.3.32 (CaZn_5) after equation 8.3.15.

8.4 How Tetrahedra and Octahedra meet in Space

With these mathematics we can also make complicated structures, like a part of the zinc blende structure, or of a shear plane as it occurs in $\text{Nb}_3\text{O}_7\text{F}$ [12], and pieces of tridymite or ice as we believe they form a part of the structure of water [13]. The equations for these structures are rather lengthy and we refer to our original publications, except for the zinc blende and a simple shear plane.

We give the equation of each tetrahedron in a unit of four, in eq. 8.4.1, using the double scale with proper coordinate shifts. This is a part of the zinc blende structure of four tetrahedra meeting at a corner as in figure 8.4.1. In 8.4.2 we show the part where the four tetrahedra meeting at high resolution to show that the function is continuous.

$$\begin{aligned}
 & e^{-(e^{-x+y-z} + e^{-x-y+z} + e^{x-y-z} + e^{x+y+z} - 22)} \\
 & + e^{-(e^{-x+y-z+8} + e^{-x-y+z} + e^{x-y-z} + e^{x+y+z-8} - 22)} \\
 & + e^{-(e^{-x+y-z+8} + e^{-x-y+z} + e^{x-y-z-8} + e^{x+y+z} - 22)} \\
 & + e^{-(e^{-x+y-z+8} + e^{-x-y+z-8} + e^{x-y-z} + e^{x+y+z} - 22)} = 2
 \end{aligned}
 \tag{8.4.1}$$

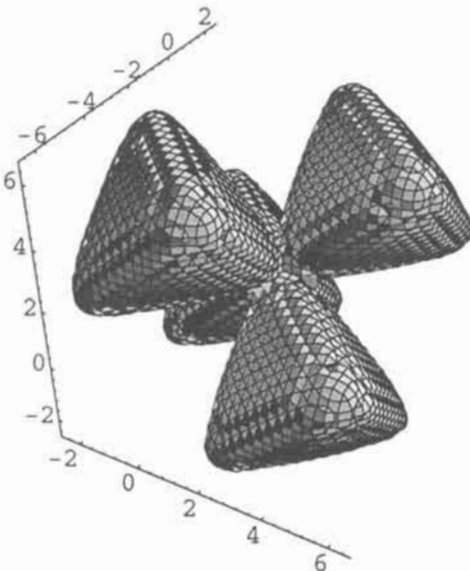


Fig. 8.4.1. Part of the zinc blende structure after equation 8.4.1.

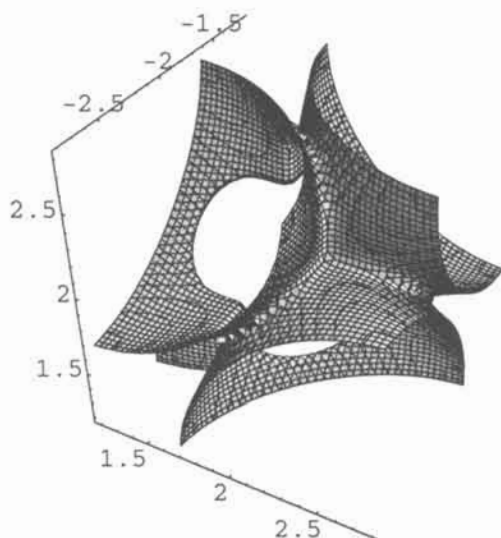


Fig. 8.4.2. High resolution of centre of fig. 8.4.1.

Octahedral edge sharing to give shear is one of the most important building operations in chemistry. Mathematically it is just translation. In eq. 8.4.2 we have four sub-equations for four octahedra, translated to give edge sharing, and they form the function on the double exponential level that gives the structure in fig. 8.4.3. We use the base of 20 to get the sharpness of the octahedra, or resolution, needed.

$$\begin{aligned} \text{oct1} = & 20^{-x+y+z} + 20^{x+y-z-4} + 20^{x-y+z} + 20^{x+y+z-4} \\ & + 20^{x-y-z} + 20^{-x-y+z+4} + 20^{-x+y-z} + 20^{-x-y-z+4} - 1500 \end{aligned}$$

$$\begin{aligned} \text{oct2} = & 20^{-x+y+z+4} + 20^{x+y-z-8} + 20^{x-y+z-4} + 20^{x+y+z-8} \\ & + 20^{x-y-z-4} + 20^{-x-y+z+8} + 20^{-x+y-z+4} + 20^{-x-y-z+8} - 1500 \end{aligned}$$

$$\begin{aligned} \text{oct3} = & 20^{-x+y+z+4} + 20^{x+y-z-4} + 20^{x-y+z-4} + 20^{x+y+z-4} \\ & + 20^{x-y-z-4} + 20^{-x-y+z+4} + 20^{-x+y-z+4} + 20^{-x-y-z+4} - 1500 \end{aligned}$$

$$\begin{aligned} \text{oct4} &= 20^{-x+y+z} + 20^{x+y-z} + 20^{x-y+z} + 20^{x+y+z} \\ &+ 20^{x-y-z} + 20^{-x-y+z} + 20^{-x+y-z} + 20^{-x-y-z} - 1500 \end{aligned}$$

$$e^{-\text{oct1}} + e^{-\text{oct2}} + e^{-\text{oct3}} + e^{-\text{oct4}} = 4$$

8.4.2

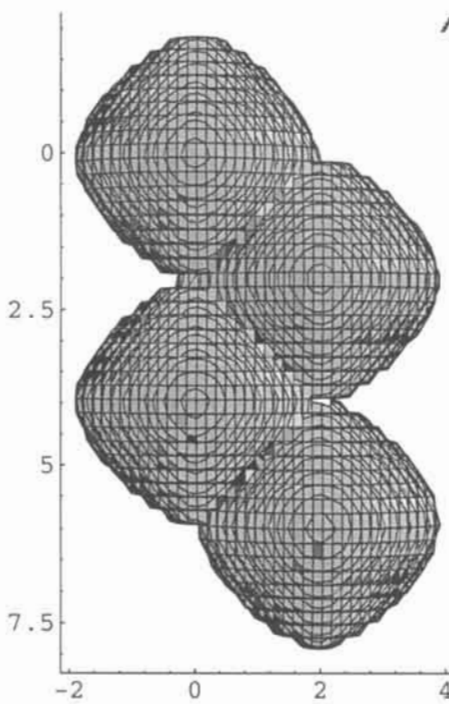


Fig. 8.4.3. Shear plane in solid state chemistry after equation 8.4.2.

Exercises 8**Exercise 8.1.**

a. Show in 3D that a cylinder may be described as built of planes.

(Hint: use equations like $x^2 + \frac{1}{10}y^2 = 1$.)

b and c. Do the same for the sphere.

(Hint: Use equation $x^2 + y^2 + Az^2 = 1$ for bigger or smaller A. And we have already shown a cylinder consists of planes.)

Exercise 8.2. Make the drop fall in fig. 8.1.11!

Exercise 8.3. Make a radiolarian more spherical.

Exercise 8.4. Plot and describe

a. $x^2 + y^2 + z = 0$

and compare with

b. $x^2 - y^2 + z = 0$

Exercise 8.5.

a. Make a string of seven spheres well separated (with the constant).

b. Make a local contact via catenoids by making one of the spheres elliptic.

c. Or via just one catenoid by adding an extra sphere of low weight.

Exercise 8.6. Describe the Diophantine equation for some n.

Answer 8.1

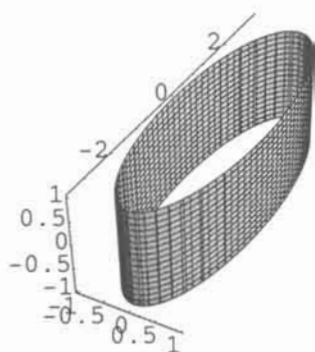
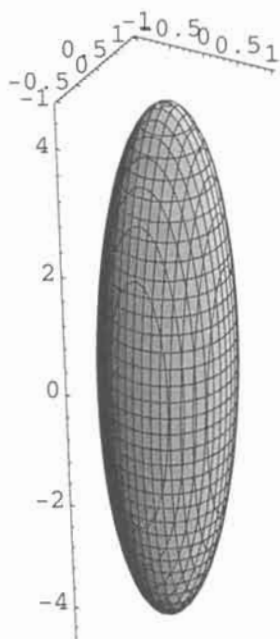
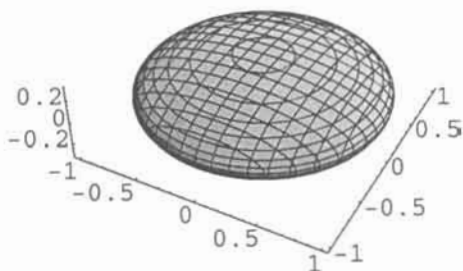


Fig. 8.1a.

Fig. 8.1b. $A=0.05$ Fig. 8.1c. $A=10$

Answer 8.2. We make the 'Gedanke'-experiment that the cylinder of some solid material is covered by a film of a liquid. In getting rid of an excess a drop is formed. Using equation

$$e^{-(x^2+y^2+z^2)} + e^{-(x^2+(z-1.92)^2)} = 0.8$$

we can increase the distance between the objects as is done in **8.2a**. Using equation

$$e^{-(x^2+y^2+z^2)} + e^{-(x^2+(z-1.9)^2)} = 0.82$$

there is fig **8.2.b**.

We can feed more liquid to the cylinder by changing constants after equation

$$e^{-(x^2+y^2+z^2)} + e^{-(x^2+(z-1.94)^2)} = 0.8$$

and the drop falls.

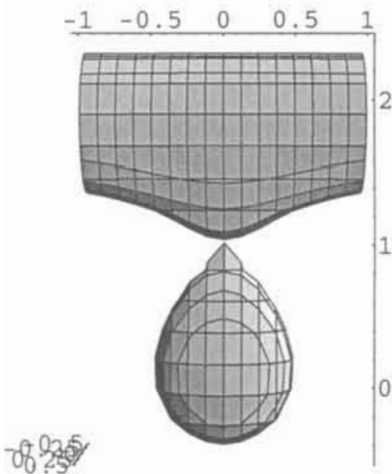


Fig. 8.2a

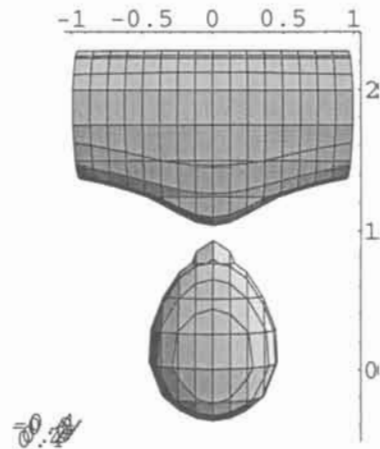


Fig. 8.2b

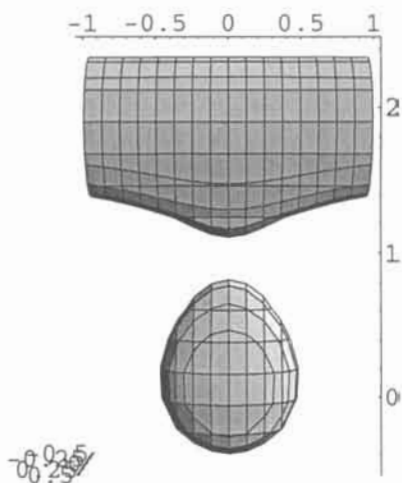


Fig 8.2c

Answer 8.3.

$$e^{-(x^2+y^2+z^2)^2} + e^{-(y^2+z^2)} = 1$$

Answer 8.4.

$x^2 - y^2 + z = 0$ is a saddle

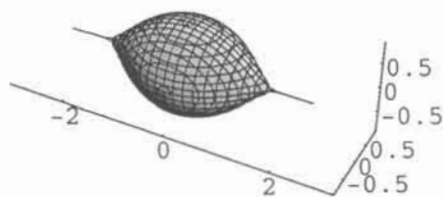


Fig. 8.3

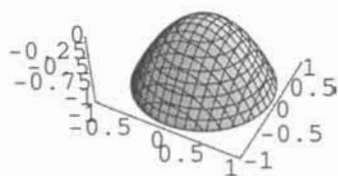


Fig. 8.4.

Answer 8.5a

$$e^{-e^{x^2+y^2+z^2}} + e^{-e^{(x-2)^2+y^2+z^2}} + e^{-e^{(x-4)^2+y^2+z^2}} + e^{-e^{(x-6)^2+y^2+z^2}} \\ + e^{-e^{(x+2)^2+y^2+z^2}} + e^{-e^{(x+4)^2+y^2+z^2}} + e^{-e^{(x+6)^2+y^2+z^2}} = 0.18$$

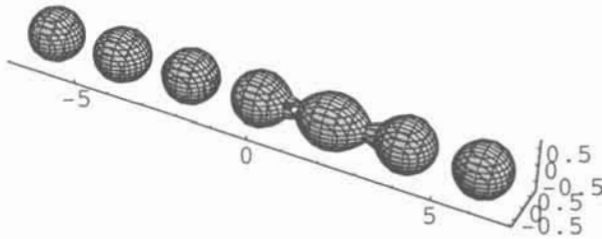


Fig. 8.5a.

Answer 8.5b

$$e^{-e^{x^2+y^2+z^2}} + e^{-e^{7((x-2)^2+y^2+z^2)}} + e^{-e^{(x-4)^2+y^2+z^2}} + e^{-e^{(x-6)^2+y^2+z^2}} \\ + e^{-e^{(x+2)^2+y^2+z^2}} + e^{-e^{(x+4)^2+y^2+z^2}} + e^{-e^{(x+6)^2+y^2+z^2}} = 0.18$$

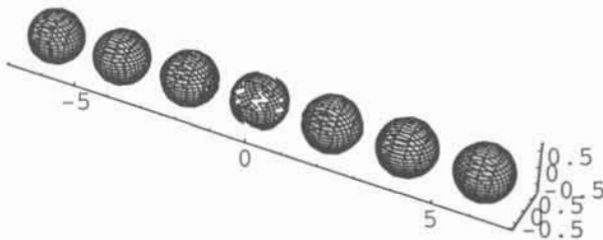


Fig. 8.5b.

Answer 8.5c. Only the part of the function where the extra small sphere gives a catenoid is shown.

$$\begin{aligned}
 & e^{-e^{x^2+y^2+z^2}} + e^{-e^{(x-2)^2+y^2+z^2}} + e^{-e^{(x-4)^2+y^2+z^2}} \\
 & + e^{-e^{(x-6)^2+y^2+z^2}} + e^{-e^{(x+2)^2+y^2+z^2}} + e^{-e^{(x+4)^2+y^2+z^2}} \\
 & + e^{-e^{(x+6)^2+y^2+z^2}} + 0.15e^{-e^{(x-1)^2+y^2+z^2}} = 0.18
 \end{aligned}$$

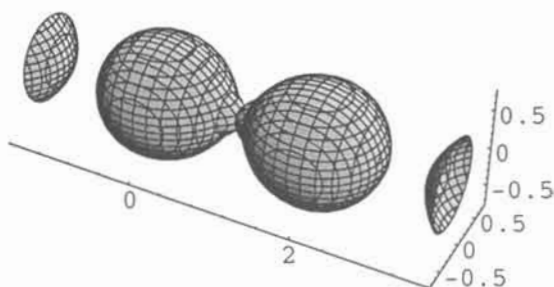


Fig. 8.5c.

Answer 8.6. The equation is:

$$x^n + y^n - z^n = 0$$

Increasing n brings out the planes.

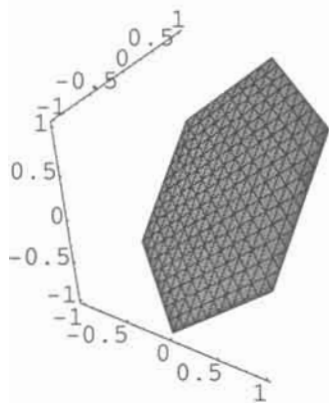


Fig. 8.6a. $n=1$

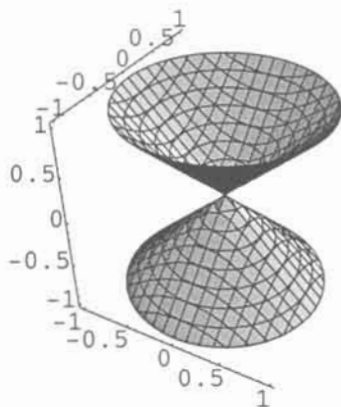


Fig. 8.6b. $n=2$

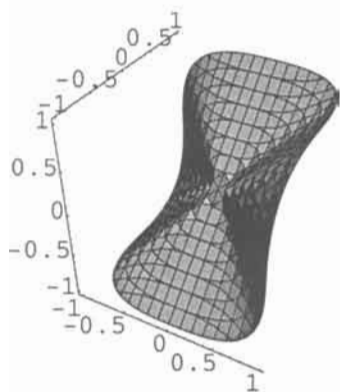


Fig. 8.6c. $n=3$

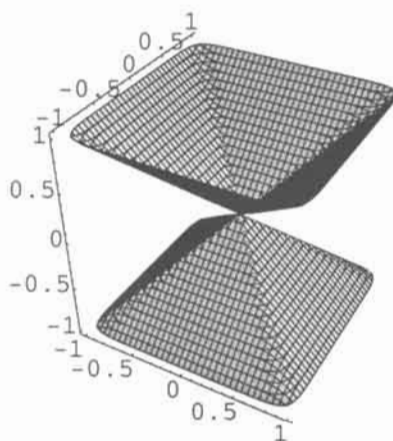


Fig. 8.6d. $n=12$

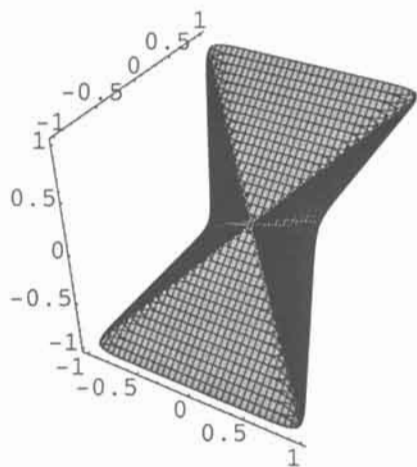


Fig. 8.6e. $n=13$

References 8

- 1 S.T. Hyde. Private communication.
- 2 S. Lidin, S. Andersson, A. Fogden, M. Jacob and Z. Blum, *Aust. J. Chem.* **45** 1519 (1992).
- 3 A. Burkhardt, U. Wedig, H. G. von Schnering and A. Savin, *Z. anorg. allg. Chem.* **619** 437 (1993).
- 4 Andersson, S.; Jacob, M., *Z. Kristallogr.* **212** (1997) 334-346.
- 5 Jacob, M, *J.Phys. II France* **7** (1997) 1035-1044.
- 6 Jacob, M. and Andersson, S.: *Z. Kristallogr.* **212** (1997) 486-492.
- 7 S. Andersson and M. Jacob, *THE MATHEMATICS OF STRUCTURES. THE EXPONENTIAL SCALE*, Oldenbourg, München, 1997.
- 8 H.G. von Schnering and R. Nesper, *Angew.Chem. Int. Ed. Engl.* **26** 1059 (1987).
- 9 H.G. von Schnering and R. Nesper, *Z. Phys. B - Condensed Matter* **83** 407 (1991).
- 10 D.B. McWhan, F.M. Rice and J.P. Remeika, *Phys.Rev. Lett.* **23** 384 (1969).
- 11 A.F. Wells, *THREE-DIMENSINAL NETS AND POLYHEDRA*, Wiley, New York, 1977.
- 12 Andersson, S.; *Acta Chem. Scand.* **18** 2339 (1964).
- 13 Jacob, M. and Andersson, S.: *Colloids and surfaces, A: Physiochemical and Engineering Aspects* **129-130** (1997) 227-237.

9 The Rods in Space

l'art d'ennuyer consiste à tout dire [1].

Here we derive the mathematics for how cylinders pack in space. We also describe the geometry when such packings condense into surfaces. We describe the rod-structure relations to crystal structures. We also make finite cubosome-like structures.

9.1 Primitive Packing of Rods

In three dimensions, $\cos(x)=C$ are planes, $\cos(y)=C$ are planes and so are $\cos(z)=C$. If all three are added, they cooperate to form the P surface in space. The function $\cos(x)+\cos(y)=C$ are parallel rods in space, and so are the pairs $\cos(x)+\cos(z)=C$ and $\cos(z)+\cos(y)=C$, as shown in figure 9.1.1, according to eq. 9.1.1.

$$\cos \frac{\pi}{2} x + \cos \frac{\pi}{2} z = 0.5 \quad 9.1.1$$

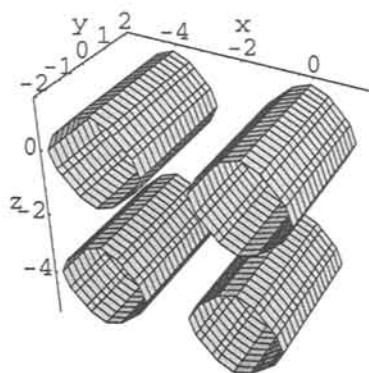


Fig. 9.1.1. Parallel rods in space after equation 9.1.1.

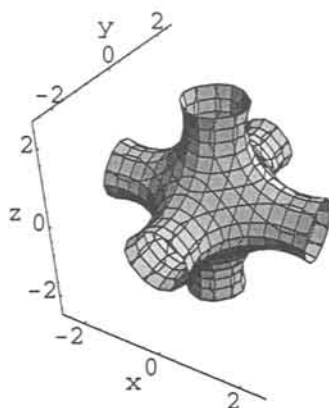


Fig. 9.1.2. Rods meet in space after equation 9.1.2.

Adding up to a function as in 9.1.2, makes the rods meet to form a P-type surface as in fig. 9.1.2.

$$e^{\cos\frac{\pi}{2}x+\cos\frac{\pi}{2}z} + e^{\cos\frac{\pi}{2}z+\cos\frac{\pi}{2}y} + e^{\cos\frac{\pi}{2}y+\cos\frac{\pi}{2}x} = 6 \quad 9.1.2$$

In order to make the rods non intersecting, we move them via translation, or a phase shift, as in equation 9.1.3 and get fig. 9.1.3.

$$e^{\cos\frac{\pi}{2}x+\cos\frac{\pi}{2}(z+2)} + e^{\cos\frac{\pi}{2}z+\cos\frac{\pi}{2}(y+2)} + e^{\cos\frac{\pi}{2}y+\cos\frac{\pi}{2}(x+2)} = 6 \quad 9.1.3$$

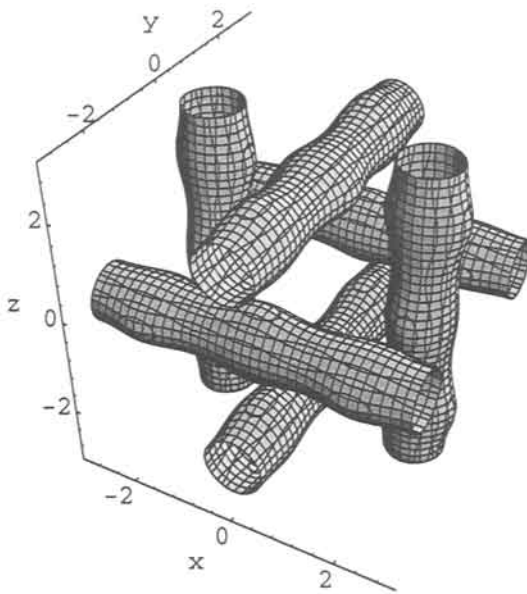


Fig. 9.1.3. Primitive packing of rods after equation 9.1.3.

So what have we done in more general terms? We go to the equation of symmetry and write it like this:

$$e^{x+y+z} + e^{x+y} + e^x = C \quad 9.1.4$$

This can equally well be written

$$e^x e^y e^z + e^x e^y + e^x = C$$

And we go circular below,

$$e^{\cos x} e^{\cos y} e^{\cos z} + e^{\cos x} e^{\cos y} + e^{\cos x} = C \tag{9.1.5}$$

We have just found experimentally that the term $\cos x + \cos y$, or $e^{\cos x} e^{\cos y}$, or the identical $e^{\cos x + \cos y}$, means a cylinder, and we can get cylinder packings by the addition on the exponential scale as above.

The GD mathematics offer another way of deriving the rod packings.

We know that $x^2 + y^2$ is a cylinder in space and we go exponentially to add rods in eq. 9.1.6, as shown in fig. 9.1.4.

$$e^{-(x^2+y^2)^2} + e^{-(y^2+z^2)^2} + e^{-(z^2+x^2)^2} = 0.65 \tag{9.1.6}$$

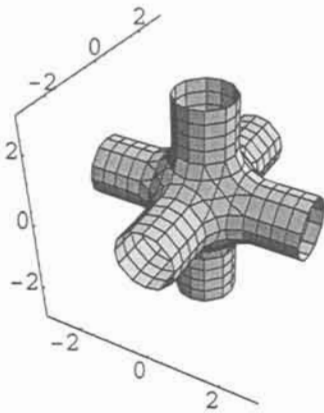


Fig. 9.1.4. Rods meet after GD function in equation 9.1.6.

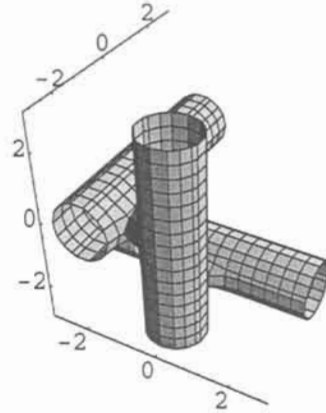


Fig. 9.1.5. Primitive packing of rods after equation 9.1.7.

By proper coordinate shifts - or translations - in eq. 9.1.7 we have non intersecting rods in fig. 9.1.5.

$$e^{-(x^2+(y+2)^2)^2} + e^{-(y^2+(z+2)^2)^2} + e^{-(z^2+(x+2)^2)^2} = 0.65 \tag{9.1.7}$$

By adding more rods as in eq. 9.1.8 we get fig 9.1.6, which is turned in 9.1.7 to show that it is nearly identical with fig. 9.1.3.

$$\begin{aligned}
 & e^{-(x^2+(y+2)^2)^2} + e^{-(y^2+(z+2)^2)^2} + e^{-(z^2+(x+2)^2)^2} \\
 & + e^{-(x^2+(y-2)^2)^2} + e^{-(y^2+(z-2)^2)^2} + e^{-(z^2+(x-2)^2)^2} = 0.65
 \end{aligned}
 \tag{9.1.8}$$

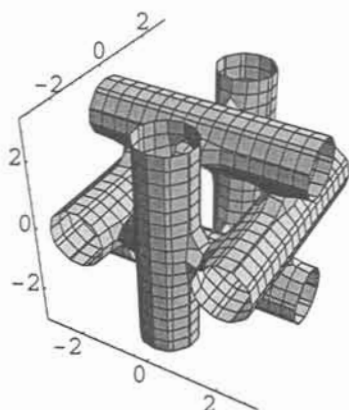


Fig. 9.1.6. More rods as after equation 9.1.8.

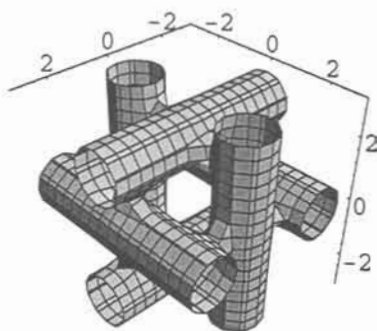


Fig. 9.1.7. Different projection after equation 9.1.8.

Expanding the original function to 9.1.9 and using two terms after below, also gives us this rod packing, as shown in fig 9.1.8.

$$\begin{aligned}
 & [\cos \frac{\pi}{2} x + \cos \frac{\pi}{2} (z+2)]^2 + [\cos \frac{\pi}{2} z + \cos \frac{\pi}{2} (y+2)]^2 + [\cos \frac{\pi}{2} y + \cos \frac{\pi}{2} (x+2)]^2 \\
 & + [\cos \frac{\pi}{2} x + \cos \frac{\pi}{2} (z+2)]^3 + [\cos \frac{\pi}{2} z + \cos \frac{\pi}{2} (y+2)]^3 + [\cos \frac{\pi}{2} y + \cos \frac{\pi}{2} (x+2)]^3 = 5.5
 \end{aligned}
 \tag{9.1.9}$$

Changing the constant to 7.6 isolates the atoms in the rod packing, which are the Nb atoms in Nb₃Sn, as shown in fig. 9.1.9.

We can also get the Sn atoms in Nb₃Sn by adding the P surface to equation 9.1.3, and get 9.1.10, and the whole structure is seen in fig. 9.1.10.

$$\begin{aligned}
 & e^{\cos \frac{\pi}{2} x + \cos \frac{\pi}{2} (z+2)} + e^{\cos \frac{\pi}{2} z + \cos \frac{\pi}{2} (y+2)} + e^{\cos \frac{\pi}{2} y + \cos \frac{\pi}{2} (x+2)} \\
 & + 2e^{\cos \frac{\pi}{2} x + \cos \frac{\pi}{2} y + \cos \frac{\pi}{2} z - 2} = 7
 \end{aligned}
 \tag{9.1.10}$$

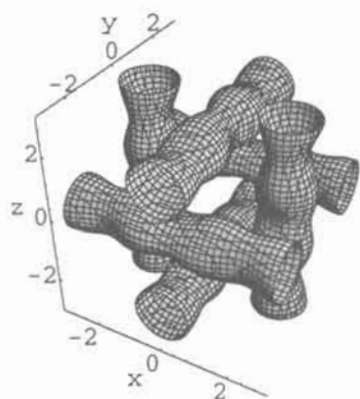


Fig. 9.1.8. Power expansion also gives this rod packing after equation 9.1.9.

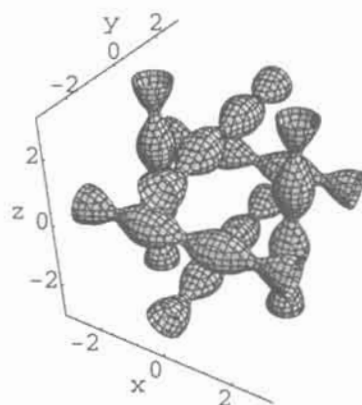


Fig. 9.1.9. Change of constant brings out bodies as the Nb atoms in Nb_3Sn , after equation 9.1.9.

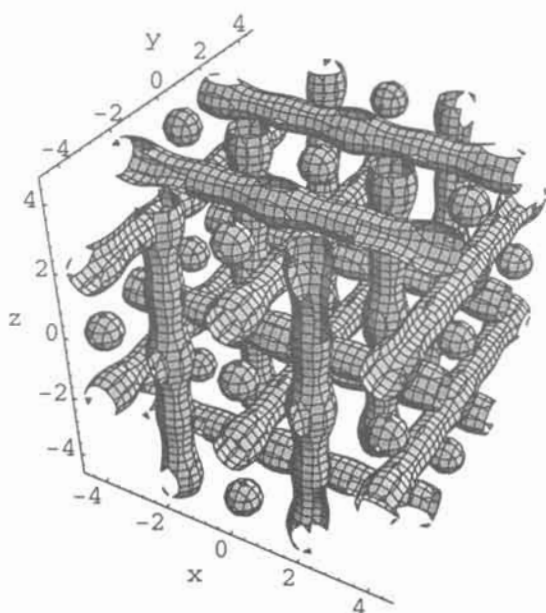


Fig. 9.1.10. Adding the P surface gives the complete structure of the superconducting Nb_3Sn .

9.2 Body Centred Packing of Rods

We constructed an algorithm saying that around a central goke you can have 3, 4 and 6 rods, and obtain fundamental packings [2]. So if we put a central goke in the primitive packing in fig. 9.1.7, and make all the rods have the same diameter and touch each other, we find that they all are space diagonals of the cube. The packing is now bcc of rods, or also the garnet packing of rods. The space group is Ia3d. The mathematics to come is just like before - permutation of the x, y, z variables following the structure of the equation of symmetry in space from eq. 3.4.1 and 4.2.10. We use the GD mathematics first as in eq. 9.2.1, and show four rods in this packing in fig. 9.2.1.

$$e^{-((x-y)^2+(y+z)^2+(x+z)^2)} + e^{-((x+y)^2+(y+z+2)^2+(x-z-2)^2)} \\ + e^{-((x-y+2)^2+(y-z-2)^2+(x-z)^2)} + e^{-((x+y-2)^2+(y-z)^2+(x+z-2)^2)} = 0.5 \quad 9.2.1$$

And with seven rods we have eq. 9.2.2, which is illustrated in fig. 9.2.2.

$$e^{-((x-y)^2+(y+z)^2+(x+z)^2)} + e^{-((x+y+2)^2+(y-z)^2+(x+z+2)^2)} \\ + e^{-((x+y)^2+(y+z+2)^2+(x-z-2)^2)} + e^{-((x-y+2)^2+(y-z-2)^2+(x-z)^2)} \\ + e^{-((x+y-2)^2+(y-z)^2+(x+z-2)^2)} + e^{-((x+y)^2+(y+z-2)^2+(x-z+2)^2)} \\ + e^{-((x-y-2)^2+(y-z+2)^2+(x-z)^2)} = 0.5 \quad 9.2.2$$

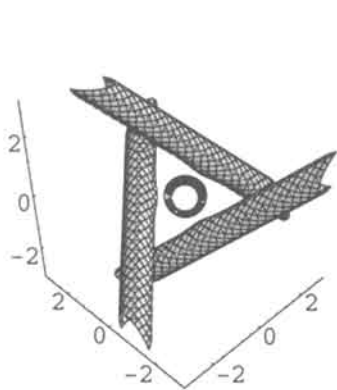


Fig. 9.2.1. Four rods in body centred arrangement after equation 9.2.1.

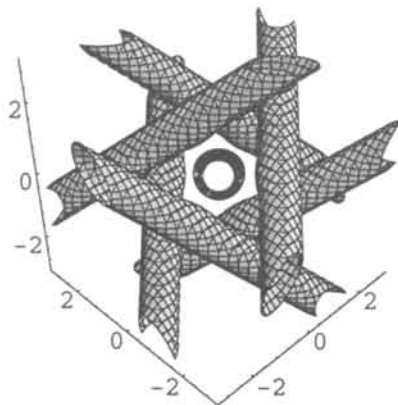


Fig. 9.2.2. Seven rods in body centred arrangement after equation 9.2.2.

We have made a bigger model in fig. 9.2.3 by using four bundles with seven rods in each after equation 9.2.3 below.

$$\begin{aligned}
 & e^{-((x+y)^2+(y+z+2)^2+(x-z-2)^2)} + e^{-((x+y)^2+(y+z-2)^2+(x-z+2)^2)} \\
 & + e^{-((x+y-4)^2+(y+z-2)^2+(x-z-2)^2)} + e^{-((x+y+4)^2+(y+z+2)^2+(x-z+2)^2)} \\
 & + e^{-((x+y+4)^2+(y+z+6)^2+(x-z-2)^2)} + e^{-((x+y-4)^2+(y+z+2)^2+(x-z-6)^2)} \\
 & + e^{-((x+y)^2+(y+z+6)^2+(x-z-6)^2)} + e^{-((x-y)^2+(y+z)^2+(x+z)^2)} \\
 & + e^{-((x-y)^2+(y+z+4)^2+(x+z+4)^2)} + e^{-((x-y+4)^2+(y+z)^2+(x+z+4)^2)} \\
 & + e^{-((x-y+4)^2+(y+z-4)^2+(x+z)^2)} + e^{-((x-y)^2+(y+z-4)^2+(x+z-4)^2)} \\
 & + e^{-((x-y-4)^2+(y+z)^2+(x+z-4)^2)} + e^{-((x-y-4)^2+(y+z+4)^2+(x+z)^2)} \\
 & + e^{-((x+y+2)^2+(y-z)^2+(x+z+2)^2)} + e^{-((x+y-2)^2+(y-z)^2+(x+z-2)^2)} \\
 & + e^{-((x+y-2)^2+(y-z-4)^2+(x+z+2)^2)} + e^{-((x+y+2)^2+(y-z+4)^2+(x+z-2)^2)} \\
 & + e^{-((x+y+6)^2+(y-z+4)^2+(x+z+2)^2)} + e^{-((x+y+6)^2+(y-z)^2+(x+z+6)^2)} \\
 & + e^{-((x+y+2)^2+(y-z-4)^2+(x+z+6)^2)} + e^{-((x-y+2)^2+(y-z-2)^2+(x-z)^2)} \\
 & + e^{-((x-y-2)^2+(y-z+2)^2+(x-z)^2)} + e^{-((x-y+2)^2+(y-z+2)^2+(x-z+4)^2)} \\
 & + e^{-((x-y-2)^2+(y-z-2)^2+(x-z-4)^2)} + e^{-((x-y+6)^2+(y-z-2)^2+(x-z+4)^2)} \\
 & + e^{-((x-y+2)^2+(y-z-6)^2+(x-z-4)^2)} + e^{-((x-y+6)^2+(y-z-6)^2+(x-z)^2)} = 0.5
 \end{aligned}$$

9.2.3

We now go circular and derive the corresponding equation:

$$\begin{aligned}
 & e^{\cos\frac{\pi}{2}(x-y)+\cos\frac{\pi}{2}(y+z)+\cos\frac{\pi}{2}(x+z)} \\
 & + e^{\cos\frac{\pi}{2}(x+y+2)+\cos\frac{\pi}{2}(y-z)+\cos\frac{\pi}{2}(x+z+2)} \\
 & + e^{\cos\frac{\pi}{2}(x+y)+\cos\frac{\pi}{2}(y+z+2)+\cos\frac{\pi}{2}(x-z-2)} \\
 & + e^{\cos\frac{\pi}{2}(x-y+2)+\cos\frac{\pi}{2}(y-z-2)+\cos\frac{\pi}{2}(x-z)} = 15
 \end{aligned}$$

9.2.4

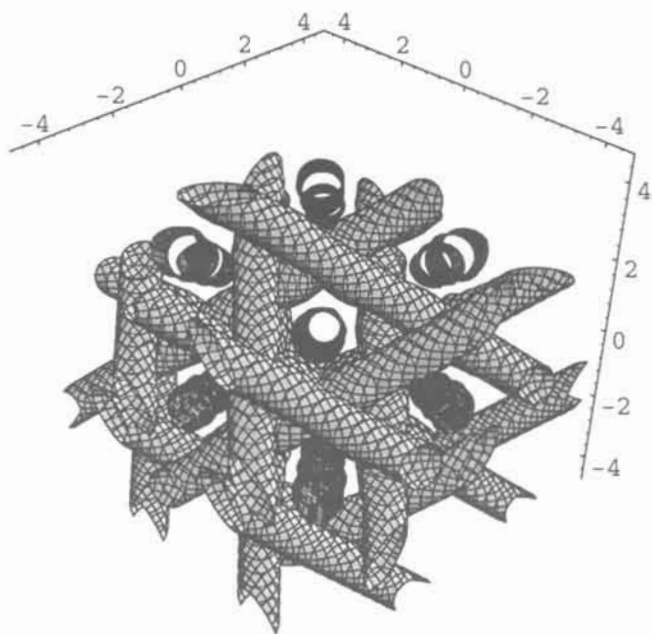


Fig. 9.2.3. Twenty eight rods in body centred arrangement after equation 9.2.3.

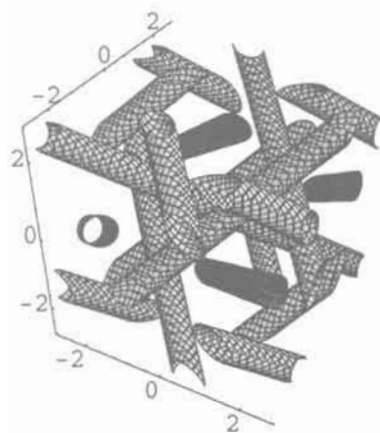


Fig. 9.2.4. Same structure but with circular functions after equation 9.2.4.

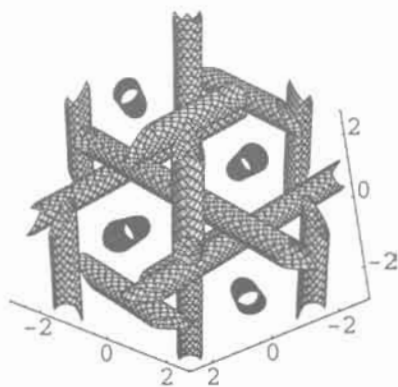


Fig. 9.2.5. Different projection.

We see again the structure in two different projections in figs. 9.2.4 and 9.2.5 from these mathematics of the circular functions. A constant is chosen so the cylinder diameter is small to give more open pictures of the structure.

O'Keefe [3] has discovered that the two packings discussed so far can interpenetrate each other, and this is shown below with two different projections in figs. 9.2.6 and 9.2.7, using only one of the four garnet rod systems (the thinner rods) to interpenetrate the primitive system. The equation is:

$$\begin{aligned}
 & e^{\cos \frac{\pi}{2} x + \cos \frac{\pi}{2} (z+2)} + e^{\cos \frac{\pi}{2} z + \cos \frac{\pi}{2} (y+2)} + e^{\cos \frac{\pi}{2} y + \cos \frac{\pi}{2} (x+2)} \\
 & + \frac{1}{4} e^{\cos \frac{\pi}{2} (x-y) + \cos \frac{\pi}{2} (y+z) + \cos \frac{\pi}{2} (x+z)} = 6.5
 \end{aligned}
 \tag{9.2.5}$$

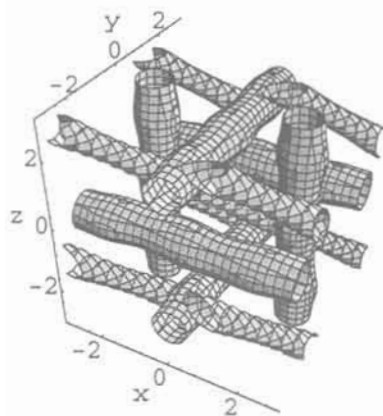


Fig. 9.2.6. The two rod structures discussed interpenetrate each other after equation 9.2.5.

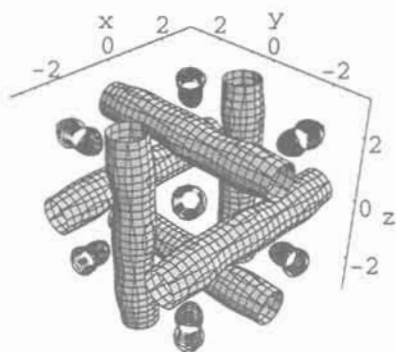


Fig. 9.2.7. Different projection.

9.3 Tetragonal and Hexagonal Packing of Rods

According to the algorithm, next is four rods around a goke, and there are different ways to obtain the mathematics. We start with the GD mathematics.

We have seen that in the packings above, the rods were parallel with a cube edge respectively a cube diagonal. We will now show that in this tetragonal packing, the rods are parallel to face diagonals (giving the structure a $c/a \neq 1$, of course). We shall demonstrate the packings directly by using the cube. Doing so we take advantage of the exponential scale as is obvious from the figures below.

We show first the packings described above in equations 9.3.1 and 2, and figures 9.3.1 and 2.

$$\begin{aligned}
 & e^{-(e^{x^2} + e^{(y+2)^2})} + e^{-(e^{y^2} + e^{(z+2)^2})} + e^{-(e^{z^2} + e^{(x+2)^2})} \\
 & + e^{-(e^{x^2} + e^{y^2} + e^{z^2} - 10)} = 0.08
 \end{aligned}
 \tag{9.3.1}$$

$$\begin{aligned}
 & e^{-(e^{(x+z)^2} + e^{(y+z+2)^2})} + e^{-(e^{(y+z)^2} + e^{(x+y+2)^2})} \\
 & + e^{-(e^{(x+y)^2} + e^{(x+z+2)^2})} + e^{-(e^{(x-1)^2} + e^{(y-1)^2} + e^{(z-1)^2} - 30)} = 0.08
 \end{aligned}
 \tag{9.3.2}$$

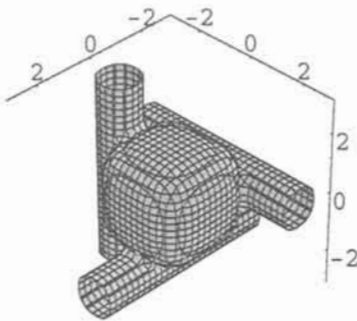


Fig. 9.3.1. P.c. packing of rods and the cube.

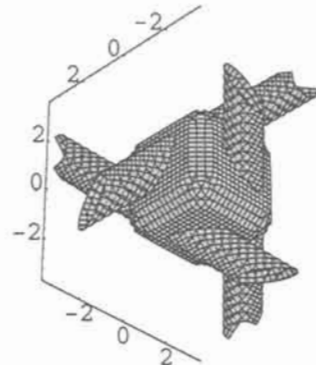


Fig. 9.3.2. Bcc packing of rods and the cube.

The relation of the tetragonal packing with the cube is shown in eq. 9.3.3 and illustrated in fig. 9.3.3.

$$\begin{aligned}
 & e^{-(e^{(x-y+z)^2 + (-x-y-z+4)^2})} + e^{-(e^{(-x-y-z)^2 + (-x+y+z-4)^2})} \\
 & + e^{-(e^{(-x+y+z)^2 + (x+y-z+4)^2})} + e^{-(e^{(x+y-z)^2 + (x-y+z-4)^2})} \quad 9.3.3 \\
 & + e^{-(e^{x^2 + e^{y^2} + e^{z^2} - 10})} = 0.08
 \end{aligned}$$

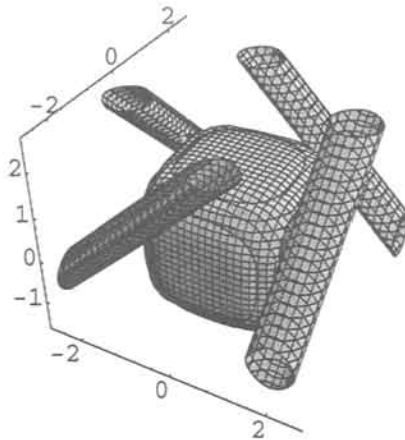


Fig. 9.3.3. Tetragonal packing of rods and the cube after equation 9.3.3.

Below we give the equation for this packing by itself, which is also shown in figs. 9.3.4 and 5.

$$\begin{aligned}
 & e^{-(x-y+z)^2 + (-x-y-z+4)^2} + e^{-(x-y-z)^2 + (-x+y+z-4)^2} \quad 9.3.4 \\
 & + e^{-(x+y+z)^2 + (x-y-z+4)^2} + e^{-(x+y-z)^2 + (x-y+z-4)^2} = 0.2
 \end{aligned}$$

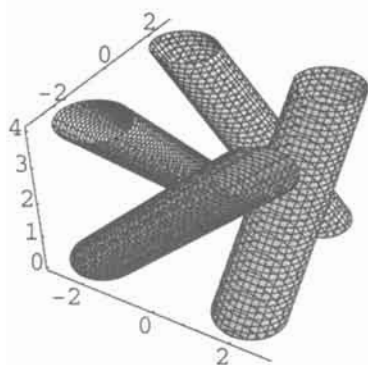


Fig. 9.3.4. Tetragonal packing of rods after equation 9.3.4.

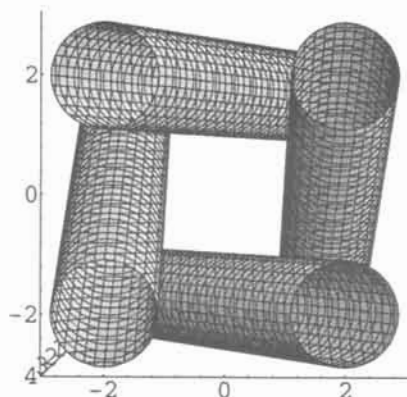


Fig. 9.3.5. Different projection.

We can add a circular goke in eq. 9.3.5 and fig. 9.3.6.

$$\begin{aligned}
 & e^{-(x-y+z)^2+(-x-y-z+4)^2} + e^{-(x-y-z)^2+(-x+y+z-4)^2} \\
 & + e^{-(x+y+z)^2+(x+y-z+4)^2} + e^{-(x+y-z)^2+(x-y+z-4)^2} \\
 & + e^{-(x^2+y^2+.5)} = 0.35
 \end{aligned} \tag{9.3.5}$$

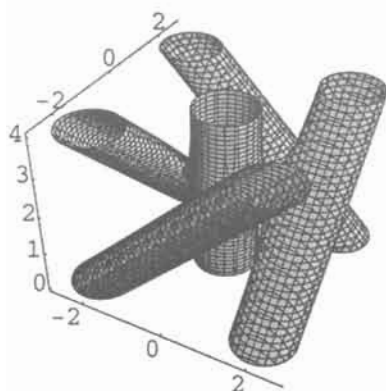


Fig. 9.3.6. A goke is added to the tetragonal packing after equation 9.3.5.

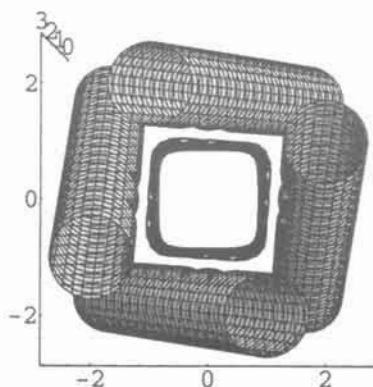


Fig. 9.3.7. A square goke is added to the tetragonal packing after equation 9.3.6.

As the structure is tetragonal we make a square goke in 9.3.6 as illustrated in fig. 9.3.7.

$$\begin{aligned}
 & e^{-(x-y+z)^2+(-x-y-z+4)^2} + e^{-(-x-y-z)^2+(-x+y+z-4)^2} \\
 & + e^{-(-x+y+z)^2+(x+y-z+4)^2} + e^{-(x+y-z)^2+(x-y+z-4)^2} \\
 & + 2e^{-(e^{x^4} + e^{y^4} - 2)} = 0.35
 \end{aligned}
 \tag{9.3.6}$$

The circular mathematics was derived accordingly, as seen in eq. 9.3.7. Because of low graphical resolution, the terms had to be squared. And the periodic packing is shown in different projections in figures 9.3.8 and 9.3.9.

$$\begin{aligned}
 & e^{(\cos\frac{\pi}{2}(x-y+z)+\cos\frac{\pi}{2}(-x-y-z+1))^2} \\
 & + e^{(\cos\frac{\pi}{2}(-x-y-z)+\cos\frac{\pi}{2}(-x+y+z-1))^2} \\
 & + e^{(\cos\frac{\pi}{2}(-x+y+z)+\cos\frac{\pi}{2}(x+y-z+1))^2} \\
 & + e^{(\cos\frac{\pi}{2}(x+y-z)+\cos\frac{\pi}{2}(x-y+z-1))^2} = 40
 \end{aligned}
 \tag{9.3.7}$$

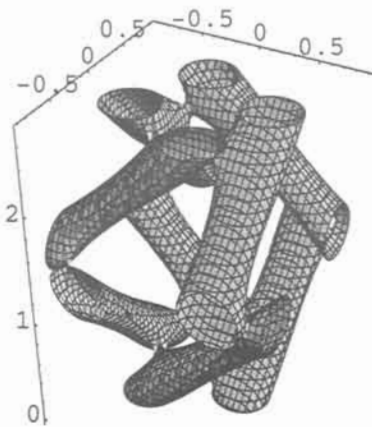


Fig. 9.3.8. Tetragonal rods with the circular functions after 9.3.7.

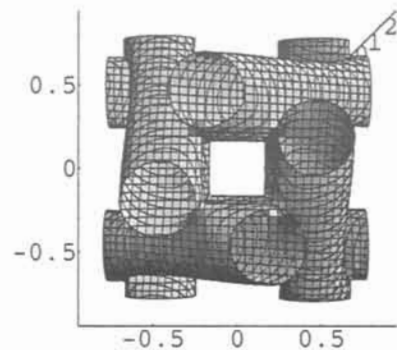


Fig. 9.3.9. Different projection.

A larger region is shown in fig. 9.3.10.

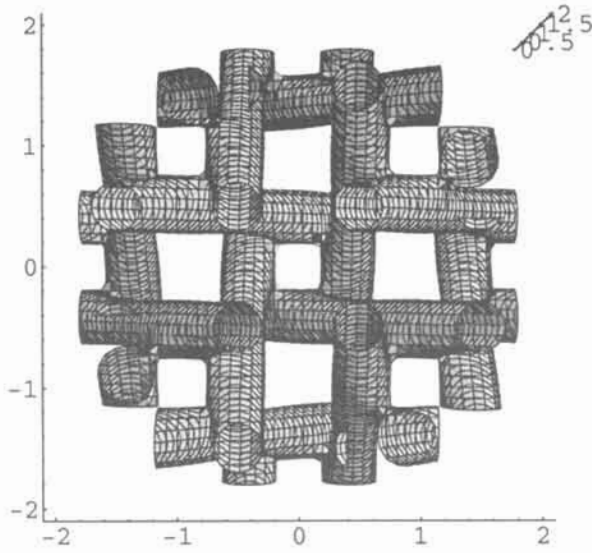


Fig. 9.3.10. A larger region.

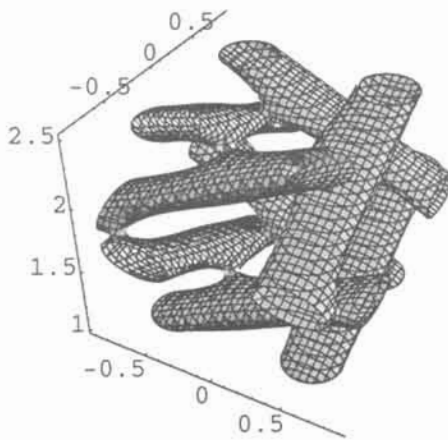


Fig. 9.3.11. Different c/a after equation 9.3.8.

And at a different c/a according to eq. 9.3.8 below gives fig. 9.3.11.

$$\begin{aligned}
 & e^{(\cos\frac{\pi}{2}(x-y+2z)+\cos\frac{\pi}{2}(-x-y-2z+1))^2} \\
 & +e^{(\cos\frac{\pi}{2}(-x-y-2z)+\cos\frac{\pi}{2}(-x+y+2z-1))^2} \\
 & +e^{(\cos\frac{\pi}{2}(-x+y+2z)+\cos\frac{\pi}{2}(x+y-2z+1))^2} \\
 & +e^{(\cos\frac{\pi}{2}(x+y-2z)+\cos\frac{\pi}{2}(x-y+2z-1))^2} = 40
 \end{aligned} \tag{9.3.8}$$

Next is the hexagonal rod packing after eq. 9.3.9 and seen in different projections in figs. 9.3.12 and 13.

$$\begin{aligned}
 & e^{-(e^{(-0.5x+\frac{\sqrt{3}}{6}y+0.4z)^2} + e^{(0.4z-\frac{\sqrt{3}}{3}y-4)^2})} \\
 & +e^{-(e^{(0.5x+\frac{\sqrt{3}}{6}y+0.4z-4)^2} + e^{(0.4z-\frac{\sqrt{3}}{3}y)^2})} \\
 & +e^{-(e^{(-0.5x+\frac{\sqrt{3}}{6}y+0.4z-4)^2} + e^{(0.5x+\frac{\sqrt{3}}{6}y+0.4z)^2})} \\
 & +e^{-(e^{(-0.5x+\frac{\sqrt{3}}{6}y-0.4z)^2} + e^{(-0.4z-\frac{\sqrt{3}}{3}y+4)^2})} \\
 & +e^{-(e^{(0.5x+\frac{\sqrt{3}}{6}y-0.4z+4)^2} + e^{(-0.4z-\frac{\sqrt{3}}{3}y)^2})} \\
 & +e^{-(e^{(0.5x+\frac{\sqrt{3}}{6}y-0.4z)^2} + e^{(-0.5x+\frac{\sqrt{3}}{6}y-0.4z+4)^2})} \\
 & +e^{-(x^2+y^2)^2} = 0.09
 \end{aligned} \tag{9.3.9}$$

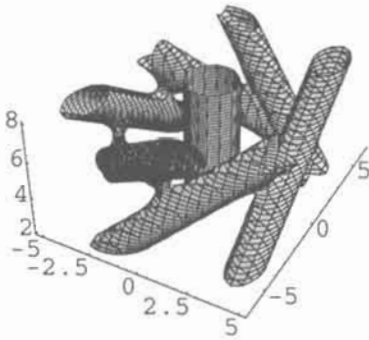


Fig. 9.3.12. Hexagonal rod packing after equation 9.3.9.

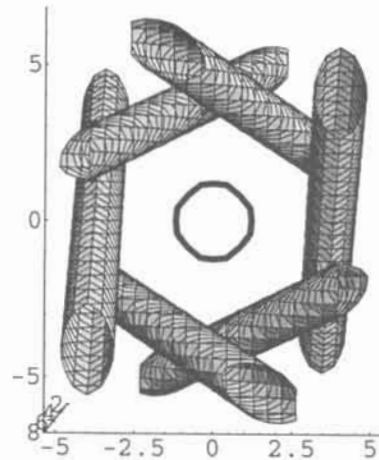


Fig. 9.3.13. Different projection.

The rods in tetragonal packing, and in hexagonal, meet after equations 9.3.10 and 11 and are shown in figs. 9.3.14 and 9.3.15.

$$\begin{aligned}
 & e^{-((-x+y+z)^2+(x+y-z)^2)} + e^{-((x+y-z)^2+(x-y+z)^2)} \\
 & + e^{-((x-y+z)^2+(-x-y-z)^2)} + e^{-((-x-y-z)^2+(-x+y+z)^2)} = 0.35
 \end{aligned} \tag{9.3.10}$$

$$\begin{aligned}
 & e^{-\left(e^{-\left(-0.5x + \frac{\sqrt{3}}{6}y + 0.4z\right)^2} + e^{-\left(0.4z - \frac{\sqrt{3}}{3}y\right)^2}\right)} \\
 & + e^{-\left(e^{-\left(0.5x + \frac{\sqrt{3}}{6}y + 0.4z\right)^2} + e^{-\left(0.4z - \frac{\sqrt{3}}{3}y\right)^2}\right)} \\
 & + e^{-\left(e^{-\left(-0.5x + \frac{\sqrt{3}}{6}y + 0.4z\right)^2} + e^{-\left(0.5x + \frac{\sqrt{3}}{6}y + 0.4z\right)^2}\right)} \\
 & + e^{-\left(e^{-\left(-0.5x + \frac{\sqrt{3}}{6}y - 0.4z\right)^2} + e^{-\left(-0.4z - \frac{\sqrt{3}}{3}y\right)^2}\right)} \\
 & + e^{-\left(e^{-\left(0.5x + \frac{\sqrt{3}}{6}y - 0.4z\right)^2} + e^{-\left(-0.4z - \frac{\sqrt{3}}{3}y\right)^2}\right)} \\
 & + e^{-\left(e^{-\left(0.5x + \frac{\sqrt{3}}{6}y - 0.4z\right)^2} + e^{-\left(-0.5x + \frac{\sqrt{3}}{6}y - 0.4z\right)^2}\right)} = 0.11
 \end{aligned} \tag{9.3.11}$$

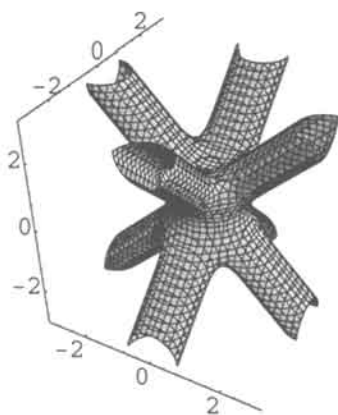


Fig. 9.3.14. Rods meet in a tetragonal structure after equation 9.3.10.

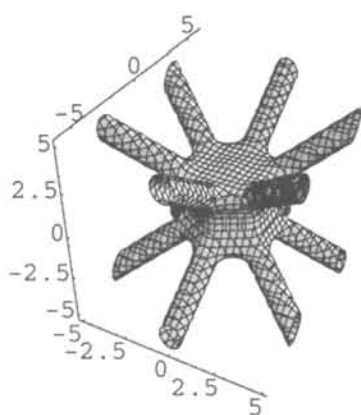


Fig. 9.3.15. Rods meet in a hexagonal structure after equation 9.3.11.

9.4 Larsson Cubosomes of Rods

We showed in chapter 5 how the Larsson cubosomes were made. We make similar structures with the rods.

We add a sphere to a cylinder after equation 9.4.1, and have a spherical torus as in fig. 9.4.1.

$$e^{-(x^2+y^2)^2} + e^{0.15(x^2+y^2+z^2)} = 1.95 \quad 9.4.1$$

In fig. 9.4.2 we have added three A15 rods to a sphere after equation 9.4.2. The structure is chiral and can be said to be a 3D propeller. This is best seen in its projection in fig. 9.4.3.

$$e^{-(x^2+(y+2)^2)^2} + e^{-(y^2+(z+2)^2)^2} + e^{-(z^2+(x+2)^2)^2} \\ + e^{0.05((x+1)^2+(y+1)^2+(z+1)^2)} = 1.9 \quad 9.4.2$$

$$\begin{aligned}
 & e^{-(x^2+(y+2)^2)^2} + e^{-(y^2+(z+2)^2)^2} \\
 & + e^{-(z^2+(x+2)^2)^2} + e^{-(x^2+(y-2)^2)^2} \\
 & + e^{-(y^2+(z-2)^2)^2} + e^{-(z^2+(x-2)^2)^2} + e^{0.04(x^2+y^2+z^2)} = 1.95
 \end{aligned}
 \tag{9.4.3}$$

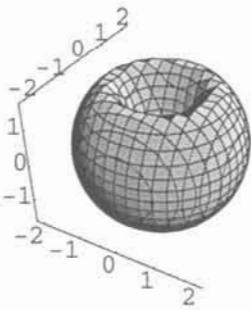


Fig. 9.4.1. Spherical torus after equation 9.4.1.

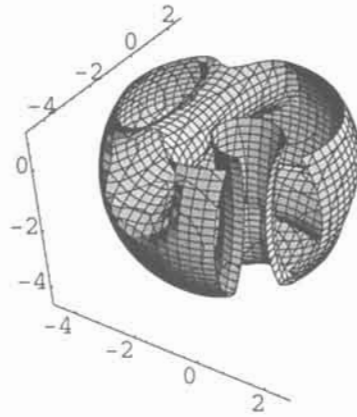


Fig. 9.4.2. Finite primitive packing of rods after equation 9.4.2.

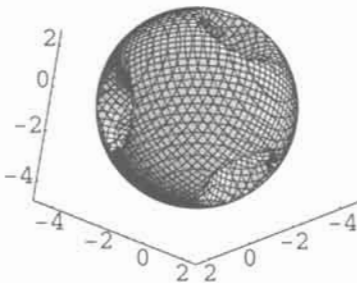


Fig. 9.4.3. Different projection.

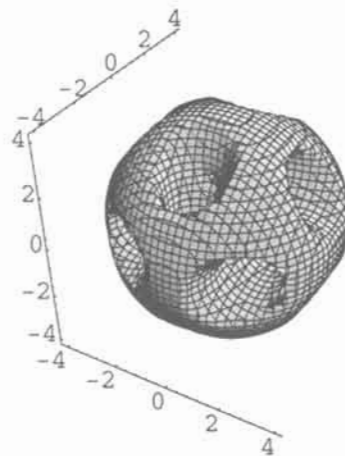


Fig. 9.4.4. Six cylinders in finite primitive packing after equation 9.4.3.

Next is to add three more cylinders in the A15 rod 3D propeller, after equation 9.4.3. Increasing the A15 packing to six cylinders in this way means a centric structure and the chirality is lost. This is a beautiful structure indeed, and is shown in fig. 9.4.4 and as a split in 9.4.5. The rod systems are non-intersecting, so this spherical body can also be used as a propeller. Blowing a thin beam of air on to the body along the three fold axis means spinning as the other rod system of opposite chirality is hidden. Organising another beam of exactly opposite direction, blowing simultaneously, would then make the body spin even better!

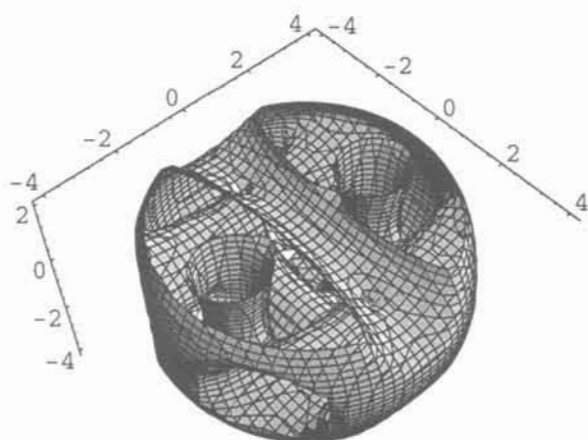


Fig. 9.4.5. Split of fig. 9.4.4.

Using the circular equation as in 9.4.4 for the bcc or garnet packing of rods and adding a sphere, we get fig. 9.4.6 and its split in 7.

$$\begin{aligned}
 & e^{\cos \frac{\pi}{2}(x-y) + \cos \frac{\pi}{2}(y+z) + \cos \frac{\pi}{2}(x+z)} \\
 & + e^{\cos \frac{\pi}{2}(x+y+2) + \cos \frac{\pi}{2}(y-z) + \cos \frac{\pi}{2}(x+z+2)} \\
 & + e^{\cos \frac{\pi}{2}(x+y) + \cos \frac{\pi}{2}(y+z+2) + \cos \frac{\pi}{2}(x-z-2)} \\
 & + e^{\cos \frac{\pi}{2}(x-y+2) + \cos \frac{\pi}{2}(y-z-2) + \cos \frac{\pi}{2}(x-z)} \\
 & + e^{0.4(x^2+y^2+z^2)} = 15
 \end{aligned}$$

9.4.4

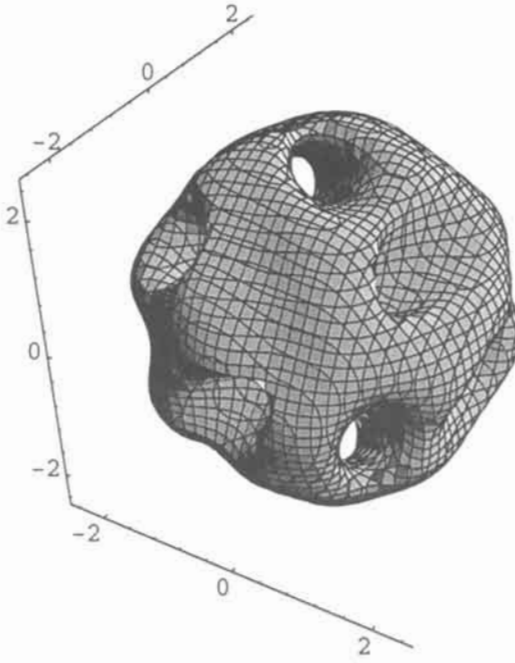


Fig. 9.4.6. Finite garnet packing of rods after equation 9.4.4.

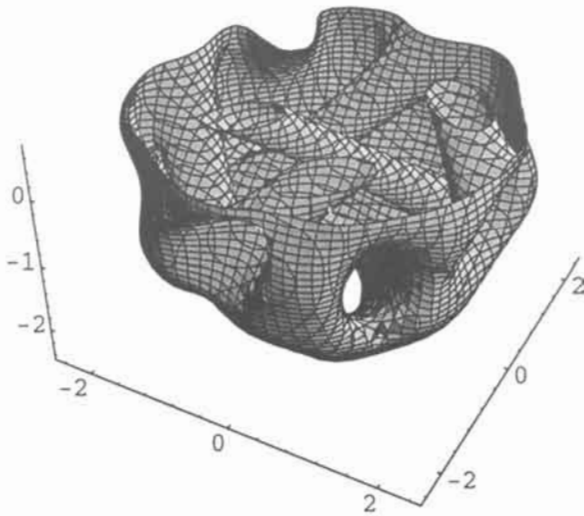


Fig. 9.4.7. Split of fig. 9.4.6.

In figures 9.4.8 and 9 there is a cylinder giving boundaries to a tetragonal rod packing after eq. 9.4.5.

$$\begin{aligned}
 & e^{-((x+z+2)^2+(y+z-2)^2)} + e^{-((y+z+2)^2+(x-z+2)^2)} \\
 & + e^{-((y-z+2)^2+(x-z-2)^2)} + e^{-((y-z-2)^2+(x+z-2)^2)} \\
 & + e^{-((y+z-10)^2+(x+z-6)^2)} + e^{-((y+z-6)^2+(x-z+10)^2)} \\
 & + e^{-((y-z+10)^2+(x-z+6)^2)} + e^{-((y-z+6)^2+(x+z-10)^2)} \\
 & + e^{0.015(y^2+x^2)} = 1.5
 \end{aligned}
 \tag{9.4.5}$$

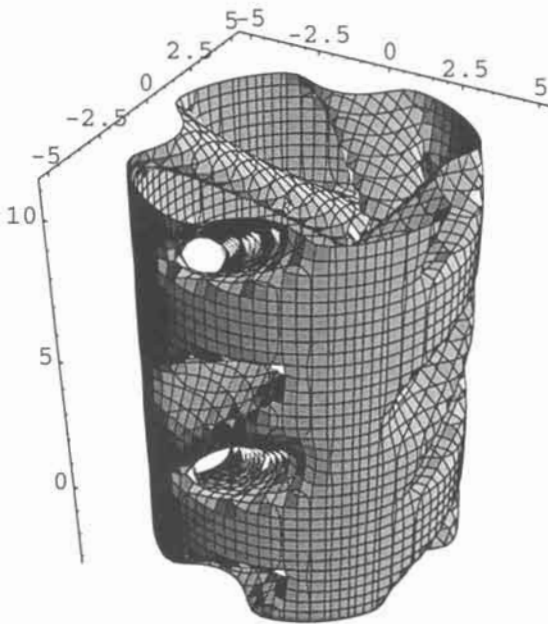


Fig. 9.4.8. Cylindrical boundary to tetragonal rod packing after equation 9.4.5.

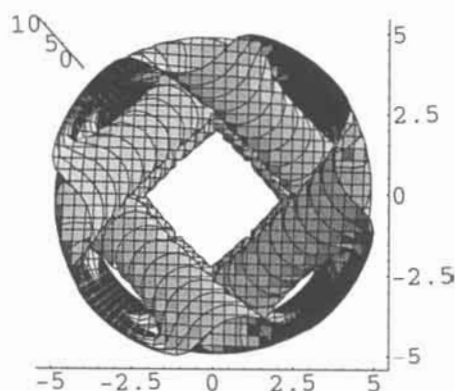


Fig. 9.4.9. Different projection.

9.5 Packing of Rods, and their Related Surfaces

Below we see the primitive packing of rods transforming to a surface. The rods approach each others by lowering the constant. At 4 there is fig. 9.5.1 and at 3.6 there is the classic IWP fig. 9.5.2. The equation is in 9.5.1.

$$e^{-\cos \pi x + \cos \pi z} + e^{-\cos \pi z + \cos \pi y} + e^{\cos \pi x - \cos \pi y} = 4 \quad 9.5.1$$

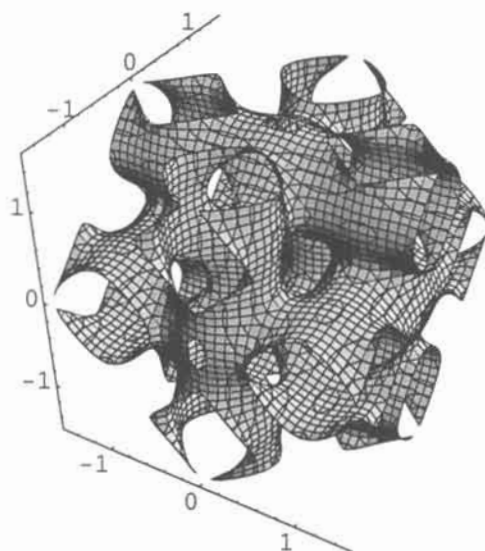


Fig. 9.5.1. Primitive rod structure transforming to a surface after equation 9.5.1. $C=4$.

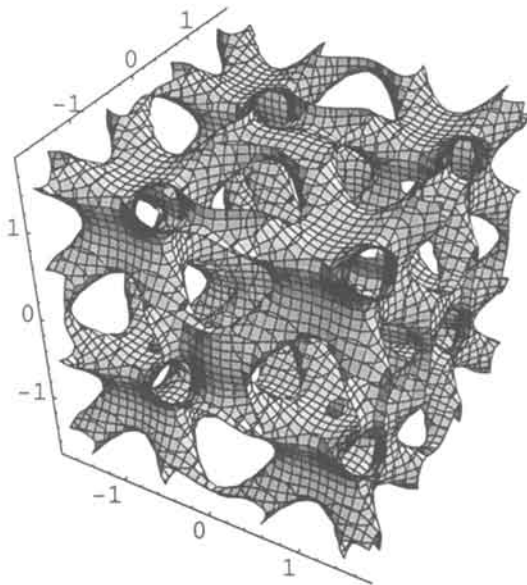


Fig. 9.5.2. At $C=3.6$ the surface is IWP.

The garnet packing - $Ia3d$ - gives a complicated surface related to the D surface and its hexagonal correspondence. We start with eq. 9.2.4 and a constant of 6, and its projection seen in figures 9.5.3 and 4.

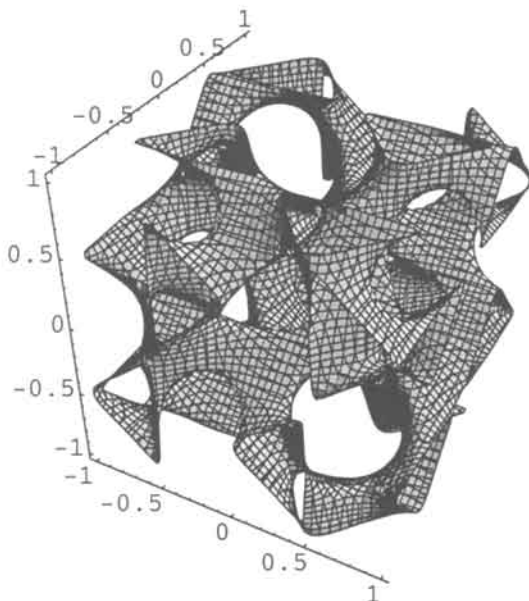


Fig. 9.5.3. Garnet packing of rods approaching a surface after equation 9.2.4 and a constant of 6.

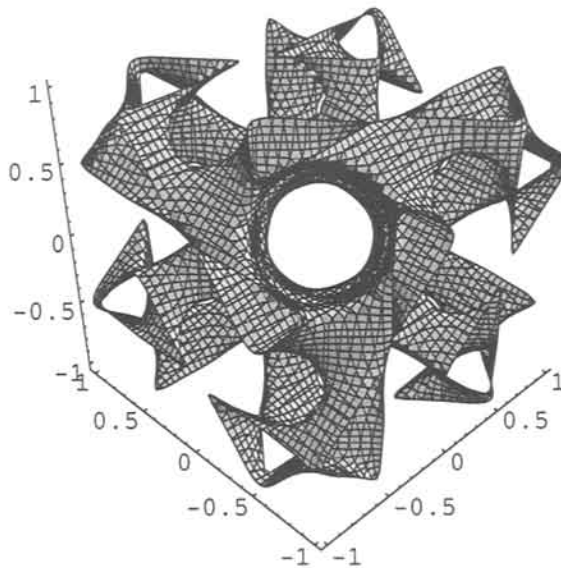


Fig. 9.5.4. Different projection.

At a constant of 4.9 a tetrahedral structure is shown in fig. 9.5.5, projected after a cubic space diagonal. A larger region is shown in fig. 9.5.6. And there are three more like that, meaning that the non-intersecting rods are kept in form of non intersecting channels of tridymite type. The tetrahedral network is created in the regions where the rods meet. The structure is intermediate in its nature to the cristobalite and the tridymite structures.

We have also used the handmade structures with the GD mathematics for this purpose. The change of constant for the primitive and the garnet, or bcc, packing of rods, also here make the rods condense into surfaces of exactly the same type as was the case for the circular functions, as shown above.

Conclusion:

The fundamental and simplest rod packings are not related to the simple and fundamental surfaces like P, D or G.

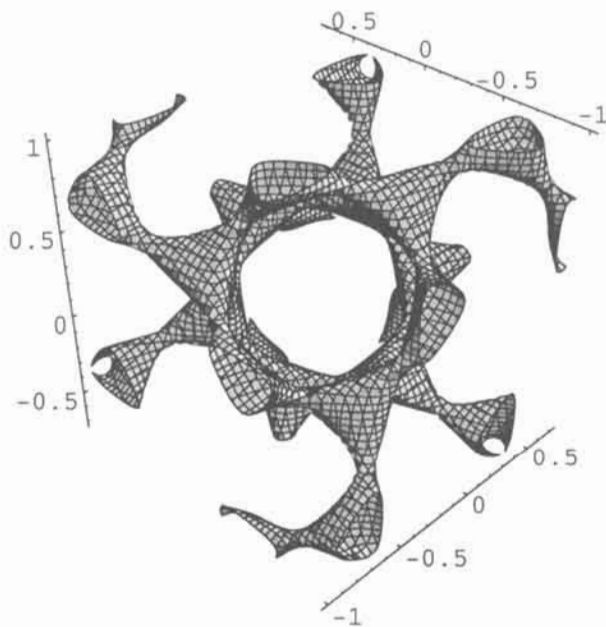


Fig. 9.5.5. At $C=4.9$ there is a tetrahedral structure projected after a cubic space diagonal.

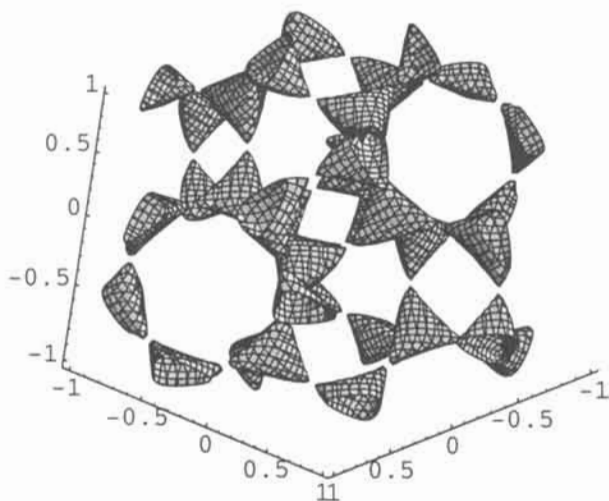


Fig. 9.5.6. A larger region of fig. 9.5.5. The structure is intermediate in its nature to the cristobalite and the tridymite structures.

Exercises 9

Exercise 9.1. Show what happens when the constant in eq 9.1.1 approaches 0.

Exercise 9.2. Make a hexagonal radiolarian.

Exercise 9.3. Make a 2D correspondence to equation 9.1.2.

Exercise 9.4. Add a perpendicular non-intersecting rod to 3.

Answer 9.1. $C=0.05$

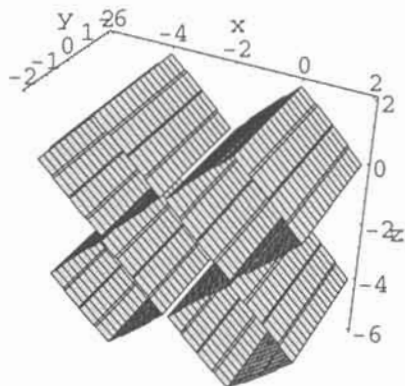


Fig. 9.1.

Answer 9.2.

$$\begin{aligned}
 & e^{-((-0.5x+0.29y+0.4z)^2+(0.4z-0.58y)^2)} + e^{-((0.5x+0.29y+0.4z)^2+(0.4z-0.58y)^2)} \\
 & + e^{-((0.5x+0.29y+0.4z)^2+(-0.5x+0.29y+0.4z)^2)} + e^{-((-0.5x+0.29y-0.4z)^2+(-0.4z-0.58y)^2)} \\
 & + e^{-((0.5x+0.29y-0.4z)^2+(-0.4z-0.58y)^2)} + e^{-((0.5x+0.29y-0.4z)^2+(-0.5x+0.29y-0.4z)^2)} \\
 & + e^{-(x^2+y^2+z^2)} - 1 = 0
 \end{aligned}$$

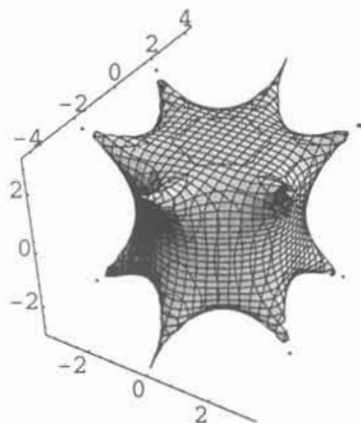


Fig. 9.2.

Answer 9.3.

$$e^{\cos\frac{\pi}{2}x + \cos\frac{\pi}{2}z} + e^{\cos\frac{\pi}{2}z + \cos\frac{\pi}{2}y} = 4.5$$

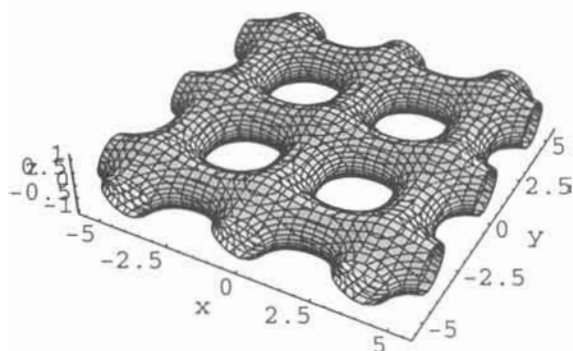


Fig. 9.3.

Answer 9.4. Note that only a part of 9.3 is used.

$$e^{\cos\frac{\pi}{2}x + \cos\frac{\pi}{2}z} + e^{\cos\frac{\pi}{2}z + \cos\frac{\pi}{2}y} + e^{\cos\frac{\pi}{2}(y+\frac{1}{2}) + \cos\frac{\pi}{2}(x+\frac{1}{2})} = 6.5$$

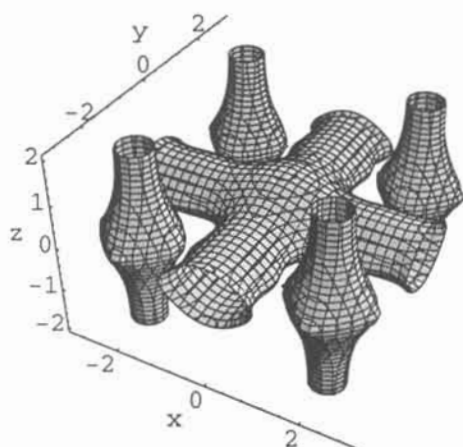


Fig. 9.4.

References 9

- 1 J.E. Gordon, *THE NEW SCIENCE OF STRONG MATERIALS or why you don't fall through the floor*, Penguin Books, England, 1975, page 18.
- 2 S. Lidin, M. Jacob and S. Andersson, *J. Solid State Chem.* **114** 36 (1995).
- 3 M. O'Keeffe, *Acta Cryst. A* **48** 879 (1992).

This Page Intentionally Left Blank

10 The Rings, Addition and Subtraction

*'...and what is the use of a book,' thought Alice,
'without pictures or conversations?'* (Lewis Carroll, from *Syngé* [1]).

Here we show examples of addition and subtraction in 3D. We add or subtract spheres to planes, cubes, the natural exponential, and show how to derive the equation of a ring or a torus.

We study the various ways of combining rings using these operations. We obtain examples of spherical and hyperbolic geometries, and we also add a torus and a periodic nodal surface.

By the subtraction of polyhedra from the sphere we obtain the hyperbolic polyhedra.

10.1 Some Simple Examples of Subtraction and Addition in 3D

We subtract a sphere from a plane, or give curvature to a plane, with a sphere after eq. 10.1.1. By gradually changing the exponential function as constant A varies from 4, 1, 0.73, to 0.65 respectively, we have the pictures below in figs 10.1.1-4.

$$x^2 + y^2 + z^2 - e^{Az} = 0 \quad 10.1.1$$

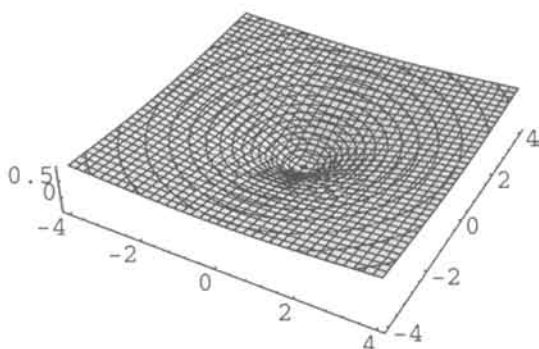
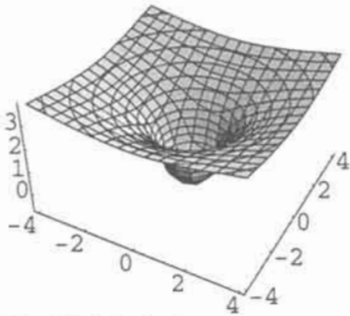
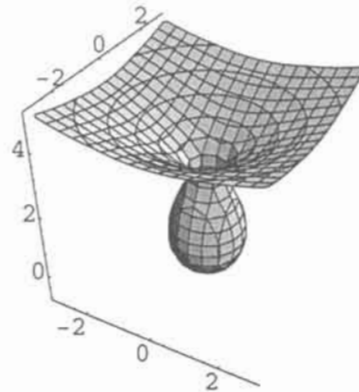
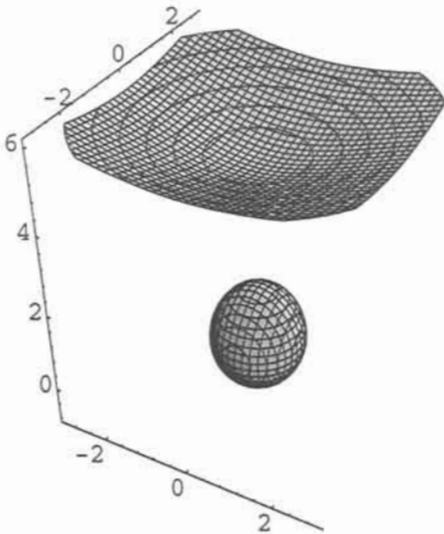


Fig. 10.1.1. A sphere subtracted from a plane after equation 10.1.1. $A=4$.

Fig. 10.1.2. $A=1$.Fig. 10.1.3. $A=0.73$.Fig. 10.1.4. $A=0.65$.

We also call it the falling drop. Or going through a wall without making a hole in it. Or that we have subtracted a sphere from a plane.

We do the same with two planes. The constant A in equation 10.1.2 is 1.5, 1.0, and 0.5 for figs 10.1.5-7. The subtraction gives a catenoidic joint of the two planes which is cylindrically elongated in fig. 10.1.6. The sphere is liberated in fig. 10.1.7.

$$x^2 + y^2 + z^2 - e^{Az} - e^{-Az} = 0$$

10.1.2

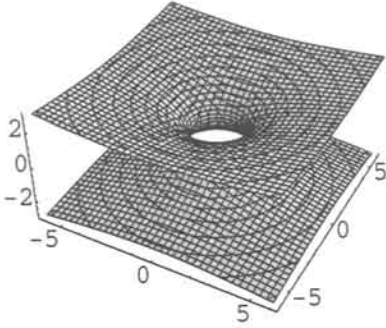


Fig. 10.1.5. A sphere subtracted from two planes after equation 10.1.2. $A=1.5$.

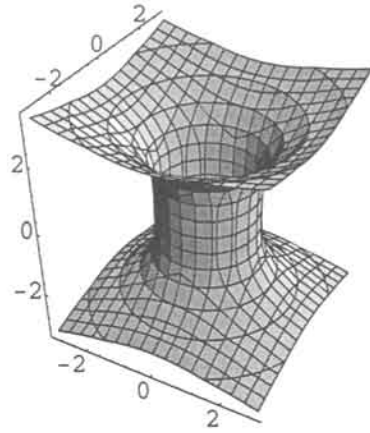


Fig. 10.1.6. $A=1$.

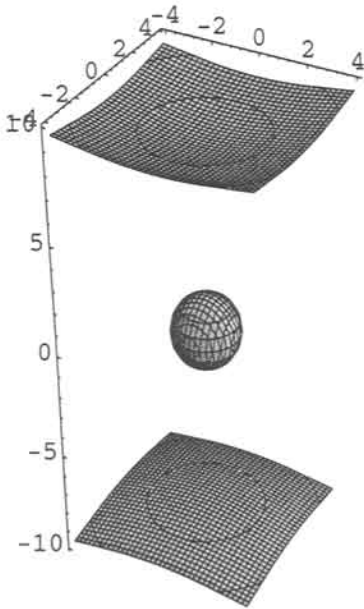


Fig. 10.1.7. The sphere is liberated at $C=0.5$.

The 3D exponential function in eq. 10.1.3 can be interpreted as a cube corner.

$$e^x + e^y + e^z = C \quad 10.1.3$$

We add and subtract the exponential function and the function of the sphere, perhaps the two most fundamental functions ever. Equation 10.1.4 gives fig 10.1.8 which obviously is a sphere added continuously to the cube corner. Fig. 10.1.9 from equation 10.1.5 is also obvious - a sphere taken away from the corner of the cube.

$$e^x + e^y + e^z + x^2 + y^2 + z^2 = 200 \quad 10.1.4$$

$$e^x + e^y + e^z - x^2 - y^2 - z^2 = 0 \quad 10.1.5$$

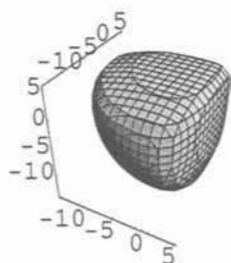


Fig. 10.1.8. A sphere added to a cube corner - or the natural exponential added to the sphere. After equation 10.1.4.

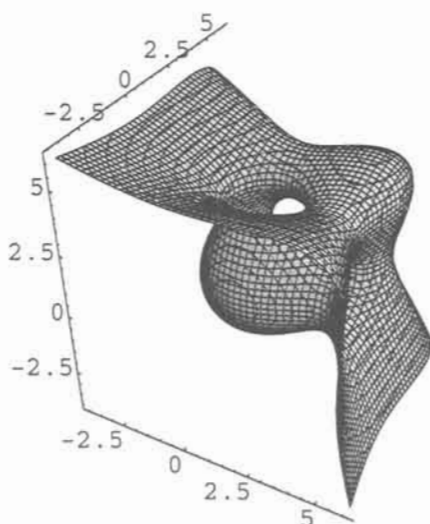


Fig. 10.1.9. A sphere taken away from a cube corner. After equation 10.1.5.

Changing the exponent shows the sphere leaving, after equation 10.1.6 and figures 10.1.10 and 10.1.11, and $A=0.69$ and 0.72 respectively.

$$e^{Ax} + e^{Ay} + e^{Az} - x^2 - y^2 - z^2 = 0 \quad 10.1.6$$

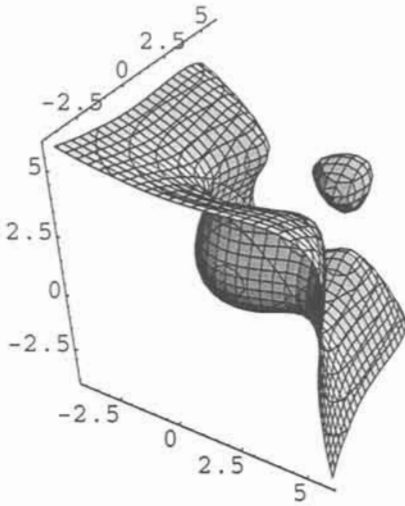


Fig. 10.1.10. The sphere is leaving after equation 10.1.6 with $A=0.69$.

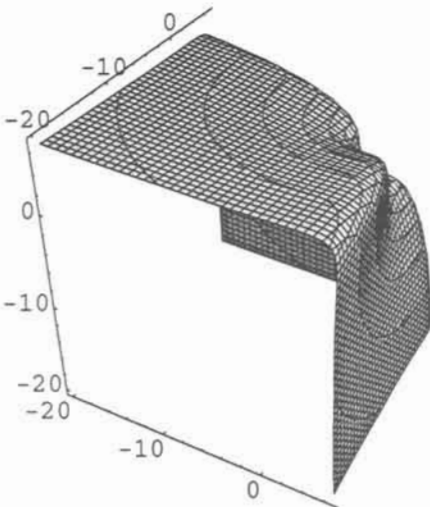


Fig. 10.1.11. $A=0.72$.

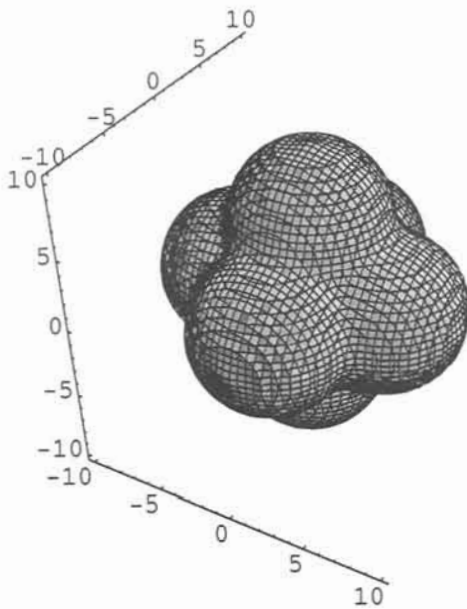


Fig. 10.1.12. A sphere subtracted from a cube after equation 10.1.7.

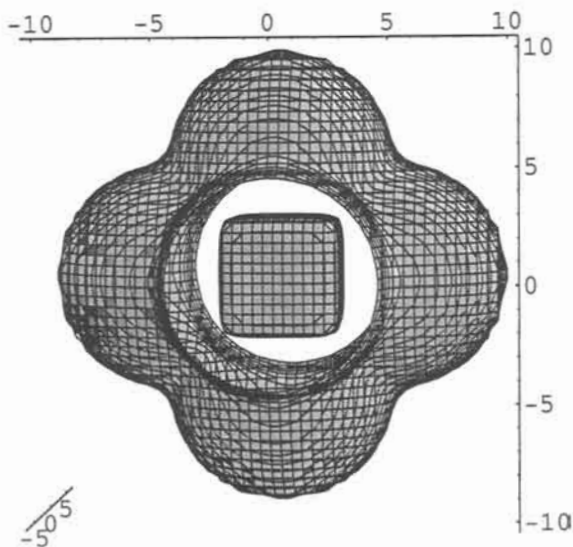


Fig. 10.1.13. The liberated cube shown in a split.

We extend to subtract the whole cube and the sphere, as in fig. 10.1.12, and the sphere is distorted. The liberated cube is shown in fig. 10.1.13, calculated with the same function, 10.1.7, but with different boundaries. At higher constants there is catenoidic contact between the sphere and the cube (not shown here).

$$10^x + 10^y + 10^z + 10^{-x} + 10^{-y} + 10^{-z} - 10^{\frac{1}{10}(x^2+y^2+z^2)} = 550 \quad 10.1.7$$

10.2 The Rings

Instead of a sphere we now take a cylinder. Closing it means adding two planes, one at each end, and opening it up means subtracting the two planes. We need to go exponential and subtract,

$$x^2 + y^2 - e^z - e^{-z} = 0 \quad 10.2.1$$

which is a slightly modified formula for the classic catenoid minimal surface, and we clearly see the cylinder and the z-planes of the surface in figs 10.2.1, and 10.2.2. We can say that the structure of this famous function is two parallel planes perpendicularly meeting a cylinder without self-intersections. So the use of an exponential scale is by no way new - it is essential to use when deriving one of the most classical surfaces ever!

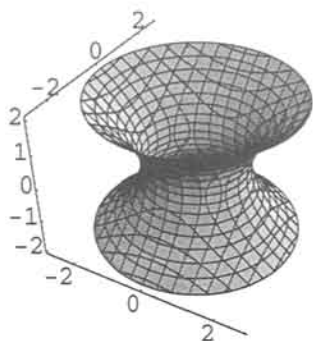


Fig. 10.2.1. A catenoid after equation 10.2.1.

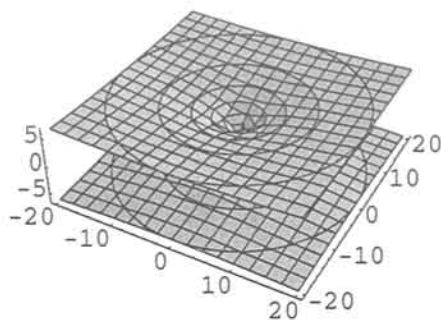


Fig. 10.2.2. Larger boundaries of fig. 10.2.1.

Adding a sphere to the catenoid means closing it. Subtracting a sphere means bending the planes so they meet and become a torus. We need to go exponential, and the constant in the exponent for the sphere is used to vary the size of the torus from $A=0.16$ in fig. 10.2.3 to 0.22 in 10.2.4.

$$x^2 + y^2 - e^z - e^{-z} - e^{A(x^2 + y^2 + z^2)} = 0 \quad 10.2.2$$

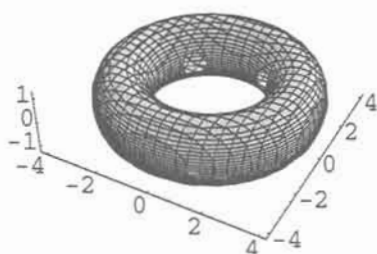


Fig. 10.2.3. Subtracting a sphere from the catenoid gives the torus after equation 10.2.2 and $A=0.16$.

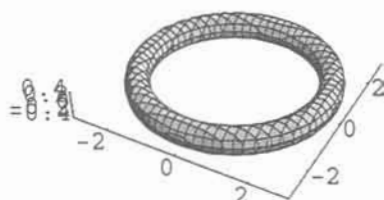


Fig. 10.2.4. $A=0.16$.

We have studied in detail how genus one is topologically derived - or how to make a hole in a sphere in a series of pictures. The equation used is

$$e^{0.15(x^2 + y^2 + z^2)} - (x^2 + y^2 - e^{0.5z} - e^{-0.5z}) = C \quad 10.2.3$$

and the value of C is given under each picture below in fig. 10.2.5 a-f.

Below is a beautiful demonstration of the rule of addition, as we see a double torus in fig. 10.2.6 (eq. 10.2.4) and triple in 10.2.7 (eq. 10.2.5). We also call them 3D pretzels.

$$\begin{aligned} &e^{(x^2 + y^2 - e^z - e^{-z} - e^{0.22(x^2 + y^2 + z^2)})} + \\ &+ e^{(x^2 + z^2 - e^y - e^{-y} - e^{0.22(x^2 + y^2 + z^2)})} = 1 \end{aligned} \quad 10.2.4$$

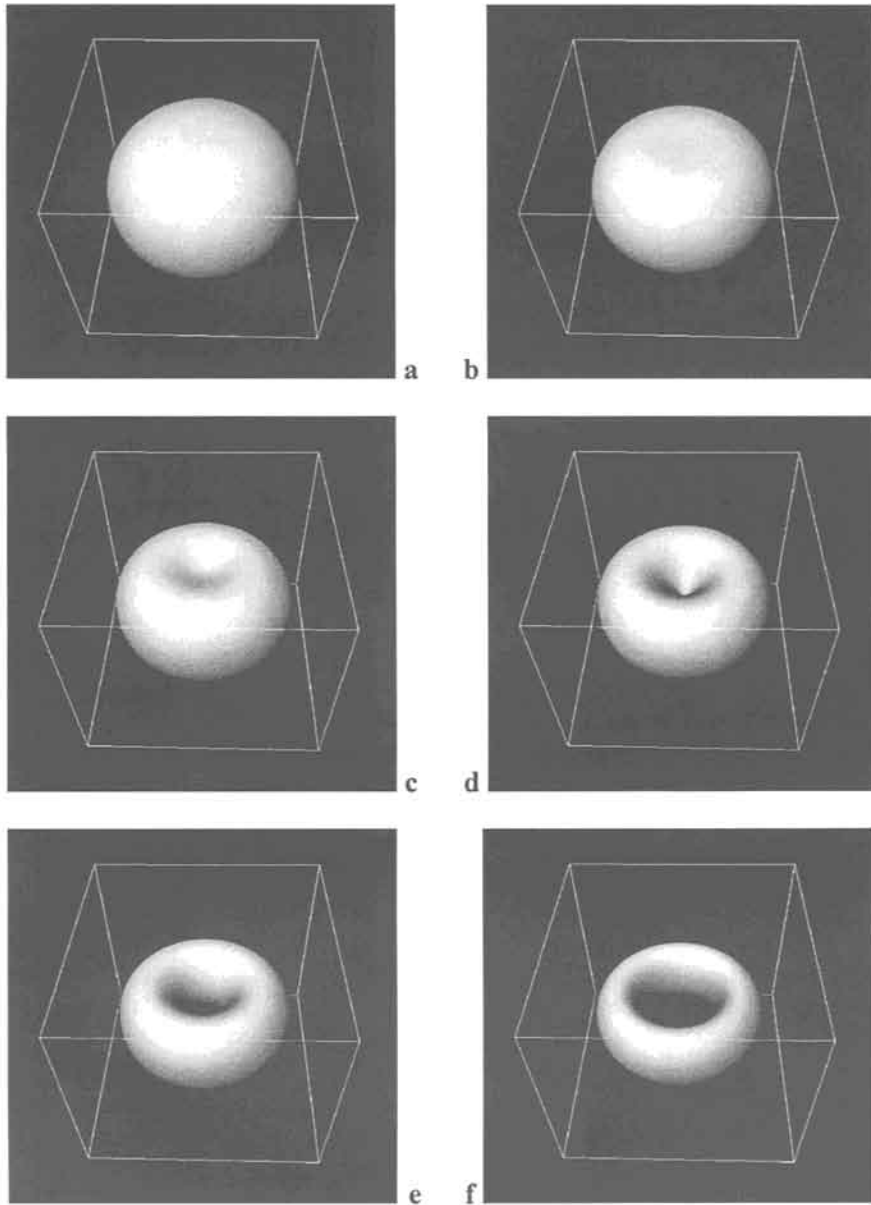


Fig. 10.2.5a-f. How to make a hole in a sphere, or how to derive genus one. From equation 10.2.3. The value of C is in (a) 20, (b) 10, (c) 5, (d) 3, (e) 2, and in (f) 0.

$$\begin{aligned}
 & e^{(x^2+y^2-e^z-e^{-z}-e^{0.22(x^2+y^2+z^2)})} + \\
 & + e^{(x^2+z^2-e^y-e^{-y}-e^{0.22(x^2+y^2+z^2)})} + \\
 & + e^{(z^2+y^2-e^x-e^{-x}-e^{0.22(x^2+y^2+z^2)})} = 1
 \end{aligned}
 \tag{10.2.5}$$

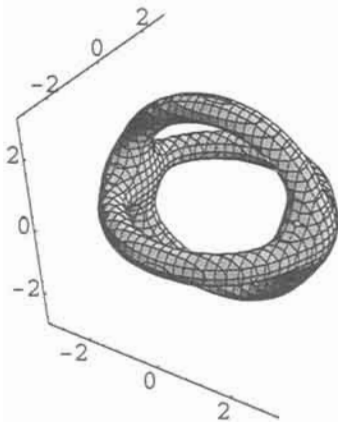


Fig. 10.2.6. Double torus after equation 10.2.4.

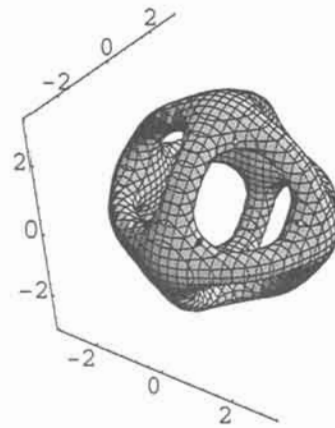


Fig. 10.2.7. Triple torus after equation 10.2.5.

K. Larsson and one of us proposed 1986 [2] that the lipid bilayer in membranes had intrinsic curvature, which gave them long range periodicity that provided a mechanism for communication. We used a ring model for the hyperbolic geometry and it is here a pleasure to give a mathematical function in equation 10.2.6 and a picture in 10.2.8.

$$\begin{aligned}
 & e^{(x^2+y^2-e^z-e^{-z}-e^{0.22(x^2+y^2+z^2)})} + \\
 & + e^{((x+5)^2+z^2-e^y-e^{-y}-e^{0.22((x+5)^2+y^2+z^2)})} + \\
 & + e^{((y+5)^2+z^2-e^x-e^{-x}-e^{0.22(x^2+(y+5)^2+z^2)})} = 1
 \end{aligned}
 \tag{10.2.6}$$

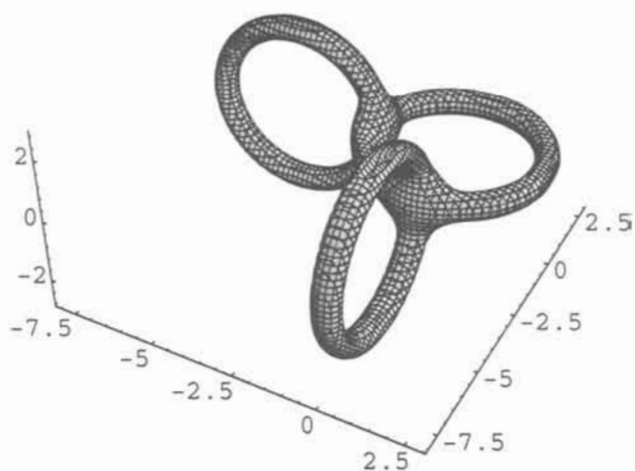


Fig. 10.2.8. Ring model for lipid bilayer after equation 10.2.6.

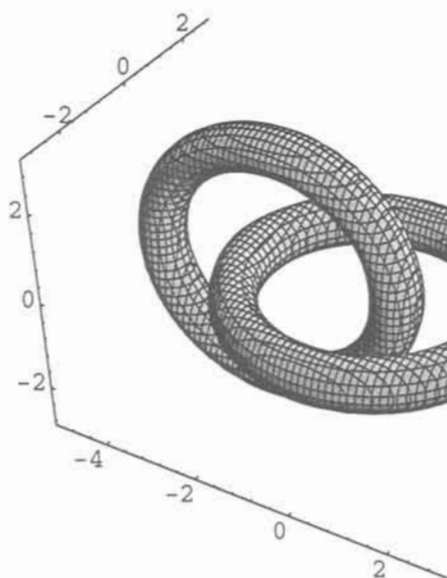


Fig. 10.2.9. Two Olympic rings after equation 10.2.7.

Next we separate the two rings in fig 10.2.6 by a simple translation in eq. 10.2.4 to get 10.2.7, and the result is shown in fig. 10.2.9.

$$e^{(x^2+y^2-e^z-e^{-z}-e^{0.22(x^2+y^2+z^2)})} + \tag{10.2.7}$$

$$e^{((x+2)^2+z^2-e^y-e^{-y}-e^{0.22((x+2)^2+y^2+z^2)})} = 0.8$$

And in eq 10.2.8 we have derived the case for three interpenetrating rings.

$$e^{((x-0.5)^2+z^2-e^y-e^{-y}-e^{0.22((x-0.5)^2+y^2+z^2)})} +$$

$$e^{((x-4)^2+y^2-e^z-e^{-z}-e^{0.22((x-4)^2+y^2+z^2)})} + \tag{10.2.8}$$

$$e^{((x-7.5)^2+z^2-e^y-e^{-y}-e^{0.22((x-7.5)^2+y^2+z^2)})} = 1$$

10.3 More Ways to make Rings

There are different ways to make rings. Below we add a cone and a cylinder - for obvious reasons we square the equation of the cylinder. For a constant of zero in equation 10.3.1 we still have the cone, but for a constant of 0.1 a torus has developed in figs. 10.3.1 and 10.3.2.

$$x^2 + y^2 - z^2 - (x^2 + y^2)^2 = C \tag{10.3.1}$$

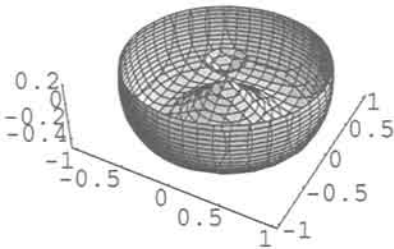


Fig. 10.3.1. Another way to make a torus after equation 10.3.1. $C=0$.

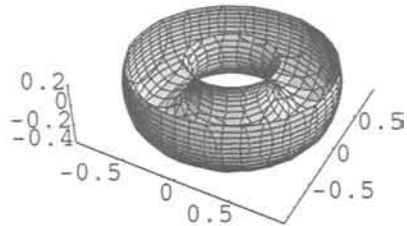


Fig. 10.3.2. $C=0.1$.

If we square we get two rings in fig. 10.3.3, and the equation is 10.3.2.

$$(x^2 + y^2 - z^2 - (x^2 + y^2)^2)^2 = 0.04 \quad 10.3.2$$

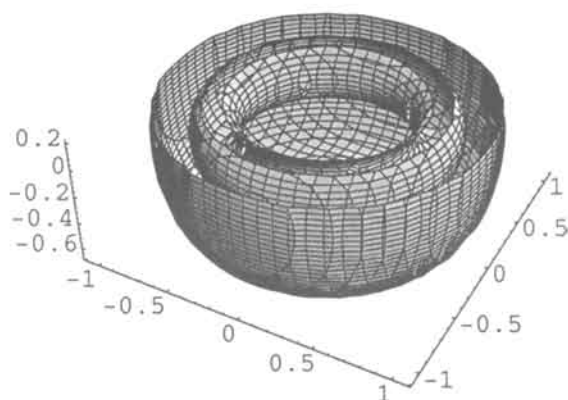


Fig. 10.3.3. The square gives a torus in a sphere after equation 10.3.2.

The ordinary equation of a torus is in eq. 10.3.3 and shown in 10.3.4.

$$((x^2 + y^2)^{0.5} - 2)^2 + z^2 = 1 \quad 10.3.3$$

And on exponential scale it is shown in fig. 10.3.5, from eq. 10.3.4.

$$e^{((x^2 + y^2)^{0.5} - 2)^2 + z^2} = 3 \quad 10.3.4$$

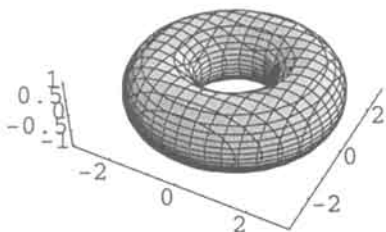


Fig. 10.3.4. The ordinary torus after equation 10.3.3.

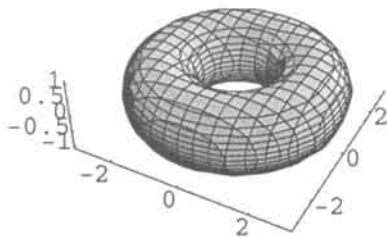


Fig. 10.3.5. The ordinary torus on the exponential scale after equation 10.3.4.

We add two spheres after equation

$$\frac{1}{2}e^{-(((x^2+y^2)^{0.5}-2)^2+z^2)} + e^{-(x^2+y^2+(z+3)^2)} + e^{-(x^2+y^2+(z-3)^2)} = 0.1$$

10.3.5

and the result is illustrated in fig. 10.3.6, and is a good picture of the ELF structure of the ClF_2^- ion [3], and as proposed the isoelectronic molecule XeF_2 [4].

We can also add just one sphere as in eq 10.3.6 and fig. 10.3.7.

$$e^{-(((x^2+y^2)^{0.5}-4)^2+z^2)} + e^{-(x^2+y^2+z^2)} = 0.2$$

10.3.6

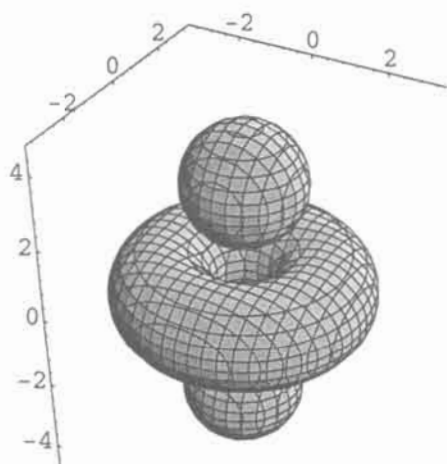


Fig. 10.3.6. The structure of the ClF_2^- ion, or the isoelectronic molecule XeF_2 after equation 10.3.5.

Or we can add a cylinder.

$$e^{-(((x^2+y^2)^{0.5}-4)^2+z^2)} + e^{-(x^2+y^2+1)} = 0.2$$

10.3.7

We made Larsson cubosomes - or a molecule - by adding the equation of a periodic surface to a sphere. Here we add the nodal P-surface to the torous and obtain similar results.

$$e^{((x^2+y^2)^{0.5}-10)^2+z^2} + e^{\cos \pi x + \cos \pi y + \cos \pi z} = 6 \tag{10.3.8}$$

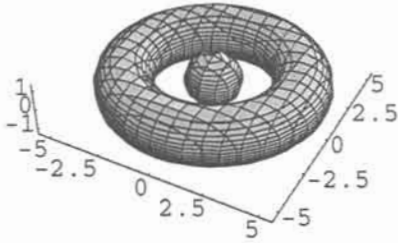


Fig. 10.3.7. After equation 10.3.6.

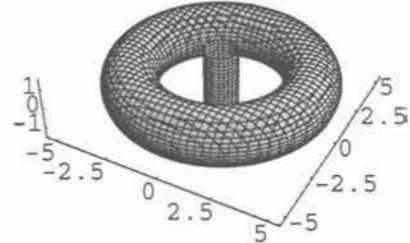


Fig. 10.3.8. After equation 10.3.7.

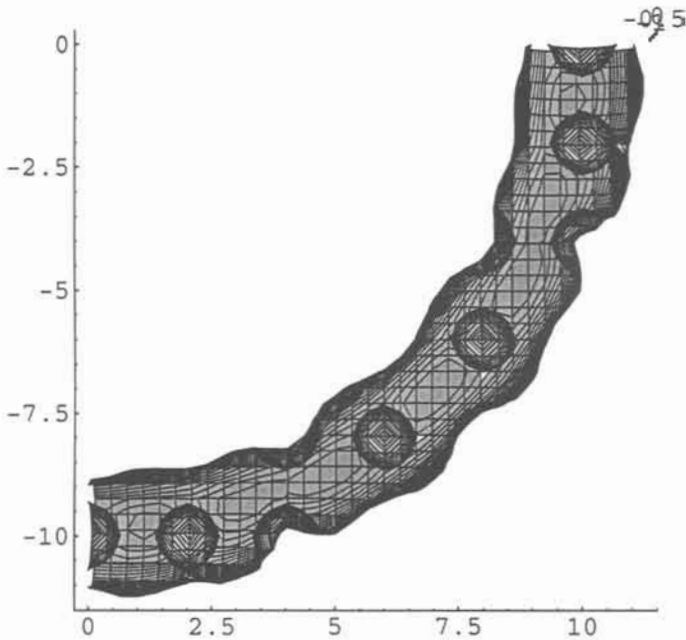


Fig. 10.3.9. A torus and the P surface in 'body' form after equation 10.3.8.

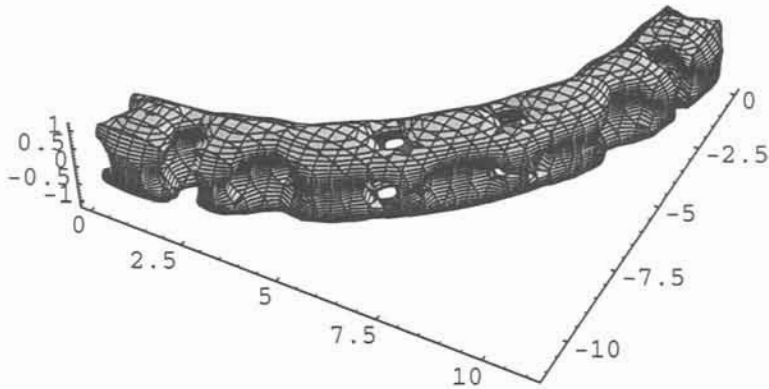


Fig. 10.3.10. A change in constant makes the surface interpenetrate the torus after equation 10.3.9.

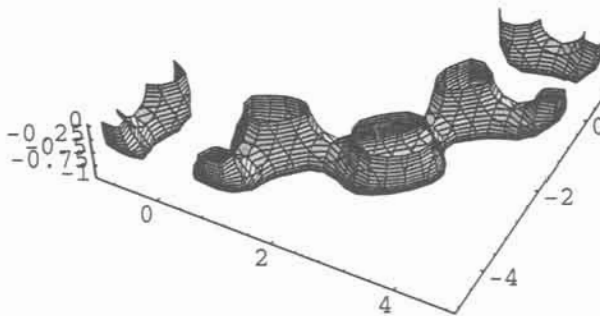


Fig. 10.3.11. A further change in the constant as in equation 10.3.10 cuts the torus into pieces of the P surfacetype.

In fig. 10.3.9 the P surface is in 'body' form and for a change in constant as in eq. 10.3.9 there is a complete surface interpenetrating the torus shown in fig. 10.3.10.

$$e^{((x^2+y^2)^{0.5}-10)^2+z^2} + e^{\cos \pi x + \cos \pi y + \cos \pi z} = 3.8 \quad 10.3.9$$

Finally a further change in the constant as in eq. 10.3.10 cuts the torus into pieces of the P surface type shown in fig. 10.3.11.

$$e^{((x^2+y^2)^{0.5}-4)^2+z^2} + e^{\cos \pi x + \cos \pi y + \cos \pi z} = 2.7 \quad 10.3.10$$

10.4 More Subtraction - Hyperbolic Polyhedra

In equation 10.4.1 we subtract two planes from a sphere and get fig. 10.4.1.

$$e^{(x^2+y^2+z^2)} - e^{x^2} = 1 \quad 10.4.1$$

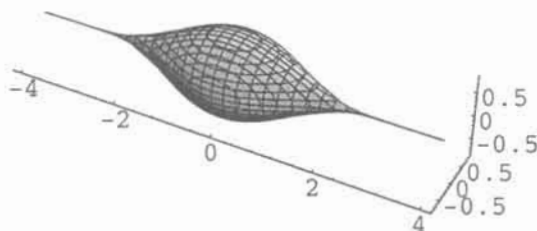


Fig. 10.4.1. Two planes subtracted from a sphere after equation 10.4.1.

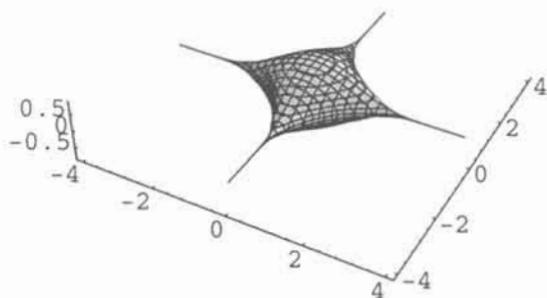


Fig. 10.4.2. Two planes subtracted from a sphere after equation 10.4.2.

We subtract two more planes in eq 10.4.2 and get fig. 10.4.2.

$$e^{(x^2+y^2+z^2)} - e^{x^2} - e^{y^2} = 0 \quad 10.4.2$$

And subtracting three planes (or a cube) as in eq. 10.4.3, we get the hyperbolic octahedron (the dual), as in fig. 10.4.3.

$$e^{(x^2+y^2+z^2)} - e^{x^2} - e^{y^2} - e^{z^2} = 0 \quad 10.4.3$$

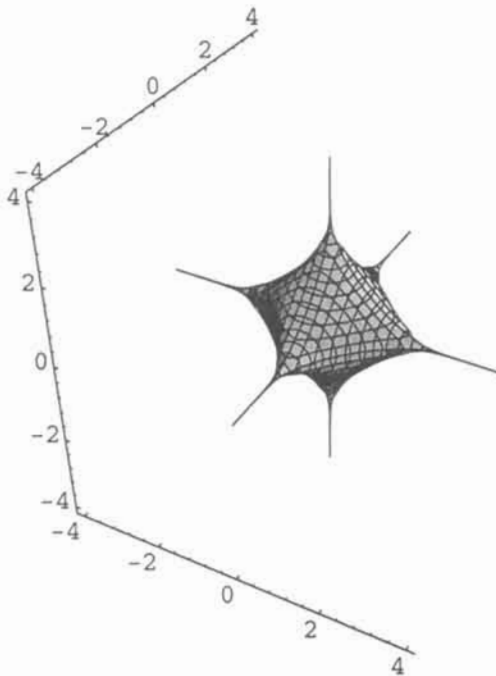


Fig. 10.4.3. A cube subtracted from a sphere after equation 10.4.3.

We subtract an octahedron from the sphere in equation 10.4.4 and get the dual as illustrated in fig. 10.4.4.

$$e^{3(x^2+y^2+z^2)} - e^{(x+y+z)^2} - e^{(x-y+z)^2} - e^{(x+y-z)^2} - e^{(y+z-x)^2} = 0$$

10.4.4

$$e^{((x^2+y^2)^{0.5}-10)^2+z^2} + e^{\cos \pi x + \cos \pi y + \cos \pi z} = 3.8 \quad 10.3.9$$

Finally a further change in the constant as in eq. 10.3.10 cuts the torus into pieces of the P surface type shown in fig. 10.3.11.

$$e^{((x^2+y^2)^{0.5}-4)^2+z^2} + e^{\cos \pi x + \cos \pi y + \cos \pi z} = 2.7 \quad 10.3.10$$

10.4 More Subtraction - Hyperbolic Polyhedra

In equation 10.4.1 we subtract two planes from a sphere and get fig. 10.4.1.

$$e^{(x^2+y^2+z^2)} - e^{x^2} = 1 \quad 10.4.1$$

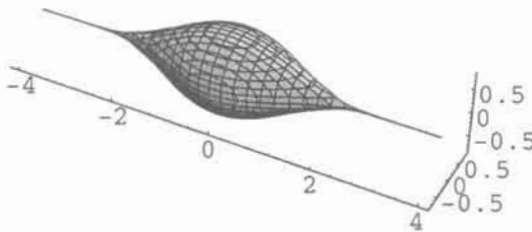


Fig. 10.4.1. Two planes subtracted from a sphere after equation 10.4.1.

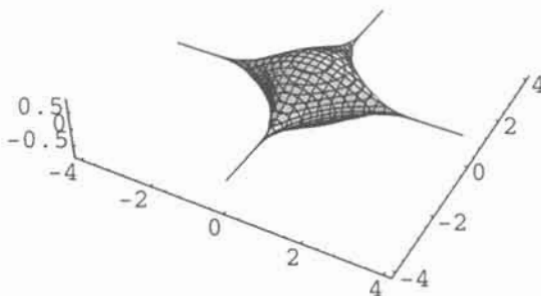


Fig. 10.4.2. Two planes subtracted from a sphere after equation 10.4.2.

In equation 10.4.5 a rhombic dodecahedron is subtracted from a sphere and fig 10.4.5 shows the dual, a hyperbolic cube octahedron.

$$\begin{aligned} e^{2(x^2+y^2+z^2)} - e^{(x+y)^2} - e^{(x-y)^2} - e^{(y+z)^2} \\ - e^{(y-z)^2} - e^{(x+z)^2} - e^{(x-z)^2} = 0 \end{aligned} \quad 10.4.5$$

In equation 10.4.6 the pentagonal dodecahedron is subtracted from a sphere, and the resulting dual - the hyperbolic icosahedron - is shown in fig. 10.4.6. Note the remarkable simplicity of the formula.

$$\begin{aligned} e^{(\tau^2+1)(x^2+y^2+z^2)} - e^{(\tau x+y)^2} - e^{(-\tau x+y)^2} \\ - e^{(\tau y+z)^2} - e^{(-\tau y+z)^2} - e^{(\tau z+x)^2} - e^{(-\tau z+x)^2} = 0 \end{aligned} \quad 10.4.6$$

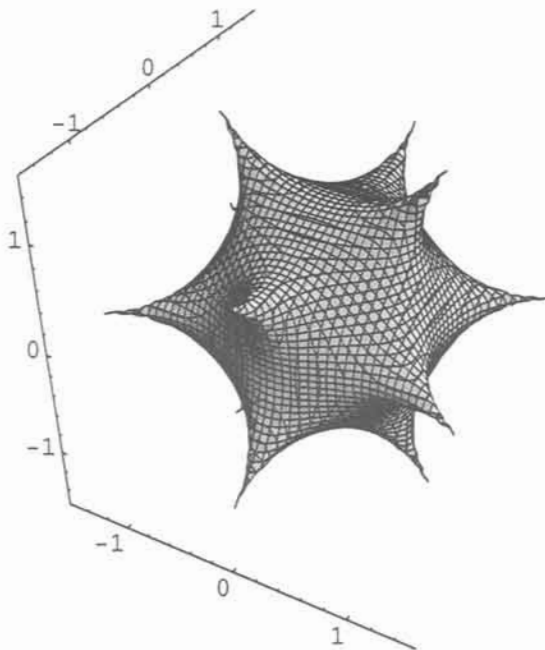


Fig. 10.4.6. The pentagonal dodecahedron subtracted from a sphere after equation 10.4.6.

Below the equation of an icosahedron is subtracted from a sphere and the result - a beautiful hyperbolic pentagonal dodecahedron - is shown in fig. 10.4.7.

$$\begin{aligned}
 &e^{(\tau^3+\tau^2+1)(x^2+y^2+z^2)} - e^{\tau^2(x+y+z)^2} - e^{\tau^2(-x+y+z)^2} \\
 &- e^{\tau^2(x+y-z)^2} - e^{\tau^2(x-y+z)^2} - e^{(x+\tau^2y)^2} - e^{(-x+\tau^2y)^2} \\
 &- e^{(z+\tau^2x)^2} - e^{(z-\tau^2x)^2} - e^{(y+\tau^2z)^2} - e^{(y-\tau^2z)^2} = 0
 \end{aligned}
 \tag{10.4.7}$$

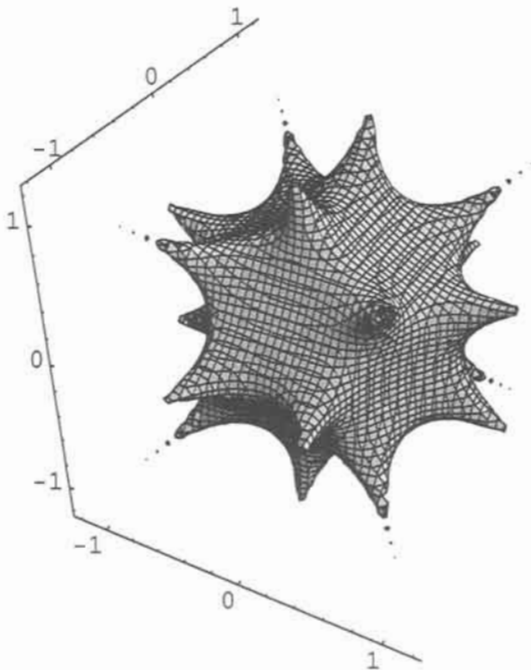


Fig. 10.4.7. An icosahedron subtracted from a sphere after equation 10.4.7.

A cube may be constructed from two dual tetrahedra, and we show in fig. 10.4.8 the result of the subtraction of a tetrahedron from a cube, after equation 10.4.8.

$$\begin{aligned}
 &e^x + e^y + e^z + e^{-x} + e^{-y} + e^{-z} \\
 &- e^{(x+y+z)} - e^{(x-y-z)} - e^{(-x-y+z)} - e^{(y-z-x)} = 0
 \end{aligned}
 \tag{10.4.8}$$

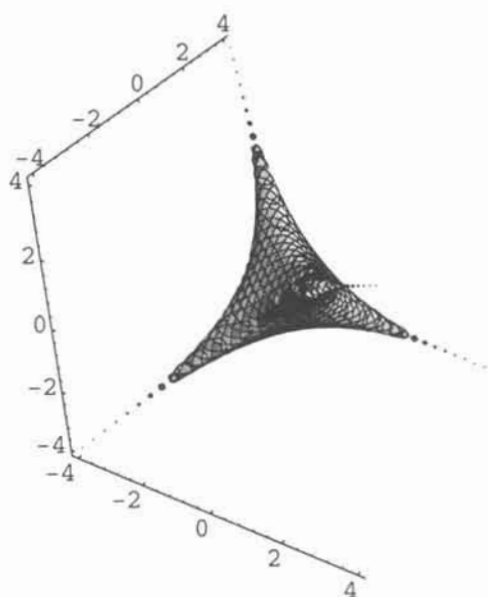


Fig. 10.4.8. A tetrahedron subtracted from a cube after equation 10.4.8.

Exercises 10

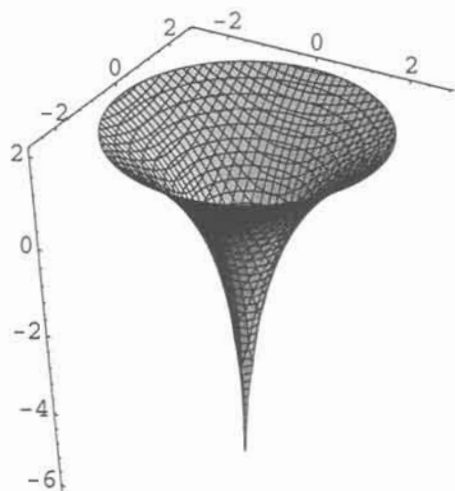
Exercise 10.1. Make a half catenoid after equation *10.2.1*.

Exercise 10.2. Subtract a tetrahedron (exponential) from a sphere (non-exponential).

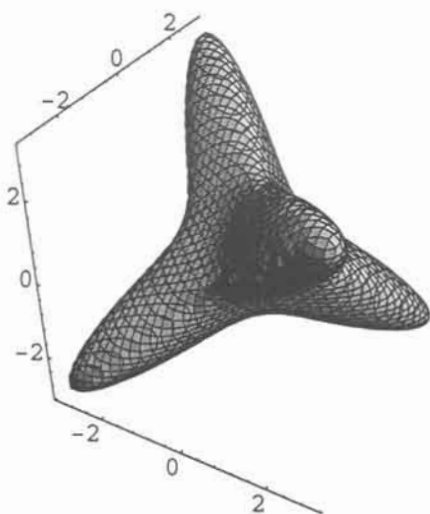
Exercise 10.3. Subtract a rhombic dodecahedron from an octahedron.

Answer 10.1

$$x^2 + y^2 - e^z = 0$$

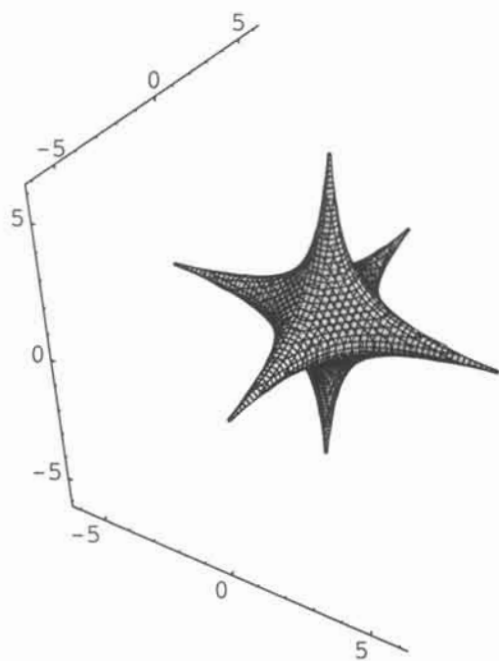
**Fig. 10.1.****Answer 10.2**

$$e^{(x+y+z)} + e^{(x-y-z)} + e^{(-x-y+z)} + e^{(y-z-x)} - 2(x^2 + y^2 + z^2) - 6 = 0$$

**Fig. 10.2.**

Answer 10.3

$$\begin{aligned}
& e^{(x+y+z)} + e^{(x-y-z)} + e^{(-x-y+z)} + e^{(y-z-x)} \\
& + e^{-(x+y+z)} + e^{-(x-y-z)} + e^{-(-x-y+z)} + e^{-(y-z-x)} \\
& - e^{(x+y)} - e^{(x-y)} - e^{(y+z)} - e^{(y-z)} - e^{(x+z)} - e^{(x-z)} \\
& - e^{-(x+y)} - e^{-(x-y)} - e^{-(y+z)} - e^{-(y-z)} - e^{-(x+z)} - e^{-(x-z)} = 0
\end{aligned}$$

**Fig. 10.3.**

References 10

- 1 J. L. Synge, *SCIENCE: SENSE AND NONSENSE*, Books for Libraries Press, New York, 1972, page 85.
- 2 K. Larsson and S. Andersson, *Acta Chem. Scand.* **B 40**, 1 (1986).
- 3 T. Fässler, Private communication.
- 4 S. Andersson, On the stereochemistry of valence bonds and the structures of XeO_3 , XeF_4 and XeF_2 , *Acta Cryst.* **B35** 1321 (1979).

11 Periodic Dilatation - Concentric Symmetry

'It shows how bold it is to draw conclusions about the area of a domain from the time it takes to sail around it' (Hildebrandt et al [1] about the coast line of Rügen, an island in the Baltic Sea).

Here we describe dilatation, in natural science called cyclic twinning. The geometry is the same as the one proposed as a structure building operation in solid state chemistry [2]. But here it is done with mathematics, and the Exponential Scale.

We give a mathematical mechanism for crystal growth - the circular function multiplied with the GD function gives the combination of translation and dilatation. The growth is exponential by the periodic property of the GD function. We also use the GD mathematics to describe the motion of solitons.

11.1 Dilatation and Translation in 2D

In photography it is called enlargement and in school geometry congruence. We may say it is a similarity that preserves angles and we call it dilatation or concentric symmetry. For an excellent description we refer to Coxeter - a good reading as background is his chapter 5 'Similarity in the Euclidean plane' [3].

What use will we have of the functions below? We surely believe they will have some importance in chemistry, physics or biology. Besides onions in botany, and multiple twins in mineralogy or crystallography. And this symmetry is also somewhat contained in the fundamental theorem of algebra which started this book. And some surfaces are very beautiful which is a reason as good as any.

We study mathematical functions that give structures which interest us. As we want periodic functions we start to study the simple and general product of a variable and its cosine, $x \cos x$, or $e^x \cos x$ or to make the 3D representation of the function sharper, $e^{nx^2} \cos x$ with n as an integer. And the product of the Gauss Distribution function and cosine, $e^{-x^2} \cos x$.

So we start in 2D with the function,

$$e^{6x^2} \cos \pi x + e^{6y^2} \cos \pi y = 0$$

11.1.1

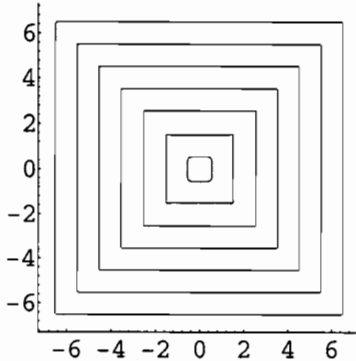


Fig. 11.1.1. Square dilatation after equation 11.1.1.

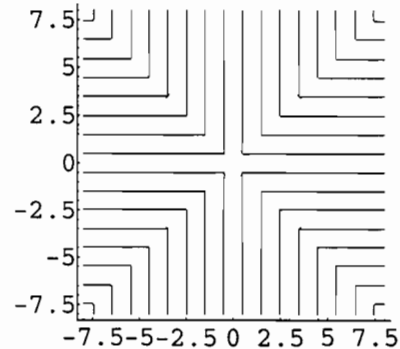


Fig. 11.1.2. Fourling operation with the corresponding GD function after equation 11.1.2.

In fig. 11.1.1 there is typical dilatation, and the structure can be regarded as a fourling of a lamellae structure. Shift to the GD as in function 11.1.2, gives a fourling operation to the whole structure as in 11.1.2.

$$e^{-6x^2} \cos \pi x + e^{-6y^2} \cos \pi y = 0$$

11.1.2

Using the property of periodicity of the GD function makes it now possible to build the mathematics for the cyclic twinning or cyclic periodicity, and we build the first function in eq. 11.1.3, which gives figure 11.1.3. Here we have the first fragment of a periodic fourling structure and we increase the size of it in 11.1.4 by adding more terms as in equation 11.1.4.

$$(e^{-6x^2} + e^{-6(x-2)^2} + e^{-6(x+2)^2}) \cos \pi x$$

$$+(e^{-6y^2} + e^{-6(y-2)^2} + e^{-6(y+2)^2}) \cos \pi y = 0$$

11.1.3

$$(e^{-6x^2} + e^{-6(x-2)^2} + e^{-6(x+2)^2} + e^{-6(x-4)^2} + e^{-6(x+4)^2}) \cos \pi x$$

$$+(e^{-6y^2} + e^{-6(y-2)^2} + e^{-6(y+2)^2} + e^{-6(y-4)^2} + e^{-6(y+4)^2}) \cos \pi y = 0$$

11.1.4

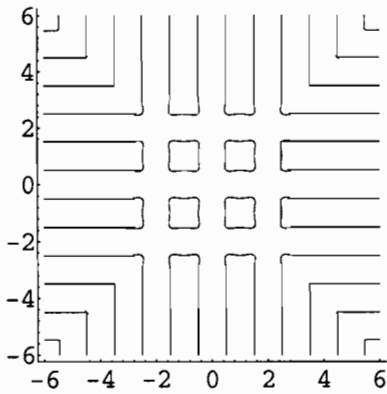


Fig. 11.1.3. The fourling unit grows with translation with equation 11.1.3.

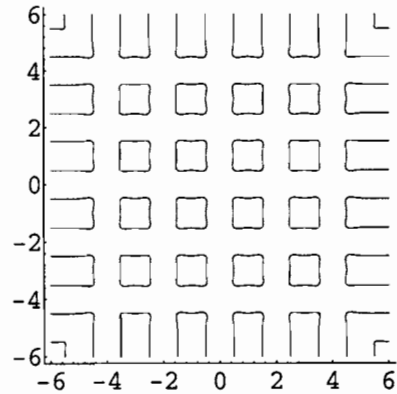


Fig. 11.1.4. Further growth with equation 11.1.4.

So far we have taken the inner square of the dilatation structure - now we want to take a larger part of the structure in fig. 11.1.1 to repeat. This is done by increased translation as in eq. 11.1.5 and 11.1.6 and the structures are in fig. 11.1.5 and 11.1.6.

$$(e^{-6x^2} + e^{-6(x-4)^2} + e^{-6(x+4)^2})\cos \pi x + (e^{-6y^2} + e^{-6(y-4)^2} + e^{-6(y+4)^2})\cos \pi y = 0 \tag{11.1.5}$$

$$(e^{-6x^2} + e^{-6(x-4)^2} + e^{-6(x+4)^2} + e^{-6(x-8)^2} + e^{-6(x+8)^2})\cos \pi x + (e^{-6y^2} + e^{-6(y-4)^2} + e^{-6(y+4)^2} + e^{-6(y-8)^2} + e^{-6(y+8)^2})\cos \pi y = 0 \tag{11.1.6}$$

We want to cut an even bigger part of the dilatation structure in fig. 11.1.1, and do so with the equations 11.1.7-8. These beautiful examples of the combined translation and dilatation are shown in figures 11.1.7-8.

$$(e^{-6x^2} + e^{-6(x-6)^2} + e^{-6(x+6)^2})\cos \pi x + (e^{-6y^2} + e^{-6(y-6)^2} + e^{-6(y+6)^2})\cos \pi y = 0 \tag{11.1.7}$$

$$\begin{aligned}
 & (e^{-6x^2} + e^{-6(x-6)^2} + e^{-6(x+6)^2} + e^{-6(x-12)^2} + e^{-6(x+12)^2}) \cos \pi x \\
 & + (e^{-6y^2} + e^{-6(y-6)^2} + e^{-6(y+6)^2} + e^{-6(y-12)^2} + e^{-6(y+12)^2}) \cos \pi y = 0
 \end{aligned}$$

11.1.8

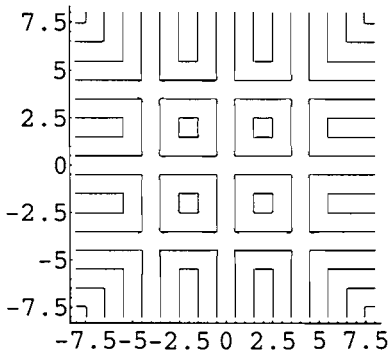


Fig. 11.1.5. Further growth includes dilatation in each building block with equation 11.1.5.

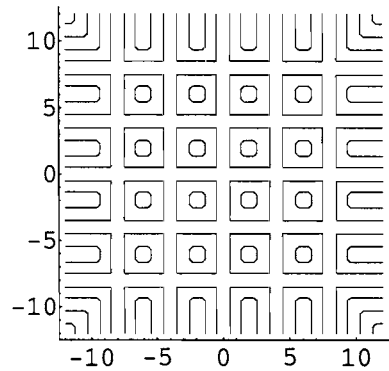


Fig. 11.1.6. Size of building block increased after 11.1.6.

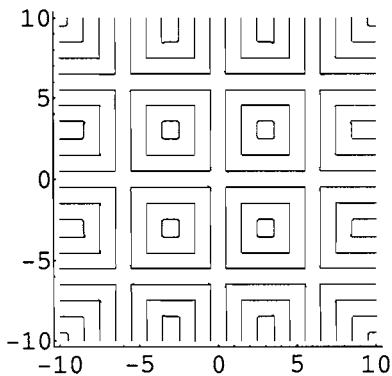


Fig. 11.1.7. Still larger size of building block increased after equation 11.1.7.

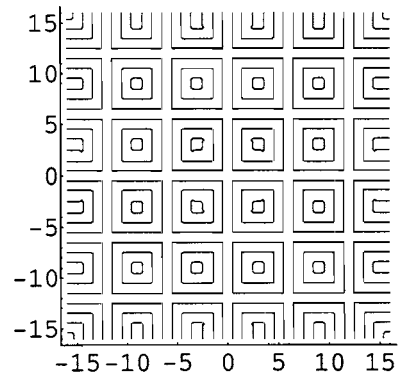


Fig. 11.1.8. Size of building block after 11.1.8.

We do the same with dilatation of the triangle after equation 11.1.9, showed in fig. 11.1.9, and we do the twin operation as in eq. 11.1.10, showed in fig. 11.1.10. The polygon trigonometry is from chapter 3.

$$\begin{aligned}
 & \cos \pi(x \cos(\pi/3) + y \sin(\pi/3))e^{6(x \cos(\pi/3) + y \sin(\pi/3))} \\
 & + \cos \pi(-x \cos(2\pi/3) - y \sin(2\pi/3))e^{6(-x \cos(2\pi/3) - y \sin(2\pi/3))} \\
 & + \cos \pi(x \cos(3\pi/3) + y \sin(3\pi/3))e^{6(x \cos(3\pi/3) + y \sin(3\pi/3))} = 0
 \end{aligned} \tag{11.1.9}$$

$$\begin{aligned}
 & \cos \pi(x \cos(\pi/3) + y \sin(\pi/3))e^{-6(x \cos(\pi/3) + y \sin(\pi/3))^2} \\
 & + \cos \pi(-x \cos(2\pi/3) - y \sin(2\pi/3))e^{-6(-x \cos(2\pi/3) - y \sin(2\pi/3))^2} \\
 & + \cos \pi(x \cos(3\pi/3) + y \sin(3\pi/3))e^{-6(x \cos(3\pi/3) + y \sin(3\pi/3))^2} = 0
 \end{aligned} \tag{11.1.10}$$

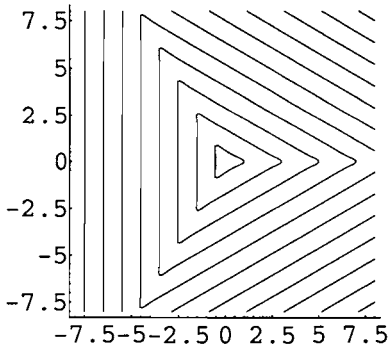


Fig. 11.1.9. Triangular dilatation after equation 11.1.9.

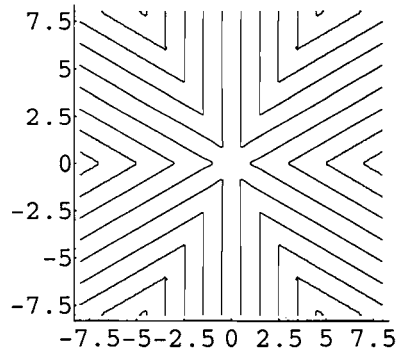


Fig. 11.1.10. Sixling operation with the corresponding GD function after equation 11.1.10.

And the repeated sixling of a rather advanced dilatation triangular block is derived in equation 11.1.11 and the formidable structure is shown in fig. 11.1.11.

$$\begin{aligned}
 & \cos \pi(x \cos(\pi/3) + y \sin(\pi/3))e^{-6(x \cos(\pi/3) + y \sin(\pi/3))^2} \\
 & + \cos \pi(-x \cos(2\pi/3) - y \sin(2\pi/3))e^{-6(-x \cos(2\pi/3) - y \sin(2\pi/3))^2} \\
 & + \cos \pi(x \cos(3\pi/3) + y \sin(3\pi/3))e^{-6(x \cos(3\pi/3) + y \sin(3\pi/3))^2} \\
 & + \cos \pi(x \cos(\pi/3) + y \sin(\pi/3) - 12)e^{-6(x \cos(\pi/3) + y \sin(\pi/3) - 12)^2} \\
 & + \cos \pi(-x \cos(2\pi/3) - y \sin(2\pi/3) - 12)e^{-6(-x \cos(2\pi/3) - y \sin(2\pi/3) - 12)^2} \\
 & + \cos \pi(x \cos(3\pi/3) + y \sin(3\pi/3) - 12)e^{-6(x \cos(3\pi/3) + y \sin(3\pi/3) - 12)^2} \\
 & + \cos \pi(x \cos(\pi/3) + y \sin(\pi/3) + 12)e^{-6(x \cos(\pi/3) + y \sin(\pi/3) + 12)^2} \\
 & + \cos \pi(-x \cos(2\pi/3) - y \sin(2\pi/3) + 12)e^{-6(-x \cos(2\pi/3) - y \sin(2\pi/3) + 12)^2} \\
 & + \cos \pi(x \cos(3\pi/3) + y \sin(3\pi/3) + 12)e^{-6(x \cos(3\pi/3) + y \sin(3\pi/3) + 12)^2} = 0
 \end{aligned}$$

11.1.11

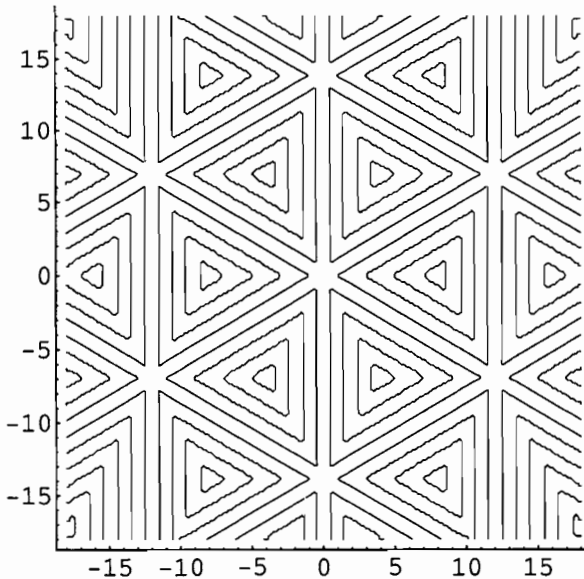


Fig. 11.1.11. Translation of a building block of triangular dilatation after equation 11.1.11.

And the pentagonal dodecahedron in equations 11.1.12 and 11.1.13 and in figures 11.1.12 and 11.1.13.

$$\begin{aligned}
 & \cos \pi(x \cos(\pi/5) + y \sin(\pi/5))e^{6(x \cos(\pi/5) + y \sin(\pi/5))} \\
 & + \cos \pi(-x \cos(2\pi/5) - y \sin(2\pi/5))e^{6(-x \cos(2\pi/5) - y \sin(2\pi/5))} \\
 & + \cos \pi(x \cos(3\pi/5) + y \sin(3\pi/5))e^{6(x \cos(3\pi/5) + y \sin(3\pi/5))} \\
 & + \cos \pi(-x \cos(4\pi/5) - y \sin(4\pi/5))e^{6(-x \cos(4\pi/5) - y \sin(4\pi/5))} \\
 & + \cos \pi(x \cos(5\pi/5) + y \sin(5\pi/5))e^{6(x \cos(5\pi/5) + y \sin(5\pi/5))} = 0
 \end{aligned} \tag{11.1.12}$$

$$\begin{aligned}
 & \cos \pi(x \cos(\pi/5) + y \sin(\pi/5))e^{-6(x \cos(\pi/5) + y \sin(\pi/5))^2} \\
 & + \cos \pi(-x \cos(2\pi/5) - y \sin(2\pi/5))e^{-6(-x \cos(2\pi/5) - y \sin(2\pi/5))^2} \\
 & + \cos \pi(x \cos(3\pi/5) + y \sin(3\pi/5))e^{-6(x \cos(3\pi/5) + y \sin(3\pi/5))^2} \\
 & + \cos \pi(-x \cos(4\pi/5) - y \sin(4\pi/5))e^{-6(-x \cos(4\pi/5) - y \sin(4\pi/5))^2} \\
 & + \cos \pi(x \cos(5\pi/5) + y \sin(5\pi/5))e^{-6(x \cos(5\pi/5) + y \sin(5\pi/5))^2} = 0
 \end{aligned} \tag{11.1.13}$$

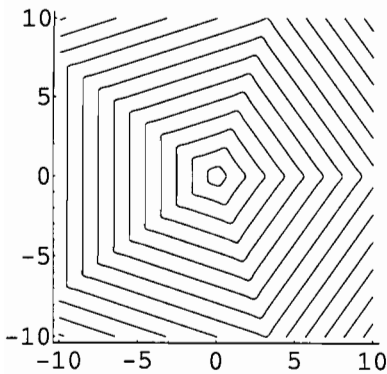


Fig. 11.1.12. Pentagonal dilatation after equation 11.1.12.

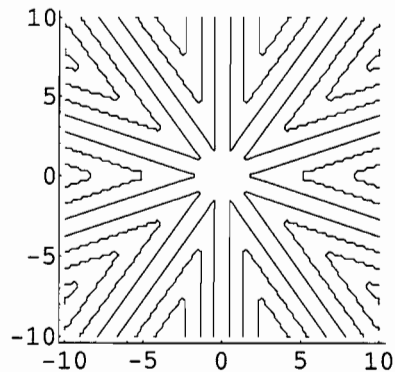


Fig. 11.1.13. Tenling operation after equation 11.1.13.

11.2 Dilatation and Translation in 3D

In 3D the first equation is 11.2.1 and its symmetry of dilatation is beautifully shown in fig. 11.2.1.

$$e^{6x^2} \cos \pi x + e^{6y^2} \cos \pi y + e^{6z^2} \cos \pi z = 0 \quad 11.2.1$$

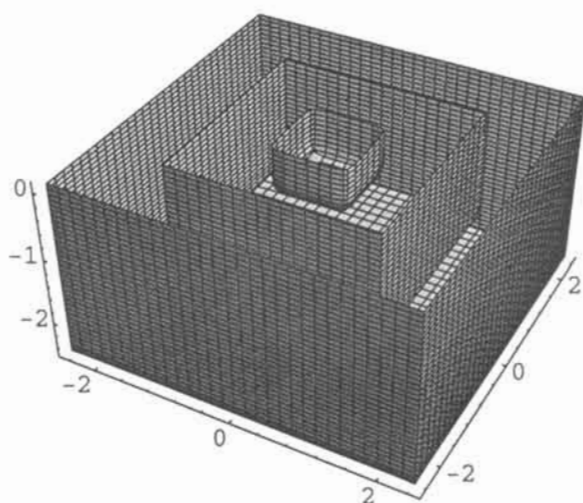


Fig. 11.2.1. Dilatation in 3D after equation 11.2.1.

An eightling operation is provided by equation 11.2.2 and the formidable structure is in fig. 11.2.2.

$$e^{-6x^2} \cos \pi x + e^{-6y^2} \cos \pi y + e^{-6z^2} \cos \pi z = 0 \quad 11.2.2$$

Before we continue we shall study the explicit function in eq. 11.2.3. This may be described as the multiplication of cosine with a damping factor like the GD function, and it is shown in fig. 11.2.3. A wave packet like this is used in quantum physics to represent a particle such as an electron. In its 3D form it describes cyclic twinning combined with dilatation.

$$y = e^{-\frac{1}{2}x^2} \cos 2\pi x \quad 11.2.3$$

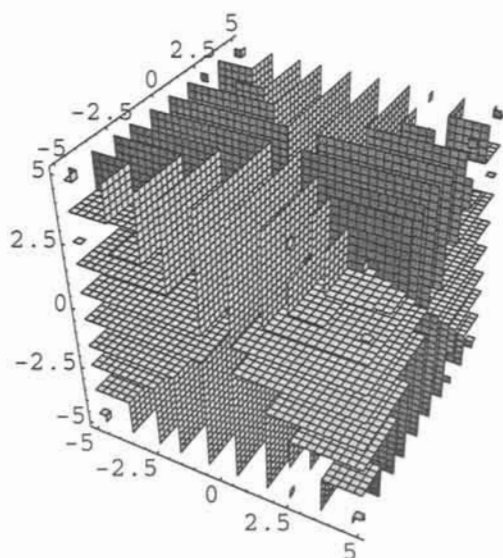


Fig. 11.2.2. Eightling operation with the corresponding GD function after equation 11.2.2.

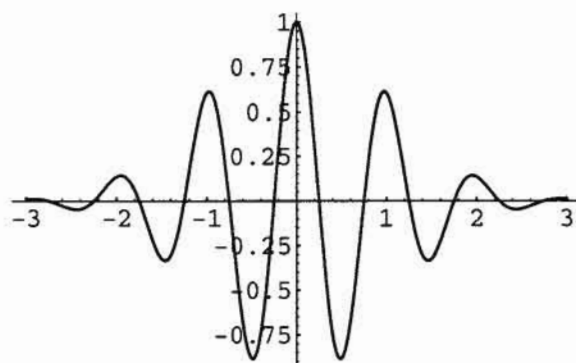


Fig. 11.2.3. Wave packet after equation 11.2.3.

As this is GD mathematics, we can add two wave packets after eq. 11.2.4, and show them in fig. 11.2.4.

$$y = e^{-\frac{1}{2}x^2} \cos 2\pi x + e^{-\frac{1}{2}(x-5)^2} \cos 2\pi x \quad 11.2.4$$

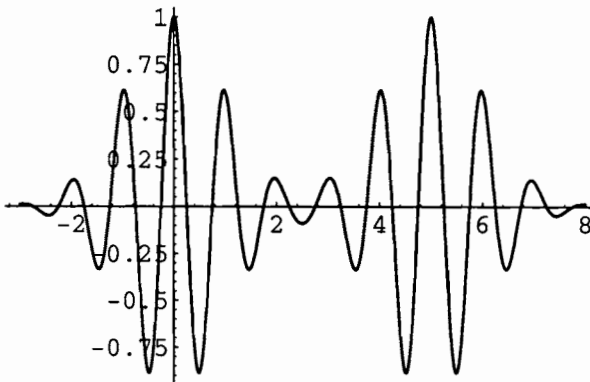


Fig. 11.2.4. Two wave packets after equation 11.2.4.

We can make one of them move and go through the other with equation 11.2.5, where n is varied 5, 3, 1, -1, -3, -5 in figure 11.2.5.

$$y = e^{-2x^2} \cos 2\pi x + e^{-2(x-n)^2} \cos 2\pi x \quad 11.2.5$$

We may of course just use two GD functions as in equation 11.2.6, where n is varied 6, 3, 0, -3, -6, and the wave packet, moving as a soliton, is going through the diffusion profile from right to left. Note the different scale after y at $n=0$.

$$y = e^{-x^2} + e^{-2(x-n)^2} \cos 2\pi x \quad 11.2.6$$

We shall now study this wave packet in 3D with the equation 11.2.7. Equation 11.2.2 showed infinite cubic dilatation in eight directions. By reducing the weight of the GD function, the cubic character is reduced (the symmetry is still cubic of course) and the cubes are joined by catenoids as shown in the split figure 11.2.7 of eq. 11.2.7. It could be described as if the P surface is enveloped by the GD function (compare with figure 7.2.5).

$$e^{-\frac{1}{2}x^2} \cos \pi x + e^{-\frac{1}{2}y^2} \cos \pi y + e^{-\frac{1}{2}z^2} \cos \pi z = 0 \quad 11.2.7$$

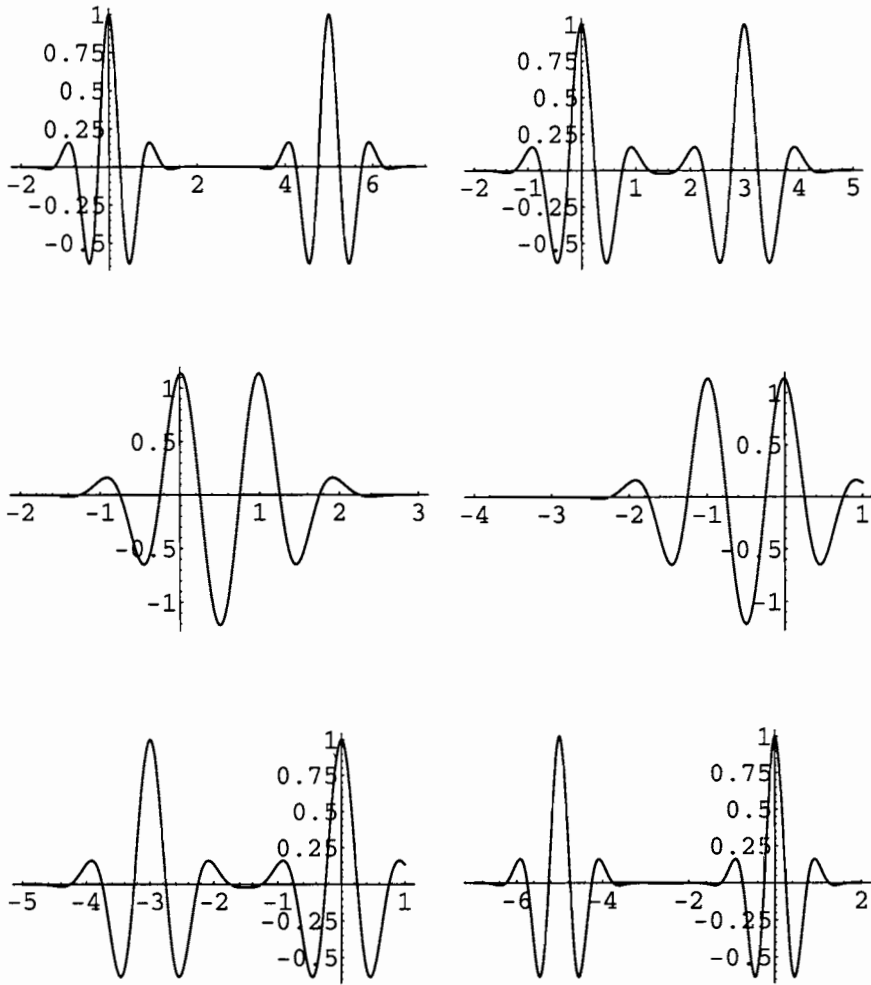


Fig. 11.2.5. One of the two wave packets move after equation 11.2.5.

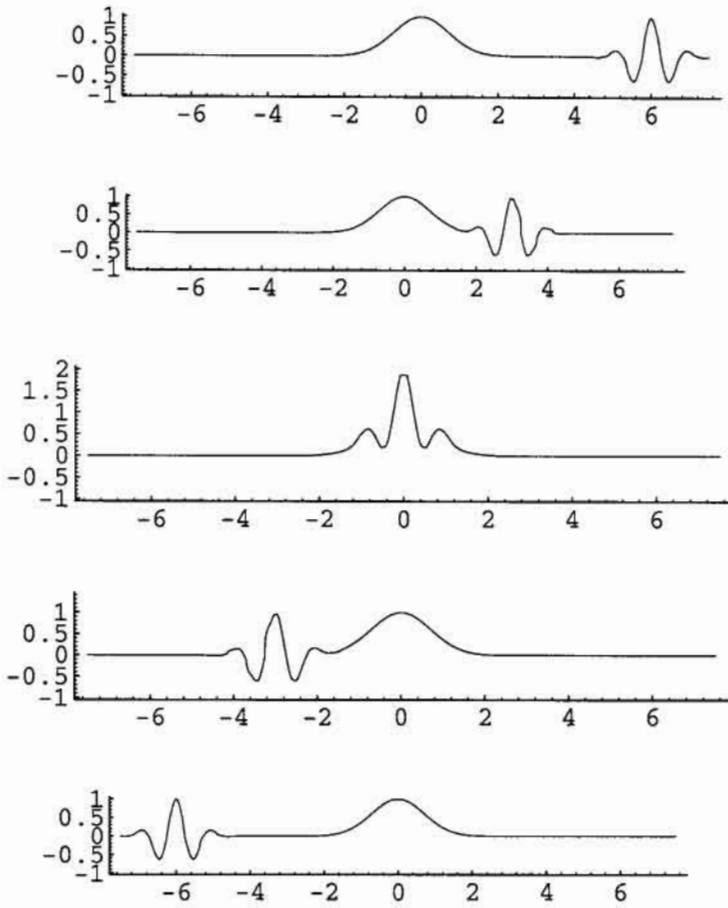


Fig. 11.2.6. One wave packet is moving through a diffusion profile after equation 11.2.6.

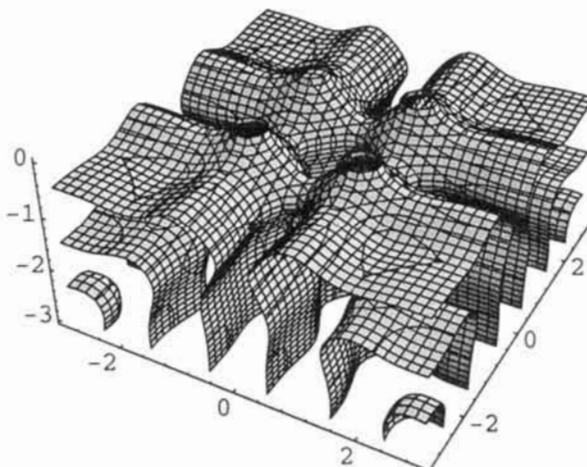


Fig. 11.2.7. Dilatation structure of the P-surface after equation 11.2.7.

As above in 2D and equation 11.1.5, we add to 3D in eq. 11.2.8, and have the beautiful picture in fig. 11.2.8 which shows the translation of a dilatation structure, all in a cyclic twin operation.

$$\begin{aligned}
 & (e^{-6x^2} + e^{-6(x-4)^2} + e^{-6(x+4)^2}) \cos \pi x \\
 & + (e^{-6y^2} + e^{-6(y-4)^2} + e^{-6(y+4)^2}) \cos \pi y \\
 & + (e^{-6z^2} + e^{-6(z-4)^2} + e^{-6(z+4)^2}) \cos \pi z = 0
 \end{aligned}
 \tag{11.2.8}$$

Next is tetrahedral dilatation in eq. 11.2.9, and the picture is in fig. 11.2.9.

$$\begin{aligned}
 & e^{6(-x+y-z)} \cos \pi(-x+y-z) + e^{6(-x-y+z)} \cos \pi(-x-y+z) \\
 & + e^{6(x-y-z)} \cos \pi(x-y-z) + e^{6(x+y+z)} \cos \pi(x+y+z) \\
 & + e^{6(-x+y-z)} \sin \pi(-x+y-z) + e^{6(-x-y+z)} \sin \pi(-x-y+z) \\
 & + e^{6(x-y-z)} \sin \pi(x-y-z) + e^{6(x+y+z)} \sin \pi(x+y+z) = 0
 \end{aligned}
 \tag{11.2.9}$$

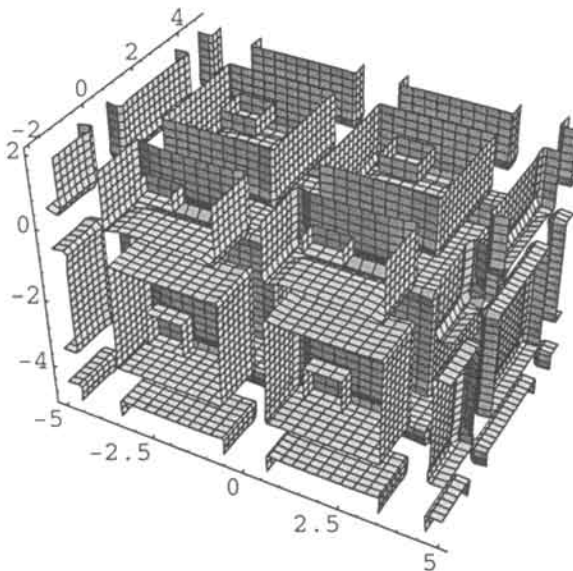


Fig. 11.2.8. Translation of a dilatation structure after equation 11.2.8.

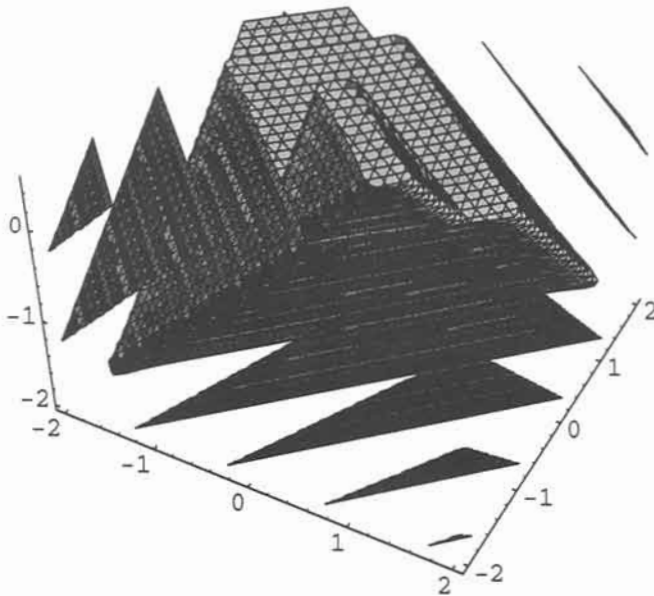


Fig. 11.2.9. Tetrahedral dilatation after equation 11.2.9.

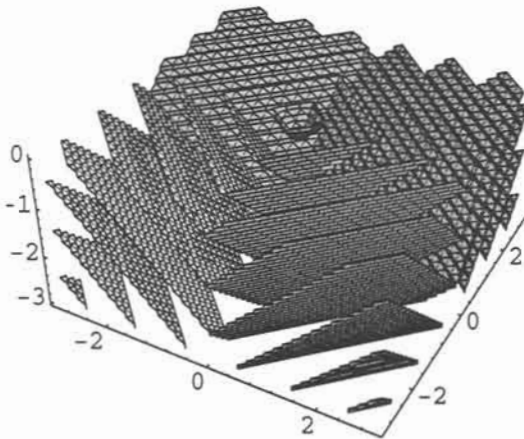


Fig. 11.2.10. Octahedral dilatation after equation 11.2.10.

And the octahedron which with dilatation from equation 11.2.10 gives figure 11.2.10 and the corresponding GD function gives figure 11.2.11 with

the fourling symmetry that has octahedral, as well as tetrahedral corners. This is more clear in a smaller region in figure 11.2.12.

$$\begin{aligned}
 & e^{6(-x+y+z)^2} \cos \pi(-x+y+z) + e^{6(x+y-z)^2} \cos \pi(x+y-z) \\
 & + e^{6(x-y+z)^2} \cos \pi(x-y+z) + e^{6(x+y+z)^2} \cos \pi(x+y+z) = 0
 \end{aligned} \tag{11.2.10}$$

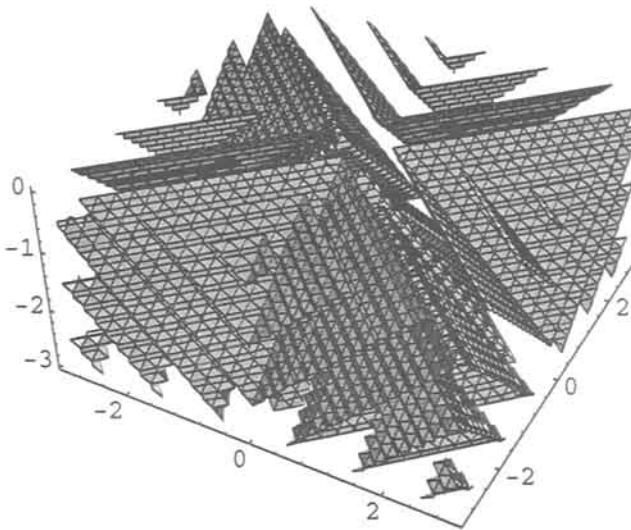


Fig. 11.2.11. Octahedral dilatation and translation making a GD function of equation 11.2.10.

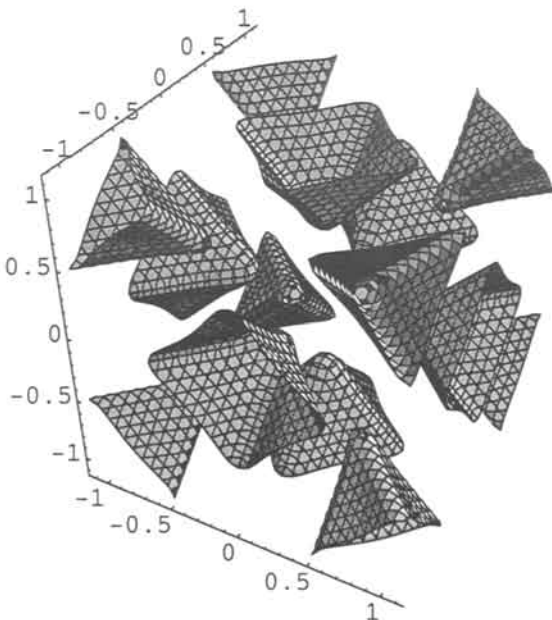


Fig. 11.2.12. Smaller region of fig. 11.2.11.

With translation as in equation 11.2.11 we only get octahedra - a ReO_3 with every second octahedron missing, as in fig. 11.2.13.

$$\begin{aligned}
 & e^{6(-x+y+z)^2} \cos \pi(-x+y+z) + e^{6(x+y-z)^2} \cos \pi(x+y-z) \\
 & + e^{6(x-y+z)^2} \cos \pi(x-y+z) + e^{6(x+y+z)^2} \cos \pi(x+y+z) \\
 & + e^{6(-x+y+z-2)^2} \cos \pi(-x+y+z) + e^{6(x+y-z-2)^2} \cos \pi(x+y-z) \\
 & + e^{6(x-y+z-2)^2} \cos \pi(x-y+z) + e^{6(x+y+z-2)^2} \cos \pi(x+y+z) \\
 & + e^{6(-x+y+z+2)^2} \cos \pi(-x+y+z) + e^{6(x+y-z+2)^2} \cos \pi(x+y-z) \\
 & + e^{6(x-y+z+2)^2} \cos \pi(x-y+z) + e^{6(x+y+z+2)^2} \cos \pi(x+y+z) = 0
 \end{aligned} \tag{11.2.11}$$

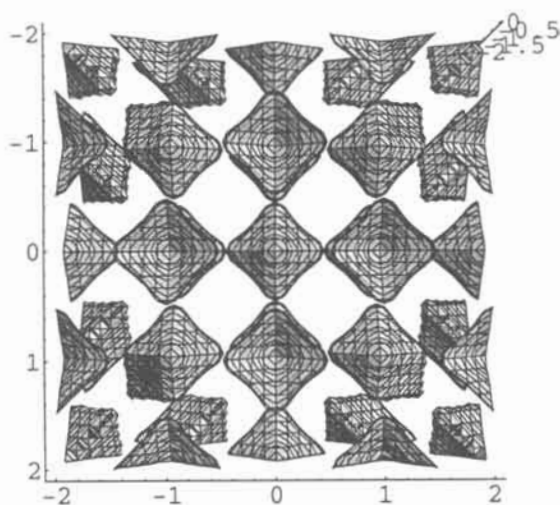


Fig. 11.2.13. With translation after equation 11.2.11 there are only octahedra within the boundaries.

We only show a small piece of dilatation symmetry of the rhombic dodecahedron after equation 11.2.12, as shown in fig. 11.2.14.

$$\begin{aligned}
 & e^{6(x+y)^2} \cos \pi(x+y) + e^{6(y+z)^2} \cos \pi(y+z) \\
 & + e^{6(x+z)^2} \cos \pi(x+z) + e^{6(x-y)^2} \cos \pi(x-y) \\
 & + e^{6(z-y)^2} \cos \pi(z-y) + e^{6(x-z)^2} \cos \pi(x-z) = 0
 \end{aligned} \tag{11.2.12}$$

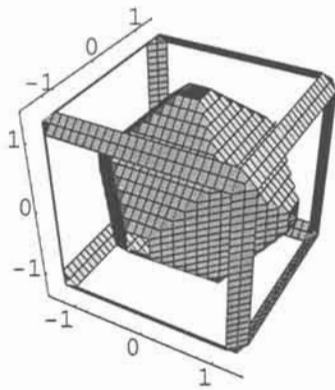


Fig. 11.2.14. Dilatation symmetry and the rhombic dodecahedron after equation 11.2.12.

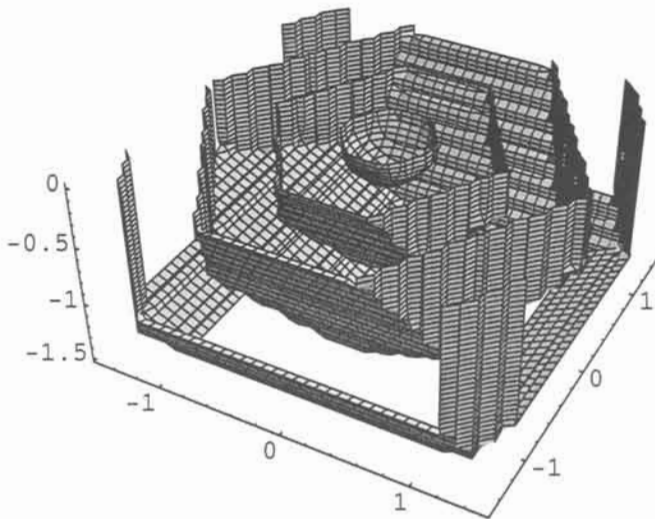


Fig. 11.2.15. Dilatation symmetry and the pentagonal dodecahedron after equation 11.2.13.

The concentric symmetry of the pentagonal dodecahedron is in fig. 11.2.15 after equation 11.2.13.

$$\begin{aligned}
 & \cos \pi(\tau x + y)e^{6(\tau x + y)^2} + \cos \pi(-\tau x + y)e^{6(-\tau x + y)^2} \\
 & + \cos \pi(\tau y + z)e^{6(\tau y + z)^2} + \cos \pi(-\tau y + z)e^{6(-\tau y + z)^2} \\
 & + \cos \pi(\tau z + x)e^{6(\tau z + x)^2} + \cos \pi(\tau z - x)e^{6(\tau z - x)^2} = 0
 \end{aligned} \tag{11.2.13}$$

The multiplication of variables with their circular function becomes complicated in 3D, and we showed above that the use of exponential equations allowed for reasonably simple and straight results. We shall below use a very simple equation to demonstrate interesting and beautiful surfaces which belong to the same symmetry as the surfaces above.

We start with equation in 11.2.14 with small boundaries as in fig. 11.2.16.

$$x \sin \pi x + y \sin \pi y + z \sin \pi z = 0 \tag{11.2.14}$$

Slightly changing the equation to 11.2.15, gives the molecule B_6H_6 again in fig. 11.2.17. The similarity to the functions of the general theorem of algebra in chapter 2 is remarkable, and now we know why.

$$x \sin \pi x + y \sin \pi y + z \sin \pi z = 1 \tag{11.2.15}$$

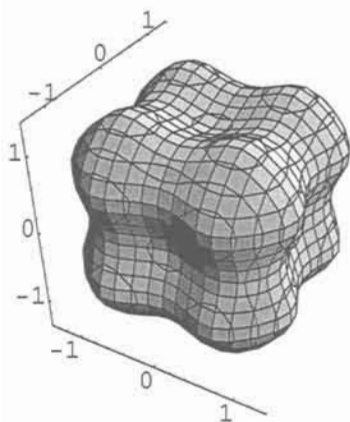


Fig. 11.2.16. After equation 11.2.14.

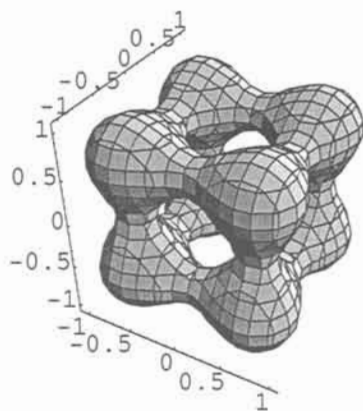


Fig. 11.2.17. With $C=1$ of equation 11.2.15 there is B_6H_6 again.

We increase boundaries and find shell after shell as in the two projections figs. 11.2.18 and 11.2.19.

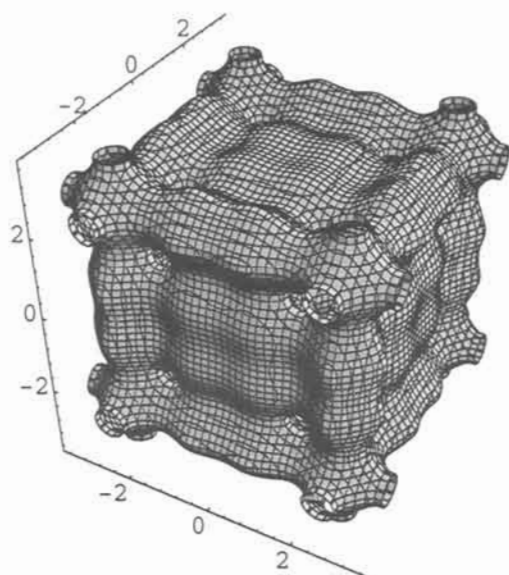


Fig. 11.2.18. Still after equation 11.2.15 with larger boundaries.

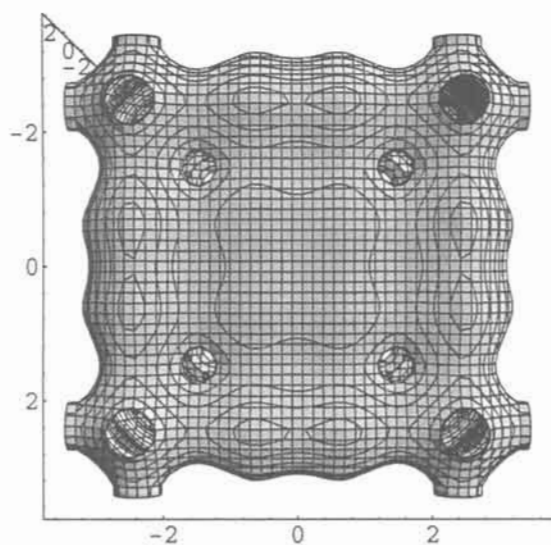


Fig. 11.2.19. Different projection.

Still bigger boundaries, as in the split of one eighth of a regular unit in fig. 11.2.20, show more layers. The general picture is that concentric cubes, joined via catenoids, build the structure.

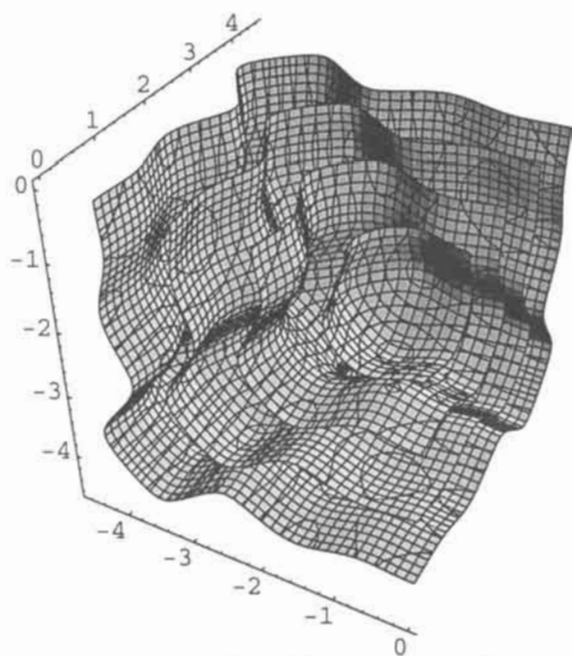


Fig. 11.2.20. Split shows that concentric cubes, joined via catenoids, build the structure.

11.3 Pure Dilatation

We start with the circle after equation 11.3.1, and obtain beautiful dilatation in fig. 11.3.1.

$$\cos 2\pi(x^2 + y^2) = 0 \quad 11.3.1$$

Next equation is eq. 11.3.2 which gives dilatation of the hyperbolas as in fig. 11.3.2.

$$\cos 2\pi(x^2 - y^2) = 0 \quad 11.3.2$$

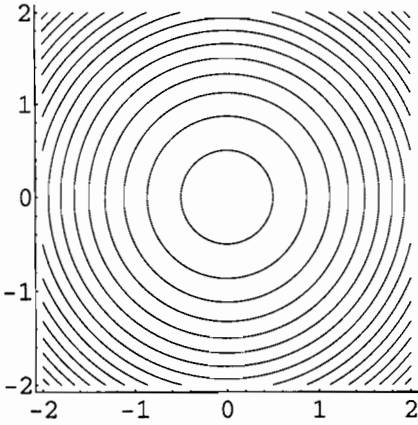


Fig. 11.3.1. Concentric circles after equation 11.3.1.

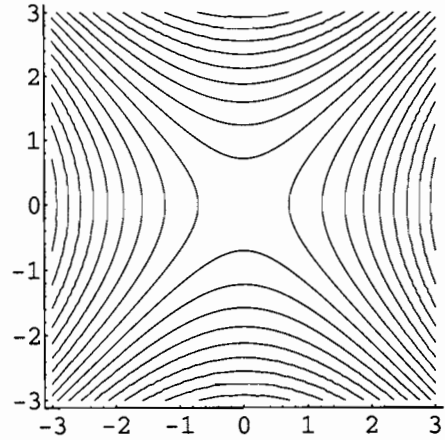


Fig. 11.3.2. Dilatation of hyperbolas after equation 11.3.2.

The simple equation of 11.3.3 gives the beautiful mixture of hyperbola and circles in fig. 11.3.3.

$$\cos \pi x^2 + \cos \pi y^2 = 0 \tag{11.3.3}$$

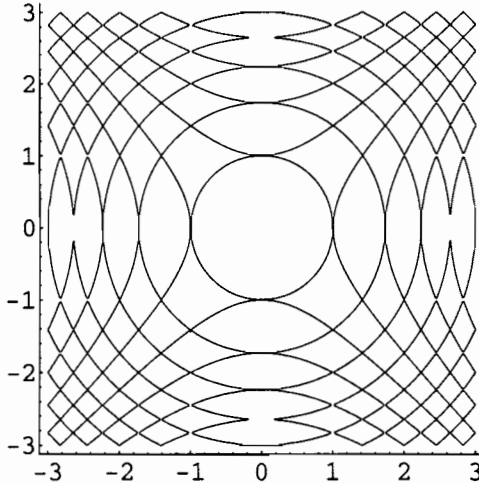


Fig. 11.3.3. Dilatation of circles and hyperbolas after equation 11.3.3.

The equation 11.3.4 gives an excellent dilatation in fig. 11.3.4.

$$\cos \pi x^2 \cos \pi y^2 = 0 \quad 11.3.4$$

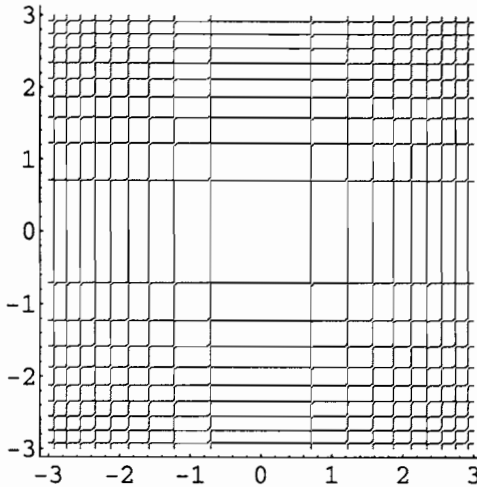


Fig. 11.3.4. Dilatation of squares after equation 11.3.4.

The dilatation of the spiral is obtained with the equation 11.3.5, and shown in fig. 11.3.5.

$$y \cos 2\pi(x^2 + y^2) + x \sin 2\pi(x^2 + y^2) = 0.4 \quad 11.3.5$$

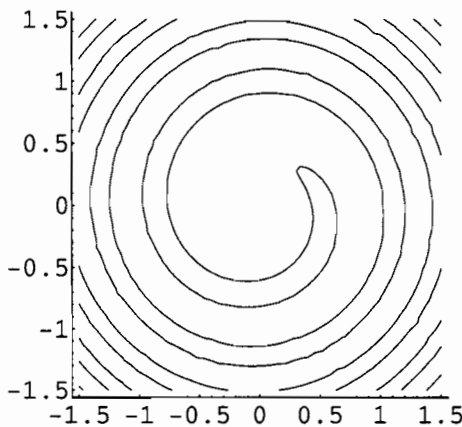


Fig. 11.3.5. Spiral dilatation after equation 11.3.5.

We do some of these simple functions in 3D and start with the concentric spheres in fig. 11.3.6 after equation 11.3.6.

$$\cos 2\pi(x^2 + y^2 + z^2) = 0 \quad 11.3.6$$

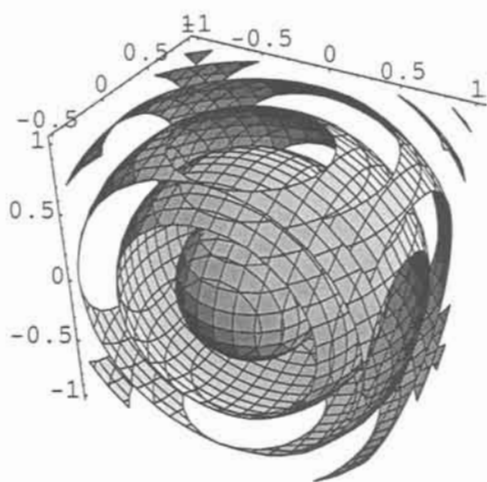


Fig. 11.3.6. Concentric spheres after equation 11.3.6.

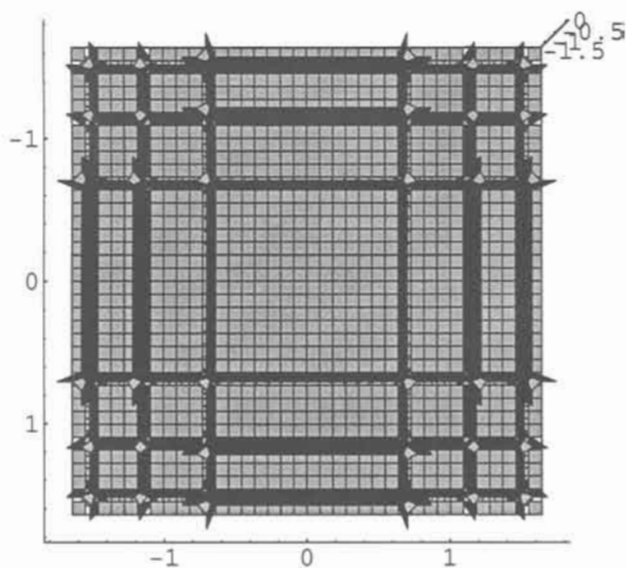


Fig. 11.3.7. Concentric cubes after equation 11.3.7.

The product in eq. 11.3.7 gives intersecting planes repeated with dilatation in fig. 11.3.7.

$$\cos \pi x^2 \cos \pi y^2 \cos \pi z^2 = 0 \quad 11.3.7$$

The sum as in eq. 11.3.8 gives the formidable dilatation of the P surface in fig. 11.3.8.

$$\cos \pi x^2 + \cos \pi y^2 + \cos \pi z^2 = 0 \quad 11.3.8$$

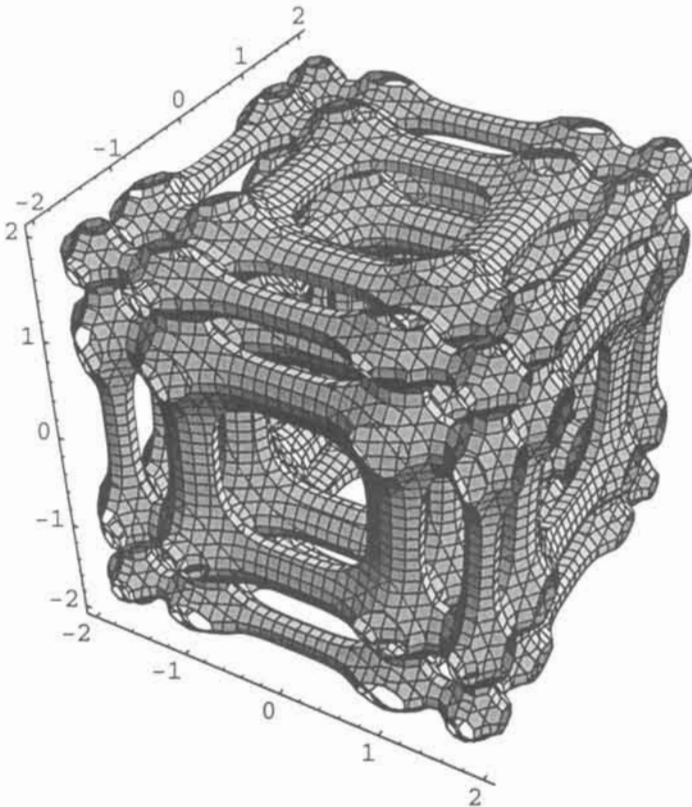


Fig. 11.3.8. Dilatation of the P surface after equation 11.3.8.

With equations of type $x \cos z^2 + y \sin z^2$ we get helicoids with pitch dilatation, and we design the equation 11.3.9 to make the spiral in fig.

11.3.9. One left handed spiral is joined to a right handed via a mirror - cylinder - and the spirals are dilatated.

$$e^{x \cos \pi z^2 + y \sin \pi z^2} + e^{x^2 + y^2} = 1.95 \tag{11.3.9}$$



Fig. 11.3.9. Two spirals and a mirror after equation 11.3.9.

Many are the surfaces which may be derived with these types of functions. We shall just show a couple of remarkable ones. The very simple equation of 11.3.10 gives the fourling of dilated P in fig. 11.3.10, with catenoids to a ‘fourling plane’ which has the topology of the fifth surface of Scherk, or also called Scherk’s tower surface, and showed earlier in chapter 2.

$$y \sin \pi x + x \sin \pi y + \sin \pi z = 0 \tag{11.3.10}$$

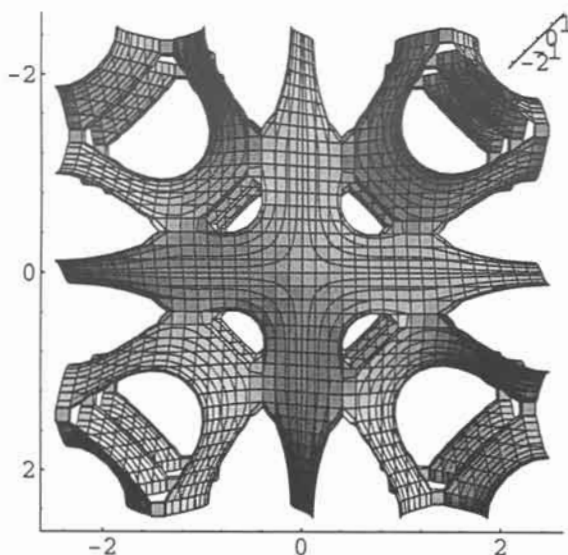


Fig. 11.3.10. A fourling of P with Scherk’s fifth surface after equation 11.3.10.

With the equation in 11.3.11 we have the remarkable eightling structure of, again, dilated P, and now with 'twin planes' built of four cube corners in fig. 11.3.11.

$$xy \sin \pi z + zy \sin \pi x + xz \sin \pi y = 0$$

11.3.11

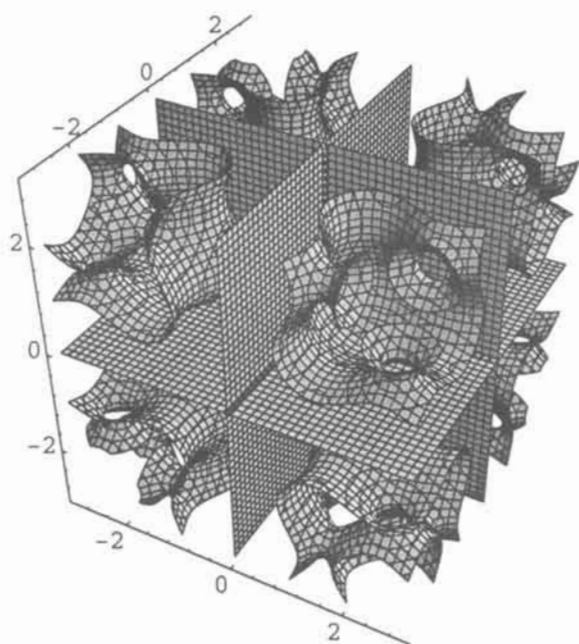


Fig. 11.3.11. An eightling of P with intersecting twin planes.

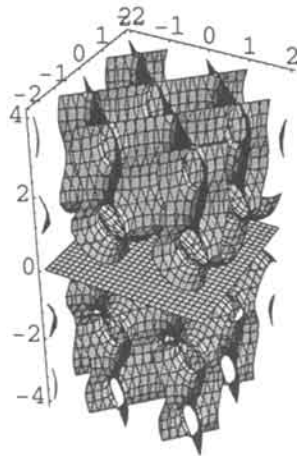


Fig. 11.3.12. Single twin plane reflecting two identical parts of the P surface after equation 11.3.12.

Finally we can give the single twin plane in a structure in figure 11.3.12, which is reflecting two identical parts of the P surface. The mathematics as given in 11.3.12 is very simple as it should be, giving a picture of a very common phenomenon in Nature.

$$\sin \pi z + z \sin \pi x + z \sin \pi y = 0 \tag{11.3.12}$$

We conclude saying that the three different twin planes as observed, topologically are minimal surfaces.

Exercises 11

Exercise 11.1. Introduce a negative sign in the equation for spherical dilatation, and describe the result.

Exercise 11.2. Do the Nautilus in 2D.

Exercise 11.3. Do the double spiral in 2D.

Exercise 11.4. Do the double Nautilus.

Exercise 11.5. Make the snail come out of Nautilus.

Exercise 11.6. Make the twin plane disappear in the structure of fig. 11.3.12 and explain why it works.

Answer 11.1. The equation is

$$\cos 2\pi(x^2 + y^2 - z^2) = 0.$$

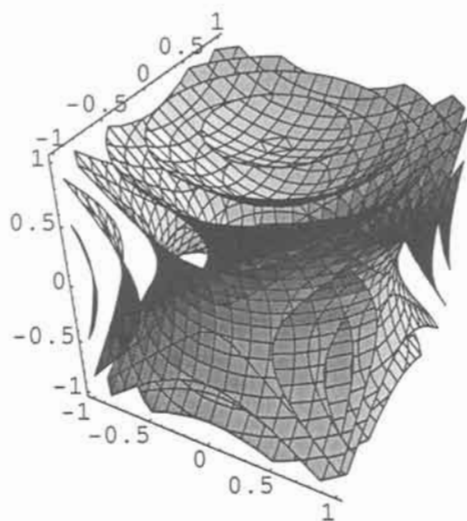


Fig. 11.1.

Answer 11.2. The equation is

$$y \cos 2\pi(x^2 + y^2)^{0.2} + x \sin 2\pi(x^2 + y^2)^{0.2} = 0$$

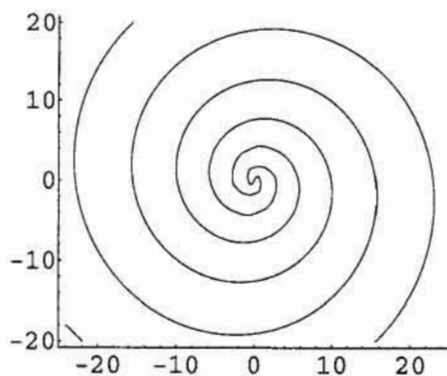


Fig. 11.2.

Answer 11.3. The equation is

$$(y \cos 2\pi(x^2 + y^2) + x \sin 2\pi(x^2 + y^2))^2 = 0.4$$

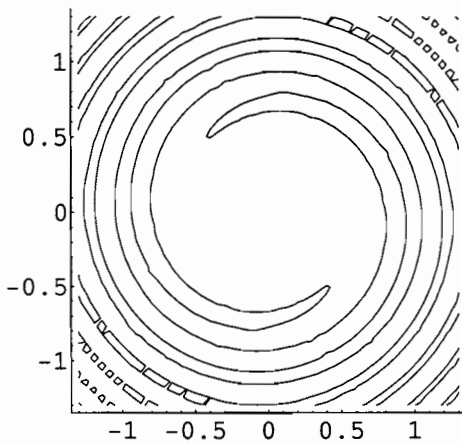


Fig. 11.3.

Answer 11.4. The equation is

$$(y \cos 2\pi(x^2 + y^2)^{0.2} + x \sin 2\pi(x^2 + y^2)^{0.2})^2 = 10$$

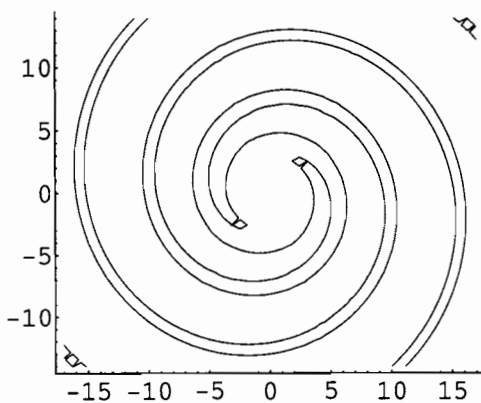


Fig. 11.4.

Answer 11.5. The equation is

$$y \cos 2\pi(x^2 + y^2)^{0.2} + x \sin 2\pi(x^2 + y^2)^{0.2} + e^{0.1(x^2 + y^2)} = 1$$

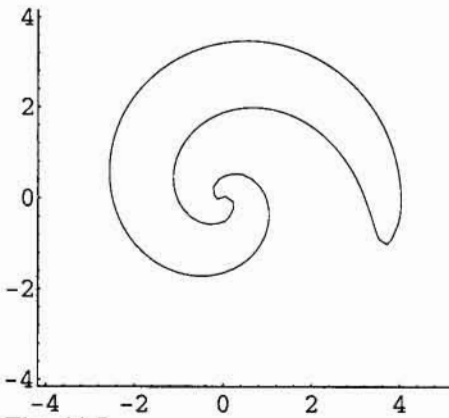


Fig. 11.5.

Answer 11.6. The equation is

$$\cos \pi z + z \sin \pi x + z \sin \pi y = 0$$

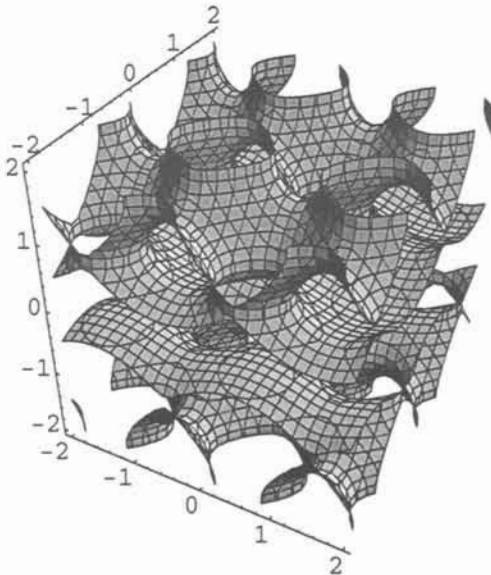


Fig. 11.6.

References 11

- 1 U. Dierkes, S. Hildebrandt, A. Kuster and O. Wohlrab, *MINIMAL SURFACES 1 and 2*, Springer Verlag, Berlin, 1991.
- 2 B.G. Hyde and S. Andersson, *INORGANIC CRYSTAL STRUCTURES*, Wiley, New York, 1988.
- 3 H.S.M. Coxeter, *INTRODUCTION TO GEOMETRY*, Wiley, New York, 1969.

Appendix 1 – Mathematica

We have been using *Mathematica*, and give here some examples. The subroutines `ContourPlot3D` and `ImplicitPlot` are for the implicit functions we use.

```
ImplicitPlot[E^y^4+E^x^4==200000,  
{x,-2,2},{y,-2,2},PlotPoints->200,Axes->False]
```

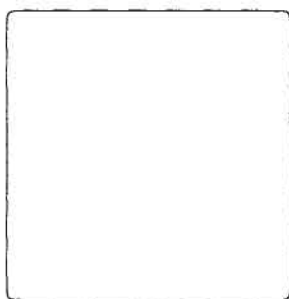


Fig. A.1.1 Square after plot above.

```
ContourPlot3D[x^10+y^10+z^10-100,  
{x,2,-2},{y,2,-2},{z,2,-2},  
MaxRecursion>2,PlotPoints->{{4,4},{4,4},{4,4}},  
Boxed->False,Axes->True]
```

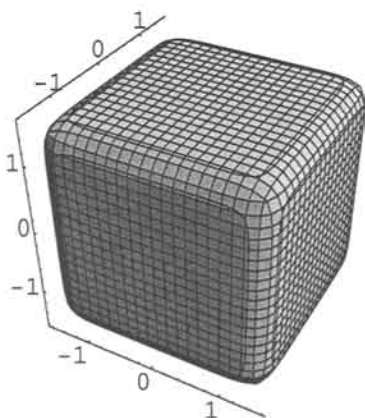


Fig. A.1.2. Cube after plot above.

Other useful programs are Plot (one-dimensional), Expand, Series, and below are examples.

First is plotted a Gauss error function and compared with an ordinary cosine function.

```
Plot[{10^-(x^2)+10^-((x-2)^2)+10^-((x-4)^2)+
10^-((x-6)^2)-.6,.4Cos[Pi x]},{x,-4,10},
PlotPoints->200,Axes->False]
```

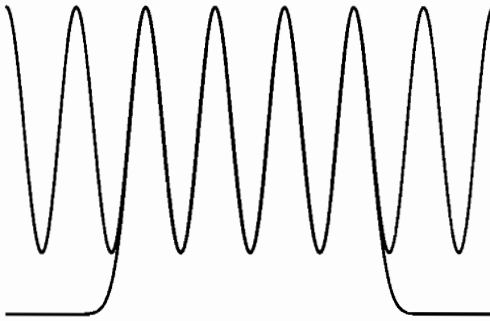


Fig. A.1.3. GD function and cosine after plot above.

```
Series[x (x^2-1)(x^2-4)(x^2-9),{x,0,8}]=x^7-14x^5+49x^3-36x
```

```
Series[E^x,{x,0,3}]=1+x+x^2/2!+x^3/3!+. . . . .
```

Appendix 2 – Curvature and differential geometry

We have introduced saddles, monkey saddles, minimal surfaces - we need a course in differential geometry with the concept of curvature.

Take a surface and let a plane rotate through a surface point in its normal. The section of this normal plane and the surface is a curve of curvature k . During the rotation, k must attain one maximum and one minimum value, k_1 and k_2 . These are called principal curvatures, and corresponding planar curves principal lines of curvature. These two curvatures are very useful in the description of the properties of surfaces. Their product is the *Gaussian curvature* (K),

$$k_1 k_2 = K \quad A\ 2.1$$

and the *mean curvature* (H) describes the sum.

A plane has both $K=0$ and $H=0$, while a cylinder has $K=0$ for every point as one of the principal curvatures is a straight line.

A point on a cylinder is called parabolic.

A point on a sphere or an ellipsoid has always positive curvature, and for the sphere $K=1/r^2$ and $H=1/r$. Such a point is called elliptic.

$$x^2 + y^2 + z^2 = 4 \quad A\ 2.2$$

$$2x^2 + y^2 + z^2 = 4 \quad A\ 2.3$$

A simple example of a surface of negative Gaussian curvature is the saddle. An example of this is shown in fig. A.2.1, with the equation

$$x^2 - y^2 - z = 0. \quad A\ 2.4$$

A point on such a surface is called hyperbolic.

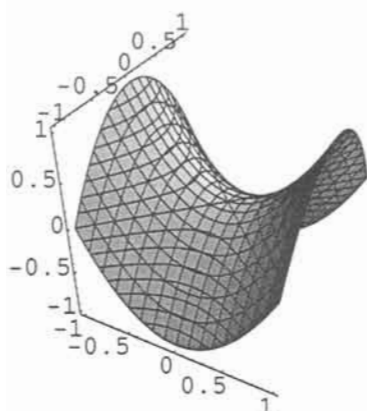


Fig. A.2.1. Saddle. After equation *A 2.4*.

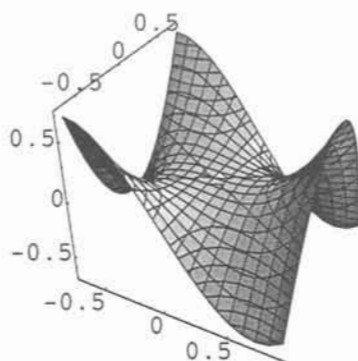


Fig. A.2.2. Monkey saddle. After equation *A 2.5*.

The monkey saddle in fig. **A.2.2** is a very remarkable surface. Hilbert gave it the name - a monkey beside its two legs also has a tail. The monkey saddle has negative Gaussian curvature everywhere, except in the centre where it is zero. Such a point is called umbilic or a flat point. We have used a simple function *A 2.5* to show the monkey saddle in fig. **A.2.2**.

$$x(x^2-3y^2) - z = 0 \quad A 2.5$$

Examples of surfaces built of saddles are the catenoid and the helicoid with the equations

$$x^2 + y^2 - \cosh z = 0 \text{ (catenoid)} \quad A 2.6$$

and

$$x \cos 4z - y \sin 4z = 0 \text{ (helicoid)} \quad A 2.7$$

Both are minimal surfaces, or soap water surfaces. Another way saying this is that $H=0$. These two surfaces are very special, they have the same Gaussian curvature on corresponding points. That means they are isometric and can be bent into each other without stretching, like a paper can be rolled into a cylinder. This has been used by us to describe phase transitions without cost of energy in liquid crystals and Martensite. It is called the Bonnet transition.

Monkey saddles and ordinary saddles build the strongly related and famous 3-periodic nodal and minimal surfaces. Some parts of this book deal with

these types of surfaces. The minimal surfaces are well characterised, having $H=0$ everywhere and $K \leq 0$. We show the nodal surface, equation A2.8, which deviates within 0.5% from the P - minimal surface, in fig. A.2.5.

$$\cos x + \cos y + \cos z = 0 \quad A\ 2.8$$

The mathematics of the 3-periodic minimal surfaces are immensely more complicated than that of the nodal surfaces.

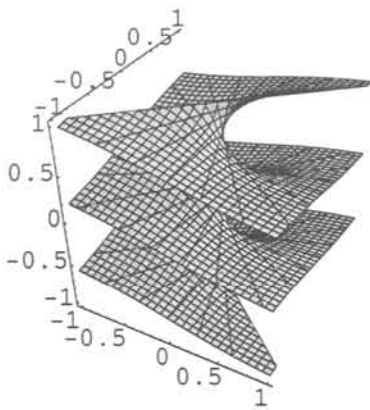


Fig. A.2.3. Helicoid after equation A 2.7.

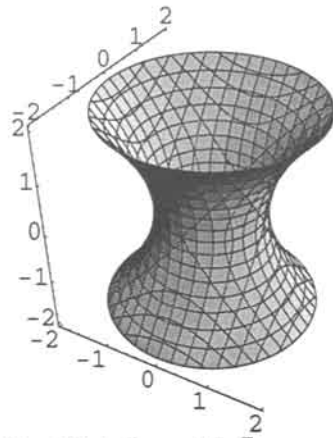


Fig. A.2.4. Catenoid after equation A 2.6.

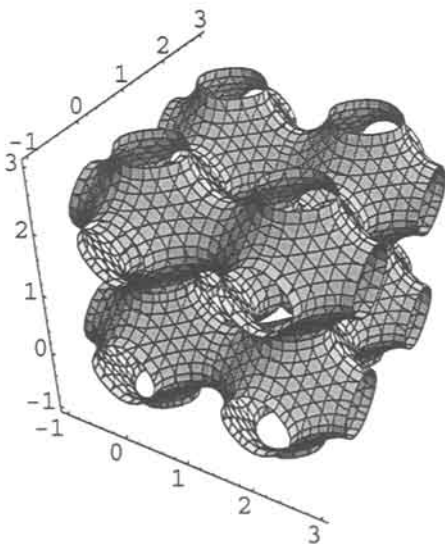


Fig. A.2.5. P-surface after equation A2.8.

Appendix 3 – Formal way to derive the shapes of polyhedra

Bodies that may be described with planes, can be given a mathematical function from the exponential scale. We derive the normal vectors of these planes and, use them in the exponents.

We will show you with the tetrahedron.

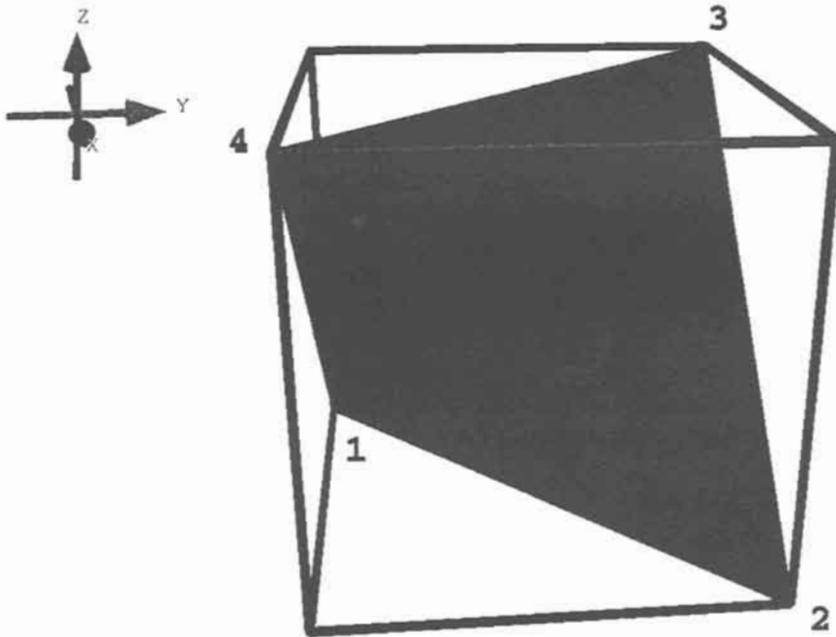


Fig. A.3.1 A suitable orientation of a tetrahedron.

Place a tetrahedron in a coordinate system, for example as shown in fig A. 3.1. The origin is in the centre of the outlined cube and the vertices (v) for the tetrahedron are:

$$v_1 = (-1 \ -1 \ -1)$$

$$v_2 = (1 \ 1 \ -1)$$

$$v_3 = (-1 \ 1 \ 1)$$

$$v_4 = (1 \ -1 \ 1)$$

In order to determine the face vectors, we need the normal vectors to the four faces. Each face is defined by three vertices;

face 1: v_1, v_2, v_3

face 2: v_1, v_3, v_4

face 3: v_1, v_4, v_2

face 4: v_2, v_4, v_3

We need five of the tetrahedrons six edges (e) to determine the normals, and the vectors for these are:

$$e_{12} = v_2 - v_1 = (2 \ 2 \ 0)$$

$$e_{13} = v_3 - v_1 = (0 \ 2 \ 2)$$

$$e_{14} = v_4 - v_1 = (2 \ 0 \ 2)$$

$$e_{23} = v_3 - v_2 = (-2 \ 0 \ 2)$$

$$e_{24} = v_4 - v_2 = (0 \ -2 \ 2)$$

The normals (n) are then the vector product of two edge vectors for the face (note that they are multiplied counter-clockwise in order to get the correct sign, or direction, of the normals);

$$n_1 = e_{13} \times e_{12} = (-4 \ 4 \ -4)$$

$$n_2 = e_{14} \times e_{13} = (-4 \ -4 \ 4)$$

$$n_3 = e_{12} \times e_{14} = (4 \ -4 \ -4)$$

$$n_4 = e_{23} \times e_{24} = (4 \ 4 \ 4)$$

For any face (even square, pentagonal or higher polygons) it is sufficient with just three vertices for the normal vector calculation, as three points define a plane.

And finally, to determine the face vectors we need a scale factor (s) for the distance of the face to the origin. This is calculated by scalar multiplication of the normal vector with an arbitrary vector to the face. For the Platonic solids the scale factors are naturally the same for all faces, but in this example we still calculate them all, and as our arbitrary vectors, we just choose one of the faces' vertex vectors;

$$s_1 = n_1 \cdot v_1 = 4$$

$$s_2 = n_2 \cdot v_1 = 4$$

$$s_3 = n_3 \cdot v_1 = 4$$

$$s_4 = n_4 \cdot v_2 = 4$$

Now, to calculate the face vectors (u), we divide the normal vectors with the corresponding scale factor, and get;

$$\begin{aligned}u_1 &= (-1 \ 1 \ -1) \\u_2 &= (-1 \ -1 \ 1) \\u_3 &= (1 \ -1 \ -1) \\u_4 &= (1 \ 1 \ 1)\end{aligned}$$

The exponential scale equation for the tetrahedron is thus:

$$\begin{aligned}10^{\text{tetr}} &= 10^{u_1 \cdot (x \ y \ z)} + 10^{u_2 \cdot (x \ y \ z)} + 10^{u_3 \cdot (x \ y \ z)} + 10^{u_4 \cdot (x \ y \ z)} = & A \ 3.1 \\&= 10^{-x+y-z} + 10^{-x-y+z} + 10^{x-y-z} + 10^{x+y+z} = C\end{aligned}$$

This method of face vector derivation is general for all polyhedra, and you can also scale and orient them as you like.

For the tetrahedron, octahedron, the icosahedron, and dodecahedron we derive accordingly the following equations, with a short notation obvious from below:

Tetrahedron

vectors: $(111), (1\bar{1}\bar{1}), (\bar{1}\bar{1}1), (\bar{1}1\bar{1})$

Octahedron

vectors: $(\pm 1, \pm 1, \pm 1)$

Icosahedron

vectors: $(\pm\tau, \pm\tau, \pm\tau), (\pm\tau^2, 0, \pm 1), (\pm 1, \pm\tau^2, 0), (0, \pm 1, \pm\tau^2)$

Dodecahedron

vectors, $(\pm\tau, \pm 1, 0), (\pm 1, 0, \pm\tau), (0, \pm\tau, \pm 1)$

$(\frac{\sqrt{5}-1}{2} \approx 1.618$ is the golden section, τ , and 2.618 is $\tau+1$, or τ^2 .)

Appendix 4 – More curvature

The following is a Mathematica Notebook code for calculation of the Gaussian and mean curvature of a function $w[x,y,z]$. It is written by Stephen Hyde, Applied Mathematics, ANU, Canberra, Australia, and works for the program Mathematica.

We show it exactly as it appears in Mathematica, except for the outputs, and we carry out the calculation of the natural exponential, or a cube corner, of the equation $e^x + e^y + e^z$ below:

```
w1[x_,y_,z_] := D[w[x,y,z],x];
w2[x_,y_,z_] := D[w[x,y,z],y];
w3[x_,y_,z_] := D[w[x,y,z],z];

w11[x_,y_,z_] := D[w1[x,y,z],x];
w12[x_,y_,z_] := D[w1[x,y,z],y];
w13[x_,y_,z_] := D[w1[x,y,z],z];

w21[x_,y_,z_] := D[w2[x,y,z],x];
w22[x_,y_,z_] := D[w2[x,y,z],y];
w23[x_,y_,z_] := D[w2[x,y,z],z];

w31[x_,y_,z_] := D[w3[x,y,z],x];
w32[x_,y_,z_] := D[w3[x,y,z],y];
w33[x_,y_,z_] := D[w3[x,y,z],z];

matrix[w_,x_,y_,z_] := {
  {w11[x,y,z]-1,w12[x,y,z],w13[x,y,z],w1[x,y,z]},
  {w21[x,y,z],w22[x,y,z]-1,w23[x,y,z],w2[x,y,z]},
  {w31[x,y,z],w32[x,y,z],w33[x,y,z]-1,w3[x,y,z]},
  {w1[x,y,z],w2[x,y,z],w3[x,y,z],0}}

det[w_,x_,y_,z_] := Det[matrix[w,x,y,z]];

a[w_,x_,y_,z_] := Coefficient[det[w,x,y,z],1,2];
b[w_,x_,y_,z_] := Coefficient[det[w,x,y,z],1,1];
c[w_,x_,y_,z_] := Coefficient[det[w,x,y,z],1,0];

meancurv[w_,x_,y_,z_] := -b[w,x,y,z]/(2*a[w,x,y,z]
* Sqrt[w1[x,y,z]^2+w2[x,y,z]^2+w3[x,y,z]^2]);
gausscurv[w_,x_,y_,z_] := c[w,x,y,z]/(a[w,x,y,z]
*(w1[x,y,z]^2+w2[x,y,z]^2+w3[x,y,z]^2));
```

Example:

$w[x, y, z] = e^x + e^y + e^z;$

`gausscurv[w, x, y, z]`

Out[108]=

$$(e^{2x+y+z} + e^{x+2y+z} + e^{x+y+2z}) / (e^{2x} + e^{2y} + e^{2z})^2$$

Instead of Gauss curvature we calculate

`meancurv[w, x, y, z]`

Out[129]=

$$(e^{2x+y} + e^{x+2y} + e^{2x+z} + e^{2y+z} + e^{x+2z} + e^{y+2z}) / 2(e^{2x} + e^{2y} + e^{2z})^{3/2}$$

If $x=y=z$ as it is in the corner, the Gaussian curvature is $1/3$ and the mean curvature is $1/\sqrt{3}$ and independent of size of the corner. These are exactly the values the cube corners converge to above in equations 3.3.2 and 3.3.3.

Appendix 5 – Raison d'être

In a description of space it is convenient to follow Coexeter[1]; The general motion is covered by a similarity, which is either an isometry or a dilative rotation. There are three kinds of isometry, rotation, translation, and reflection. These combine in commutative pairs to form the twist (screw displacement), glide reflection and rotary reflection. Which gives the crystallographic groups.

The *continuous rotation* of a point gives the circle - the *continuous dilatation* gives the line. And the combination in the plane - the *continuous dilative rotation* - of a point gives the equiangular spiral, or the logarithmic spiral, or in Nature the Nautilus.

The simple *twist*, a combination of continuous rotation and continuous dilatation of a point perpendicular to the plane of rotation, gives a space curve which is the circular helix or the screw. Or half the DNA molecule.

We can think of curves in space as paths of a point in motion. These words by Struik form the background to the modern description of space curves, physics of particle motion and symmetry in space.

In certain parametrisations of curves motion along the curve the *speed* of a curve or the *acceleration* of a curve are defined.

We exemplify with the circle and the circular helix:

$$x = a \cos u, y = a \sin u, z = 0 \text{ (circle)}$$

$$x = a \cos u, y = a \sin u, z = bu \text{ (circular helix)}$$

a is the radius of the circle (projected for the helix), $2\pi b$ is the pitch, in French *pas*, in German *Ganghöhe*, in Swedish *stigning*. With b positive the helix is right handed, if negative the helix is left handed.

It is often convenient to think of u as the time and define speed, acceleration, and force accordingly. Relations between curvature and energy may be obtained.

While curvature for a curve measures the deviation from a tangent, the torsion measures the deviation for a curve from sitting in a plane. Planar curves have only curvature while space curves have curvature and torsion. If κ is curvature and τ is torsion they are related to radius and pitch by the equations

$$\kappa = \frac{a}{a^2 + b^2}$$

and

$$\tau = \frac{b}{a^2 + b^2}$$

As u increases, the arc length s increases. s may be described as

$$ds^2 = dx^2 + dy^2 + dz^2$$

or

$$s = \int \sqrt{x^2 + y^2 + z^2} du$$

A so called natural parametrisation can be made with s , torsion and curvature, which provide general equations for space curves as a reduction of the Riccati equations.

A simple example is the blowing up of a circle or a sphere. Time and curvature become synonyms which is a tempting description of time in mathematics. But the application to more complicated space curves is not transparent.

Going to surfaces the Gaussian curvature is the product of two principal curvatures, and the mean curvature the sum. The torsion is now included in this.

So we conclude that in a geometric description of curves and surfaces the ordinary curvature, the torsion, the Gaussian curvature, and the mean curvature are tools to make the properties of these things available for our perception. Parametrisation brings in a variable like time and the notion of point motion in space curves allows for a definition of physical concepts like speed, acceleration and force. Which also then are useful for the description of the space curve itself.

As time is not a mathematical concept we shall avoid it here and use implicit functions. In particular we study the change of the constant belonging to an implicit function. This is not an ordinary parametrisation but it is an auxiliary variable we have found great use to vary. Again we take the sphere as an example - a change of radius (blowing up the balloon) is a change of constant, or curvature, or time.

We shall see that the change of constant for more advanced functions means drastic changes of curvature and topology, and offers descriptions of reactions in mathematics without the use of the physical notions of time or speed.

Reference

- 1 H.S.M. Coxeter, INTRODUCTION TO GEOMETRY, Wiley, New York, 1969.

This Page Intentionally Left Blank

Subject Index

A

A15 · 253; 255
admantane · 167
AlB₂ · 123; 133
algebraic equation · 10; 14; 16
Alhambra ornaments · 74; 123
alloys · 86; 137; 209
apatite · 73; 128
auxiliary parameter · 63; 64; 206

B

B₄H₄ · 24; 25; 119; 213
B₆H₆ · 21; 24; 95; 113; 202; 213; 310
B₈H₈ · 24; 25; 213
bcc · 79; 84; 86; 87; 117; 133; 161; 205; 209; 210; 242; 255; 260
body centred packing · 2; 24; 25; 164; 205
Bonnet transition · 328
Boyle · 7; 8
building blocks · 2; 64; 65; 99

C

CaF₂ · 91
catenoids · 83; 88; 90; 91; 183; 205; 206; 209; 210; 211; 218; 219; 222;
229; 302; 312; 317
CaZn₅ · 123; 134; 135; 225
centaur function · 63; 194
chirality · 99; 255
circular functions · 2; 74; 75; 80; 99; 123; 147; 156; 175; 179; 244; 245;
249; 260
CLP minimal surface · 119
complex exponential · 1; 2; 3; 73; 74; 80; 81; 82; 83; 115; 157; 162; 163
compound polyhedra · 39
concentric cubes · 312
concentric spheres · 315
concentric structure · 95; 198
cone · 193; 198; 199; 278

congruence · 293
cosh · 2; 19
CsCl · 87
CuAl₂ · 123; 135; 136; 139; 140
cube · 2; 12; 18; 19; 24; 31; 39; 48; 49; 50; 51; 52; 53; 54; 55; 56; 57; 58;
61; 63; 67; 78; 83; 91; 115; 116; 117; 118; 157; 183; 197; 204; 213;
214; 215; 217; 222; 242; 246; 247; 270; 272; 273; 284; 286; 287; 288;
318; 330; 333; 334
cube corner · 2; 12; 18; 55; 56; 217; 270; 318; 333
cubeoctahedron · 222
cubic dilatation · 302
cubic equation · 19; 20
cubic ice · 83
cubosome · 3; 5; 115; 117; 118; 119; 160; 161; 162; 163; 167; 169; 222;
237
cyclic twinning · 293; 294; 300

D

D'Arcy Thompson · 1; 7
de Moivre · 81
defect structure · 11
definitions of sine · 13
diamond · 2; 24; 25; 83; 84; 85; 117; 132; 161; 167; 205; 218; 219
differential geometry · 1; 7; 327
diffusion equation · 179; 185
dilatation · 2; 73; 147; 175; 293; 294; 295; 296; 297; 298; 299; 300; 302;
305; 306; 307; 308; 312; 314; 316; 320; 335
dilatation of the spiral · 314
Diophantine equation · 229
disc surfaces · 107
DNA · 2; 62; 73; 99; 108; 112; 147; 150; 151; 152; 153; 335
double diamond · 84
double ice · 84
double torus · 274
dual · 21; 25; 171; 191; 202; 211; 213; 214; 215; 217; 225; 284; 286; 287

E

eigenfunctions · 123
eightling operation · 300
electron structure · 21; 213
ELF structure · 26; 113; 119; 202; 213; 280
enzyme · 73; 112
equation of symmetry · 2; 39; 82; 115; 156; 238; 242
Euclid · 141

Euler · 39
Exponential Scale · 1; 5; 7; 19; 39; 293

F

face centred cubic · 2; 13; 76; 79
falling drop · 268
Fibonacci · 31; 175; 176
finite · 2; 13; 19; 21; 31; 99; 112; 123; 147; 156; 162; 197; 237; 254
fourling · 136; 294; 295; 307; 317
fourling plane · 317
fundamental polyhedra · 7; 24; 39; 57
fundamental theorem of algebra · 1; 3; 7; 13; 16; 34; 123; 132; 147; 186;
293

G

G surface · 79
garnet · 162; 242; 245; 255; 256; 259; 260
garnet packing of rods · 242; 255; 256; 259
Gauss distribution function · 3; 74
Gaussian curvature · 52; 53; 54; 55; 196; 327; 328; 334; 336
general saddle equation · 1; 29; 123; 136; 142
genetic code · 147
genus one · 274; 275
gmelinite · 129; 130
goke · 104; 242; 246; 248; 249
grooves · 147; 152
gyroid · 82; 85; 86; 117; 118; 161; 162; 163; 164; 219; 221; 222

H

handmade periodicity · 156; 180
hanging drop · 191; 194
Hardy · 7; 38; 39; 71; 74; 98; 190
helical saddle tower surfaces · 106
helicoid · 31; 34; 35; 100; 102; 103; 110; 114; 328
heptadecagon · 67
hexagonal close packing · 123; 133; 134; 205; 222
hexagonal rod packing · 251
hierarchy · 39; 62
hyperbolic plane · 191; 197
hyperbolic polyhedra · 2; 267

I

ice · 73; 83; 84; 85; 224; 226
icosahedron · 39; 59; 60; 286; 287; 332
incommensurate · 140; 141
infinite products · 13; 147
interpenetrating gyroid · 221
interstitial · 204; 218
isometry · 73; 335
isosurface constant · 8; 52; 55; 76; 99

K

Kant · 7
Kepler star · 91
Kepler's stella octangula · 66; 215; 216
Klemm · 216

L

Larsson cubosome · 115; 118; 162; 169; 253; 281
LaVallée Poussin · 73; 75
Liesegang rings · 182
lipid bilayer · 276; 277

M

martensite · 328
Mathematica · 7; 52; 82; 94; 97; 186; 325; 333
mean curvature · 52; 54; 55; 69; 327; 333; 334; 336
minimal surfaces · 1; 7; 26; 30; 73; 79; 205; 217; 319; 327; 328; 329
 Mo_6Cl_8 · 66; 216
monkey saddles · 19; 327
multiple eigenvalues · 123
multiple twins · 293
myoglobine · 112

N

natural exponential · 2; 39; 55; 67; 75; 115; 156; 267; 270; 333
 $\text{Nb}_3\text{O}_7\text{F}$ · 226
 Nb_3Sn · 240; 241
 NbO · 87
Neovius · 82
Nesper · 38; 79; 86; 98; 236
Neurosedyne · 99

NIntegrate · 186; 187
nodal surfaces · 2; 26; 79; 80; 205; 329

O

O'Keeffe · 4; 245; 265
octahedron · 18; 24; 26; 39; 48; 49; 57; 58; 59; 60; 65; 66; 67; 69; 157;
170; 176; 177; 202; 211; 213; 214; 215; 217; 218; 284; 285; 286; 289;
306; 308; 332
octahemioctahedron · 173; 174
olympic rings · 277
optimal organisation · 62
oxide chemistry · 191

P

P surface · 20; 21; 22; 26; 79; 83; 85; 95; 116; 206; 207; 237; 240; 241;
281; 282; 283; 302; 316; 319
pentagonal dodecahedron · 39; 61; 286; 287; 299; 309
periodic fourling · 294
Perovskite · 213
pitch · 107; 108; 152; 316; 335; 336
planar groups · 131
polygon · 44; 47; 297
polynomial additions · 7
precipitation · 181
pretzels · 274
primitive cubic · 21; 24; 26; 78; 85; 205
primitive hexagonal packing · 225
primitive packing of rods · 254; 258
propeller · 253; 255
protein molecules · 74
pseudosphere · 196
pyrite · 61
pyritohedron · 61

Q

quasi · 123; 136; 137

R

radiolarian · 147; 229; 262
repulsion · 3; 191; 200
rhombic dodecahedron · 18; 24; 26; 39; 55; 57; 58; 59; 60; 61; 162; 209;
285; 286; 289; 308; 309

rings · 182; 267; 273; 277; 278; 279
rods in space · 109; 237
roots · 1; 3; 7; 9; 10; 12; 14; 15; 16; 19; 20; 22; 24; 26; 82; 147; 148
Rutile · 213; 215

S

saddle equation · 1; 26; 29; 123; 130; 136; 142
saddle tower surfaces · 30; 106
sail · 293
Scherk · 27; 31; 34; 120; 317
screw · 35; 74; 75; 99; 112; 335
shear plane · 226
sinh · 19
skeletons · 185
Skiena · 139; 146
snake's head · 110; 111
sodalite · 90
solitons · 293
sphere packings · 7
spiral surface · 100; 110
stainless steel · 86; 209
structure of water · 197; 226
Synge · 73; 98; 267; 292

T

Terasaki · 182; 190
tetrahedral · 11; 12; 65; 91; 96; 117; 213; 260; 261; 305; 307
tetrahedron · 18; 24; 26; 39; 48; 49; 57; 59; 67; 69; 117; 170; 171; 211;
226; 287; 288; 289; 330; 332
tetrahemihexahedron · 174
theorem of algebra · 1; 3; 7; 13; 16; 34; 123; 132; 147; 186; 293; 310
TiH₂ · 91; 92
topology · 19; 55; 73; 95; 119; 150; 152; 191; 196; 197; 198; 205; 210;
317; 337
torus · 253; 254; 267; 274; 276; 278; 279; 281; 282; 283
tower surface · 27; 30; 31; 102; 106; 107; 108; 317
translation vector · 73; 74
tridymite · 224; 226; 260; 261
trigonal bipyramid · 133; 225
trigonal prism · 225
triple · 104; 274
twin plane · 174; 318; 319; 320

V

VO₂ · 213

von Schnering · 4; 38; 79; 86; 98; 122; 202; 236

W

wave equation · 13

wave packets · 301; 302; 303

WC · 225

Wells · 86; 98; 123; 146; 219; 221; 222; 236

Whittaker & Watson · 75

X

XeF₂ · 280; 292

Z

zeolite · 129; 130; 140; 161

zinc blende · 226

This Page Intentionally Left Blank